

VOLUME 12

NUMBER 2

2019

ISSN 2218-7979
eISSN 2409-370X

International Journal of
Biology
and **Chemistry**



Al-Farabi Kazakh National University

International Journal of Biology and Chemistry is published twice a year by al-Farabi Kazakh National University, al-Farabi ave., 71, 050040, Almaty, Republic of Kazakhstan
website: <http://ijbch.kaznu.kz/>

Any inquiry for subscriptions should be sent to:
Prof. Mukhambetkali Burkitbayev, al-Farabi Kazakh National University
al-Farabi ave., 71, 050040, Almaty, Republic of Kazakhstan
e-mail: Mukhambetkali.Burkitbayev@kaznu.kz

EDITORIAL

The most significant achievements in the field of natural sciences are reached in joint collaboration, where important roles are taken by biology and chemistry. Therefore publication of a Journal, displaying results of current studies in the field of biology and chemistry, facilitates highlighting of theoretical and practical issues and distribution of scientific discoveries.

One of the basic goals of the Journal is to promote the extensive exchange of information between the scientists from all over the world. We welcome publishing original papers and materials of biological and chemical conferences, held in different countries (after the process of their subsequent selection).

Creation of special International Journal of Biology and Chemistry is of great importance, because a great amount of scientists might publish their articles and it will help to widen the geography of future collaboration. We will be glad to publish also the papers of the scientists from the other continents.

The Journal aims to publish the results of the experimental and theoretical studies in the field of biology, biotechnology, chemistry and chemical technology. Among the emphasized subjects are: modern issues of technologies for organic synthesis; scientific basis of the production of physiologically active preparations; modern issues of technologies for processing of raw materials; production of new materials and technologies; study on chemical and physical properties and structure of oil and coal; theoretical and practical issues in processing of hydrocarbons; modern achievements in the field of nanotechnology; results of studies in the fields of biology, biotechnology, genetics, nanotechnology, etc.

We hope to receive papers from a number of scientific centers, which are involved in the application of the scientific principles of biological and chemical sciences on practice and carrying out research on the subject, whether it relates to the production of new materials, technologies and ecological issues.

¹*O.K. Khamdiyeva , ²S. Pack , ¹Z.M. Biyasheva ,
²Z. Abdullaev , ³D.R. Kaidarova , ⁴N.P. Kabysheva 

¹Al-Farabi Kazakh National University, Almaty, Kazakhstan

²The Chromosome Pathology Unit, Laboratory of Pathology, National Cancer Institute,
National Institutes of Health in Bethesda, MD, USA

³Kazakh Institute of Oncology and Radiology, Almaty, Kazakhstan

⁴Kazakh Scientific Center of Quarantine and Zoonotic Diseases, Almaty, Kazakhstan

*e-mail: azadahamdieva@gmail.com

Mutation and expression of the *C-KIT* gene on population of Kazakhstan

Abstract: Lung cancer is still a leading cause of death from malignant tumors worldwide. Due to late diagnosis, results of treatment remain unsatisfactory. In Kazakhstan about 3,669 new cases of lung cancer are detected every year, with a 5-year survival rate for 2016 equal to 48.0%. The aim of the current work is to study the expression of C-KIT protein and identify mutations in patients with lung cancer living in Almaty region. Literature data showed that anomalous expression of the corresponding gene and presence of mutations lead to a number of malignant neoplasms. Creation of drugs targeting C-KIT protein, promotes the development of clinical diagnosis and treatment of cancer. Blood samples and biopsy material obtained from patients diagnosed with lung cancer, treated at the Almaty Oncology Center and residing in Almaty region served the objects of the study. Written informed consent was obtained from all patients. Analysis of restriction fragment length polymorphism and immunohistochemical analysis followed the polymerase chain reaction. For immunohistochemical analysis tissue fixed in formalin and embedded in paraffin blocks was used. The presence of mutations in codon 557 was revealed by the genetic analysis of 11 exon of *C-KIT* gene. RFLP analysis and sequencing showed mutations in the codon. Immunohistochemical analysis revealed overexpression of *C-KIT* gene in four (9.09%) patients, 14 (31.82%) patients had moderate expression, 24 (54.54%) patients had weak expression and two (4.55%) patients had no expression. In total, 18 (40.91%) patients had a positive response to immunohistochemical analysis. This suggests that the disorders occur in the cells of tumor tissue and are not inherited. In fact, in most cases the occurrence of lung cancer can be associated with smoking.

Key words: *C-KIT* gene, mutation, expression, immunohistochemical analysis.

Introduction

Cancer remains the leading cause of death worldwide, despite impressive advances in the early diagnosis and treatment of patients with malignant neoplasms. Incidence rates in Kazakhstan are highest among CIS countries [1]; with 36 813 cases detected in 2016 [2]. Lung cancer is one of the most common types of cancer and the leading cause of death from cancer worldwide [3]. This type of cancer is the most common in the world, and in 2016, it amounted to 9.9% of the total number of new cases of cancer in Kazakhstan. In 2016, about 3,635 new cases of lung cancer were detected in Kazakhstan, with five-year survival equal to 48.0%, and 2,498 death cases [2]. High mortality from lung cancer is believed to be

caused by aggressiveness, invasive and metastatic disease potential, as well as difficulties in detecting it in the early stages. Therefore, the search for pathogenetic approaches in the treatment of cancer remains an urgent problem today. The lack of significant achievements in the fight against cancer is largely due to an insufficient level of diagnosis. For the vast majority of people, the cancer is still diagnosed in the late stages of development (73.5%), in which the possibilities of modern treatment methods cannot be fully realized, as patients may have resistance to chemotherapy and targeted drugs. Ten years ago, therapeutic strategies for treating lung cancer were based on a histological type of classification. However, in recent years, one of the most interesting advances in the treatment of lung cancer has been the

understanding of genetic changes in cells. Achievements in genomic sequencing and identification of molecular markers over the past decade have clearly demonstrated that cancer is a heterogeneous disease [4; 5].

The studies using some modern methods of molecular biology have allowed us to fundamentally change our ideas about the characteristics of the various forms of the disease that arise and, consequently, the treatment tactics and its predicted course. Developments in genotyping have changed the clinical practice of treating lung cancer and have shown that genetic changes in the *EGFR*, *ALK*, *ROS1*, *HER2*, *KIT* and *BRAF* genes are powerful predictive biomarkers in the treatment of lung cancer [6-10].

In this regard, the purpose of the current research was to study the expression of C-KIT protein and identify mutations in patients with lung cancer living in Almaty region.

Materials and methods

Patients. Surgical specimens were obtained during the surgery from patients diagnosed with a lung cancer. All patients underwent a survey, which contained information on clinical data, gender, age and bad habits. Patients signed a voluntary informed consent before participating in the study. The study protocol was approved by the local ethics committee of the medical faculty of the Higher School of Public Health at Al-Farabi Kazakh National University (Almaty, Kazakhstan) – protocol No. IRB – A024 from September 22, 2017.

DNA preparation. Genomic DNA was isolated and purified from formalin-fixed paraffin-embedded tissues using the GeneJet Genomic DNA Purification Kit (Thermo Fisher Scientific, USA). Purified DNA samples were aliquoted and stored in a freezer at -20°C.

PCR and RFLP analysis. Specific primers (forward 5'-GATCTATTTTCCCTTCTC-3' and reverse 5'-AGCCCCTGTTTCATACTGAC-3') were designed using the PrimerQuest Tool. Each PCR reaction mixture contained forward and reverse primers (10 pmol each), 25 ng of genomic DNA, 10 µL of Mmix (2x, Thermo Fisher Scientific, USA) and nuclease-free water. PCR was performed in 0.2 mL microtubes on Mastercycler^R Nexus thermal cycler (Thermocycler EppendorfTM, USA). PCR conditions consisted of initial denaturation step at 95°C for 4 min, then 35 cycles of 94°C for 30 sec, 56°C for 30 sec, and 72°C for 45 sec, and final extension step at 72°C for 5 min.

The PCR products were analyzed using electrophoresis on 1% agarose gel. The correspondence of the obtained fragments was evaluated using the DNA Ladder Gene Ruler 100 bp marker (Thermo Fisher Scientific, USA). Restriction endonucleases were selected using WatCut online software for SNP-RFLP analysis. The PCR products were digested with restriction endonucleases SsiI and FokI. 5 µL of the PCR product and 10U of endonuclease were used in the reaction carried out at 37°C for 3 h. Restricted DNA was analyzed on 8% polyacrylamide gel. The polyacrylamide gel was stained with ethidium bromide. DNA Ladder Gene Ruler 100 bp (Thermo Fisher Scientific, USA) was used for detection of the restriction fragments length.

Tissue microarrays. Before creating a Tissue Microarrays (TMAs) slide, all tumor tissues were classified according to the international classification of stages of malignant neoplasms – TNM [11].

As a material for the creation of TMAs slides and immunohistochemical analysis, 44 histological materials obtained from patients with lung cancer fixed in formalin and embedded in paraffin blocks were used. Each selected area of lung tissue was analyzed by a qualified pathologist to determine histological types of tumors. From selected sites, selected tissue was carefully taken with a hollow cylinder (2 mm in diameter) and transferred into one common paraffin block. Then, a 3-4 micron thick section was cut from this block using a microtome (RM2255, Leica, Wetzlar, Germany) and placed on a glass slide [12] (Figure 1).

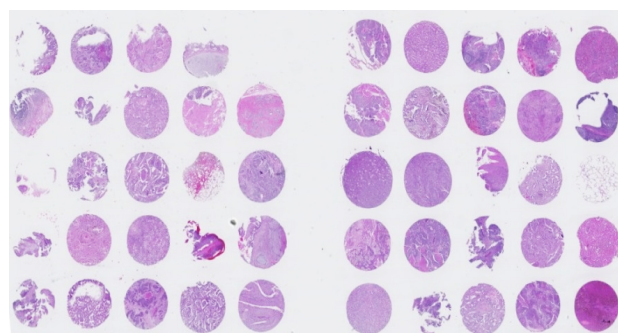


Figure 1 – Tissue Microarrays, slid with cores of 2 mm in diameter

Figure 1 shows the location of all TMAs samples on a glass slide. All 44 samples were divided into 5 rows of 9 samples (5th row – 8 samples).

Immunohistochemistry. Immunohistochemical staining was performed on slides using TMAs. For staining polyclonal antibodies CD117 (DAKO, Glos-

trup, Denmark) were used at dilution of 1:500. The preparations were analyzed using a NanoZoomer-XR C12000 digital slide scanner (Hamamatsu Photonics, Japan) with NDP.scan 2.5 software. The evaluation of immunohistological staining was distributed as follows: 0, no stained cells or weak staining intensity, with less than 10% of tumor cells; 1+, pale or weak color intensity, with more than 10% of tumor cells; 2+, moderate staining intensity; and 3+, strong, granular staining intensity; 2+ and 3+ were identified as positive, and 0 and 1+ as negative [13].

Results and discussion

The patients with lung cancer included in this study were treated at the Oncology center from Janu-

ary, 2013 to February, 2016. Questionnaires and voluntary informed consent were collected prior to the collection of the biomaterial. The main characteristics of the patients are shown in Table 1.

As can be seen from the Table 1, among 44 patients, 70.45% were men and 29.55% women, which corresponds to the data on more frequent cases of this type of cancer in men. Tumors were classified according to TNM criteria, and patients were divided by the following stages of cancer: stage I – 10 cases (22.73%), stage II – 15 cases (34.09%), stage III – 15 cases (34.09%), and stage IV – 4 cases (9.09%). According to the histological type, the distribution was as follows: squamous cell lung cancer – 63.6%, adenocarcinoma – 34.1%, small cell lung cancer – 2.3%.

Table 1 – The characteristics of the lung cancer case and control cohorts

Cohort (persons)	Years of birth (average age)	Sex, persons (%)		Ethnicity, persons (%)		Smoking habit, persons (%)		
		Males	Females	Asians (Kazakhs, Uigur, Koreans)	Russian	Smokers	Non-smokers	Ex-smokers
Case (44)	1937-1967 (62.6±7.7)	31 (70.45)	13 (29.55)	23 (52.27)	21 (47.73)	31 (70.45)	12 (27.27)	1 (2.27)
Control (50)	1934-1968 (61.7±9.2)	32 (64.00)	18 (36.00)	35 (70.00)	15 (30.00)	13 (26.00)	36 (72.00)	1 (2.0)
t_{st}	0.075	0.381	0.533	1.147	1.374	2.348	2.207	0.103
P	*0.952	0.768	0.688	0.456	0.400	0.256	0.271	0.935

Analysis of the restriction products for the presence of the Trp557Arg and Val559Asp mutations was analysed on 8% polyacrylamide gel. When analyzing restriction products for the presence of the Trp557Arg mutation, the normal allele in homozygous state has a single fragment of 258 bp in size. The mutant allele in homozygous state has two fragments 169 bp and 89 bp. Consequently, the heterozygous genotype has 3 fragments of 258 bp, 169 bp and 89 bp. RFLP analysis of 11 exon for the presence of Val559Asp mutation homozygous wild allele has one fragment of 258 bp, a homozygous mutant allele – two fragments of 150 and 108 bp, and the heterozygous allele – three fragments of 258 bp, 150 bp and 108 bp (Figure 2).

Figure 2 shows that sample number seven has three fragments measuring 258 bp, 169 bp and 89 bp, which indicates the heterozygosity of this gene for Trp557Arg mutations.

After RLFP analysis DNA samples were sent for sequencing analysis (9, 11 and 13 exons) to the National Cancer Institute, the National Institutes of Health in Bethesda, Maryland. The sequence analysis also did not reveal genetic abnormalities in the *C-KIT* gene, with the exception of the Trp557Arg mutation in sample number 7.

Figure 3 shows the level of expression of the *C-KIT* gene, which may be the cause of the development of cancer; immunohistochemical staining is applied.

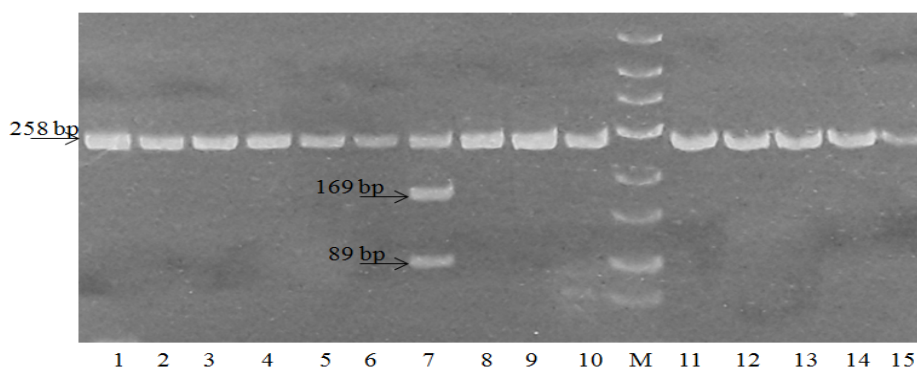


Figure 2 – The electropherogram of the restriction products of the *C-KIT* gene (11 exon, Trp557Arg and Val559Asp). Note: M – molecular weight marker 25bp; 1–6, 8–10 PCR products without mutations Trp557Arg; 7 – PCR products with mutation Trp557Arg; 11–15 PCR products without mutations Val559Asp

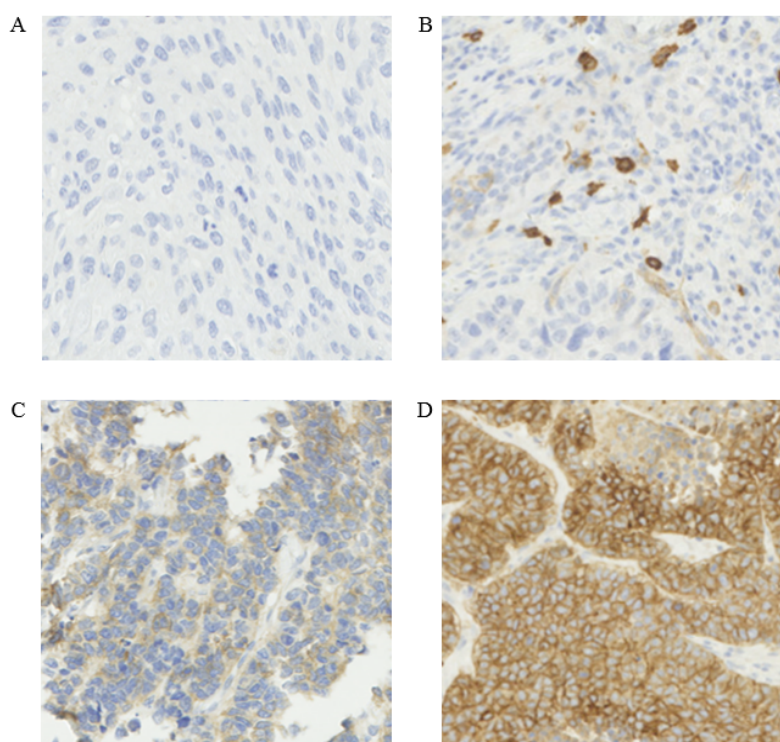


Figure 3 – Immunohistochemical analysis of histological material of lung cancer patients

Figure 3.A shows negative staining, indicating lack of expression; Figure 3.B – a sample of tissue with weak staining shows moderate expression; Figures 3. C and 3.D – the samples of tissue with moderate staining (2+) and strong staining (3+) show a high level of expression of the analyzed gene.

Table 2 shows the results of the immunohistochemical analysis. Immunohistochemical staining revealed 4 patients (9.09%) had overexpression of the *C-KIT* gene, 14 (31.82%) had moderate expression (more than 10%), 24 (54.54 %) showed weak expression of 1+ (less than 10%) and 2 patients (4.55%) did not have expression.

Table 2 – The results of the immunohistochemical analysis

Number of analyzed patients	The number of patients not having the C-KIT gene expression (0)	The number of patients with low expression of the C-KIT gene (1+)	The number of patients with moderate expression of the C-KIT gene (2+)	The number of patients with high expression of the C-KIT gene (3+)
44	2 (4.55 %)	24 (54.54%)	14 (31.82%)	4 (9.09%)

As can be seen from the Table 2, patients having a positive response to immunohistochemical analysis amounted to 40.91%, what could be the cause of the lung cancer. Accordingly, the cause of the lung cancer in these patients may be an increased expression of the *C-KIT* gene.

The *C-KIT* gene is an oncogene that regulates cell division and interacts with cell cycle factors. Solid tumors such as breast cancer, neuroblastoma, colon cancer, gynecological tumors, glioma, and SCLC reported to express *C-KIT* [14]. Autocrine or paracrine activation of the C-KIT receptor using GFR has been postulated for the treatment of lung cancer. The receptor can also be constitutionally activated independent of the ligand by specific mutations of the *C-KIT* gene. The receptor can also be constitutively activated independently on the ligand by specific mutations of the *C-KIT* gene. Expression of C-KIT protein was detected in 79-88% of SCLC cell lines, and during the inactivation of *C-KIT* the tyrosine kinase inhibitor imatinib had an inhibitory effect on SCLC cell growth [15].

Micke et al. showed that *C-KIT* expression is associated with reduced survival [16], however Blackhall et al. in their studies demonstrated *C-KIT* expression in 51% of tumors and concluded that *C-KIT* expression is not a predictor of survival [17]. Studies of the correlation between the level of C-KIT protein synthesis and the rate of the cancer development have led to the conflicting results. In some cases, the correlation was significant, while in other experiments it was absent [18; 19].

However, there is a little information on the mutations in the studied gene and protein expression in non-small cell lung cancer. Antonescu et al. revealed a Trp557Arg mutation in the gastrointestinal stromal tumor [20]. Like other *C-KIT* mutations occurring in exon 11, this mutation is thought to be associated with increased sensitivity to imatinib and other *C-KIT* inhibitors [21].

In our studies, a mutation in the *C-KIT* gene was detected in one patient with a diagnosis of adenocarcinoma and with a stage of the disease – T2aN-0M0G2R0. The results of immunohistochemical analysis showed that this patient has a moderate

level of expression of C-KIT protein (2+). However, despite the data obtained, our results showed that for non-small cell lung cancer, the expression of the *C-KIT* gene is not associated with mutations and are rare as in other researchers. Analysis of the expression level showed that 40.91% of patients had increased expression of the *C-KIT* gene, which is a high indicator for the development of cancer. Thus, the relationship between gene expression and mutations was not observed in our studies, as well as the relationship between expression and cancer stages in patients. *C-KIT* gene expression level may be due to gene amplification rather than mutations.

Conclusion

Our results show that the level of C-KIT gene expression is high for patients with lung cancer in Kazakhstan and is much more common than genetic disorders in this gene. Due to the high frequency of expression of this gene (40.91%), it is highly recommended for patients to undergo various forms of lung screening tests.

This will help to find the spectrum of causes of the disease and find the right treatment for the targeted therapy. There was not any relationship between disease stages and survival, despite the high level of *C-KIT* gene expression.

Acknowledgment

This work was supported by the grant AP05133577 “Radiogenic cancer damage of the population by radon isotopes and its modeling with rays of alpha particles in the biotests” received from the Committee of Science, Ministry of Education and Science of Republic of Kazakhstan for 2018-2020 yy.

References

1. Nurgaziev K.Sh., Seitkazina G.D., Baypeisov D.M., Seisenbaev G.T., Azhmagambetova A.E., Zhylkaidarova A.Zh. (2015) Indicators of oncology service in the Republic of Kazakhstan for 2015. KazIOR. 138 p.

2. Analytical material of the expanded board of the Ministry of Health of the Republic of Kazakhstan [Analiticheskij material rasshirenoj kollegii ministerstva zdavoohranenija Respubliki Kazahstan], 2017, Astana, 35 p.
3. Siegel R.L., Miller K.D., Jemal A. (2019) Cancer statistics, 2019. *CA Cancer J Clin.*, vol. 69, no. 1, pp. 7-34.
4. Tsang E.S., Shen Y., Chooback N., Ho C., Jones M., Renouf D.J., et al. (2019) Clinical outcomes after whole-genome sequencing in patients with metastatic non-small-cell lung cancer. *Cold Spring Harb Mol Case Stud.*, vol. 5, no. 1, pii: a002659.
5. Udagawa C., Horinouchi H., Shiraishi K., Kohno T., Okusaka T., Ueno H., Tamura K., Ohe Y., Zembutsu H. (2019) Whole genome sequencing to identify predictive markers for the risk of drug-induced interstitial lung disease. *PLoS One.*, vol.14, no. 10, e0223371.
6. Hung W.Y., Chang J.H., Cheng Y., Chen C.K., Chen J.Q., Hua K.T., Cheng C.W., Hsiao M., Chung C.L., Lee W.J., Chien M.H. (2018) Leukocyte cell-derived chemotaxin 2 retards non-small cell lung cancer progression through antagonizing MET and EGFR activities. *Cell Physiol Biochem.*, vol. 51, no. 1, pp. 337-355.
7. Yoshida R., Sasaki T., Umekage Y., Tanno S., Ono Y., Ogata M., Chiba S., Mizukami Y., Ohsaki Y. (2018) Highly sensitive detection of ALK resistance mutations in plasma using droplet digital PCR. *BMC Cancer*, vol. 18, no. 1, pp. 1136.
8. Colombino M., Paliogiannis P., Cossu A., Santeufemia D.A., et al. (2019) EGFR, KRAS, BRAF, ALK, and cMET genetic alterations in 1440 Sardinian patients with lung adenocarcinoma. *BMC Pulm Med.*, vol. 19, no. 1, p. 209.
9. Liu L., Wu J., Zhao W., Huang M.J. (2017) Atrial fibrillation was changed into sinus bradycardia in a ROS1-positive advanced lung adenocarcinoma patient who achieved durable response to Crizotinib: A case report and literature review. *Medicine (Baltimore)*, vol. 96, no. 21, e6979.
10. Hsu C.C., Liao B.C., Liao W.Y., Markovets A., Stetson D., Thress K., Chih-Hsin Yang J. (2019) Exon-16-skipping HER2 as a novel mechanism of osimertinib-resistance in EGFR L858R/T790M-positive non-small-cell lung cancer. *J Thorac Oncol.*, pii: S1556-0864(19)33307-6
11. Leslie H. S., Mary K.G., Christian W. (2011) TNM Classification of Malignant Tumours, 7th Ed. Wiley, pp. 336 ISBN: 978-1-444-35896-4
12. Fowler C.B., Man Y.G., Zhang S., O'Leary T.J., Mason J.T., Cunningham R.E. (2011) Tissue microarrays: construction and uses. *Methods Mol Biol.*, vol. 724, pp. 23-35.
13. Boldrini L., Ursino S., Gisfredi S., Faviana P., Donati V., Camcci T., Lucchi M., Mussi A., Basolo F., et al. (2004) Expression and mutational status of C-KIT in small-cell lung cancer: prognostic relevance. *Clin Cancer Res.*, vol. 15, pp. 4101-4108.
14. Pittoni P., Piconese S., Tripodo C., Colombo M.P. (2011) Tumor-intrinsic and -extrinsic roles of c-Kit: mast cells as the primary off-target of tyrosine kinase inhibitors. *Oncogene*, vol. 30, pp. 757-769.
15. Cheng Y., Li H., Ma L., Zhang S., et al. (2014) Detection of c-kit mutational status in small-cell lung cancer in a Chinese cohort. *Thorac Cancer.*, vol. 5, no. 3, pp. 225-231.
16. Micke P., Basrai M., Faldum A., Bittinger F., Rönstrand L., Blaukat A., Beeh K.M., Oesch F., Fischer B., Buhl R., Hengstler J.G. (2003) Characterization of c-kit expression in small cell lung cancer: prognostic and therapeutic implications. *Clin Cancer Res.*, vol. 9, no. 1, pp. 188-194.
17. Blackhall F.H., Pintilie M., Michael M., et al. (2003) Expression and prognostic significance of kit, protein kinase B, and mitogen-activated protein kinase in patients with small cell lung cancer. *Clin Cancer Res.*, vol. 9, pp. 2241-2247.
18. Krystal G.W., Honsawek S., Kiewlich D., Liang C., Vasile S., Sun L., McMahon G., Lipson K.E. (2001) Indolinone tyrosine kinase inhibitors block KIT activation and growth of small cell lung cancer cells. *Cancer Res.*, vol. 61, pp. 3660-3668.
19. Spigel D.R., Hainsworth J.D., Simons L., et al. (2007) Irinotecan, carboplatin, and imatinib in untreated extensive-stage small-cell lung cancer: a phase II trial of the Minnie Pearl Cancer Research Network. *Thorac Oncol.*, vol. 2, pp. 854-861.
20. Antonescu C.R., Sommer G., Sarran L., et al. (2003) Association of KIT exon 9 mutation with nongastric primary site and aggressive behavior: KIT mutation analysis and clinical correlates of 120 gastrointestinal stromal tumors. *Clin Cancer Res.*, vol. 9, pp. 3329-3337.
21. Yu T.M., Morrison C., Gold E.J., Tradonsky A., Layton A.J. (2019) Multiple biomarker testing tissue consumption and completion rates with single-gene tests and investigational use of oncomine dx target test for advanced non-small-cell lung cancer: a single-center analysis. *Clinical Lung Cancer*, vol. 20, no. 1, pp. 20-29.

¹N. Ghasempour , ¹A.H. Elhami Rad , ^{2*}M. Javanmard,
³E. Azarpazhouh , ¹M.Armin 

¹Department of Food Science and Technology, Islamic Azad University, Sabzevar, Iran

²Food technologies group, Chemical Engineering Institute,

Iranian Research Organization for Science and Technology (IROST), Tehran, Iran

³Agricultural Engineering Research Department, Khorasan Razavi Agricultural and
Natural Resources Research and Education Center, AREEO, Mashhad, Iran

*e-mail: javanmard@irost.ir

Optimization of conditions of ultrasound-assisted extraction of phenolic compounds from orange pomace (*Citrus sinensis*)

Abstract: Every year millions of tons of fruit peels, such as that from apples, oranges and pomegranates are disposed of as juice factory wastes in our country as well as globally. As we know today special attention is given to the optimum use of plant wastes and extraction of bioactive compounds, namely, antioxidants and antimicrobials. Unfortunately, Iran with a 15.2-30% green waste production, currently holds the first place in the world fruit waste production. The current study was carried out with the goal of optimizing the ultrasound-assisted extraction of antioxidant compounds from orange pomace. In this optimization by use of the response surface method, a Box-Behnken design was evaluated for three variables consisting of ultrasonication amplitude (20, 60 and 100%), ultrasonication time (15, 35 and 55 min) and ultrasonication temperature (35, 50 and 65°C). The results showed if the extraction time, extraction temperature and ultrasonication Amplitude were to be set at 26.43 min, 35°C and 65.66%, respectively, the highest antimicrobial antioxidant compound extraction efficiency would be reached. Under such conditions, phenolic compounds amount of 91.96 mg of gallic acid, free radical inhibition of 57.89% and extraction efficiency of 10.62% were attained. The results demonstrated that ultrasonication could be a very effective method for continuous extraction of antioxidant compounds from fruit waste.

Key words: antioxidant, Box-Behnken design, orange pomace extract, total phenolic compound, ultrasound.

Introduction

Every year millions of tons of fruit peels, such as that from apples, oranges and pomegranates are disposed of as juice factory wastes in our country as well as globally. As we know it today special attention is given to the optimum use of plant wastes and extraction of biologically active compounds, namely, antioxidants and antimicrobials [1]. Unfortunately, Iran with a 15.2-30% green waste production, currently holds the first place in the world fruit waste production. On the one hand, wastes lead to loss of national resources, on the other hand, the disposal of which causes some difficulties. For example, wastes rich in phenolic compounds, which are usually buried in the ground, in addition to being expensive, cause environmental problems [2].

From another point of view, the pursuit of finding replacements for synthetic antioxidants has led to examination of numerous antioxidants from plant sources. Examinations have shown that antioxidant activity of some fruits and vegetables is dependent on the total amounts of phenolic compounds in them. Taking the fact that plants are natural sources of antioxidants, research in this field is increasing. Citrus fruits possess considerable antioxidant activity, containing large numbers of flavonoids. Recent research has been to explore ways of natural development of these compounds; it has been established that the antioxidant amount varies in different numbers and structures.

Choice of the extraction method is one of the main factors, which can affect the properties of the effective constituents of extracts [3]. Usually, extraction by conventional methods requires a long pe-

riod of time, high temperature and solvent amount. Thermal extraction causes antioxidant degradation and reduces the antioxidant activity of the produced extract. There are different extraction methods from plants and fruits [1; 3; 4]. The use of novel and practical methods, such as the ultrasound process for extraction of higher quality, more stable, soluble in water and remaining safe extracts along with reduced related expenses (high efficiency and low energy and water consumption), seems important [5-7]. Ultrasound-assisted extraction, can lead to higher extraction of effective constituents from orange pomace. More than 88 000 000 tons of various citrus fruits are produced worldwide each year, of which wastes account for about 15 000 000 tons. Citrus wastes usually consist of water, soluble sugars, fiber, organic acids, amino acids, protein and minerals of different amounts. Considering the vast amounts of protein and fibers present in citrus wastes they can be used as a high-energy source in livestock diet.

In recent years, various researches have been carried out in the field of application of ultrasound waves in processing of food materials. For instance, Sharayei *et al.* performed a study with the purpose of optimum use of pomegranate peel as the residue of agriculture and pomegranate juice factories, and extraction of biologically active compounds (antioxidant and antimicrobial), employing the ultrasound-assisted method. Results showed that all aqueous extracts of pomegranate and peel, possessed the antioxidant activity and antioxidant potency of 6% aqueous extract of pomegranate peel, was roughly the same as that of synthetic butylated hydroxytoluene antioxidants [8]. A study was carried out on the effects of high-powered ultrasound waves on ground olive grains. It was determined that in the presence of these waves, cell walls and plant tissues are disrupted and more antioxidant compounds (polyphenols and tocopherols) and pigments (chlorophyll and carotenoid) found a way into the oil and led to an increase in nutrition rating [9]. Rosangela *et al.* examined the chemical composition of yerba mate tea (*Ilex paraguariensis* leaves) using the ultrasound-assisted method. The use of ultrasound waves led to improved caffeine and palmitic acid amounts efficiencies in methanol solvent [12]. In this study, optimization of ultrasound-assisted extraction of phenolic compounds from orange pomace, and later comparison between the two methods, *i.e.*, maceration and ultrasonication are under the scope.

Materials and methods

Plant materials. Orange wastes were purchased from Iran Citrus Co. (Tonekabon, Mazandaran Province) in August, 2016. The wastes, after drying at room temperature and away from sunlight, were completely dried and grounded using an electric grinder and passed through a mesh strainer No. 20 and kept at a dark, cold and dry place.

Chemicals and reagents. All chemicals and reagents used in this study, were analytical grade, including Folin-Ciocalteu reagent (FC), gallic acid, DPPH (2,2-diphenyl-1-picrylhydrazyl) reagent obtained from Sigma-Aldrich Corp. (St. Louis, MO), chemical and organic solvents purchased from Merck KGaA (Darmstadt, Germany).

Extraction procedures. In order to produce extracts from orange wastes, the maceration and ultrasound-assisted methods were used. The solvent used in both methods was 70% ethanol.

Maceration extraction method. For this purpose, 100 g of powdered orange pomace was carefully weighed and poured into a 1000 mL beaker containing 70% ethanol solvent and stirred for 24 h at room temperature. The solution was then filtered under vacuum and concentrated up to the point of full dewatering using a rotary dryer (Laborota 4000, Germany) at 45°C in an oven until reaching constant weight under vacuum.

Ultrasound-assisted extraction method. For this purpose, a 100 g of powdered orange pomace was carefully weighed and poured into a 1000 mL beaker containing 70% ethanol solvent and moved to the special ultrasonication chamber. For ultrasonication, the ultrasonic device model (UP400S, Heilscher, Germany) with 400 W power and H7 type probe made from titanium; diameter – 7 mm, length – 100 mm was used. For extraction, parameters of ultrasonication changed as follows: time – 15, 35 and 55 min, amplitude – 20, 60 and 100%, temperature – 35, 50 and 65°C; with the sound frequency of 24 kHz based on the variables surfaces predicted in the Box-Behnken design, according to Table 1, were selected.

Statistical analysis. In order to study the effect of time, temperature and amplitude of the process on optimization of extraction conditions of phenolics, tests were performed based on an RSM design in 3 factors and 3 design surfaces and a Box-Behnken design. The software in use was Design Expert and graphs were drawn by Microsoft Excel. The coded and actual levels of each of the variables are given in Table 2.

Table 1 – Random treatments of the Box-Behnken design experimentation

Treatment	Time (min) (A)	Temperature (°C) (B)	Amplitude (%) (C)
1	55	35	60
2	55	65	60
3	35	65	20
4	15	65	60
5	35	65	100
6	15	50	20
7	55	50	100
8	15	35	60
9	35	50	60
10	55	50	20
11	35	35	100
12	35	35	20
13	15	50	100
14	35	50	60
15	35	50	60

Table 2 – Valuable codes, independence variables and actual value used in ultrasound method

Independence variables	Valuable codes	Actual value
Time	-1, 0, +1	15, 35, 55
Temperature	-1, 0, +1	35, 50, 65
Amplitude	-1, 0, +1	20, 60, 100

Measurement of TPC. The total phenolic content (TPC) in the extract produced from the two extraction methods, maceration and ultrasonication, was determined with Folin-Ciocalteu [11]. For that 500 µL of the extract solution were poured into a test tube and then 500 µL of the diluted Folin-Ciocalteu solution with a 1:10 ration and 6 c.c. of distilled water were added to the solution. 8 minutes later, 1.5 mL of 20% sodium carbonate were added and adequately stirred. The compound within the test tube was incubated for 30 min at room temperature and the absorbency read at 765 nm on the spectrophotometer with the following formula (Eq.1).

$$P = \frac{Y}{W} * 1000,$$

where

P – TPC (mg gallic acid per g)

Y – TPC (mg gallic acid per mL)

W – sample weight (g)

The total phenolic content from the drawn linear equation based on gallic acid (0, 30, 70, 110, 150,

190 and 200 ppm in 70% ethanol), was expressed as mg of gallic acid per g of dried extract.

Estimation of antioxidant capacity. Estimation of the free radical-scavenging activity was performed through the use of the DPPH test and 2,2-diphenyl picrylhydrazyl reagent [12]. The DPPH reagent was obtained by adding 0.009 g of 2,2-diphenyl picrylhydrazyl reagent to 75 mL of methanol. A ml of the aforementioned solution was added to the 500 µL sample and then 3.5 mL of methanol was added to it. Then stirring was carried out for 30 s. The solution produced was incubated at room temperature for 90 min and the absorbency of the sample reported at 512 nanometers on the spectrophotometer device in the following formula (Eq.2).

$$\text{DPPH (\%)} = \frac{A_{\text{count}} - A_{\text{sample}}}{A_{\text{count}}} * 100,$$

where

A_{count} – Absorbance of control

A_{sample} – Absorbance of sample

Extraction yield. The extraction efficiency is given by the following formula (Eq. 3):

$$EY = \frac{\text{Dried extraction weight}}{\text{initial sample weight}} * 100$$

Results and discussion

Model fitting. After data analysis with the goal of finding the best-suggested model from the five existing: mean, cubic, 2FI, linear, variance analysis, for which the sum of squares had significant differences, and the lack of fit was insignificant, the best model was selected. Given this subject and after examining the results obtained and a comparison between the existing regression models, the results indicated that the Quadratic model for TPC, DPPH free radical-scavenging capacity and measured extraction efficiency tests in this study, had a significant difference compared to the other models. There models for which the Lack of

fit was undefined (Table 3). Consequently, the Quadratic model was selected for examining the trend of variations of the parameters measured in this study. After selecting the best model in the desired statistical surface (1% or 5%), in order to examine the effective parameters in the study, with regard to the variance table, the parameter for which the F test insignificant ($P > 0.05$), is eliminated and the rest of parameters which had significant differences were kept.

It is worth mentioning that in the case that the linear parameter of a variable in a model, does not have a significant effect, yet its mutual effect with one of the other variables, which has a significant effect in the model, does have a significant effect, then that parameter is kept in the model and afterward the general equation is derived for any parameter, by the given coefficients. Ultimately, from amongst the different parameters, the parameter which has the highest sum of squares is selected as the most effective parameter.

Table 3 – Analysis of variance of the regression coefficients of the obtained models over the response variables (quantitative and qualitative properties) of orange pomace extract

Source	df	EY (%)		TPC (mg GA/100 g)		DPPH (%)	
		Coefficient	Sum of Squares	Coefficient	Sum of Squares	Coefficient	Sum of Squares
Model	9	3.56*	48.97	-183.29*	9911.71	36.93**	1732.43
Linear							
Time (A)	1	0.09*	7.26	0.025*	3257.05	-0.097 ^{ns}	0.0015
Temperature (B)	1	0.01 ^{ns}	0.80	7.87 ^{ns}	904.83	0.366*	208.28
Amplitude (C)	1	0.19*	12.70	3.28*	1371.83	0.774**	633.86
Quadratic							
A*A	1	^{ns} -0.0029	5.14	-0.0084 ^{ns}	41.87	-0.019*	228.91
B*B	1	-0.0004 ^{ns}	0.044	-0.064 ^{ns}	780.33	-0.0087 ^{ns}	14.42
C*C	1	-0.0013**	18.12	-0.016*	2639.61	-0.0021 ^{ns}	44.04
Interaction							
A*B	1	0.002 ^{ns}	2.82	-0.018 ^{ns}	121.88	0.029**	320.77
A*C	1	0.00036 ^{ns}	0.34	0.0079 ^{ns}	160.53	-0.0002 ^{ns}	0.198
B*C	1	-0.0014 ^{ns}	3.06	-0.024 ^{ns}	876.75	-0.014**	305.20
Residuals	5		4.84		195.15		82.71
Lack of Fit	3		0.95		128.66		14.76
Pure Error	2		3.88		66.49		67.95
Total	14		53.80		12077.7		1815.14
Std. Dev		0.98		15.04		4.07	
Mean		8.93		63.37		45.36	
CV (%)		11.02		23.73		8.97	
R ²		0.91		0.89		0.95	
Adj R ²		0.74		0.71		0.87	

Note: ^{ns} – no significant effect at level >0.1; Std. Dev (standard deviation) – *P<0.05; **P<0.01; ***P<0.001

Investigating the effect of independent variables on qualitative and quantitative properties of orange pomace: effects of process variables on TPC extraction. The results from the variance analysis of the extract, extracted from orange pomace, quantitative and qualitative – experimental and predicted properties produced from the central combined design in the orange pomace extract production process, are given in Table 4.

With regard to Equation. 4 and Table 3, the parameters A and C² were selected as the most effective factors in the extraction of phenolic compounds, using Eq.4.

$$\text{TPC} = -183.29 + 0.025A + 7.87B + 3.28C - 0.018AB + 0.0079AC - 0.024BC - 0.0084A^2 - 0.064B^2 - 0.016C^2$$

In the RSM methodology, there is a step called Verification. In this step, the value for total phenolic compounds extraction in the extermination step

should be statistically compared to the value predicted by the model. In this examination, after having carried out this step, the observed values were compared to the predicted values and the calculations may be seen in Table 4; the results are demonstrative of the good correlation between results obtained from the experimental method and the values predicted with the statistical method.

The significance of the quadratic temperature term shows that the rising trend of the amount of phenolics extraction continues until around 49 °C and declines with further increase in temperature (Figure 1-A). This phenomenon which has been reported in various studies is probably due to the destruction and oxidization of some of the heat-sensitive polyphenols at higher temperatures [13; 14]. Additionally, the rise of temperature also expands the level of phenolic compounds extraction and because of the increase in solubility of phenolics, the rate of mass and heat transfer occurs faster [15].

Table 4 – Dependent and independent variables

Time (min)	Temp. (°C)	Amplitude (%)	EY (%)		TPC (mg GA/100 gr)		DPPH (%)	
			Real Values	Predicted Values	Real Values	Predicted Values	Real Values	Predicted Values
55	35	60	10.14	9.94	60	65.25	38.03	38.77
55	65	60	11.4	10.99	26.49	32.94	44.81	46.48
35	65	20	10.3	10.29	30.08	36.98	59.6	59.56
15	65	60	7.2	7.40	89.59	84.34	29.28	28.54
35	65	100	5.8	6.02	41.66	33.56	25.18	24.29
15	50	20	8.2	8.01	72.14	70.49	49.02	49.80
55	50	100	7.2	7.39	54.68	56.33	32.8	32.02
15	35	60	9.3	9.72	101.02	94.57	58.32	56.65
35	50	60	9.65	10.80	71.15	87.18	46.51	52.46
55	50	20	8.9	9.32	30.82	17.47	51.9	50.27
35	35	100	8.4	8.41	91.34	84.44	51.93	51.97
35	35	20	9.4	9.18	20.54	28.64	51.41	52.30
15	50	100	5.32	4.90	70.66	84.01	30.81	32.44
35	50	60	12.35	10.80	98.25	87.18	52.71	52.46
35	50	60	10.4	10.80	92.14	87.18	58.16	52.46

Results acquired from the Ahmadian and Niazmand study illustrate the specific effect of the mean temperature (43 °C) on the extraction of polyphenolic compounds from the saffron petal [16]. The effect of temperature on increasing extraction efficiency is

most probably due to the improvement of mass transfer at a higher temperature and therefore increasing the solubility of phenolic compounds, increasing the penetration rate and decreasing the coefficient of viscosity, of the solvent. In addition, the rise in extrac-

tion temperature, bringing about the dissociation of the bonds of the phenolic compounds with the rest of the compounds and affecting the membrane structure of plant cells can be responsible for extraction procedure facilitation.

As apparent from Figure 1-B, by increasing the time from 15 to 25 min, the extraction efficiency amount increases. The underlying reason for these results may be explained in such a way that a prolonged contact time (the extraction time) leads to oxidization of phenolic compounds due to light or oxygen expression [17].

According to the investigation carried out in the research on ultrasound-assisted extraction of phenolic compounds from wheat bran, the extraction amount of these compounds markedly increased from 15 to 30 min but then roughly decreased from 30 to 50 min [11].

With regard to Figure 1-C by raising the device power up to 60%, the amount of polyphenolics ex-

traction efficiency increases and until 80% a marginally rising trend was observed and declined thereafter. Ultrasonic waves generate numerous physical and chemical reactions, by means of creation and growth of bubbles in the environment and their implosion under mechanical forces. When ultrasonic waves pass through a liquid, given a high enough ultrasonic natural Amplitude, as a result of the negative applied pressure, small bubbles are made and periodic pressures and turbulences are formed. The bubbles implode with differing intensities and give rise to physical and chemical changes, this phenomenon is called cavitation [18]. The principal mechanism of ultrasound-assisted extraction is due to the cavitation phenomenon which leads to the generation of micro bubbles and subsequently an implosion within the liquid mass. The implosion of these bubbles is often accompanied by release vast amounts of energy which is exerted on the nearby environment in the form of shear stress [19].

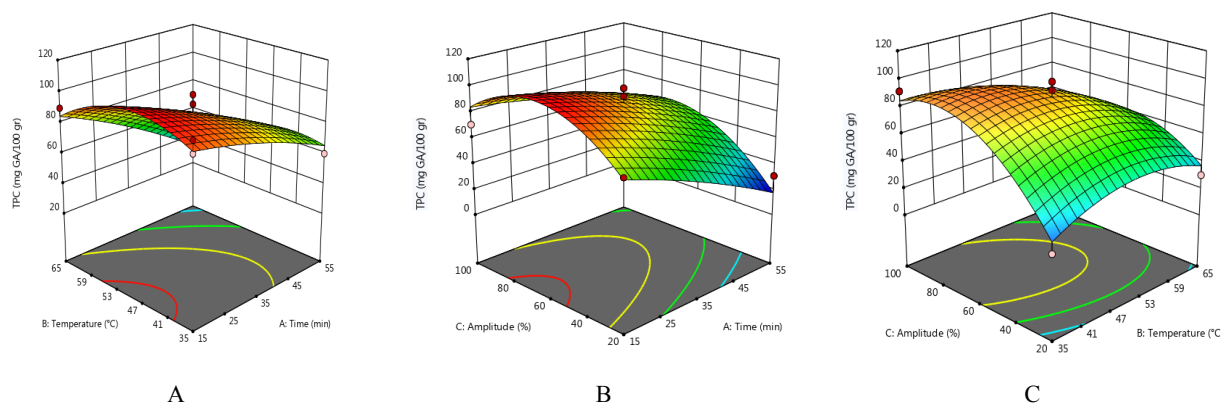


Figure 1 – The effect of extraction conditions on the amount of extracted polyphenol extract from orange pomace.
Note: A – time and temperature effects, B – time and amplitude effects, C – temperature and amplitude

Effects of process variables on antioxidant activity. Investigation of the DPPH free radical inhibition activity is one of the techniques of determining antioxidant activity. In this method, the purple color of the DPPH free radicals is neutralized and made colorless under the influence of the existent antioxidants in the extract. Thus, the degree of colorlessness of this compound is descriptive of the free radical inhibition capacity of the existent antioxidants. The results from the variance analysis demonstrate the significance of temperature, amplitude, quadratic of time and also the interaction terms of temperature and ultrasonication Amplitude and the temperature and time interaction. With regard to Eq.

5, the Amplitude was reported as to possessing the most effective parameter upon the scavenging of free radicals.

$$\text{DPPH} = 36.93 - 0.097A + 0.366B + 0.774C + 0.029AB - 0.002AC - 0.014BC - 0.019A^2 - 0.0087B^2 - 0.0021C^2$$

According to the response surface diagram in Figure 2-A, by increasing the time up to 40 minutes, an increase in inhibition percentage was observed. Heidari *et al.* investigated the antioxidant properties of *Flomidoschema parviflora* [20]. These researchers reported that by means of increasing the time, the

free-radical scavenging has risen which is because of the growth of phenolic compounds extraction with the increase in time and their inhibition effect on the free radicals. Yet, with increasing time (times greater than 46 min) this trend has become very gradual and the free-radical scavenging amount declines, with which study, the results from the relation by increasing time to 36 min, agree.

Taking into consideration the response surface diagram related to the inhibition percentage, which is represented in Figure 2-B, the extraction temperature parameter has caused a rise in the capacity with a further increase in temperature. In the research on grape peels conducted by Ghafoor in order to optimize the conditions of ultrasound-assisted extraction, by means of the two extraction temperature and ultrasonication amplitude parameters, it was determined that with rises in the extraction temperature and ultrasonication amplitude the free-radical scavenging capacity increases [21].

According to Figure 2-C related to the free-radical inhibition effect, the amplitude parameter, originally increased the capacity of up to 80%, and then led to its decrease. The reason behind the aforementioned results can be described as the rise in amplitude, by means of cavitation, brings about the breakage of the plant cell membrane and further solvent penetration into the inside of the plant cell, as well as improving the mass transfer and the contact surface between the solid and liquid phases, through membrane decomposition and its release and fast spread into the liquid phase. In the research carried out by Ahmadian and Niazmand, the results showed that with an increase in the amplitude, the free-radical scavenging amount has grown, in such a way that at 100% of amplitude, the highest inhibition percentage was observed [16]. In fact, this is a result of the higher polyphenolic compounds extraction at this amplitude and therefore increasing cell wall destruction and expanded exit and access of such materials.

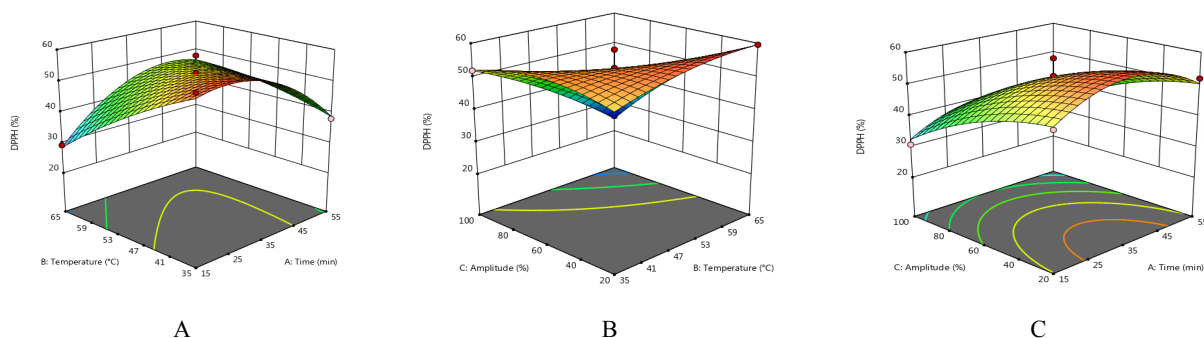


Figure 2 – The effects of the extraction conditions on the free-radical scavenging percentage of the extracted orange pomace extract. Note: A – the effects of temperature and time. B – the effects of temperature and amplitude. C – the effect of time and amplitude

Effects of process variables on extraction yield.

Examination of the variance analysis table (Table 3) and Eq. 6 shows that the time, amplitude and quadratic of amplitude have the stronger effect on the amount of extraction efficiency.

$$\text{YELD} = 3.56 + 0.09A + 0.01B + 0.19C + 0.002AB + 0.00036AC - 0.0014BC - 0.0029A^2 - 0.00048B^2 - 0.0013C^2$$

With regard to the extraction efficiency response surface diagram displayed in Figure 3-A, with an increase in time up to 46 min, growth in the efficiency amount was observed. Time increases the mass

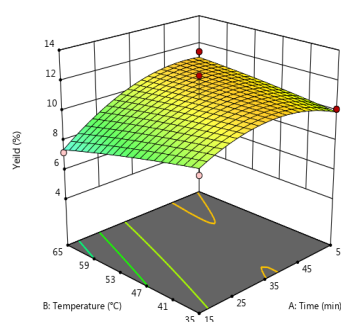
transfer period. The drop in the effective constituent extraction amount with an increase in time from 43 to 55 min is probably caused by the destruction of some active natural compounds. One can describe that the longer time period, having brought about the enhanced cell wall disruption, leads to the extraction of insoluble compounds within the solvent, which results in the lower solvent penetration of cells [22; 23].

Furthermore, bearing in mind the significance of the temperature parameter, it is validated that with an increase in the extraction temperature, the extraction efficiency amount is expanded. Temperature is one of the key factors in the extraction efficiency

amount, in a way that the rise in temperature has caused an increase in the solvent penetration rate (Figure 3-B).

According to the response surface diagram, with an increase in the device output up to 76%, an enhancement in extraction efficiency amount was observed (Figure 3-C). The extraction amount growth by an increase in Amplitude is probably because of

the cavitation phenomenon resultant of the ultrasonication; the cavitation phenomenon leads to increased plant tissue [24]. The decline in the effective constituents' extraction amount, caused by increasing the ultrasonication amplitude from 80% to 100%, is probably a result of the destruction of some active natural compounds because of the high amplitude of the waves [24].



A

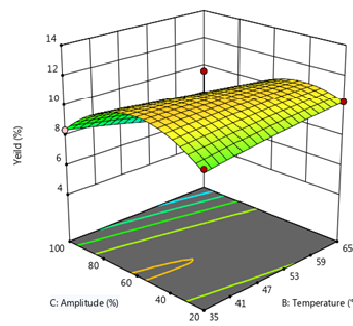


Figure 3-B

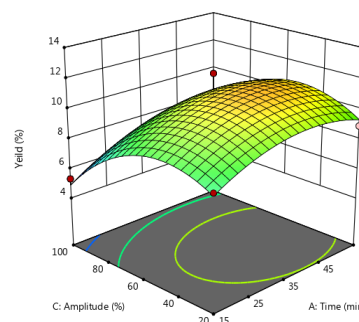


Figure 3-C

Figure 3 – The effects of the extraction conditions on the extraction yield of the extracted orange pomace extract.

Note: A – the effects of temperature and time; B – the effects of temperature and amplitude; C – the effect of time and amplitude

Optimization comparison ultrasound-assisted extraction with conventional extraction. The measurement of total phenolic compounds, free-radical scavenging, and extraction efficiency amount through maceration and ultrasonication methods demonstrated the method of extraction has a profound effect on the total amount of phenolic compounds in terms of gallic acid. As apparent, the ultrasonication method has extracted more phenolic compounds compared to the maceration method (for the ultrasonication method, the phenolic compounds amount in terms of gallic acid was obtained as 91.96 mg, the free-radical scavenging amount as 57.89% and the extraction efficiency as 10.62% and for the maceration method the phenolic compounds amount was obtained as 11.10 mg of gallic acid, the free-radical scavenging as 2.79% and the extraction efficiency as 4.46% per 5 g of the initial powder). It can be said the shear stress exerted by ultrasonic waves lead to the breakdown of large polymer molecules, which in turn results in the better extraction of phenolic compounds compared to the maceration method. These results are in accordance with the report by Albu *et al.*, who reported that utilization of the ultrasonication method led to additional extraction of carnosic acid from rosemary [26].

Findings related to the corrosion activity of free radicals in the different extraction methods, i.e. ultrasonication and maceration, is indicative of the notable difference between methods [20]. The extract produced from the ultrasonication method possesses obtains higher free-radical corrosive activity than that of the maceration method and one can state that the enhanced phenolic compounds extraction in the ultrasonication method, in comparison to the maceration method, has led to the increased antioxidantal activity in the ultrasonication method.

Conclusion

Orange pomace has agreeable antioxidant activity due to high amounts of polyphenolic compounds. With regard to the rich vegetation of the country in terms of the area under cultivation and production of orange fruits, considering its nutritional and pharmaceutical rating, it is possible to have it introduced as a natural antioxidant source within the food industry. Analysis of the Box-Behnken design response surface with three independent variables consisting of time, temperature and device ultrasonication amplitude serving as effective parameters on the extraction of antimicrobial compounds from orange

pomace was carried out. The finding signaled that the response surface methodology can be used satisfactorily in the evaluation of the efficiency of the extraction procedure employed. All three ultrasonication extraction parameters: temperature, time and amplitude led to the increased antioxidant activity. Suggested models have high R^2 and R^2 (adj.) values with insignificant lack of fit value and low coefficient of variations showing their suitability in predicting the evaluated parameters. On the one hand, by utilizing the models, adjustment of the extraction conditions is made possible, and on the other, considering the utilized extraction conditions, predict and rectify the desired properties.

Acknowledgment

Financial support was provided by the Agricultural Engineering Research Department, Khorasan Razavi Agricultural and Natural Research and Education, AREEO Mashhad, Iran.

References

1. Sagdic O., Ozturk I., Kisi O. (2012) Expert systems with applications. Modeling antimicrobial effect of different grape pomace and extracts on *S. aureus* and *E. coli* in vegetable soup using artificial neural network and fuzzy logic system. no. 39, pp. 6792-6798.
2. Martin J., Porto E., Correa C., Alencar M., Gloria E., Cabral I., Aquino L. (2012) Antimicrobial potential and chemical composition of agro-industrial wastes. *J Nat Prod.*, no. 5, pp. 27-36.
3. Adamez J., Samino E.G., Sanchez E.V., Gomez D.G. (2012) In vitro estimation of the antibacterial activity and antioxidant capacity of aqueous extracts from grape-seeds (*Vitis vinifera* L.). *Food Control*, no. 24, pp. 136-141.
4. Liu S., Yang F., Zhang C., Ji H., Hong P., Deng C. (2009) Optimization of process parameters for supercritical carbon dioxide extraction of *Passiflora* seed oil by response surface methodology. *J Supercrit Fluid.*, no. 48, pp. 9-14.
5. Corrales M., Garcia A., Butz P., Tauscher B. (2009) Extraction of anthocyanins from grape skins assisted by high hydrostatic pressure. *J Food Eng.*, no. 90, pp. 415-421.
6. Pompeu D., Silva E., Rogez H. (2009) Optimization of the solvent extraction of phenolic antioxidants from fruits of *Euterpe oleracea* using response surface methodology. *Biores Technol.*, no. 100, pp. 6076-6082.
7. Wijngaard H., Hossain M.B, Rai D.K., Brunton N. (2012) Techniques to extract bioactive compounds from food by-products of plant origin. *Food Res Int.*, no. 46, pp. 505-513.
8. Sharayei P., Azarpazhouh A. Investigating the effect of ultrasound on antioxidant and antifungal properties of pomegranate peel. Agricultural and Natural Resources Research and Education Center, AREEO, Mashhad, Iran. 2017.
9. Jimenez A., Beltran G. (2007) Ultrasonics sonochemistry. High-power ultrasound in olive paste pretreatment. Effect on process yield and virgin olive oil characteristics. vol. 6, no. 14, pp. 725-731.
10. Porto C.D., Porretto E., Decorti D. (2013). Comparison of ultrasound-assisted extraction with conventional extraction methods of oil and polyphenols from grape (*Vitis vinifera* L.) seeds. *Ultrasonics Sonochem.*, no. 20, pp. 1076-1080.
11. Wang J., Sun B., Cao Y., Tian Y., Li X. (2008) Optimization of ultrasound-assisted extraction of phenolic compounds from wheat bran. *Food Chem.*, vol. 2, no. 106, 804-810.
12. Von Gadow A., Joubert E., Hansmann C.F. (1997) Comparison of the antioxidant activity of aspalathin with that of other plant phenols of rooibos tea (*Aspalathus linearis*), α -tocopherol, BHT, and BHA. *J Agric Food Chem.*, vol. 3, no. 45, 632-638.
13. Silva E., Rogez H., Larondelle Y. (2007) Optimization of extraction of phenolics from *Inga edulis* leaves using response surface methodology. *Sep Purif Technol.*, vol. 3, no. 55, pp. 381-387.
14. Wissam Z., Ghada B., Wassim A., Warid K. (2012) Effective extraction of polyphenols and proanthocyanidins from pomegranate's peel. *Int J Pharm Sci.*, vol. 3, no. 4, pp. 675-682.
15. Negro C., Tommasi L., Miceli A. (2003) Phenolic compounds and antioxidant activity from red grape marce extracts. *Bioresource Technol.*, no. 87, pp. 41-44.
16. Ahmadian Koochaksarayee Z., Niazmand R. (2016) Optimization of extraction of effective compounds from saffron petals by ultrasound-assay method. *Novel Food Tech.*, no. 13, pp. 121-135.
17. Chan S., Lee C., Yap C., Mustapha W.A.W., Ho C. (2009) Optimization of extraction conditions for phenolic compounds from limau purut (*Citrus hystrix*) peels. *Int Food Res. J.*, vol.2, no. 16, pp. 203-213.
18. Chemat F., Zill-e-Huma, and Khan M.K. (2011) Applications of ultrasound in food technology: processing, preservation and extraction. *Ultrason Sonochem.*, vol. 4, no. 18, pp. 813-835.

19. Ji J., Lu X., Cai M., Xu Z. (2006) Ultrasonics sonochemistry. Improvement of leaching process of *Geniposide* with ultrasound. vol. 5, no. 13, pp. 455-462.
20. Heydari Majd M., Mortazavi A., Asili J., Boulourian Sh. (2012) Herbal medicine. optimization of extraction of phenolic compounds from *Flomidoschema parviflora* by ultrasound-assay method, no 1, pp. 7-13.
21. Ghafoor K., Choi Y., Yeong Jeon, Ju and Hee Jo (2009) Optimization of ultrasound-assisted extraction of phenolic compounds, antioxidants, and anthocyanins from grape (*Vitis vinifera*) seeds. *Agric Food Chem.*, vol. 11, no. 57, pp. 4988-4994.
22. Rosangela J., Lisiane F., Valeria P., Claudio D., Ana Paula O., Jose O. (2007) Ultrasonics sonochemistry. The use of ultrasound in the extraction of *Ilex paraguariensis* leaves: a comparison with maceration. no. 14, pp. 6-12.
23. Tian Y., Xu Z., Zheng B., and Lo Y.M. (2013) Optimization of ultrasonic-assisted extraction of pomegranate (*Punica granatum* L.) seed oil. *Ultrasonics Sonochem.*, no. 20, pp. 202-208.
24. Vilku K., Mawson R., Simons L., Bates D. (2008) Applications and opportunities for ultrasound assisted extraction in the food industry – a review. *Innov Food Sci Emerg Technol.*, vol. 2, no. 9, pp. 161-169.
25. Lianfu Z., Zelong L. (2008) Ultrasonics sonochemistry. Optimization and comparison of ultrasound/microwave assisted extraction (UMAE) and ultrasonic assisted extraction (UAE) of lycopene from tomatoes. vol. 5, no. 15, pp. 731-737.
26. Albu S., Joyce E., Paniwnyk L., Lorimer J., Mason T. (2004) Potential for the use of ultrasound in the extraction of antioxidants from *Rosmarinus officinalis* for the food and pharmaceutical industry. *Ultrason Sonochem.*, vol. 3, no. 11, pp. 261-265.

^{1*}Z. Inelova , ¹S. Nesterova , ²Z. Zakaria ,
¹Y. Zaparina , ¹A. Sayakhmet 

¹Al-Farabi Kazakh National University, Almaty, Kazakhstan
²Universiti Sains Malaysia, Minden, Penang, Malaysia
*e-mail: Zarina.Inelova@kaznu.kz

Systematic analysis of flora of Atyrau city

Abstract: Currently, a great deal of attention is attracted to the study of regional flora as part of the solution to the problem of the study and conservation of biodiversity. Complete information on the composition of the flora of a particular region is important; it allows to establish the structure and genesis of its components, identify individual characteristics, restore the history of formation and trends. Therefore, the study of the flora of any region will always be relevant. The most important qualitative indicator of the flora it is a systematic structure. This article presents the results of a study obtained during a systematic analysis of the flora of Atyrau. It was revealed that the flora of the study area includes 27 families, of which 10 leading families make up 73.4% of the total species composition. The leading families in this taxonomic composition are the following families: *Chenopodiaceae* (90 species, 26 genera), *Asteraceae* (70 species, 32 genera), *Poaceae* (55 species, 30 genera). Dominant genera are: *Artemisia*, *Astragalus*, *Salsola*. Endemic species in the city of Atyrau revealed – 8, rare species – 6. Flora was studied using geobotanical and floristic research methods, the main of which was route-reconnaissance. Based on the analysis of literature data, viewing the herbarium of KazNU, materials collected in the framework of the scientific and technical program 0200/PTF14 on the topic: “Risk assessment of the impact of anthropogenic impact on the population of the Kazakhstan part of the Caspian region”, as well as their own research on the study and collection of plants in Atyrau, a list of flora has been compiled, including 534 species belonging to 243 genera and 57 families.

Key words: flora, Atyrau city, systematic analysis, plant biodiversity, taxonomic composition, floristic spectrum.

Introduction

Under the conditions of a constantly growing anthropogenic impact on nature, one of the most pressing environmental problems is the conservation of biodiversity as an important factor in the stable functioning of the biosphere and the development of human society. At present, a lot of attention is paid to the problem of conservation of biological diversity; it is put forward as a priority. At the present stage of the development of society, when a person involves in production all new natural objects and territories, a comprehensive study of regional flora is of great importance. Full information about the composition of the flora of a particular region is important as it allows establishing the structure and genesis of its components, identification of individual characteristics, restoration

of the history of formation and trends of change. Therefore, the study of the flora of any region will always be relevant [1-5].

In this work, an analysis of the flora of the city of Atyrau is carried out, which is subject to increased anthropogenic impact on the environment, which leads to a deterioration in the quality of the natural environment, and in the long run is the reason for the reduction of biodiversity [6-9].

Atyrau is the administrative center of the Atyrau region. The city is better known to the general public as the “oil capital” of the Republic of Kazakhstan. The climate of Atyrau is sharply continental, arid. Summer is dry, long, hot; winter is not snowy, cold. The average temperature in January is 8-11 °C, in July +24 +25 °C. Annual snowfall is 100-200 mm. The major rivers flowing through the territory of the region are the Urals (total length 2534 km, within

Kazakhstan 1084 km), Emba (712 km), Sagyz (511 km), Oyyl (800 km). The large lake of the region is Inder (110.5 sq. Km). The soil cover of the territory is very diverse, due to the diverse conditions of soil formation and the history of formation. The desert zone is divided into subzones of the northern desert and brown soils into the subzone of the southern desert with gray-brown soils. The northeastern part belongs to the desert-steppe zone with light chestnut soils. A distinctive feature of the vegetation cover is its spatial heterogeneity. Among the leading factors determining the spatial distribution of vegetation are moistening conditions, salinity, soil composition and topography [9]. Currently, the city of Atyrau has been surrounded by industrial enterprises with a large number of harmful substances. Within the city are: Atyrau oil refinery, Atyrau Heat and Power Plant, washing station "PPS Oil Trade", oil depot LLP "Caspiypromstroy real estate" (KPSN), New oil depot, LLP "Akzhayyk-7" (repair and washing of railway rolling stock), oil depot in Shirina village, Asphalt plant, solid waste landfill, Atyrau oil pipeline department, Caspian pipeline consortium, Bolashak complex oil and gas treatment unit. Flora analysis plays a key role in solving the problems of biodiversity conservation in various regions. The work of both domestic and foreign authors is devoted to this problem: Mukhitdinov N.M. [10], Dimieva L.A. [11], Inelova Z.A. [12; 13], Ogar N.P. [14], Ivashchenko A.A. [15], Ganeshaiyah K.N. [16], Conti F. [17], Sivtceva-Maksimova P.S. [18], Ivanov A.L. [19].

A systematic analysis is necessary to identify the taxonomic structure of the flora. This analysis determines the hierarchical sequence of taxa of the rank of family and genus, which refers to the specific features of this flora, shows its difference from other flora, and also determines the affiliation of the flora to large phytocenoses of the globe. From this point of view, the systematic structure of the flora. Thus, the aim of this work was to conduct a systematic analysis of Atyrau, one of the most developed industrial centers, to take measures to preserve the biological diversity of Kazakhstan.

Materials and methods

The material of the studies was the herbarium material of the Department of Biodiversity and

Bioresources of the Kazakh National University named after al-Farabi, materials collected during the period of 2014-2017 in the framework of the scientific and technical program 0200/PTF14 on the topic: "Risk assessment of the impact of anthropogenic impact on the population of the Kazakhstan part of the Caspian region", and own collection of species composition conducted during the period of 2018-2020.

In the field, a classical methods of floristic and geobotanical research are used [20]. The main method of investigation was route-reconnaissance, the essence of which was to identify the main patterns of distribution of species composition and vegetation in the study area.

Before starting work, a route was laid according to which studies were conducted. During the route, a geobotanical description of vegetation was carried out in separate, small areas, collection and herbarization of species, their entry in special forms. The route was planned in such a way that it passed through various phytocenoses, capturing a variety of habitats [21].

When determining the herbarium samples were used as sources of the "Flora of Kazakhstan volume 1-9" [22], "Illustrated determinant of plants of Kazakhstan volume 1-2" [23], the definition of families and genera was carried out with the help of "Flora of Kazakhstan" by M.S. Baitenov [24].

The location of species and supraspecific categories in the flora and floristic spectrum carried out according to the system of A. L. Takhtajan [25]. The spelling of Latin names, the nomenclatural changes of the taxa were verified in accordance with S. K. Cherepanov [26].

The rare and endemic species distribution was verified according to the Red Book of Kazakhstan [27].

Results and discussion

As a result of the analysis of the plant species composition, compiled on the basis of our own and published data [11; 14; 28], the flora of Atyrau includes 243 genera and 534 species from 57 families. The most important qualitative indicator of the flora is its systematic structure. Figure 1 presents the data on the systematic composition of families, genera, and species of flora in Atyrau.

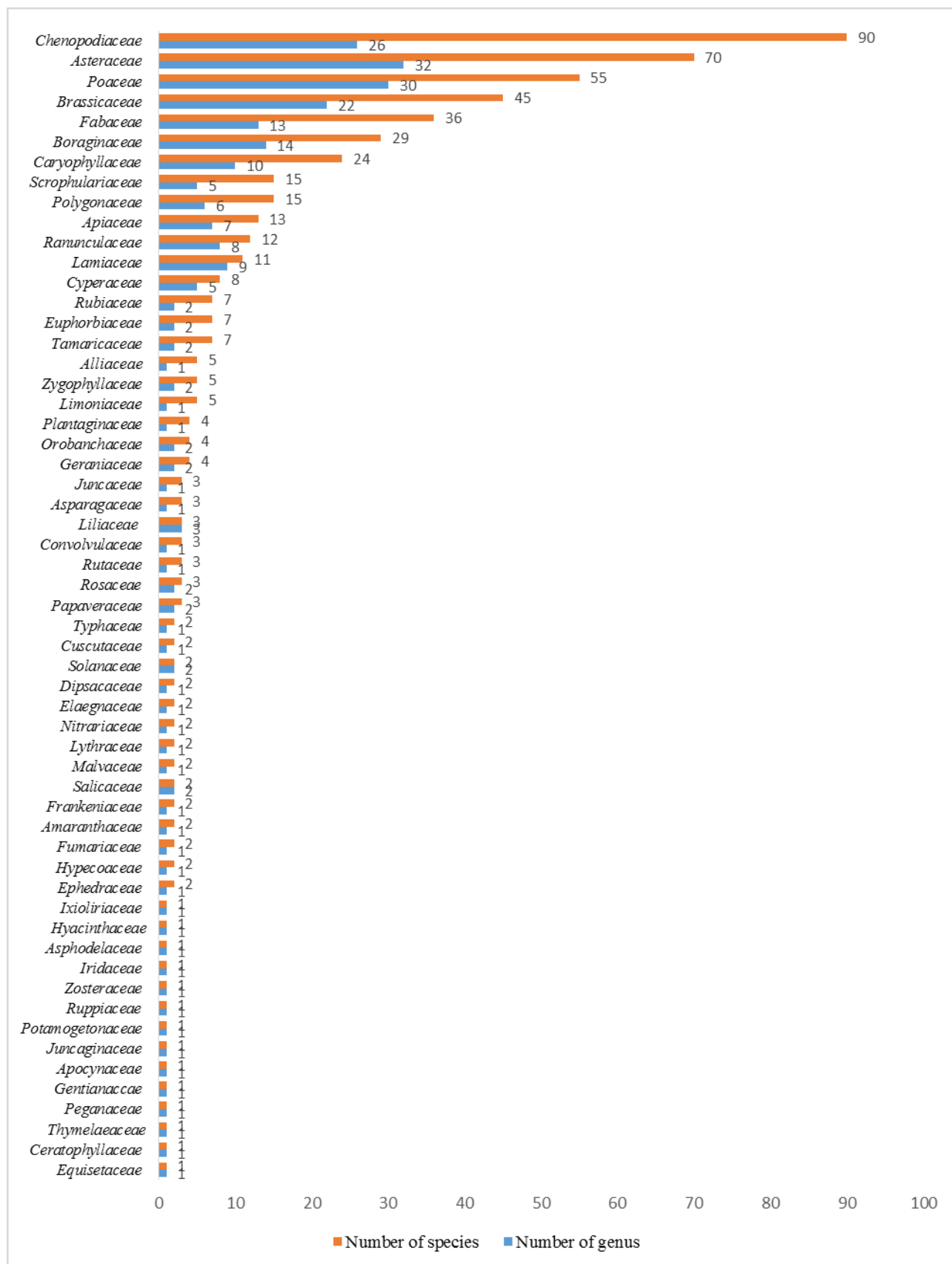


Figure 1 – Total taxonomic structure of flora of of Atyrau city

According to the Figure 1, a wealth of species families: *Asteraceae* Dumort. (32 genera: *Acantholepis*, *Acroptilon*, *Amberboa*, *Artemisia*, *Carthamus*, *Centaurea*, *Chondrilla*, *Cichorium*, *Cirsium*, *Cousinia*, *Echinops*, *Epilasia*, *Erigeron*, *Heteracia*, *Hyalea*, *Inula*, *Jurinea*, *Karelinia*, *Koelpinia*, *Lactuca*, *Mausolea*, *Microcephala*, *Onopordum*, *Rhaponticum*, *Scorzonera*, *Senecio*, *Serratula*, *Takhtajiantha*, *Tanacetum*, *Taraxacum*, *Tragopogon*, *Xanthium*), *Chenopodiaceae* Vent. (26 genera: *Agriophyllum*, *Anabasis*, *Atriplex*, *Bassia*, *Camphorosma*, *Ceratocarpus*, *Chenopodium*, *Climacoptera*, *Corispermum*, *Girgensohnia*, *Halimocnemis*, *Halocnemum*, *Halogeton*, *Halopeplis*, *Halostachys*, *Halothamnus*, *Haloxylon*, *Horaninovia*, *Kalidium*, *Kirilowia*, *Kochia*, *Nanophyton*, *Petrosimonia*, *Salicornia*, *Salsola*, *Suaeda*), *Poaceae* Barahart (30 genera: *Achnatherum*, *Aeluropus*, *Agropyron*, *Alopecurus*, *Anisantha*, *Bromus*, *Calamagrostis*, *Catabrosella*, *Crypsis*, *Cynodon*, *Echinochloa*, *Elymus*, *Elytrigia*, *Eragrostis*, *Eremopyrum*, *Festuca*, *Hordeum*, *Leymus*, *Lolium*, *Melica*, *Phragmites*, *Poa*, *Polypogon*, *Psathyrostachys*, *Puccinellia*, *Secale*, *Setaria*, *Stipa*, *Stipagrostis*, *Trisetaria*), *Brassicaceae* Burnett (22 genera: *Alyssum*, *Arabidopsis*, *Barbarea*, *Camelina*, *Cardaria*, *Clypeola*, *Crambe*, *Cryptospora*, *Descurainia*, *Erysimum*, *Goldbachia*, *Hymenolobus*, *Lepidium*, *Leptaleum*, *Matthiola*, *Megacarpaea*, *Meniococus*, *Pachypterygium*, *Sisymbrium*, *Strigosella*, *Tauscheria*, *Tetracme*), *Boraginaceae* Juss (*Argusia*, *Arnebia*, *Asperugo*, *Cynoglossum*, *Gastrocotyle*, *Heterocaryum*, *Lappula*, *Lycopsis*, *Myosotis*, *Nonea*, *Paracaryum*, *Rindera*, *Rochelia*, *Suchtelenia*), *Faba-*

ceae Vent. (13 genera: *Alhagi*, *Ammodendron*, *As-tragalus*, *Caragana*, *Eremosparton*, *Ewersmannia*, *Glycyrrhiza*, *Halimodendron*, *Lathyrus*, *Medicago*, *Melilotus*, *Onobrychis*, *Trigonella*) achieved through generic diversity. However, the systematic structure of the flora of Atyrau is also characterized by the significant participation of single-species families: *Equisetaceae* Rich. ex DC. (*Equisetum ramosissimum* Desf.), *Ceratophyllaceae* S.F. Gray (*Ceratophyllum demersum* L.), *Thymelaeaceae* Juss. (*Diarthron vesiculosum* (Fisch. and Mey. ex Kar. and Kir.) C.A. Mey.), *Peganaceae* (Engl.) Tiegh. ex Takht. (*Pegatum harmala* L.), *Gentianaceae* Juss (*Centaurium pulchellum* (Sw.) Druce), *Apocynaceae* Juss. (*Trachomitum scabrum* (Russan.) Pobed.), *Juncaginaceae* Rich. (*Triglochin palustre* L.), *Potamogetonaceae* Engl. (*Potamogeton pectinatus* L.), *Ruppiaceae* Hutch. (*Ruppia maritima* L.), *Zosteraceae* Dumort (*Zostera noltii* Hornem.), *Iridaceae* Juss. (*Iris tenuifolia* Pall.), *Asphodelaceae* Juss. (*Eremurus inderiensis* (Stev.) Regel), *Hyacinthaceae* Batsch (*Ornithogalum fischerianum* Krasch.), *Ixioliriaceae* Nakai (*Ixiolirion tataricum* (Pall.) Roem. and Schult.). The share of 15 single-species families accounts for only 2.62% of the total number of species. The presence in the flora of one – two-species families is always of great interest, because centers of their species diversity are found in other climatic regions.

The floristic spectrum of Atyrau city and the following systematic groups, presented in Table 1, shows that flowering plants were prevailing, while the horsetail and gymnosperms occupied the lowest share.

Table 1 – Distribution of plants of Atyrau city by the systematic groups

Systematic group	Number of families	Number of genus	Number of species	% of the total number of species
Horsetail	1	1	1	0.19
Gymnosperms	1	1	2	0.37
Angiosperms:				
- dicotyledonous	40	191	444	83.14
- monocotyledons	15	50	87	16.29
Total:	57	243	534	100

The species composition of the flora of Atyrau city is dominated by the divisions of *Magnoliophyta*, which accounts for 531 species (99.43%) and only a small number of species (3 or 0.56 %) belongs to *Pinophyta* and *Equisetophyta* (Figure 2).

The total number of dicotyledons in the flora of the study area includes 40 families (*Ceratophyllaceae* S.F. Gray., *Ranunculaceae* Juss., *Papaveraceae* Juss., *Hypocoaceae* (Dumort.) Willk., *Fumariaceae* D.C., *Caryophyllaceae* Juss., *Amaranthaceae* Juss.,

Chenopodiaceae Vent., *Polygonaceae* Juss., *Limoniaceae* Ser., *Tamaricaceae* Link, *Frankeniaceae* S.F. Gray, *Salicaceae* Mirbel, *Brassicaceae* Burnett, *Malvaceae* Juss., *Euphorbiaceae* Juss., *Thymelaeaceae* Juss., *Rosaceae* Juss., *Lythraceae* J. St.-Hil., *Fabaceae* Lindl., *Rutaceae* Juss., *Zygophyllaceae* Lindl., *Nitrariaceae* Bercht. et J. Presl., *Peganaceae* (Engl.) Tigh. ex Takht., *Geraniaceae* Juss., *Elaeagnaceae* Juss., *Apiaceae* Lindl., *Dipsacaceae* Juss., *Rubiaceae* Juss., *Gentianaceae* Juss., *Apocynaceae* Juss., *Solanaceae* Juss., *Convolvulaceae* Juss., *Cuscutaceae* Dumort., *Boraginaceae* Juss., *Scrophulariaceae* Lindl., *Orobanchaceae* Vent., *Plantaginaceae* Lindl., *Lamiaceae* Lindl., *Asteraceae* Dumort.), containing 191 genera and 444 species, which is 83.14% of the

total number of species. Monocotyledons includes 15 families (*Juncaginaceae* Rich., *Potamogetonaceae* Engl., *Ruppiaceae* Hutch., *Zosteraceae* Dumort., *Iridaceae* Juss., *Liliaceae* Juss., *Alliaceae* J. Agardh., *Asphodelaceae* Juss., *Hyacinthaceae* Batsch, *Ixioliriaceae* Nakai, *Asparagaceae* Juss., *Juncaceae* Juss., *Cyperaceae* Juss., *Poaceae* Barahart, *Typhaceae* Juss.) containing 50 genera and 87 species or 16.29% of the total species, the spore plants (*Equisetaceae* Rich. ex DC.) and gymnosperms (*Ephedraceae* Dumort.) – 3 species (0.56%).

There is a clear tendency in the ratio of the number of monocotyledonous and dicotyledonous genera towards increasing role of dicotyledonous, which is even more evident on the level of the families.

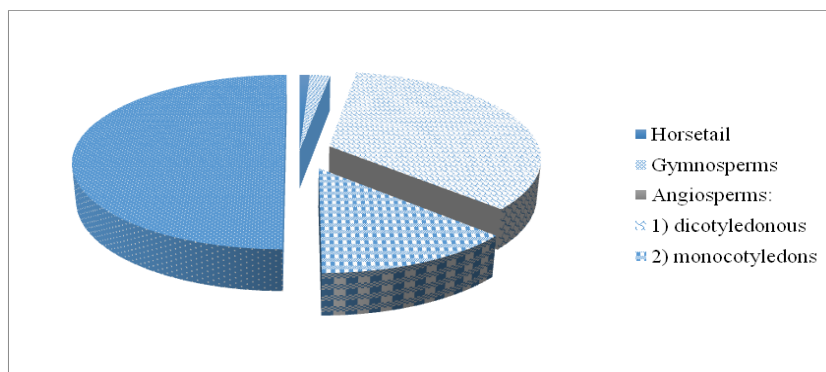


Figure 2 – Ratio of systematic groups of flora of Atyrau city

Accordingly, in the studied flora, most families, genera, and species are angiosperms, among which dicotyledons predominate.

On the territory of Atyrau city 57 families of plants were identified. Traditionally, in floristic works 10 large families of plants are considered in descending order of the number of species, which is called the family spectrum of flora. Analysis of the largest families of the flora of Atyrau city has allowed identifying the 10 largest families in the greatest number of species.

The first 10 families (*Chenopodiaceae*, *Asteraceae*, *Poaceae*, *Brassicaceae*, *Fabaceae*, *Boraginaceae*, *Caryophyllaceae*, *Polygonaceae*, *Scrophulariaceae*, *Apiaceae*) contain 392 species of plants, which is about 73.4% of the total number of species.

Figure 3 shows the spectrum of the 10 largest families in the flora of Atyrau city.

According to the data, the first place in the number of species and genera is occupied by the family

Chenopodiaceae (90 species, or 16.85 % of the total number of species, 26 genus), then the second place is occupied by the *Asteraceae* family (70 species or 13.11 %, 32 genus). The third place is occupied by the *Poaceae* family, which contains 30 genera, 55 species, or 10.3% of the total number of genera. This is followed by the family *Brassicaceae* – 45 species (8.43%), 22 genera. The family *Fabaceae* – 36 species (6.74 %), numbers of genus 13. *Boraginaceae* family contains 29 species (5.43%), 14 genera, *Caryophyllaceae* – 24 species (4.49%), 10 genera. This is followed by the families *Polygonaceae* and *Scrophulariaceae*, which contain the same number of species – 15 (2.81%), but a different number of genera – 6 and 5, respectively. In tenth place is the *Apiaceae* family with 13 species (2.43%) and 7 genera. The above 10 families include 73.4 % of the total species composition of the flora of the studied region. Other families are characterized by more low species and generic diversity.

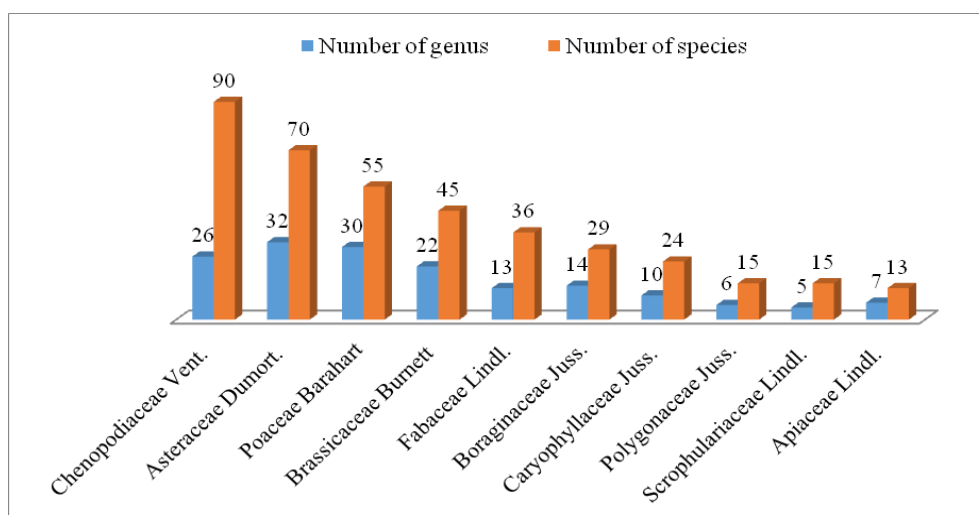


Figure 3 – Number of species and genera in 10 leading families of flora of Atyrau city

Table 2 provides information on the number of species for the largest genera of flora Atyrau city. The largest and largest genera mainly belong to the leading families of the studied flora (*Asteraceae*, *Fabaceae*, *Chenopodiaceae*). The species of these genera under appropriate environmental conditions create a common floral background.

Table 2 – Number of species in the largest genera of flora of Atyrau city

Genus	Number of species	% of the total number of species
<i>Artemisia</i>	16	3
<i>Astragalus</i>	14	2.62
<i>Salsola</i>	12	2.45
<i>Suaeda</i>	10	1.87
<i>Atriplex</i>	9	1.48
<i>Climacoptera</i>	8	1.5
<i>Anabasis</i>	7	1.31
<i>Tamarix</i>	6	1.12
<i>Gypsophila</i>	5	0.94
<i>Agropyron</i>	4	0.75
Total – 10	91	17.04

According to the data presented in the Table 2 the largest genera are *Artemisia* (16 species or 3%), *Astragalus* (14 species or 2.62 %), *Salsola* (12 species, 2.45 %), *Suaeda* (10 species or 1.87 %). Can also be noted by the number of species: *Atriplex* (9

species, 1.48 %), *Climacoptera* (8 species, 1.5 %), *Anabasis* (7 species, 1.31 %), *Tamarix* (6 species, 1.12 %), *Gypsophila* (5 species, 0.94 %), *Agropyron* (4 species, 0.75%).

Accordingly, for 10 genera (4.11 % of the total number of genera) 91 species of flora are present in Atyrau city. On the territory of Atyrau city 8 endemic and 6 rare species were identified. In the study area, the following plants are endemic species: *Atriplex pungens* Trautv., *Rubia cretaceae* Pojark., *Saponari aspathulifolia* (Fenzl) Vved., *Gypsophila krascheninnikovii* Schischk., *Stemmacantha nitida* (Fisch.) M. Dittrich (= *Rhaponticum nitidum* Fisch., *Jurinea tenuiloba* Bunge, *Corispermum laxiflorum* Schrenk, *Suaeda kossinskyi* Iljin. The rare species: *Crambe tatarica* Sebeok, *Lepidium meyeri* Claus, *Rubia cretaceae* Pojark., *Linaria cretacea* Fisch. ex Spreng., *Tulipa biflora* Pall., *Ornithogalum fischeranum* Krasch.

Conclusion

Flora analysis plays a key role in solving the problems of biodiversity conservation in various regions. In accordance with the Convention on Biodiversity, the first step for conservation is an inventory of flora and natural plant resources, which is the foundation for the development of a scientifically based algorithm for the rational use of plant wealth.

On the basis of the literature review and analysis of the herbarium, collected within the framework of scientific and technical program 0200/PTF14 “Risk assessment of the impact of anthropogenic impact on the population of the Kazakhstan part of the Caspian region” and additional research on the study of

Atyrau flora, a list of plants has been compiled, including 534 species belonging to 243 genera and 57 families. The first ten leading families contain 392 species and make up 73.4% of the total species composition of the flora of the study area. The leading families in this taxonomic composition are *Chenopodiaceae* (90 species, or 16.85% of the total number of species, 26 genera), *Asteraceae* (70 species or 13.11%, 32 genera), *Poaceae* (55 species, which is 10.3% of the total, 30 genera). Dominant genera are *Artemisia* (16 species or 3%), *Astragalus* (14 species or 2.62%), *Salsola* (12 species or 2.25%). Endemic plants in the city of Atyrau revealed – 8 species, rare – 6 species.

The results of the research will serve as the basis for the rational use of flora and vegetation in Atyrau, as well as the conservation of biodiversity.

The data obtained as a result of the study can be used to compile a floristic summary of Atyrau, the analysis of which serves as the basis for recommendations on the protection of the plant gene pool, which under the conditions of increasing anthropogenic pressure will serve as material for long-term environmental monitoring of the ecosystems of the region.

The results of a systematic analysis of the flora of Atyrau allow us to identify centers of endemism and relictness, as well as to solve the issues of the place and role of this flora in a number of other adjacent flora.

References

- Fenu G., Bacchetta G., Giacanelli V.D. (2017) Conserving plant diversity in Europe: outcomes, criticisms and perspectives of the Habitats Directive application in Italy. *Biodivers Conserv.*, no. 26, pp. 309-328. doi 10.1007/s10531-016-1244-1
- Handa I.T. (2014) Consequences of biodiversity loss for litter decomposition across biomes. *Nature*, vol. 509, pp. 218-221. doi 10.1038/nature13247
- Cunningham S.D., Ow D.W. (1996) Promises and Prospects of Phytoremediation. *Plant Physiology*, vol. 110, pp. 715-719. doi 10.1104/pp.110.3.715
- Hillebrand H., Matthiessen B. (2009) Biodiversity in a complex world: consolidation and progress in functional biodiversity research. *Ecol. Lett.*, vol. 12, pp. 1405-1419. doi 10.1111/j.1461-0248.2009.01388.x
- Cardinale B.J., Gonzalez A., Allington G. (2018) Is local biodiversity declining or not? A summary of the debate over analysis of species richness time trends. *Elsevier Ltd.*, vol. 219, pp. 175-183. doi 10.1016/j.biocon.2017.12.021
- Duffy J.E., Carinale B.J., France K.E., McIntyre P.B., Loreau M. (2007) The functional role of biodiversity in ecosystems: incorporating trophic complexity. *Ecol. Lett.*, vol. 10, pp. 522-538. doi 10.1111/j.1461-0248.2007.01037.x
- Bracken M.S., Friberg S.E., Gonzalez-Dorantes C.A., Williams S.L. (2008) Functional consequences of realistic biodiversity changes in a marine ecosystem. *Ecol. Lett.*, vol. 105, no. 3, pp. 924-928. doi 10.1073/pnas.0704103105
- Cardinale B.J., Duffy J.E., Gonzalez A. (2012) Biodiversity loss and its impact on humanity. *Nature*, vol. 486, pp. 59-67. doi 10.1038/nature11148
- Dimeeva L.A., Sultanova B.M., Usen K., Permitina V.N., Sadvokasov R.E., Kerdyashkin A.V., Imanalinova A.A. (2014) Transformatsiya pustynnoy rastitelnosti Kazakhstana v regionah neftegazodobyichi I vozmozhnosti ee reabilitatsii [Transformation of the desert vegetation of Kazakhstan in the regions of oil and gas production and the possibility of its rehabilitation]. Almaty, 136 p.
- Muhitdinov N.M., Inelova Z.A. (2008) Sistematicheskiy analiz floryi doliny I srednego I nizhnego techeniya r. Ili [A systematic analysis of the flora of the valley of the middle and lower reaches of the river]. *Izvestia*, vol.1, no. 265, pp. 43-47.
- Dimeeva L.A., Sinyaeva N.I., Lyisenko V.V. (1998) Otsenka bioraznoobraziya Atyrauskoy oblasti dlya organizatsii ohranyaemykh territoriy [Assessment of the biodiversity of the Atyrau region for the organization of protected areas]. *Search, Series: Natur. Sci.*, no. 3, pp. 28-39.
- Inelova Z., Nesterova S., Yerubaeva G., Zaparina Ye., Aitzhan M. (2019) Systematic analysis of the flora of the Talgar, Enbekshikazakh districts of the Almaty region. *Exper. Biol.*, vol. 1, no. 78, pp. 20-27.
- Inelova Z.A., Nesterova S.G., Erubaeva G.K., Korotkov V.S., Tolyimbek K., Kadyrbek R. (2014) Sistematicheskiy analiz floryi Zharkentskoy kotloviny Ile-balhashskogo regiona [A systematic analysis of the flora of the Zharkent basin of the Ile-Balkhash region]. *Bulletin of KazNU. Ser. Ecol.*, no. 3 (42), pp. 169-174.
- Ogar N.P., Stogova L.P. (2002) Spisok floryi Kazhastanskoy chasti poberezhya Kaspiyskogo morya [List of flora of the Kazakhstan part of the Caspian Sea coast]. Almaty, 318 p.
- Ivaschenko A.A. (2015) Materialy k flore Ile-Alatauskogo natsionalnogo parka i prilgayushih territoriy [Materials for the flora of the Ile-Alatau Na-

tional Park and adjacent territories]. Astana: Zhasyl Orda, vol.1, pp. 29-71.

16. Ganeshaiah K.N., Sanjappa M., Rao R., Murugan, C. Shivaprakash K.N. (2019) Spatial distribution pattern of taxonomic and phylogenetic diversity of woody flora in Andaman and Nicobar Islands, India. *Forest Ecosystems*, vol. 6, no. 38, pp.1-14. doi.10.1186/s40663-019-0196-9

17. Conti F., Ciaschetti G., Martino L.D., Bartolucci F. (2019) An annotated checklist of the vascular flora of Majella National Park (Central Italy). *Phytotaxa*, vol. 412, pp.1-90. doi.10.11646/phytotaxa.412.1.1

18. Sivtceva-Maksimova P.S., Sivtseva S.S. (2019) Toward the scientific research of A.E. Kulakovsky: Floristic analysis of the northern region of Russia, *Amazon research*, vol. 8, no. 21, pp. 365-371.

19. Ivanov A.L. (2018) Cistematicheskii analiz flory rossiyskogo Kavkaza [A systematic analysis of the flora of the Russian Caucasus] *Bull. Samara Sci. Cent. Rus. Ac. Sci.*, vol. 5, no. 4, pp. 631-636.

20. Degtyareva, S., Dorofeeva V. (2019) The relationship of spore (mosses) and seed plants with mesorelief types of oak forests. International jubilee scientific and practical conference innovative directions of development of the forestry complex, vol. 226, pp. 237-346. doi.10.1088/1755-1315/226/1/012004

21. Lavrenko E.M., Korchagina A.A. (1959) *Polevaya geobotanika* [Field geobotany]. Botanical

Institute named after V.L. Komarova Academy of Sciences of the USSR, vol. 1-2, 444 p.

22. Pavlov N.V. (1956-1966) *Flora Kazakhstana* [Flora of Kazakhstan]. Alma-Ata: Nauka, vol. 1, 359 p.; vol. 2, 291 p.; vol. 3, 457 p.; vol. 4, 547 p.; vol. 5, 514 p.; vol. 6, 464 p.; vol. 7, 436 p.; vol. 8, 446 p.; vol. 9, 635 p.

23. Goloskokov V.P. (1969-1972) *Illyustrirovannyi opredelitel rasteniy Kazakhstana* [Illustrated identifier of plants of Kazakhstan]. Alma-Ata: Science, vol.1, 525 p.; vol.2, 568 p.

24. Baytenov M.S. (1999-2001) *Flora Kazakhstana* [Flora of Kazakhstan]. Almaty: Science, vol.1, 400 p.; vol. 2, 280 p.

25. Takhtadzhyan A.L. (1987) *Sistema magnoliolitov* [*Magnoliophyte* system]. L.: Science. 439 p.

26. Cherepanov S.K. (1981) *Sosudistyie rasteniya SSSR* [Vascular plants of the USSR]. L.: Science, 509 p.

27. *The Red Book of Kazakhstan (plants)*, (2014). ArtPrintXXI LLP: Astana, vol. 2, 830 p.

28. Nesterova S.G., Inelova Z.A., Erubaeva G.K. (2017) *Rekomendatsii ob urovne riska upotrebleniya kormovyih nazemnyih rasteniy Kazahstanskoy chasti Prikaspiya* [Recommendations on the risk level of the use of forage terrestrial plants of the Kazakhstan part of the Caspian region] Almaty: Qazaq Universiteti, 30 p. ISBN 978-601-04-2913-0.

¹M. Irfan , ¹S. Sadia , ¹J. Bakhtawar ,
²H.A. Shakir , ²M. Khan , ³S. Ali 

¹Department of Biotechnology, University of Sargodha, Sargodha, Pakistan,
²Department of Zoology, University of the Punjab new campus, Lahore, Pakistan,
³Department of Zoology, Government College University, Lahore, Pakistan
*e-mail: irfan.ashraf@uos.edu.pk

Utilization of peanut shells as substrate for cellulase production in submerged fermentation through Box-Behnken Design

Abstract: Increasing environmental pollution and global warming encourage bioengineers and biotechnologists to find renewable and environmental friendly sources of energy. Conversion of biomass especially agro-industrial biomass consisting of lignocellulosic material into different products and energy is the modern and promising scheme for this purpose due to their abundance in nature, lower cost and easy handling. These properties made them potential producers of biofuels in near future. In current research, *Bacillus paralichniformis* potential for cellulase production was analyzed using submerged fermentation, for which peanut shell waste was used as a substrate. Nutritional factors were optimized for best enzyme production using Box-Behnken Design (BBD) of response surface methodology (RSM). Results illustrated the maximum enzyme production of 12.838 IU for CMCase and 40.956 IU for FPase after 24 h of fermentation period. These results were obtained at 3 g/mL substrate concentration, 0.45 g/mL yeast extract and 0.01 g/mL MgSO₄ for CMCase and 3g/mL substrate, 0.45 g/mL yeast extract and 0.3 g/mL MgSO₄ for FPase. These results proposed the possibility of utilization of this strain for production of cellulase to endorse its use in industry.

Key words: *Bacillus* sp., cellulase, peanut shells, RSM, CCD, submerged fermentation.

Introduction

Increasing environmental pollution and global warming encourage bioengineers and biotechnologists to find renewable and environmental friendly sources of energy [1]. Conversion of biomass especially agro-industrial biomass consisting of lignocellulosic material into different products and energy is the modern and promising scheme for this purpose due to their abundance in nature, lower cost and easy handling. These properties made them potential producers of biofuels in near future [2]; if the product recovery and purification steps use limited and optimized water, solvents and energy [3; 4]. On the other hand conversion of lignin gasification (LG) biomass into simple units remains the major problem due to complex chemical nature of LG material. However, enzymatic hydrolysis, physical or biological degradation methods made it easy and economical for industrial uses [5]. These processes effect saccharification of cellulose enzymatically [6]. Cellulose is the most abundant

and naturally renewable source of energy which can compete with many of the existing but expensive and nonrenewable resources of energy. It is a plant biopolymer with complex structure having a hydrolytic enzyme system for the cleavage of bonds and its conversion into simple sugar like D-glucose units [7].

Cellulases are the enzymes that catalyze cellulose into fermentable sugars which is now considered the feasible process to reduce the risk of environmental pollution, easy and useful dumping and degradation of plant and cellulosic waste. In industry these have great importance in paper and pulp, textile, detergents, food and feed additives, bio-ethanol production and processing of chemicals. The prerequisite for easy and economical use of cellulases is to search for best microbial strains which produce high enzyme titer and to optimize media that could be affordable for industry. There are many microorganisms studied and searched for the production of cellulases but lesser number of them are able to produce it in economically feasible

and industrially significant quantities of enzyme [8]. Microorganisms are genetically the most diverse group due to high metabolic flexibility and multiple enzyme based reactions which in turn catalyze complex structures like cellulose in D-glucose with the help of enzymes called cellulase. Microorganisms have high impact on biotechnological applications due to these significant features [7]. Bacteria are emerging as hotspots of versatility and variety genetically and functionally. They can degrade lignocellulosic materials involving complex system of lignocellulolytic enzymes [9].

The complex cellulase enzyme system consists of three enzymes which are endoglucanases, exoglucanases and cellobioases [10]. Endoglucanases are β -1,4-D glucan-4-glucano-hydrolase and carboxymethyl cellulase, while exoglucanases are β -1,4-D glucan-4-gluco-hydrolase and cellobiohydrolase and cellobioases termed as CBH and cellobioases are β -D glucoside glucohydrolase and β -1,4-D-glucosidase, all free enzymes present in 57 of glycosyl hydrolase families [11; 12]. Cellulolytic enzymes would be of great industrial use with the promising environmental and economical sustainability if their media could be improved with the proper optimized conditions for achieving best enzyme titer that eventually lessens its cost [13].

The optimization of cellulase production and selection of ideal substrate are major and important steps having significant enzyme titer at the end. Limited information was available for *Bacillus* species enzymology and its cellulolytic activities. Bacterial cellulases usually reported to be extracellular and production can be optimized by adjusting nutritional parameters and physical properties like temperature and pH, etc. The major factor has always been carbon source but nitrogen phosphorus and metal ions sources are also of great importance [14].

Determination of cellulolytic potential of microorganism is carried out via fermentation process. There are two types used commonly one is solid state fermentation and second is submerged fermentation. Solid state fermentation is carried out in the absence of free liquids as microorganisms grow on firm surfaces holding up as substrates [15]. This type has been used mostly for filamentous fungi where solid substrate acts as natural surface for filamentous growth of fungi [16].

Submerged fermentation usually denoted as SMF is a type of fermentation which requires large amount of liquid substrates as compared to solid state fermentation. These may be water, molasses or

broths. The products which mainly are secondary metabolites or enzymes are secreted in and collected form liquid media. Continuous replenishment of substrates or nutrient may be required according to the use of substrates in fermentation process. Microbes which need high moisture content for their growth such as bacteria usually best for this type of fermentation. The advantage of this technique is easy purification and product recovery [17; 18]. Submerged fermentation is preferred for bacterial cultures due to ease of purification, sterilization and process control. The culture conditions and media optimization are the major steps to be considered [19]. During early 1970's, cellulase production was started commercially via submerged fermentation. Mega scale use of cellulase as animal feed additive and for stonewashing denim was practiced in industry during 1980's [20].

Formulation of media is specific for the organism and its optimization is necessary for best production of required substance hence any general media composition cannot be used for optimum growth and cellulase production [21]. Response surface methodology (RSM) is the statistical analysis modeling used to optimize and evaluate many biotechnological processes and enzymatic hydrolysis [22]. RSM is affected by many parameters and variable factors affecting the results and then these are optimized for the best conditions using different designs of RSM with the interpolation of first or second polynomial equations in sequential testing procedure [23; 24]. This technique, RSM integrates mathematical and statistical approaches and analyzes defined independent parameters on response without having any previous information about the relation between response function and variable parameters [25-27]. RSM is being used now statistically, as an appropriate methodology for experiment designing, statistical model building, evaluation of factors affecting the optimum conditions for required response and in turn, decreasing the number of experiments for the required response [28]. In biotechnological processes, RSM evaluate the optimum conditions for the growth of microorganism and product formation [29; 30]. Here, RSM was used to determine optimal conditions for novel bacterial strain *Bacillus parlichniformis* and the factors that affect the response of cellulase production. Peanut shell waste has been taken as carbon source and cellulolytic potential of *Bacillus parlichniformis* was investigated in submerged fermentation with optimal medium conditions.

Materials and methods

Object. Samples of *Bacillus paralichniformis* isolated from soil were provided by the Laboratory of Microbial Biotechnology, Department of Biotechnology, University of Sargodha. The strain was maintained on nutrient agar slants and used for cellulase production in subsequent study.

Enzyme production. Submerged fermentation was performed for the production of enzyme having medium ingredients of peanut shell waste, yeast extract and MgSO₄. Concentration of these ingredients was optimized as per experimental design. The medium components were sterilized and inoculated with 1ml of 24 h old vegetative cell culture and placed in a shaking incubator for 24 h with a shaking speed of 120 rpm at 35°C. Culture broth was consequently centrifuged at 10,000 x g and 4°C for 10 min. Centrifuged pure extract without cellular material was used as source of crude enzyme extract for further processing.

Cellulase assay. Carboxymethyl cellulase (CMCase) and filter paper activity (FPase) was estimated as described in our earlier reports [31].

Saccharification of peanut shell. In 500 mL conical flask, 100 mL of crude cellulase enzymes with 4% substrate was incubated at 50 °C for various time intervals. After termination of enzymatic hydrolysis, centrifugation of material was performed at 10,000 rpm for 10 min. Saccharification (%) was calculated using the following formulae [32].

$$\text{Saccharification (\%)} = \frac{\text{Reducing sugars released (mg/ml)}}{\text{Substrate used (mg/ml)}} \times 100$$

Experimental design. Box–Behnken design (BBD) was used for optimization of medium components in this study. The independent and noteworthy variables used were peanut shell (substrate) concentration (X₁), yeast concentration, (X₂) and MgSO₄ (X₃) and their levels are mentioned in Table 1. The relation between actual and coded values was described by the following equation;

$$x_i = \frac{X_i - X_0}{\Delta X_i}$$

where x_i and X_i are the coded and actual values of the independent variable, X₀ is the actual value of the independent variable at the center point and ΔX_i is the change of X_i. The response is calculated from

the following equation using STATISTICA software (99th ed.).

$$Y = \beta_0 + \beta_1 X_1 + \beta_2 X_2 + \beta_3 X_3 + \beta_{11} X_1^2 + \beta_{22} X_2^2 + \beta_{33} X_3^2 + \beta_{12} X_1 X_2 + \beta_{13} X_1 X_3 + \beta_{23} X_2 X_3$$

Y is the response, X₁, X₂ and X₃ are the independent variables, β₀ is the intercept, β₁, β₂ and β₃ are linear coefficient, β₁², β₂² and β₃² are square coefficients, β₁₂, β₁₃ and β₂₃ are interaction coefficients.

Results and discussion

Cellulases were produced by *Bacillus paralichniformis* in SMF. Media optimization for best enzyme titer was carried out using three independent variables such as substrate (peanut shell waste) concentration (X₁), Yeast extract (X₂) and MgSO₄ (X₃) and their levels are mentioned in Table 1. The response was calculated by second degree polynomial regression equation (Eq. 3; 4) using Minitab software version 9.

With the optimized conditions of media, the best enzyme production obtained for CMCase was 12.838 IU with optimized conditions of substrate concentration of 3 (%), yeast extract 0.45 (%) and MgSO₄ 0.01(%) after 24 h of incubation. This value was in close proximity with the predicted value of 12.38850 IU as shown in table 2. Highest FPase production (40.956 IU) was observed with substrate concentration of 3 (%), 0.45% of yeast extract and MgSO₄ concentration of 0.3 (%) having predicted value of 31.5108 IU.

Table 1 – Coded and actual levels of the factors for three factors Box-Behnken design

Independent variables	Symbols	Coded and actual values		
		-1	0	+1
Peanut shell waste	X ₁	0.5	1.75	3
Yeast extract	X ₂	0.1	0.45	0.8
MgSO ₄	X ₃	0.01	0.155	0.3

$$\begin{aligned} \text{CMCase (IU)} = & -3.55 + 7.13 X_1 + 18.15 X_2 \\ & + 12.96 X_3 - 0.574 X_1 * X_1 - 19.62 X_2 * X_2 - \\ & 64.2 X_3 * X_3 - 3.366 X_1 * X_2 - 4.59 X_1 * X_3 \\ & + 20.59 X_2 * X_3 \text{Equation (3)} \end{aligned}$$

$$\begin{aligned} \text{FPase (IU)} = & 10.7 + 4.5 X_1 + 30.4 X_2 - 40 X_3 \\ & + 1.36 X_1 * X_1 - 40.4 X_2 * X_2 - 141 X_3 * X_3 - 9.8 X_1 * X_2 \\ & + 17.1 X_1 * X_3 + 88 X_2 * X_3 \text{Equation (4)} \end{aligned}$$

Table 2 – Cellulase production by *B. paralicheniformis* using Box-Behnenken design from peanut shells

Run #	X ₁	X ₂	X ₃	CMCase activity (IU)			FPase activity (IU)		
				Observed	Predicted	Residual	Observed	Predicted	Residual
1	0.5	0.45	0.01	3.204	3.49975	-0.29575	7.238	16.68313	-9.4451
2	1.75	0.8	0.01	5.04	4.61963	0.420375	17.979	8.13738	9.84162
3	0.5	0.45	0.3	3.055	3.50450	-0.44950	7.238	6.48912	0.74888
4	3	0.8	0.155	6.557	7.42688	-0.86987	11.746	20.83875	-9.0927
5	0.5	0.8	0.155	3.024	3.14863	-0.12462	10.2	10.59650	-0.3965
6	1.75	0.1	0.3	4.085	4.50538	-0.42037	0.901	10.74263	-9.8416
7	3	0.45	0.3	9.358	9.06225	0.295750	40.956	31.51088	9.44513
8	3	0.1	0.155	12.043	11.91838	0.124625	36.45	36.05350	0.39650
9	1.75	0.45	0.155	9.358	9.36167	-0.00366	17.541	21.84300	-4.3020
10	1.75	0.45	0.155	9.019	9.36167	-0.34266	25.063	21.84300	3.22000
11	3	0.45	0.01	12.838	12.38850	0.449500	28.592	29.34088	-0.7488
12	1.75	0.1	0.01	7.682	8.25613	-0.57412	24.084	23.73163	0.35237
13	1.75	0.8	0.3	5.623	5.04888	0.574125	12.75	13.10238	-0.3523
14	1.75	0.45	0.155	9.708	9.36167	0.346333	22.925	21.84300	1.08200
15	0.5	0.1	0.155	2.62	1.75013	0.869875	17.709	8.61625	9.09275

All the data was statistically analyzed using analysis of variance for significance of the model (Table 3). The significance of model and response for coefficients is mainly dependent on F-value and P-values. The higher the F-value resulting in lower P-value described the high accuracy and significance of regression model [33]. Therefore, higher computed Fischer's F-value for CMCase was 26.07 and for FPase 1.14 with P-value 0.001 and 0.468 respectively. The model for CMCase was highly significant while FPase was found not significant. The fitness of model was further analyzed by the determination coefficient R² for CMCase and FPase. The R² value for CMCase and FPase were 97.91% and 67.17%, which revealed that 2.09% and 32.67% variation was not determined by model respectively. Higher value of R square of CMCase showed the accuracy of the model (Figure 1).

Interaction effect of parameters. The interaction effect of substrate concentration (X₁), yeast extract

(X₂) and MgSO₄(X₃) has been described in contour plots. Different pattern of colors in these plots depicted levels of enzyme production with one variable constant or zero level and two parameters with different levels (Figure 2). These plots indicated that each parameter significantly affect enzyme production.

The results were validated further by repeated experiments of optimized values of significant parameters as predicted in desirability diagrams (Figure 3). Results were in the close range with predicted values. This figure depicted that at optimized levels of peanut shell waste 1.75%, yeast extract 0.45% and MgSO₄ 0.155%, the maximum CMCase production was 13.678 IU which was confirmed by repeated experiments. The predicted optimized value for FPase was 1.75% peanut shell waste, 0.45% yeast extract and 0.155% MgSO₄ yielded 41.016 IU enzyme production which were almost similar after experiments.

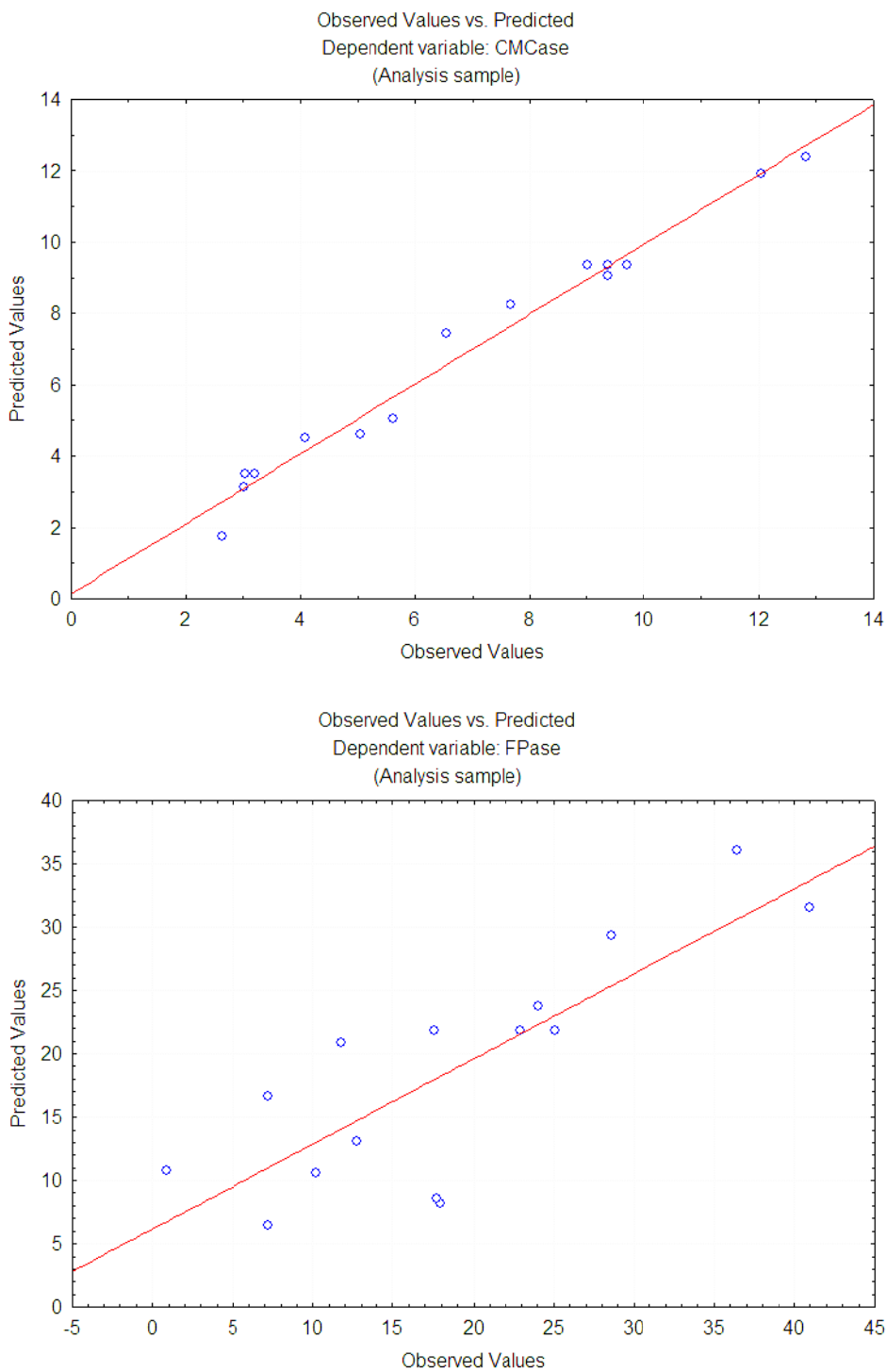


Figure 1 – Observed vs predicted values of independent variables for maximum enzyme production

Table 3 – Analysis of variance for cellulase production from *B.paralichniformis* in submerged fermentation

CMCase (IU)	Sources	DF	Adj SS	Adj MS	F value	P value
	Model	9	158.320	17.591	26.07	0.001
	Linear	3	114.650	38.217	56.64	0.000
	X ₁	1	104.351	104.351	154.66	0.000
	X ₂	1	4.783	4.783	7.09	0.045
	X ₃	1	5.516	5.516	8.18	0.035
	Square	3	27.855	9.285	13.76	0.008
	X ₁ ²	1	2.972	2.972	4.41	0.090
	X ₂ ²	1	21.329	21.329	31.61	0.002
	X ₃ ²	1	6.736	6.736	9.98	0.025
	2 Way interaction	3	15.815	5.272	7.81	0.025
	X ₁ *X ₂	1	8.673	8.673	12.85	0.016
	X ₁ *X ₃	1	2.774	2.774	4.11	0.098
X ₂ *X ₃	1	4.368	4.368	6.47	0.052	
Error	5	3.374	0.675	8.81	0.104	
Lack of fit	3	3.136	1.045			
Pure error	2	0.237	0.119			
Total	14	161.693				
FPase (IU)	Sources	DF	Adj SS	Adj MS	F value	P value
	Model	9	1164.71	129.41	1.14	0.468
	Linear	3	829.64	276.55	2.43	0.181
	X ₁	1	709.87	709.87	6.24	0.055
	X ₂	1	87.58	87.58	0.77	0.421
	X ₃	1	32.19	32.19	0.28	0.618
	Square	3	142.35	47.45	0.42	0.749
	X ₁ ²	1	16.76	16.76	0.15	0.717
	X ₂ ²	1	90.37	90.37	0.79	0.414
	X ₃ ²	1	32.51	32.51	0.29	0.616
	2 way interaction	3	192.72	64.24	0.56	0.662
	X ₁ *X ₂	1	73.92	73.92	0.65	0.457
	X ₁ *X ₃	1	38.22	38.22	0.34	0.587
X ₂ *X ₃	1	80.59	80.59	0.71	0.439	
Error	5	569.22	113.84	11.96	0.078	
Lack of fit	3	539.18	179.73			
Pure error	2	30.05	15.02			
Total	14	1733.93				

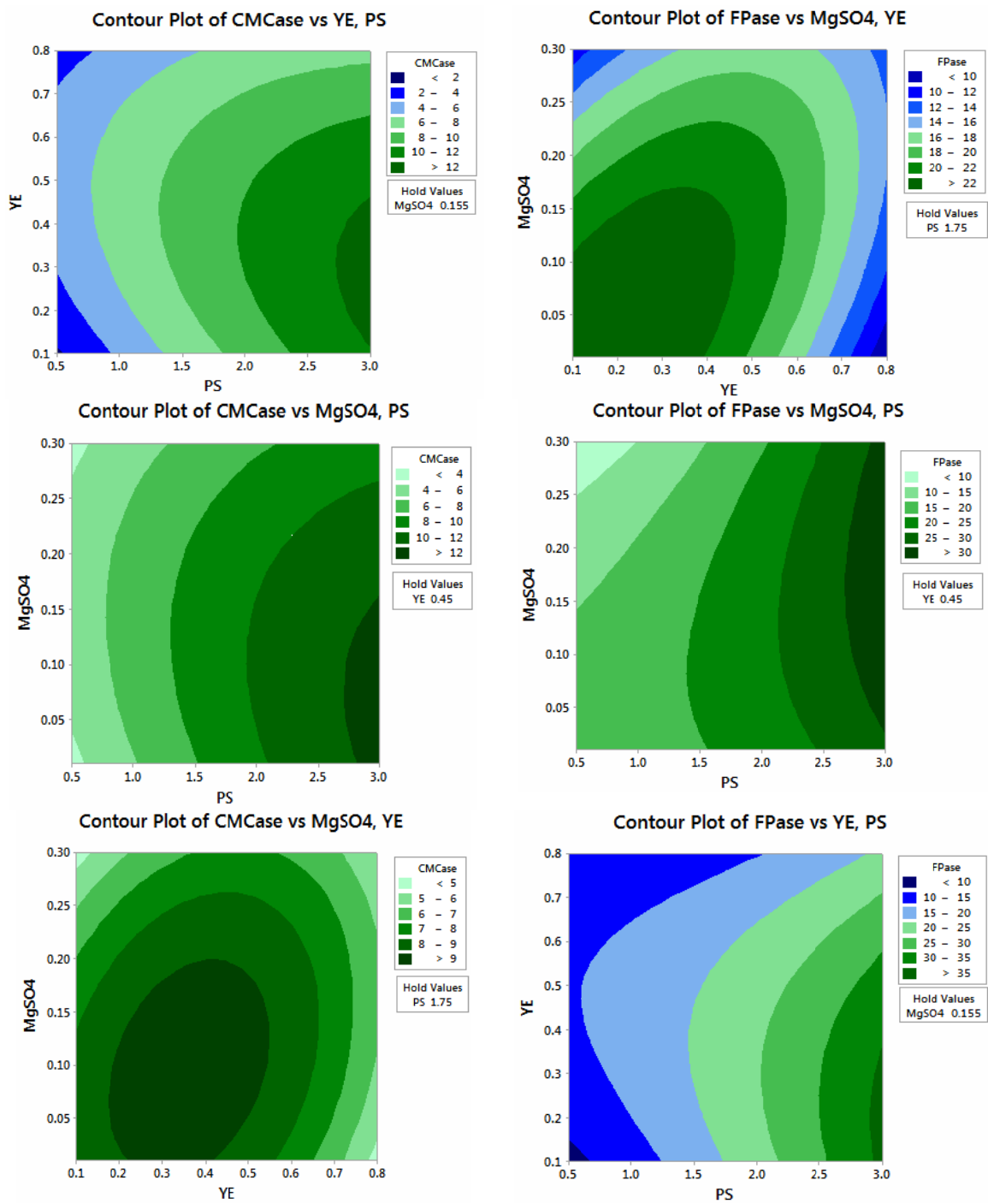


Figure 2 – Contour plots for CMCase (IU) and FPase (IU) production from peanut shells by *Bacillus paralicheniformis* submerged fermentation

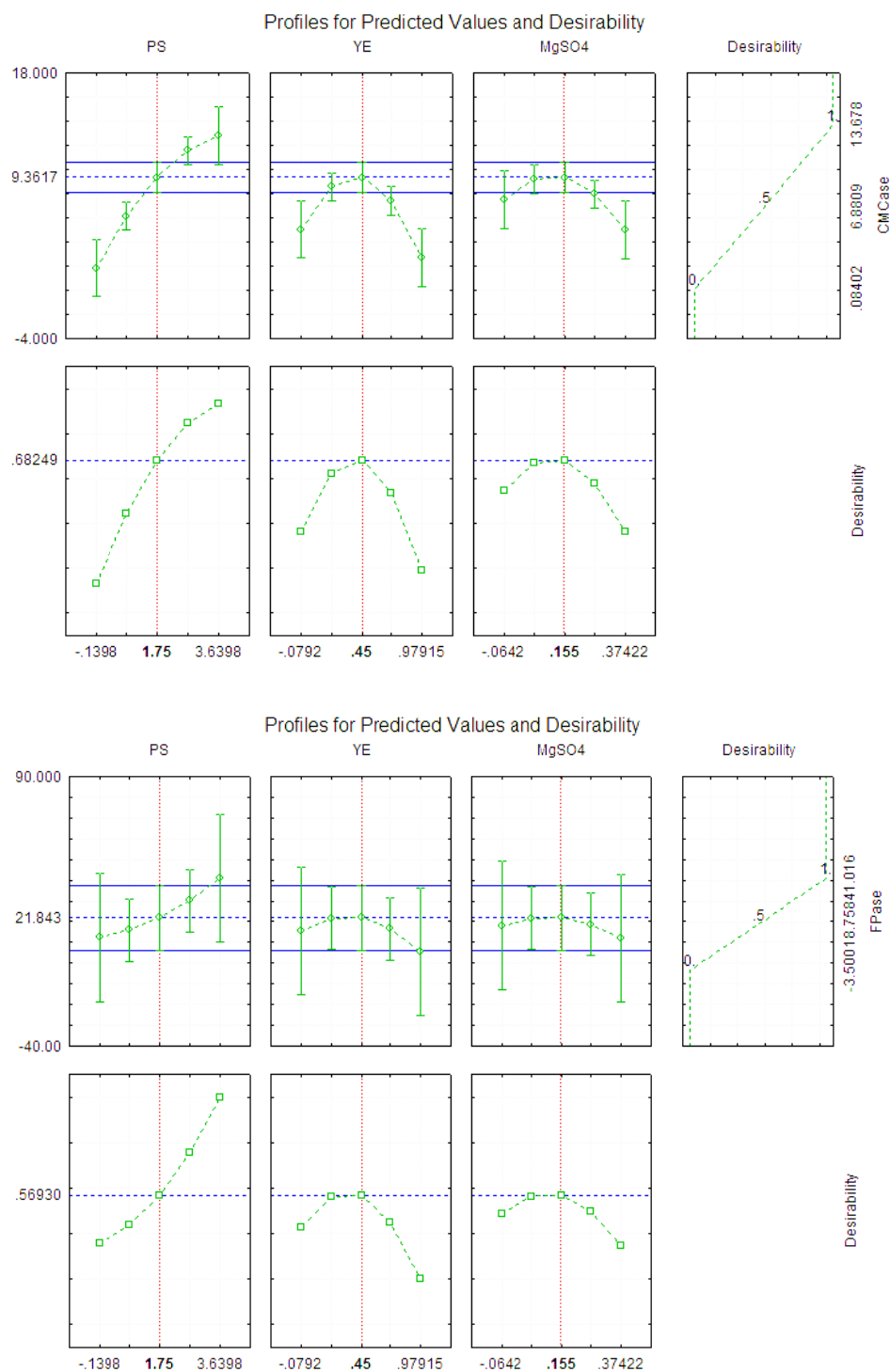


Figure 3 – Desirability of CMCCase and FPFase production

Saccharification. The crude enzyme which was produced from *Bacillus paralichniformis* in submerged fermentation was applied to hydrolyze peanut shell waste. The experiment was carried out for

different time periods and results (Figure 4) depicted the maximum total sugar (38.0 ± 0.23 mg/mL) production was observed at 8 h. Further increased time of incubation declined sugar production.

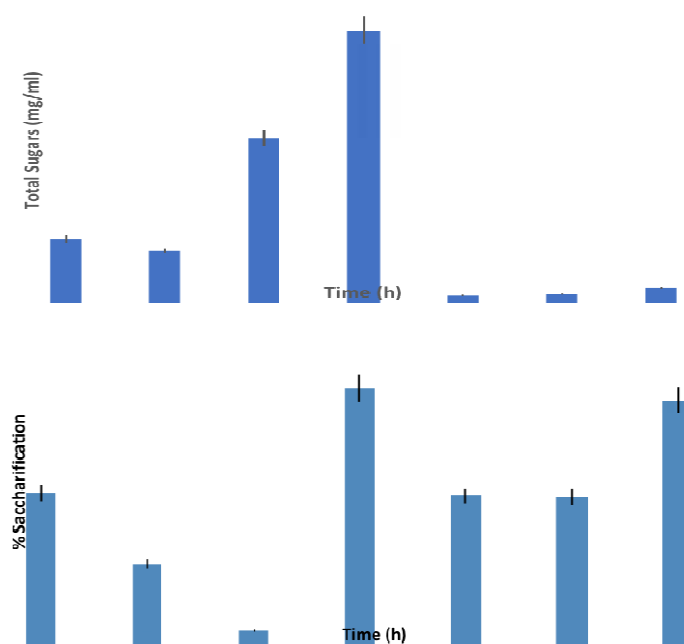


Figure 4 – Sugars released after enzymatic hydrolysis at various time period

As we know cellulase has major industrial role and now the increasing demands of renewable energy sources motivate biotechnologist to search for novel and better microbial strains and easy renewable sources of substrate, like agro-industrial wastes for the production of enzymes, using novel strain. *Bacillus subtilis* K18 had tremendous potential of cellulase production using a variety of substrates like saw dust [34], eucalyptus leaves [35], cotton stalk, peanut shells [36], potato peels [46], *Saccharum spontaneum* [37] and banana peduncle [31] through response surface methodology. Another study reported 0.037 IU/mL/min of CMCase from *Bacillus* sp. C1AC5507 using bagasse through RSM in submerged fermentation [38]. *Bacillus aquimaris* isolated from the gut of *Labeo rohita* has maximum endoglucanase producing potential of 437.3833 IU/mL/min in submerge fermentation [39].

Bacillus pumilis strain had potential of using sugarcane bagasse as carbon source for CMCase 13.6 IU/mL/min production in submerge fermentation [40]. *Aeromonas bestiarum* isolated from the gut of *Labeo rohita* gave the endoglucanase titer of 3.766 IU using sugarcane bagasse as substrate [41]. Medium components and type of substrate significantly affects cellulase production in submerge fermentation as described in previous study [42].

The ongoing study has been carried out with this perspective of easily available and renewable plus economical agro waste, i.e. peanut shell waste with a novel strain of *Bacillus paralichniformis*. The cellulase enzyme produced from this bacterium was further used for saccharification of peanut shells, which gave maximum sugar after 8 h of incubation period (Figure 4).

Another study reported maximum sugar production at 6 h for sugar beet pulp [43]. Saccharification of *Saccharum spontaneum* releasing maximum total sugars of 12.71 mg/mL after 20 h of incubation at 50°C [37]. Cellulase produced by the *Bacillus subtilis* K-18 has stimulated the 54.389% saccharification of pine needles [44]. Cellulase mediated saccharification by *Bacillus cereus* produced maximum total sugars of 31.42 mg/mL released after 6 h of incubation at 50 °C [45]. Wheat straw fermented with *Saccharomyces cerevisiae* under optimized condition of 2 % wheat straw, 0.5% enzyme concentration and 6 h of time period has been resulted in 40.15 % of saccharification [33]. Asghar et al. also reported 8 h of incubation time for maximum saccharification of wheat straw [46].

Conclusion

Results obtained within the current study prove that the novel strain *Bacillus paralichniformis* has

good industrial potential for cellulase production to perform cellulolytic functions, and it can also be used to convert lignocellulosic biomass into ethanol by saccharification.

Acknowledgment

This study was supported by Office of Research, Innovation and Commercialization, University of Sargodha, wide grant number UOS/ORIC/2016/39.

References

- Zhang W., Barone R. and Renneckar S. (2016). Enhanced enzymatic saccharification of pretreated biomass using glycerol thermal processing (GTP). *Bioresour Technol.*, vol. 199, pp. 148-154.
- Bhalla A., Bansal N., Kumar S., Bischoff M. and Sani K. (2013). Improved lignocellulose conversion to biofuels with thermophilic bacteria and thermostable enzymes. *Bioresour Technol.*, vol.128, pp. 751-759.
- Barakat A., de Vries H. and Rouau X. (2013). Dry fractionation process as an important step in current and future lignocellulose biorefineries: a review. *Bioresour Technol.*, vol. 134, pp. 362-373.
- Sun F., Zhao X., Hong J., Wang L., Sun H. (2016). Industrially relevant hydrolyzability and fermentability of sugarcane bagasse improved effectively by glycerol organosolv pretreatment. *Biotechnol Biofuels*, vol. 9, pp. 1-13.
- Chen M., Jia Z., Hu H., Zhao B. and Liu H. (2015). A comparison of several organosolv pretreatments for improving the enzymatic hydrolysis of wheat straw: substrate digestibility, fermentability and structural features. *Appl Energy*, vol. 150, pp. 224-232.
- Barakat A., Chuetor S., Monlau F., Solhy A. and Rouau X. (2014). Eco-friendly drychemo-mechanical pretreatments of lignocellulosic biomass: impact on energy and yield of the enzymatic hydrolysis. *Appl Energy*, vol.113, no.1, pp. 97-105.
- Hussain S., Siddique T., Saleem M., Arshad M. and Khalid A. (2009). Impact of Pesticides on Soil Microbial Diversity, Enzymes, and Biochemical Reactions. *Adv Agron.*, vol.102, pp. 160-190.
- Shin C.S., Lee J.P., Lee J.S. and Park S.C. (2000). Enzyme production of *Trichoderma reesei* Rut C-30 on various lignocellulosic substrates. *Appl Biochem Biotechnol.*, pp. 237-245
- López-Mondéjar R., Algora C. and Baldrian P. (2019). Lignocellulolytic systems of soil bacteria: a vast and diverse toolbox for biotechnological conversion processes. *Biotechnol adv.*, vol.37, no. 6, 03.013.
- Joachim H.J., Patrick A.N. (2008). Selected soil enzymes: examples of their potential roles in the ecosystem. *Afr J Biotechnol.*, vol. 7, no. 3, pp.181-191.
- Siddiqui K.S., Saqio A.A.N., Rashid M.H. and Rajoka M.I. (2000). Carboxyl group modification significantly altered the kinetic properties of purified carboxymethyl cellulase from *Aspergillus niger*. *Enzyme Microb Technol.*, vol. 27, pp. 467-474.
- Rashid B., Baba Z.A., Malik M.A., Mir A.H., Akhter F., Asif M., Zargar M.Y., Rashid N., Rashid N. and Maqbool S. (2019). Characterization of cellulolytic bacteria from waste dumping sites of Kashmir Himalaya. *Int J Curr Microbiol App Sci.*, vol. 8, no. 01, pp. 2033-2048.
- Patel A.K., Singhania R.R., Sim S.J. and Pandey A. (2019). Thermostable cellulases: current status and perspectives. *Bioresour Technol.*, vol. 279, pp. 385-392.
- Sreeja S.J., Jeba Malar P.W., Sharmila Joseph F.R., Steffi T., Grasian I. and Palavesam A. (2013). Optimization of cellulase production by *Bacillus altitudinis*. APS MSU and *Bacillus licheniformis* APS2 MSU, gut isolates of fish *Etroplus suratensis*. *IJOART*, vol. 2, pp. 401-406.
- Jecu L, (2000). Solid state fermentation of agricultural wastes for endoglucanase production. *Ind Crops Prod.*, vol. 11, no. 1, pp. 1-5.
- Sajith S., Priji P., Sreedevi S., and Benjamin S. (2016). An overview on fungal cellulases with an industrial perspective. *J Nutr Food Sci.*, vol. 6, no.1, p. 461.
- Sirohi R., Singh A. and Malik S. (2018). Production, characterization and industrial applications of cellulase derived from agro-waste. *Cur J Appl Sci Tech.*, pp. 1-9.
- Subramaniyam and Vimala R (2012). Solid state and submerged fermentation for the production of bioactive substances; a comparative study. *Int J Sci Nat.*, vol. 3, no. 3, pp. 480-486.
- Vidyalakshmi R., Paranthaman R. and Indhumathi J. (2009). Amylase production on submerged fermentation by *Bacillus spp.* *World J Chem.*, vol. 4, no.1, pp. 89-91.

20. Tolan J.S. and Foody B. (1999). Cellulase from submerged fermentation. In: Recent progress in bioconversion of lignocellulosics. Springer, Berlin, Heidelberg, pp. 41-67.
21. Tholudur A., Ramirez W.F. and McMillan J.D. (1996). Mathematical modeling and optimization of cellulase protein production using *Trichoderma reesei* RL-P37, *Biotechnol Bioeng.*, vol. 66, no.1, pp. 1-16.
22. Alvira P., Tomás-Pejó E. and Ballesteros M. (2010). Pretreatment technologies for an efficient bioethanol production process based on enzymatic hydrolysis. *Biores Technol.*, vol. 101, pp. 4851-4861.
23. Li C., Knierim B. and Manisseri C. (2007). Comparison of dilute acid and ionic liquid pretreatment of switchgrass: biomass recalcitrance, delignification and enzymatic saccharification. *Biores Technol.*, vol. 101, pp. 4900-4906.
24. Ferreira S., Duarte A.P., Ribeiro M.H., Queiroz J.A. and Domingues F.C. (2009). Response surface optimization of enzymatic hydrolysis of *Cistus ladanifer* and *Cytisus striatus* for bioethanol production. *Biochem Eng J.*, vol. 45, pp. 192-200.
25. Puri S., Beg Q.K. and Gupta R. (2002). Optimization of alkaline protease production from *Bacillus sp.* by response surface methodology. *Curr Microbiol.*, vol. 44, pp. 286-290.
26. Balusu R., Paduru R.R., Kuravi S.K., Seenayya G. and Reddy G. (2005). Optimization of critical medium components using response surface methodology for ethanol production from cellulosic biomass by *Clostridium thermocellum* SS19. *Process Biochem.*, vol. 40, pp. 3025-3030.
27. Wang Q., Ma H., Xu W., Gong L., Zhang W. and Zou D. (2008). Short communication: ethanol production from kitchen garbage using response surface methodology. *Biochem Eng J.*, vol. 39, pp. 604-610.
28. Coninck D.J., Bouquelet S., Dumortier V., Duyme V., Verdier and Denantes I. (2000). Industrial media and fermentation processes for improved growth and protease production by *Tetrahymena thermophila*. *J. Ind. Microbiol. Biotechnol.*, vol. 24, pp. 285-290.
29. Mei X., Liu R., Shen F and Wu H. (2009). Optimization of fermentation conditions for the production of ethanol from stalk juice of sweet sorghum by immobilized yeast using response surface methodology. *Energy Fuels*, vol. 23, pp. 487-491.
30. Shankar T. and Isaiarasu L. (2012). Statistical optimization for cellulase production by *Bacillus pumilus* EWBCM1 using response surface methodology. *Global J Biotech and Biochem.*, vol. 7, no.1, pp. 01-06.
31. Arooj A., Irfan M., Tabsum F., Shakir H.A., Qazi J.I. (2017). Effect of dilute sulphuric acid pretreatment on cellulase production by *Bacillus subtilis* K-18 through response surface methodology. *Proc Pak Ac Sci B; Life and Env Sci.*, vol. 54, no. 1, pp. 11-20.
32. Irfan M., Asghar U., Nadeem M., Nelofer R., Syed Q., Shakir H.A. and Qazi J.I. (2016). Statistical optimization of saccharification of alkali pretreated wheat straw for bioethanol production. *Waste Biomass Valor.*, vol. 7, pp.1389-1396.
33. Long C., Ou Y., Guo P., Liu Y., Cui J., Long M. and Hu Z. (2009). Cellulase production by solid state fermentation using bagasse with *Penicillium decumbens* L-06. *Annals Microbiol.*, vol. 59, pp. 517-523.
34. Anjum A., Irfan M., Tabsum F., Shakir Ha and Qazi J.I. (2017). Optimization of sulphuric acid pre-treatment of *Acacia* saw dust through Box-Bhenken Design for cellulase production by *B.subtilis*. *Adv Life Sci.*, vol. 5, no. 1, pp.19-24.
35. Iqbal S., Irfan M., Tabassum F., Shakir H.A., Qazi J.I. (2017). Application of Box-Behnken Design for optimization of different pretreatment conditions for cellulase production. *J Northeast Agric Univ. (eng.)*, vol. 24, no. 3, pp. 51-59.
36. Arshad F., Irfan M., Shakir H.A., Tabsum F. and Qazi J.I. (2017). Optimization of dilute sulphuric acid pre-treatments of peanut shells through Box-Bhenken Design for cellulase production by *Bacillus subtilis* K-18. *Punjab Univ J Zool.*, vol. 32, no. 1, pp. 81-90.
37. Ghazanfar M., Irfan M., Tabssum F., Shakir H.A. and Qazi J.I. (2018). Effect of different pretreatment conditions on *Saccharum spontaneum* for cellulase production by *B. subtilis* K-18 through Box-Bhenken Design. *Iran J Sci Technol A.*, vol. 42, no. 2, pp. 313-320.
38. Padilha Q.M., Carvalho L.C.T., Dias P.V.S., Grisi C.S.L., Honorato da Silva F.L., Santos S.F.M. and Araujo D.A.M. (2015). Production and characterization of thermophilic carboxymethyl cellulase synthesized by *Bacillus sp.* growing in sugarcane bagasse in submerged fermentation. *Braz J Chem.*, vol. 32, no. 1, pp. 35-42.
39. Khalid S., Irfan M., Shakir H.A., Qazi J.I. (2017). Endoglucanase producing potential of *Bacillus* species isolated from the gut of *Labeo rohita*. *J Mar Sci Tech.*, vol. 25, no. 5, pp. 581-587.
40. Chaudhary N., Qazi J.I. and Irfan M. (2017). Isolation and Identification of Cellulolytic

and Ethanologenic Bacteria from Soil. *Iran J Sci Technol Trans Sci.*, vol. 41, pp. 551-555.

41. Majeed H.S., Irfan M., Shakir H.A. and Qazi J.I. (2016). Filter paper activity producing potential of *Aeromonas* species isolated from the gut of *Labeo rohita*. *Pak J Zool.*, vol. 48, no. 5, pp. 1317-1323.

42. Arshad M., Irfan M., Rehman A., Nadeem M., Huma Z., Shakir H.A., Syed Q. (2017) Optimization for medium and substrate for CMCase production by *Bacillus subtilis* – BS06 in submerged fermentation and its applications in saccharification. *Punjab Univ J Zool.*, vol. 32, no.2, pp. 179-188.

43. Berłowska J., Pielech-Przybylska K., Balcerek M., Dziekońska-Kubczak U., Patelski P., Dziugan P. and Kręgiel D. (2016). Simultaneous saccharification and fermentation of sugar beet pulp

for efficient bioethanol production. *BioMed Res Int.*, 2016.

44. Irfan M., Mushtaq Q., Tabssum F., Shakir H.A. and Qazi J.I. (2017). Carboxymethyl cellulase production optimization from newly isolated thermophilic *Bacillus subtilis* K-18 for saccharification using response surface methodology. *AMB Express*, vol. 7, no. 1, p. 29.

45. Tabssum F., Irfan M., Shakir H.A., Qazi J.I. (2018). RSM based optimization of nutritional conditions for cellulase mediated Saccharification by *Bacillus cereus*. *J Med Biol Eng.*, vol. 12, no. 1, p. 7.

46. Asghar M., Irfan M., Iram Z., Huma R. Nelofer, Nadeem M., Syed Q. (2015). Effect of alkaline pretreatment on delignification of wheat straw. *Nat Prod Res.*, vol.29, no.2, pp. 125-131.

^{1*}S.Zh. Kolumbayeva , ¹A.V. Lovinskaya ,
¹N.T. Bekmagambetova , ^{2,3}S.K. Abilev 

¹Al-Farabi Kazakh National University, Almaty, Kazakhstan

²Vavilov Institute of General Genetics, Russia, Moscow

³Lomonosov Moscow State University, Russia, Moscow

e-mail: saule.kolumbayeva@kaznu.kz

Antimutagenic activity of medicinal plants *Salvia officinalis* L. and *Origanum vulgare* L. (family *Lamiaceae*)

Abstract: The search for effective protectors of natural origin to correct mutagenic and toxic effects does not lose its relevance due to the increase of environmentally hazardous factors in the environment. The mutagenic and antimutagenic effect on chromosomal aberrations in root tips of barley seeds germinated under infusions of medicinal plants of oregano (*Origanum vulgare*) and sage (*Salvia officinalis*) of the *Lamiaceae* family were investigated. The studied infusion with different methods of preparation (concentrated, diluted, and phytotea) did not show a mutagenic effect, the frequency of structural mutations in barley seeds treated with infusions was at the level of negative control. The ability of oregano and sage infusions to reduce induced mutagenesis was also established. The frequency of mutagen-induced chromosomal aberrations decreased statistically significant ($p < 0.01$) in the combined pre- and posttreatment of each infusion with methyl methanesulfonate (MMS, positive control). The level of inhibition of the mutation process depended on the sequence of treatment to infusions and mutagen, as well as the type of infusion. A comparative analysis of the results of combined treatment of barley seeds with mutagen and infusions of oregano and sage showed that the pretreatment infusions before mutagen more effectively reduces the level of induced mutagenesis than the posttreatment. The effectiveness of the antimutagenic action of the studied infusions evaluated by the reduction factor. The reduction factor in the infusion of diluted oregano and oregano tea was above 60%, which indicates the ability to inhibit MMS induced mutagenesis by *Origanum vulgare* infusions by 60%. The reduction factor of the concentrated sage infusion in barley seeds pretreatment with it was 51%, diluted sage infusions and tea was 70% and 71%, respectively. The reduction factor indicates the ability of *Salvia officinalis* infusions to inhibit MMS-induced mutagenesis by 50-70% with pretreatment on barley seeds. The obtained results indicate the presence of antimutagenic activity in the studied medicinal herbs due to the presence of different biologically active compounds. Infusions of medicinal plants of oregano and sage can recommend for the development of means of protecting the body from chemical mutagenic factors.

Key words: medicinal plants, biologically active compounds, mutagenic and antimutagenic activity, chromosomal aberrations.

Introduction

The ecological situation in Kazakhstan, as well as in the whole world, is far from prosperous and firstly caused by large-scale pollution of the environment by ecologically dangerous factors with toxic and mutagenic activity. Recently, an increase in the frequency of oncological and hereditary diseases has been observed, which poses a severe threat to the human population [1-3]. There is an increase in the genetic load in the populations of almost all species of organisms, which can lead and is already leading to a sharp decline in the number

and even the extinction of entire species. Sources of pollution, including road transport (flue gases), various industries (industrial waste, garbage), agriculture (pesticides, fertilizers), mining and processing industry, space industry are everywhere and contaminate the environment [4; 5]. The vast majority of environmental pollutants have toxic, cytotoxic, teratogenic effects. They are also likely to have carcinogenic and mutagenic activity [6]. In the body, they can activate free radicals, inhibit repair, or interact directly with DNA molecules. An essential role in the protection of genetic material and heredity is played by antimutagens, which can

neutralize the mutagen before it interacts with DNA and suppress its action, as well as activate the repair system [2; 7]. Therefore, the development and search for new sources of compounds with protective properties are undoubtedly relevant [8; 9]. Currently, chemically pure compounds and extracts from plants are used for this purpose. Antimutagenic properties have been identified in vitamins, amino acids, polyamines, endogenous antioxidants, and others. However, pure chemical compounds with antimutagenic action can have side effects. In this regard, drugs of natural origin are of great interest [7]. Besides, the process of obtaining drugs from plants is often more economically preferable than chemical synthesis [8].

Currently, medicinal plants arouse great interest as a promising source of biologically active compounds (BACs) with antioxidant and antimutagenic properties. Such substances can be used for a long time without harmful effects and have a complex effect on the body, as well as are relatively less allergenic in comparison with the synthetic analogs [10-13].

In Kazakhstan grows such medicinal species of plants of *Lamiaceae* family as *Salvia* (sage), *Mentha* (mint), *Melissa* (melissa), *Leonurus* (motherwort). Due to the phytochemical composition, medicinal plants of our republic have a broad pharmacological spectrum [14]. Therefore, screening of plants for genoprotective and antimutagenic potential is extremely promising. Screening and sampling of the most effective medicinal plants will allow us to offer certain species to create a collection of medicinal herbs that has genoprotective activity. The aim of the current research is the cytogenetic study of the mutagenic and antimutagenic activity of oregano (*Origanum vulgare*) and sage (*Salvia officinalis*) infusions of the *Lamiaceae* family on barley.

Materials and methods

Research objects. Barley of Baisheshek variety, which is zoned in Kazakhstan, was used for cytogenetic studies. Seeds of double-row barley (*Hordeum vulgare* L.) are widely used in cytogenetic studies, due to the small number ($2n=14$) and large size of chromosomes (length 6-8 microns). Another advantage of barley as a test object is the low natural mutation rate. At the same time, barley seeds have a sufficiently high sensitivity to various factors with mutagenic activity. Also, barley is widely used in various

studies on the biotesting of xenobiotics for mutagenicity and antimutagenicity [15].

Medicinal plants of the *Lamiaceae* family – oregano (*Origanum vulgare*) and sage (*Salvia officinalis*) were tested for antimutagenic activity. These herbs are rich in tannins, ascorbic acid, alkaloids, flavonoids, so they are in demand in traditional medicine. The natural level of mutation in seeds germinated on distilled water served as negative control. The standard mutagen methyl methanesulfonate (MMS, $C_2H_6O_3S$), a potent direct-acting alkylating agent, was used as positive control at a concentration of 10 mg/L [16]. MMS in standard short-term *in vivo* and *in vitro* tests shows mutagenic activity, in the *umu*-test induces the SOS response, in bacteria in the absence of metabolic activation induces point mutations. It also causes somatic and sex-linked recessive lethal mutations in *Drosophila*, induces neoplastic transformation in rodent cell cultures, *in vivo* causes mutations in germ cells of mice and in human cells *in vitro* causes the formation of micronuclei, single-strand DNA breaks, unscheduled DNA synthesis, gene mutations, and sister chromatid exchanges. The wide range of genetic activity shown above in the battery of different test systems explains the choice of methyl methanesulfonate as a positive control of genotoxic and mutagenic agents [16; 17].

Seed germination and cytogenic test. Barley seeds were treated separately with infusions of medicinal plants and mutagen before germination. Infusions were prepared according to the recipe on the pharmacy packaging. Three types of infusions were studied for mutagenic/antimutagenic activity: concentrated (according to the recipe), diluted (concentrated infusion diluted 2 times) and phytotea. To identify the antimutagenic activity of the studied plants, a combined treatment of barley with infusions and mutagen was performed. Seeds were taken in each infusion for 4 h. The treated seeds were washed and germinated in Petri dishes on filter paper moistened with distilled water in a thermostat at 25 ± 1 °C. A day later, germinated seeds with a length of primary roots 0.5 cm were transferred to filter paper moistened with a solution of 0.01% colchicine for 4 hours to accumulate metaphase plates. Then the roots were fixed using fixative (1:1 ethyl alcohol: glacial acetic acid), and after 24 h, they were transferred to 70% ethanol for long-term storage [18].

The fixed material was cold hydrolyzed in a diluted aqueous (1:1) cooled HCl solution for 40-50 min at 4°C. As a result of weak DNA hydrolysis,

free aldehyde groups are formed, which interact with the stain, and the chromosomes acquire a bright purple color. After staining, the roots were washed with freshly prepared sulphurous water to remove the stain that had not reacted with DNA from the cells. Next, maceration was carried out with the help of cytase (a mixture of cellulosic enzymes of the salivary gland of the grape snail), which destroys the intercellular substance and plant cell walls, contributing to the distribution of a monolayer of metaphase plates on the slide. The obtained cytological preparations were kept in a refrigerating chamber for 24 h at $74\pm 1^\circ\text{C}$ to obtain permanent preparations.

To determine the mutagenic/antimutagenic potential of infusions of medicinal plants, we used a metaphase method of chromosome analysis. It is widely used by researchers cytogenetic test provides information about the types of structural mutations and their frequency [1; 19]. Metaphase plates were analyzed on the optical microscope Olympus BX 43F (Olympus, Japan). About 500 metaphases were analyzed in each variant. The effectiveness of reducing the frequency of MMS-induced chromosomal aberrations (the effectiveness of antimutagens) was determined by the reduction factor (RF). The antimutagenic effect was considered moderate for 25-40% inhibition, strong for more than 40%,

and not recognized as a positive result for less than 25% inhibition.

Statistical analysis. Statistical analysis of the results was carried out using the Analysis ToolPak in Microsoft Excel, Star Plus, and WinPepi. In each variant, the mean values and the standard errors of the means were calculated. Student's test was used to establish the reliability of differences between mean values of the different variants. The differences between the data were considered statistically significant with a confidence probability of 0.95.

Results and discussion

Analysis of the genetic activity of oregano and sage infusions was performed in two stages. At the first stage, mutagenic activity of infusions of different concentrations was studied in order to select such variants that would not give a mutagenic effect. At the second stage, DNA-protective activity of infusions was studied at combined action with mutagen on barley seeds.

The study of mutagenic and antimutagenic activity of oregano (Origanum vulgare L.). The results of cytogenetic study of the root tip cells of barley seeds separately and combined treated with MMS and infusions of different concentrations of oregano presented in Table 1.

Table 1 – Frequency and spectrum of structural chromosome disorders induced in barley seeds by separate and combined treatment with methyl methanesulfonate and oregano infusions

Experiment variation	Total studied cells	Frequency of aberrant cells (M \pm m%)	Number of chromosomal aberrations per 100 metaphase cells		
			total aberrations	chromosomal type	chromatid type
Water (negative control)	480	1.25 \pm 0.51	1.46 \pm 0.55	0.83 \pm 0.41	0.63 \pm 0.36
MMS, 10 mg/L (positive control)	450	5.33 \pm 1.06*	6.44 \pm 1.16*	2.22 \pm 0.69	4.22 \pm 0.95*
Concentrated infusion	495	1.82 \pm 0.60	2.22 \pm 0.66	0.81 \pm 0.40	1.41 \pm 0.53
Diluted infusion	500	1.20 \pm 0.49	1.20 \pm 0.49	0.60 \pm 0.35	0.60 \pm 0.35
Phytotea	490	1.22 \pm 0.50	1.43 \pm 0.54	0.61 \pm 0.35	0.82 \pm 0.41
Concentrated infusion + MMS	500	3.60 \pm 0.83	3.80 \pm 0.86	1.40 \pm 0.53	2.40 \pm 0.68
Diluted infusion + MMS	490	2.24 \pm 0.67*	2.24 \pm 0.67**	0.82 \pm 0.41	1.43 \pm 0.54*
Phytotea + MMS	490	2.04 \pm 0.64**	2.24 \pm 0.67**	1.02 \pm 0.45	1.22 \pm 0.50**
MMS + concentrated infusion	480	4.17 \pm 0.91	4.58 \pm 0.95	1.67 \pm 0.58	2.92 \pm 0.77
MMS + diluted infusion	490	2.86 \pm 0.75	3.06 \pm 0.78*	1.02 \pm 0.45	2.04 \pm 0.64
MMS + phytotea	510	2.94 \pm 0.75	3.33 \pm 0.79*	1.18 \pm 0.48	2.16 \pm 0.64

Note: * – $p < 0,001$ in comparison with the negative control;
 • – $p < 0,05$; ** – $p < 0,01$ compared to methyl methanesulfonate

From the results, the frequency of aberrant cells in the control variant, when the seeds were germinated on distilled water, was 1.25 %. The number of chromosomal aberrations per 100 analyzed metaphases was already higher because in 1 cell were observed 2 chromosome structural abnormalities. The ratio of chromosomal and chromatid rearrangements was almost equal and amounted to 0.83% and 0.63%, respectively.

The frequency of aberrant cells and the number of chromosomal aberrations per 100 metaphases in the cells of the root tip cells of MMS-treated seeds dramatically increased, compared to the control variant. The frequency of aberrant cells and the number of chromosomal aberrations per 100 metaphases significantly ($p < 0.001$) increased by 4.3

times. The increase in the level of chromosome rearrangements occurred both due to structural mutations of chromosomal and chromatid types. Moreover, the frequency of chromatid-type abnormalities increased by 6.7 times ($p < 0.001$), and the chromosome type – by 2.7 times. The obtained results indicate a high sensitivity of the genetic material to the mutagenic action of MMS in the synthesis phase (S) and postsynthetic phase (G_2) of the cell cycle. The spectrum of chromosomal aberrations was quite wide. Paired terminal deletions, paired point fragments represented chromosomal rearrangements, chromatid-type were represented by single terminal fragments and acentric single rings. Besides, it was noted abnormal anaphases, which were absent in the negative control (Figure 1).

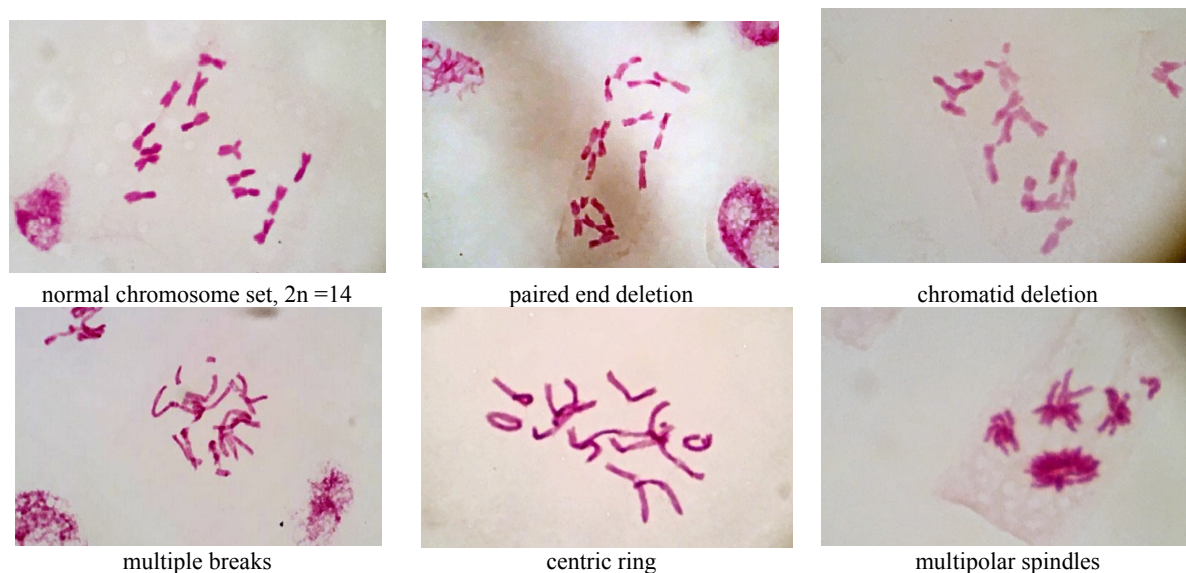


Figure 1 – Structural chromosome disorders induced by MMS, x1000

Treatment of seeds with oregano infusions of different concentrations did not show any mutagenic effect. The level of chromosomal aberrations in all three variants of seed treatment with infusions was at the same level as control. There was an increase of 1.5 times in the frequency of aberrant cells and the number of chromosomal aberrations per 100 metaphases in the treatment of seeds with a concentrated oregano infusion compared to the

control, but this difference was not statistically significant. Therefore, the results obtained in this series of experiments indicate the absence of mutagenic activity in oregano infusions in the used concentrations.

In the next series of experiments was studied, the ability of oregano infusions to modify the mutagenic effect of methyl methanesulfonate in their combined effect on barley seeds (Table 2).

Table 2 – Frequency and spectrum of structural chromosome disorders induced in barley seeds by separate and combined treatment with methyl methanesulfonate and sage infusions

Experiment variation	Total studied cells	Frequency of aberrant cells (M ± m%)	Number of chromosomal aberrations per 100 metaphase cells		
			total aberrations	chromosomal type	chromatid type
Water (negative control)	480	1.25±0.51	1.46±0.55	0.83±0.41	0.63±0.36
MMS, 10 mg/L (positive control)	450	5.33±1.06*	6.44±1.16*	2.22±0.06	4.22±0.95*
Concentrated infusion	510	2.16±0.64	2.94±0.75	1.18±0.48	1.76±0.58
Diluted infusion	490	1.43±0.54	1.63±0.57	0.82±0.41	0.82±0.41
Phytotea	475	1.68±0.59	1.68±0.59	1.05±0.47	0.63±0.36
Concentrated infusion + MMS	540	2.78±0.71*	3.15±0.75*	1.30±0.49	1.85±0.58*
Diluted infusion + MMS	510	1.76±0.58**	1.96±0.61***	0.78±0.39	1.18±0.48**
Phytotea + MMS	490	1.84±0.61**	1.84±0.61***	0.82±0.41	1.02±0.45**
MMS + concentrated infusion	480	3.13±0.79	3.75±0.87	1.46±0.55	2.29±0.68
MMS + diluted infusion	515	3.11±0.76	3.30±0.79*	1.36±0.51	1.94±0.61*
MMS + phytotea	510	3.14±0.77	3.53±0.82*	1.18±0.48	2.36±0.67

Note: * – p<0.001 in comparison with the negative control;
 • – p<0.05; ** – p<0.01 compared to methyl methanesulfonate

As can be seen from the presented results, pretreatment of barley seeds with concentrated infusion of oregano reduced the occurrence of MMS-induced structural mutations by 1.7 times. However, the observed decrease was not statistically significant.

As a result of pretreatment of seeds with diluted oregano infusion and oregano phytotea with subsequent treatment of MMS, a statistically significant decrease in the level of MMS-induced mutagenesis was observed. In the variant with a diluted infusion, the frequency of aberrant cells induced by MMS was reduced by 2.3 times (p<0.05). The number of chromosomal aberrations per 100 metaphases decreased by 2.9 times (p<0.01) compared to the MMS treatment. The decrease in the level of chromosomal aberrations occurred both due to rearrangements of chromosomal and chromatid types. There was a statistically significant (p<0.05) decrease in the level of chromatid rearrangements.

Oregano phytotea also significantly reduced the frequency of aberrant cells and the level of chromosomal aberrations induced by the mutagen. Thus, the frequency of cells with chromosome rearrangements induced by MMS decreased from 5.33% to 2.04%, i.e., 2.6 times (p<0.01). The number of chromosomal aberrations per 100 cells decreased from 6.44% to 2.24%, which was 2.9 times (p<0.01). At the same time, there was a statistically significant decrease in the level of

structural rearrangements of chromatid type (p<0.01).

In the seed posttreatment (first mutagen, and then treatment with infusion), the modifying effect mutagenic action of MMS was slightly different. So, in the posttreatment of concentrated oregano infusion after mutagen, the frequency of aberrant cells decreased by 1.3 times compared to the variant of separate treatment of MMS, and the number of chromosomal aberrations per 100 cells – by 1.4 times. The level of chromosomal rearrangements decreased by 1.3 times, and chromatid type – by 1.5 times. However, the observed decrease in MMS-induced mutagenesis was not statistically significant. In variants with seed posttreatment with diluted oregano infusion and oregano phytotea after MMS, a statistically significant decrease in the number of chromosomal aberrations per 100 cells was observed, by 2.1 times (p<0.05) and 1.9 times (p<0.05), respectively.

The obtained results indicate the ability of oregano infusions to modify methyl methanesulfonate-induced mutagenesis in the direction of its decrease. This fact allows us to assume that the complex of biologically active compounds contained in oregano has antimutagenic activity. Moreover, the antimutagenic activity of oregano infusions depends on their concentration. In this case, the concentrated infusion, in contrast to the diluted infusion and oregano tea, did not give a statistically significant antimutagenic effect.

Comparative analysis of the results of combined treatment of barley seeds with mutagen and oregano infusions showed that the pretreatment of infusions effectively reduces the level of induced mutagenesis than the posttreatment.

The effectiveness of the antimutagenic action of oregano was evaluated by the reduction factor. The reduction factor in the diluted oregano infusion and oregano tea was above 60%. It indicates the ability of *Origanum vulgare* infusions to inhibit the mutagenesis MMS-induced mutagenesis by 60%. The obtained results suggest a strong antimutagenic effect, given by diluted infusions of the medicinal plant oregano that contains biologically active compounds.

The study of the mutagenic and antimutagenic activity of infusions from the medicinal plant sage (Salvia officinalis L.). Results of cytogenetic study of the barley root meristem cells separately and mutually treated with MMS and sage infusions of different concentrations are presented in Table 2. All variants of sage infusions in barley seed treatment did not significantly increase the frequency of aberrant cells and the level of chromosomal aberrations by 100 metaphases compared to the negative control. So, if these indicators in the control were 1.25% and 1.46 per 100 metaphases, then after seed treatments with concentrated, diluted infusions and phytotea indicators show – 2.16% and 2.94, 1.43% and 1.63, 1.68% and 1.68, respectively. However, it should be noted that in the treatment with concentrated sage infusion, these indicators were higher by 1.7 and 2.0 times, respectively, but the difference was not statistically significant. The results in these experiment series indicate the absence of mutagenic activity in sage infusions in the used concentrations.

In the next series of experiments, barley seeds were successively treated first with sage infusions, and then with MMS mutagen in order to establish the presence or absence of antimutagenic potential in the infusions of this medicinal plant. In «concentrated infusion + MMS» combination (pretreatment) sage significantly reduced the frequency of aberrant cells and the number of chromosomal aberrations per 100 metaphases by 1.9 times ($p < 0.05$) and 2.0 times ($p < 0.05$), respectively, compared to MMS treatment. At the same time, there was a statistically significant decrease in the number of chromatid-type structural aberrations (single terminal fragments, acentric rings, micro fragments) by 2.3 times ($p < 0.05$).

As a result of barley seed pretreatment with diluted sage infusion and sage phytotea, the inhibition degree of MMS-induced mutagenesis significantly increased. Thus, in the variant with a diluted sage infusion, the frequency of aberrant cells and the number of chromosomal aberrations per 100 metaphases decreased by 3.1 ($p < 0.01$) and 3.3 times ($p < 0.001$), respectively, compared to treatment with MMS. A statistically significant decrease in these indicators happened due to structural rearrangements of the chromatid type ($p < 0.01$). Pretreatment with sage phytotea before MMS significantly reduced the occurrence of mutagen-induced chromosomal aberrations. Also, the level of aberrant cells fell from 5.33% to 1.84% ($p < 0.01$), and the number of chromosomal aberrations per 100 metaphases decreased from 6.44 to 1.84 ($p < 0.001$). In this variant, was observed a statistically significant ($p < 0.01$) decrease in the frequency of chromatid type rearrangements by 4.1 times.

In the seed posttreatment (MMS + sage), the effect of sage modification of MMS-induced mutagenesis was significantly weaker and was not noticed in all treatment variants. Thus, with barley posttreatment after a mutagen with concentrated infusion, there was a tendency to a decrease in all studied parameters, that is, the frequency of aberrant cells, the number of chromosomal aberrations by 100 metaphases and the number of rearrangements of the chromosomal and chromatid types. However, the observed decrease in the level of MMS-induced mutagenesis was not statistically significant.

In variants with seed posttreatments with diluted sage infusion and sage phytotea after MMS, there was a statistically significant decrease in the number of chromosomal aberrations per 100 cells by 2.0 and 1.8 times ($p < 0.05$), respectively. The number of structural mutations of chromatid type ($p < 0.05$) also significantly decreased in the variant with seed posttreatment with diluted infusion after MMS.

The obtained results indicate the ability of sage infusions, depending on its concentration, to significantly modify the level of induced mutagenesis in the direction of its decrease. When sage infusions exposures combined with mutagen, there was a statistically significant decrease in the frequency of chromosomal aberrations induced by MMS. It should be noted, that the degree of inhibition of induced mutagenesis depended not only on the concentration of infusions, but also on the sequence of their treatment on the studied test object.

This fact allows us to assume that the complex of biologically active compounds contained in sage, has antimutagenic activity. Comparative analysis of the results of combined treatment of barley seeds with mutagen and sage infusions showed that the pretreatment of infusions reduces the level of induced mutagenesis more effectively than the posttreatment, same as in the case of oregano.

The effectiveness of the antimutagenic action of sage was evaluated by the reduction factor. The reduction factor in the pretreatment of barley seeds with concentrated infusion was 51%, with diluted sage infusion and sage phytotea was 70% and 71%, respectively. The reduction factor indicates the ability of *Salvia officinalis* infusions to inhibit MMS-induced mutagenesis by 50-70% in case of barley pretreatment. The reduction factor at the posttreatment after MMS influence of infusions was 49-45%. The obtained results indicate the presence of antimutagenic activity in sage infusions, due to the presence of different biologically active compounds in plants of this species.

Thus, cytogenetic studies were carried out on barley seeds, separately and combined treated with infusions of different concentrations of two species of medicinal plants from the family *Lamiaceae* – oregano (*Origanum vulgare* L.) and sage (*Salvia officinalis* L.). The established antimutagenic activity of infusions from medicinal plants was presented in a statistically significant decrease in the level of chromosomal aberrations induced by the classical mutagen methyl methanesulfonate. There were no statistically significant differences in the level of modification of the mutagenic effect of MMS with the studied infusions containing biologically active compounds.

Environmental pollution by hazardous agents with genetic activity significantly increases the risk of hereditary pathologies in newborns, malignant neoplasms and other diseases in the population. Therefore, one of the priorities of the state is its genetic safety. Within the framework of this problem, there is increasing interest in the process of reducing and leveling spontaneous or induced mutagenesis and in the general phenomenon of antimutagenesis. Therefore, the search and detection of compounds with antimutagenic activity are one of the most promising areas of research in recent years [9].

Numerous studies indicate that plants play an important role in maintaining human health. According to the World Health Organization, more than half of the world's population uses alternative

medicine based on medicinal plants along with traditional medicine [20-22]. In recent decades, natural antioxidants have attracted attention for their protective effect, against toxicity and genotoxicity, caused by various physical and chemical agents. Many researchers note that the use in everyday life of various natural antimutagenic and antigenotoxic compounds that can reduce genetic material damage can prevent the development of cancer in humans [21-23]. There are two groups of antimutagens – desmutagens and bioantimutagens. The desmutagen removes genotoxic agents from the body or inactivates mutagens partially or completely before interacting with DNA. Bioantimutagen can participate in the processes of repairing damaged DNA. The mechanism, effectiveness, and spectrum of action of antimutagens can be different [1; 9; 24].

Currently, a large number of antimutagens of different nature have been revealed. The mechanism of action of many of them is still completely unknown, which is why they have not been widely used [24; 25]. In addition, the assessment of their harmlessness to the human has not been fully done, traditional pharmacotoxicological studies have not been carried out. This is why the search for inhibitors of induced mutagenesis among medicinal plants widely used in traditional medicine is the most promising. The antimutagenic effect of herbal preparations is due to the presence of biologically active compounds in them, primarily vitamins, phenols, polyphenols, pigments, amino acids and others [26; 27].

Based on the above, we performed cytogenetic studies of antimutagenic activity of two species of medicinal plants from the family *Lamiaceae* that widely used in traditional medicine – oregano (*Origanum vulgare* L.) and sage (*Salvia officinalis* L.). Antimutagenic activity of infusions of these medicinal plants was demonstrated in a significant decrease in the frequency of chromosomal aberrations induced by the classical mutagen methyl methanesulfonate. There were no statistically significant differences in the level of modification of the mutagenic effect of MMS by infusions of different concentrations. Also, there were no statistically significant differences in the degree of antimutagenic activity of oregano and sage infusions with MMS-induced mutagenesis.

Origanum and *Salvia* plants from *Lamiaceae* family have anti-inflammatory, antioxidant, sedative, antibacterial, wound healing, toning, antiseptic effects, which are used in diseases of the upper respiratory tract and gastrointestinal tract.

Sage leaves contain essential oils (up to 2%) that include camphor, cineol, D- α -pinene, α - and β -thujone, D-borneol, tannins, alkaloids, some acids, sodium, potassium, calcium, vitamins A, C, E, K, fiber and flavonoids. Oregano herb contains 0.3 to 1% essential oil, which includes phenols (up to 44%) – thymol and its isomer carvacrol, bi- and tricyclic sesquiterpenes (12.5%); tannins, ascorbic acid, and flavonoids.

The composition of medicinal plants includes many natural phenolic antioxidants, which cause their antioxidant, anti-inflammatory, antimicrobial, antispasmodic and neuroprotective effects. Phenolic and polyphenolic compounds are involved in redox reactions and in the processes of neutralization of reactive oxygen species. There is data on the presence of antimutagenic and anticancerogenic activity of polyphenols [28].

Phytochemicals influence the processes of metabolism and neutralization of xenobiotics, including carcinogens and mutagens. They can bind free radicals and reactive metabolites of xenobiotics, inhibit enzymes that activate xenobiotics, and activate detoxification enzymes [24]. A comprehensive study of plant compounds as potential protectors for the toxic, genotoxic and mutagenic effects of various environmental pollutants on the body is required.

Conclusion

In the present study, cytogenetic studies were carried out on barley seeds, separately and mutually with infusions of different concentrations of two species of medicinal plants from the family *Lamiaceae* – oregano (*Origanum vulgare* L.) and sage (*Salvia officinalis* L.). Antimutagenic activity of infusions from medicinal plants was noted by a statistically significant decrease in the level of chromosomal aberrations induced by the classical mutagen methyl methanesulfonate. No statistically significant differences in the level of modification of the mutagenic effect of MMS with the studied infusions containing biologically active compounds were revealed.

References

1. Abilev S.K., Glazer V.M. (2015) Mutagenez s osnovami genotoksikologii [Mutagenesis with the basics of genotoxicology]. Moscow; Saint-Petersburg: Nestor-Istoriya, 304 p.
2. Mukhametzhanova Z.T. (2017) Sovremennoe sostoyanie problemy zagryazneniya okruzhayushchey sredy [Current state of the problem of environmental pollution]. *Gigiena truda i meditsinskaya ekologiya*, vol. 55, no 2, pp. 11-20.
3. Moroz V.V., Smirnova S.G., Ivanova O.V., Poroshenko G.G. (2007) Mutatsii i antimutageny v meditsine kriticheskikh sostoyaniy [Mutations and antimutagens in critical state medicine]. *Obshchaya reanimatologiya*, no. 5-6, pp. 213-217.
4. Kolumbayeva S.Zh., Begimbetova D.A. (2013) Mutagennye efekty khimicheskikh zagryazniteley okruzhayushchey sredy [Mutagenic effects of chemical environmental pollutants]. Almaty: Qazaq universiteti, 196 p.
5. Ilyushina N.A., Egorova O.V., Masal'tsev G.V., Aver'yanova N.S., Revazova Yu.A. (2017) Mutagennost' i kantserogennost' pestitsidov, opasnost' dlya zdorov'ya cheloveka. Sistemicheskiy obzor. [Mutagenicity and carcinogenicity of pesticides, danger to human health. Systematic review]. *Zdravookhranenie Rossiyskoy Federatsii*, vol. 61, no. 2, pp. 96-102.
6. Carpenter D.O. (2013) Exposure to chemicals and radiation during childhood and risk for cancer later in life. *Journal of Adolescent Health*, vol. 52, no. 5, pp. S21-S29. doi: 10.1016/j.jadohealth.2013.01.027
7. Durnev A.D. (2018) Antimutagenez i antimutageny [Antimutagenesis and antimutagens]. *Fiziologiya cheloveka*, vol. 44, no. 3, pp. 116-137.
8. Efimov S.N., Dmitruk S.I., Il'inskiy N.N. (2004) Antimutagennaya aktivnost' lekarstvennykh rasteniy Sibirskogo regiona. [Antimutagenic activity of medicinal plants of the Siberian region] *Byulleten' sibirskoy meditsiny*, no. 3, pp. 17-26.
9. Słoczyńska K., Powroźnik B., Pękała E., Waszkielewicz A.M. (2014) Antimutagenic compounds and their possible mechanisms of action. *J. Appl. Gen.*, vol. 55, no. 2, pp. 273-285. doi: 10.1007/s13353-014-0198-9
10. Safonov N.N. (2013) Lekarstvennye rasteniya: illyustrirovanny atlas. [Medicinal plants: illustrated atlas]. M.: Eksmo, pp. 305-307.
11. Goncharova R.I., Kuzhir T.D. (2005) Molekulyarnye osnovy primeneniya antimutagenov v kachestve antikantserogenov. [Molecular basis of applying antimutagens as anticarcinogens] *Ekologicheskaya genetika*, vol. 3, no. 3, pp. 19-32.
12. Uzun F., Kalender S., Durak D. et al. (2009) Malathion-induced testicular toxicity in male rats and the protective effect of vitamins C and E. *Food*

Chem. Toxic., vol. 47, no. 8, pp. 1903-1908. doi: 10.1016/j.fct.2009.05.001

13. Chen K.-H., Wang, K.-J., Wang K.-M. et al. (2014) Applying particle swarm optimization-based decision tree classifier for cancer classification on gene expression data. *Appl. Soft Comp.*, vol. 24 (C), pp. 773-780. doi: 10.1016/j.asoc.2014.08.032.

14. Loseva I.V. (2008) Syr'evaya baza lekarstvennykh rasteniy Kazakhstana i ee ratsional'noe ispol'zovanie [The raw material base of medicinal plants of Kazakhstan and its rational use]. Karaganda, 110 p. (In Russian).

15. Georgieva M., Gecheff K. (2013) Molecular Cytogenetic Characterization of a New Reconstructed Barley Karyotype. *Biotechnology and Biotechnological Equipment*, vol. 27, no. 1, pp. 3577-3582. doi: 10.5504/BBEQ.2012.0126

16. Oshida K., Iwanaga E., Miyamoto K., Miyamoto Y. (2010) Comet assay in murine bone-marrow cell line (FDC-P2). *Toxicol in vitro*, vol. 24, no. 3, pp. 1039-1044. doi: 10.1016/j.tiv.2009.11.014

17. Smirnikhina S.A., Strel'nikov V.V., Voronina E.S., Tanas A.S., Lavrov A.V. (2013) Mutagen influence with different mechanisms of action on DNA global methylation in human whole-blood lymphocytes *in vitro*. *Rus J Gen.*, vol. 49, no. 7, pp. 765-770. doi: 10.1134/S1022795413060124

18. Pausheva Z.P. (1988) Praktikum po tsitologii rasteniy [Practicum on plant cytology]. Moscow: Agropromizdat, 271 p.

19. Daev E.V., Dukel'skaya A.V., Barabanova L.V. (2014) Tsitogeneticheskie metody indikatsii ekologicheskoy napryazhennosti v vodnykh i nazemnykh biosistemakh [Cytogenetic methods for indicating environmental stress in aquatic and terrestrial biosystems]. *Ekol. genetika*, vol.12, no. 2, pp. 3-12.

20. Mendoza-Pérez J.A., Fregoso-Aguilar T.A. (2013) Chemistry of natural antioxidants and studies performed with different plants collected in Mexico. Rijeka, Croatia: InTech, pp. 59-85.

21. Barranco-Pedraza L.M., Batista-Hernández I.L. (2013) Social contribution of traditional and natural medicine in the Cuban public health. *Rev. Human Med.*, vol.3, no. 13, pp. 713-727.

22. López-Romero D., Izquierdo-Vega J.A., Morales-González J.A., Madrigal-Bujaidar E., Chamorro-Cevallos G., Sánchez-Gutiérrez M., Betanzos-Cabrera G., Álvarez-González I., Morales-González Á., Madrigal-Santillán E. (2018) Evidence of Some Natural Products with Antigenotoxic Effects. Part 2: Plants, Vegetables, and Natural Resin. *Nutrients*, vol. 10, no. 12, pp. 1954. doi: 10.3390/nu10121954

23. Madrigal-Santillán E., Madrigal-Bujaidar E., Cruz-Jaime S., Valadez-Vega M.C., Sumaya-Martínez M.T., Pérez-Ávila K.G., Morales-González J.A. (2013) The Chemoprevention of Chronic Degenerative Disease Through Dietary Antioxidants: Progress, Promise and Evidences. Rijeka, Croatia: InTech, pp. 155-185.

24. Morales-González J.A., Madrigal-Bujaidar E., Sánchez-Gutiérrez M., Izquierdo-Vega J.A. (2019) Garlic (*Allium sativum* L.) A brief review of its antigenotoxic effects. *Foods*, vol. 8, no. 8, pp. 343. doi: 10.3390/foods8080343

25. Mosovska S., Mikulasova M., Brindzova L. (2010) Genotoxic and antimutagenic activities of extracts from pseudocereals in the *Salmonella* mutagenicity assay. *Food Chem. Toxicol.*, Vol. 48, no. 6, pp. 1483-1487.

26. Ammosov A.S., Litvinenko V.I. (2003) Fenol'nye soedineniya rodov *Glycyrrhiza* L. i *Meristotropis* Fisch. et Mey [Phenolic compounds of the genera *Glycyrrhiza* L. and *Meristotropis* Fisch. et Mey]. *Farmakom.*, no. 2, pp. 34-80.

27. Vasilyeva I.M., Shagirova Zh.M., Sinelshikova T.A., Mavletova D.A., Kuzmina N.S., Zasukhina G.D. (2009) Protection of radiosensitive human cells against the action of heavy metals by antimutagens and adapting factors: association with genetic and protein polymorphisms. *Rus J Gen.*, vol. 45, no. 6, pp. 659-662. doi: 10.1134/S1022795409060040

28. Maslennikov P.V., Chupakhina G.N., Skrypnik L.N. (2013) Soderzhanie fenol'nykh soedineniy v lekarstvennykh rasteniyakh botanicheskogo sada. [The content of phenolic compounds in medicinal plants of the botanical garden] *Izvestiya RAN. Seriya biologicheskaya*, no. 5, pp. 551-557.

¹S. Abbaszadeh, ²M. Nikbakht, ^{3*}P. Ramezannezhad,
⁴M. Sagharjoghi Farahani, ⁵S.A.Y. Ahmadi, ¹A. Safarzadeh

¹Department of Clinical Biochemistry, Lorestan University of Medical Sciences, Khorramabad, Iran

²Department of Medical Nanotechnology, Tehran University of Medical Sciences, Tehran, Iran

³Cellular and Molecular Research Center, Shahrekord University of Medical Sciences, Shahrekord, Iran

⁴Islamshahr Branch, Islamic Azad University, Islamshahr, Iran

⁵Pediatric Growth and Development Research Center,

Institute of Endocrinology and Metabolism; University of Medical Sciences, Tehran, Iran

*e-mail: ramezannezhad.p@gmail.com

Some issues of nanometals applications in cancer treatment

Abstract: Nanotechnology and the use of innovative materials, such as nanoparticles, have created a new and effective approach to fight cancer. Several achievements in cancer therapy using metal nanoparticles and challenges facing them are presented in the current review. Cancer therapy requires teamwork with a multidisciplinary approach. It has different levels according to the type of cancer, including chemotherapy (induction, neoadjuvant, adjuvant, consolidation or maintenance chemotherapy), radiotherapy and surgical resection. Nanometals and nanodrugs may be used on the different levels of cancer therapy, especially in chemotherapy. Platinum (Pt)-based drugs are one group of the most effective drugs used for cancer chemotherapy. Gold nanoparticles are the other group of nanometals commonly used in cancer treatment. Although effectiveness of nanometals including gold-, silver-, and iron-based, has been investigated on different cancer cell lines and animal models both *in vitro* and *in vivo*, their effectiveness should also be explored from the viewpoints of evidence-based medicine.

Key words: cancer, chemotherapy, nanoparticle, nanometal, platinum, gold, silver.

Introduction

Cancer therapy is a multidisciplinary effort that requires involvement of different specialties, each providing specific services to the patient with the aim of ensuring that the patient receives optimum care and support. However, any innovation cannot be used directly in clinical practice, since any novel idea may intervene in the accepted procedure of therapy. Such challenges are now going to be solved thanks to evidence-based medicine (EBM) [1; 2]. Use of innovative materials, such as up-conversion nanoparticles, nanogold, quantum dots, magnetic nanoparticles and nanodiamonds has created a new and effective approach to fight cancer. Use of nanoparticles led to many opportunities in cancer diagnosis and treatment. Hybrid proteins and nanostructures can be used to affect in different ways affecting the tumor, for instance, by creating magnetic field, temperature, light, etc. To date, substantial accomplishments have been achieved, but in spite of all successes, many problems like biocompatibility, selective drug trans-

fer, pharmacokinetics, safety and success of the chosen treatment remain unresolved [3].

In this regard, we performed this review to discuss novel achievements of metal nanoparticles in cancer therapy and challenges facing them.

Multi-subject cancer therapy

Cancers are usually represented by hematologic malignancies and malignant solid tumors [4]. Solid tumors are mainly carcinoma (epithelial origin) and sarcoma (mesenchymal origin), transition from epithelial origin to mesenchymal origin may occur as well [5; 6].

The general protocol of cancer therapy includes different levels of chemotherapy, radiotherapy, medical and palliative therapy, and surgery. In hematologic malignancies, the first level is induction [7]. The chemotherapy at this level results in reduction of malignant cell numbers from 10^{11} to 10^9 (approximately 99%) within one month. The clinical manifestation of this reduction is named complete remis-

sion [8]. Patients are then prepared for consolidation therapy (a 1 to 2-month period). Thereafter, the remaining malignant cells should be destroyed during a 1 to 2-year period of maintenance therapy [9]. In solid tumors, surgical resection is essential. Steps preceding and following it may be or not to be performed according to the type of cancer, its stage and clinical judgement of practitioners. Neoadjuvant chemotherapy precedes the surgical resection. It results in clearance of tumor margins and helps surgeons to differentiate tumor margins during resection. Although level wise neoadjuvant chemotherapy of solid tumors is equivalent to induction level in treatment of hematologic malignancies, reduction of malignant cell numbers from 10^{11} to 10^9 in solid tumors occurs after surgical level [10]. Level after surgical resection is called adjuvant chemoradiotherapy. The resection procedure can be R0 (without microscopic residue), R1 (without macroscopic residue) or R2 (with macroscopic residue). R2 is also called as palliative resection. Palliative therapy is used for the patients who are at end stages, have older ages or poor prognosis. Such patients are referred to palliative medicine ward [11]. We have indicated a comparison of cancer therapy levels in hematologic and

solid malignancies through the lens of number of malignant cells in Figure 1 and Table 1.

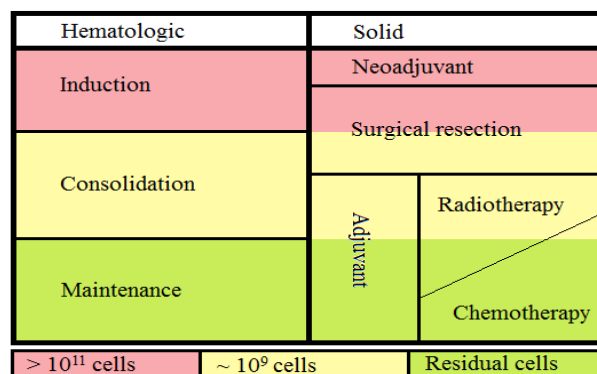


Figure 1 – Comparison of cancer therapy levels in hematologic and solid malignancies assessed by the number of malignant cells

Figure 1 shows that different levels are required to reduce the number of cancer cells in patient. All the levels should be completed to reduce the probability of recurrence. Nanodrugs can be used at these levels. For solid tumors, surgical resection is always necessary, except metastatic cancers.

Table 1 – Levels and principles of cancer therapy in general

Type of malignancy (cancer)					
Hematologic			Solid tumor		
Level of therapy	Method	Outcome	Level of therapy	Method	Outcome
Induction	Chemotherapy	Complete remission	Neoadjuvant	Chemotherapy	Visibility of margins
Consolidation	Chemotherapy/ BMT	Clearance of malignant cells	Resection	Surgery	Clearance of malignant cells
Maintenance	Chemotherapy/ Radiotherapy	Prevention of relapse	Adjuvant	Radiotherapy/ Chemotherapy	Prevention of relapse
Palliative (if failure to cure)	Clinical and medical care	Increased quality of life	Palliative (if failure to cure)	Clinical and medical care	Increased quality of life

Note: BMT: bone marrow transplantation

Table 1 shows the levels of cancer therapy in detail. Complete remission belongs the signs and symptoms which patients have them at the time of diagnosis. In solid tumors, neoadjuvant chemotherapy helps to increase visibility of the tumor margins for better surgical resection; in addition, a partial remission may be observed.

Molecular bases of cancer and mTOR signaling pathway

In general, if cell replication signals uncontrollably overcome cell cycle suppression signals a neoplastic tissue will be formed. Genes activating cell cycle are called proto-oncogenes and genes inhibit-

ing cell cycle are called tumor-suppressor genes. The examples of proto-oncogenes are human epidermal growth factor receptor 2 (*Her2*), *KRAS*, *beta-catenin*, *cyclin D1*, *c-Kit*, vascular endothelial growth factor (*VEGF*) and other. Monoclonal antibodies are used to target the products of these genes. For instance, trastuzumab targets Her2, imatinib targets c-Kit and bevacizumab targets VEGF [12].

Mammalian target of rapamycin (mTOR) is a center for multiple cell growth pathways and can be connected with multiple other proteins, which play important roles in cell growth. This system consists of two complexes; one of them is mTOR complex 1 and the other one is mTOR complex 2, which manage cellular processes by phosphorylation of major translation regulators, such as ribosomal S6 kinase and eukaryote initiation factor 4E binding protein. mTOR is sensitive to physiological responses dependent on cellular levels of oxygen, nutrients and energy. Due to its important roles in various cellular processes and diseases, mTOR is considered the molecular aim. mTOR is involved in obesity, depression and cancer and the importance of these diseases lead to production of the

rapamycin, which in turn can inhibit mTOR and its analogs. mTOR signaling can be disrupted by genetic mutations, such as mutation in phosphatase and tensin homolog (*PTEN*) gene and cause several cancers like prostate, melanoma, breast, lung, endometrial, brain, thyroid, bladder and renal cancers. mTOR activity in both normal and cancer cells has been inhibited using different types of nanoparticles and results in reduction in the level of phosphorylated mTOR and subsequently mTORC1 catalytic activity [13-16].

Use of metals and metal nanoparticles in diagnosis and treatment of cancer

Nanometals (metal nanoparticles) can be used both in diagnosis and treatment of cancer, including targeted drug delivery [17], tracking of malignant cells [18], magnetic-based hyperthermia treatment [18], etc. The latter results in expression of heat shock proteins by tumor cells and induction of apoptosis [19]. We summarized specific nanoparticles used for the specific cancer cell lines in Table 2 [20-37].

Table 2 – Effects of specific metal nanoparticles on specific cancer cell lines

Nanoparticle (type)	Cancer (cell line)	Summary of findings	Ref.
Gold (PEGylated)	Reticulo-endothelial system	The aim of this study was to produce gold nanoparticles using plant-mediated phytochemical extracts and take the conjugate particularly to the tumor. It was proved that PEGylated gold nanoparticles can be used as delivery vehicle for targeting small biomolecules (antibody etc.) to the tumor location.	[23]
Gold (Au@QCS-GA-FA)	Lung cancer cells (CHAGO)	Quaternized chitosan-gallic acid-folic acid stabilized gold nanoparticles (Au@QCS-GA-FA) has enough potential to use as an anti-cancer agent.	[29]
Gold (Dox*FA-GO@Au)	Ehrlich Ascites Tumor cells); EAT cells(-breast cancer); MCF-7 cell line	This study showed that gold nanoparticles can play important role in tumor management.	[21]
Gold (lycopene-nanogold nanoemulsion)	colon cancer cell line (HT-29)	The aim of this study was to produce a nanoemulsion by the use of gold nanoparticles and lycopene and study the effect of this nanoemulsion on HT-29 colon cancer cell line. According to this study LP-nanogold nanoemulsion have sufficient effect the treatment of colon cancer.	[27]
Gold (Hyaluronic acid-fabricated nanogold)	Lung cancer cell line (A549)	Inhibitor of apoptosis protein-2 (IAP-2) was driven into A549 cells by the use of gold nanoparticle and hyaluronic acid (AuNP-HA) and results to a reduction in the cell proliferation.	[31]
Silver (Biogenic silver nanoparticles)	Human breast cancer (MCF-7 cell lines)	Biogenic silver nanoparticles showed their impressive role in inhibiting of MCF-7 cell lines.	[30]
Silver (Plant derived silver-nanoparticle)	Colorectal cancer cell line (HCT116)	PD-AgNP leads to apoptosis in colon cancer cells.	[34]
Nanoparticle paclitaxel (NP PTX)	Lung Cancer	Nanoparticle paclitaxel (NP PTX) caused G2/M phase cell cycle pause and changed the microtubule dynamics resulting in cell death.	[25]

Continuation of Table 2

Nanoparticle (type)	Cancer (cell line)	Summary of findings	Ref.
Silver	Human breast cancer cells (MCF-7)	AgNPs signified sufficient cytotoxicity impact against MCF-7 at minimal dosage.	[35]
Nanodiamond/nanoplatinum	Breast cancer cells (4T1)	nanodiamond/nanoplatinum can be used as cancer therapy agent owing to its ability to reduce cell stiffness.	[24]
Silver	Prostate cancer cells (PC3)	Prostate cancer cells can be destroyed by cytotoxic effects of Nanosilver.	[22]
Silver (TAT-modified nanosilver)	Multidrug-resistant (MDR) cancer-melanoma	AgNP-TAT is a strong anticancer nanoparticle and can inhibit MDR, non-resistance cells and the tumor growth.	[32]
Silver	Human oral squamous cell carcinoma (HSC-3)	The main purpose was the comparison of intracellular impacts between silver nanoparticles (AgNPs) conjugated with nuclear and cytoplasmic targeting peptides and peptide-conjugated gold nanoparticles (AuNPs). Treated cell with AgNPs showed DNA damage and apoptosis.	[20]
Epigallocatechin-3-gallate-gold nanoparticles (EGCG-pNG)	Bladder cancer	EGCG-pNG as a antitumor agent can inhibit tumor cell growing owing to apoptosis.	[26]
Fluorophore-nanoparticle	Breast cancer	fluorophore-nanoparticle can be utilized as a designed complex to target breast cancer by emitting fluorescence conditionally.	[36]
Gold	Liver cancer	Nanogold revealed its potential for inhibiting of the angiogenesis and growth of liver cancer cells because of inhibition of the VEGF165-induced signaling.	[33]
Gold	Breast cancer	The aim was to develop a tumor-specific multi-functional, nano-entity which is able to detect and treat cancer. gold-coated Fe ₃ O ₄ nanoparticles are tumor-specific nano-agents and can play important roles in detection and hyperthermia for breast cancer.	[28]
Gold	Colorectal carcinoma cell line (HT29)	The goal was to study that AuNPs can influence the epithelial origin cell lines: continuous and oncogenic. Cell line of HT29 showed sensitiveness to the effects of AuNPs.	[37]

Based on results, platinum (Pt)-based drugs are some of the most effective drugs used for cancer chemotherapy. One of the efficient Pt-based anti-tumor drugs is Cisplatin (Cis-diamminedichloroplatinum-II). It was approved in 1978 and is used for treatment of various cancers such as testicular, prostate, bladder and lung cancers. Therapeutic function of Pt-based drugs is binding to DNA and stopping its replication. Cisplatin cannot be used for all types of cancers and resistance to it has been observed. Pt-based complexes showed promising cytotoxic effect due to their structural properties [38; 39]. Other than conventional use of this metal, Pt-based nanoparticles have been studied. These particles have radiosensitizing properties in comparison to metal atoms of Pt [40].

Gold (Au) nanoparticles are commonly used in cancer treatment and diagnostics. For instance, combinations of gold nanoparticles with anti-tumor

marker antibodies have been used as biosensors [41]. Due to their physiochemical properties, gold nanoparticles can be used for hyperthermia-based treatment of cancer [42]. Their possibility to act as radiosensitizers has also been shown [40].

Silver (Ag) is known as a metal with antimicrobial and anticancer effects. Previously, silver containing compounds have been shown to have antimicrobial and anticancer effects via induction of necrosis and late apoptosis [43]. According to these effects, nanoparticles of silver are also used [44]. Silver nanoparticles are usually synthesized by medicinal plants (green nanoparticles) [45].

Iron is another metal used in cancer therapy. It is suitable for heat induction. It has been previously proved that magnetic nanoparticles can destroy tumor cells by heat delivery and use of alternating electromagnetic field. Magnetic materials, such as iron oxide (Fe₂O₃ or Fe₃O₄) are the most used materials

for hyperthermia. Nanoparticles can be employed as tumor hyperthermic treatment because of their ability to be utilized as a heat guide, where their sufficiency depends on their size. The best size of the particles to get heated well is within the range of 10-30 nm. Non-invasive hyperthermic therapy may be feasible by heating a tumor model containing nanoparticles. Absorption of near-infrared reflectance can be improved using gold nanoparticles. Utilization of coated Fe_3O_4 nanoparticles with gold is a useful method for optical/thermal markers for seamless diagnosis and therapy in a minimally invasive way. This approach has been used towards the breast cancer cell lines [46; 47].

Medical plants and antioxidants can be used for their anticancer effects as well as their pain relieving effects [48]. For pathophysiology of cancers, role of mutilation in apoptotic related genes [49] and angiogenic factors was investigated [50]. We also found that immune cells, such as natural killers might be involved in cancer [51].

Conclusion

This review was aimed to investigate the use of nanometals gold-based, silver-based, platinum-based and iron-based in cancer treatment. According to literature, specific metal nanoparticles can inhibit cell lines of different cancers based on *in vitro* experimental studies. *In vivo* studies were focused on magnetic, heat induction and ability to track effects. Metals (as single atom or in combination with other compounds) had been previously used in different diseases. Cancer had been a major concern and hence metals were studied for cancer treatment. Nanotechnology was added to this idea and therefore metal nanoparticles were innovated. They are used according to their targeted effect, magnetic potencies and heat induction as well as tracking cancer cells for diagnostic aims. Use of nanoparticles should not intervene with the accepted levels of cancer therapy. Therefore, such agents should be used as a combination therapy and levels of evidence should be regarded and updated.

Acknowledgement

We would like to express our gratitude to Dr. M. Rafieian Kopaei for his valuable help in pharmacology.

References

1. Kaasa S., De Conno F. (2001) Palliative care research. *Europ J Cancer*, vol. 37, no 8, pp. 153-159.

2. Brescia F.J. (2001) Lung cancer – a philosophical, ethical, and personal perspective. *Crit Rev Oncol Hematol.*, vol. 40, no. 2, pp. 139-148.

3. Deyev S., Lebedenko E. (2017) Targeted bifunctional proteins and hybrid nanoconstructs for cancer diagnostics and therapies. *Mol Biol.*, vol. 51, no. 6, pp. 788-803.

4. Jordan C.T. (2004). Cancer stem cell biology: from leukemia to solid tumors. *Curr Opin Cell Biol.*, vol. 16, no. 6, pp. 708-712.

5. Christiansen J.J., Rajasekaran A.K. (2006). Reassessing epithelial to mesenchymal transition as a prerequisite for carcinoma invasion and metastasis. *Cancer Res.*, vol. 66, no. 17, pp. 8319-8326.

6. Thiery J.P. (2002) Epithelial-mesenchymal transitions in tumour progression. *Nat Rev Cancer*, vol. 2, no. 6, p. 442.

7. Johnson S.B., Park H.S., Gross C.P., James B.Y. (2018). Complementary medicine, refusal of conventional cancer therapy, and survival among patients with curable cancers. *JAMA oncology*, vol. 4, no. 10, pp. 1375-1381.

8. Ronghe M.D., Murphy D. (2016). Chemotherapy and novel cancer targeted therapies, *Surgery Childhood Tum.*, pp. 135-152.

9. Jacene H.A., Tirumani S.H., Wahl R.L. (2017). Radionuclide Therapy of Lymphomas. In: Strauss H., Mariani G., Volterrani D., Larson S. (eds.) *Nuclear Oncology*. Springer.

10. Funt S.A., Chapman P.B. (2016). The role of neoadjuvant trials in drug development for solid tumors. *Clin Cancer Res.*, vol. 22, no. 10, pp. 2323-2328.

11. Hong T.S., Ryan D.P. (2015). Adjuvant chemotherapy for locally advanced rectal cancer: is it a given. *J Clin Oncol.*, vol. 33, no. 17, pp. 1878-1880.

12. Chial H. (2008). Proto-oncogenes to oncogenes to cancer. *Nat Educ.*, vol. 1, no. 1, pp. 33.

13. Serej F.A., Pourhassan-Moghaddam M., Kallan M.E., Mehdipour A., Serej Z.A., Ebrahimi-Kalan A. (2018). Targeting the PI3K/Akt/mTOR signaling pathway: applications of nanotechnology. *Crescent J Med Biol Sci.*, vol. 5, no. 1, pp. 7-13.

14. Xu Y., Islam M.A., Zope H., Mahmoudi M., Langer R.S., Shi J., et al. (2017). Restoration of tumor suppression *in vivo* by systemic delivery of PTEN mRNA nanoparticles. *J Clin Oncol.*, vol. 35, no. 15, pp. 11582-11582.

15. De Araújo Jr R.F., Pessoa J.B., Cruz L.J., Chan A.B., De Castro Miguel E., Cavalcante R.S., et al. (2018). Apoptosis in human liver carcinoma caused by gold nanoparticles in combination with carvedilol is mediated via modulation of MAPK/

Akt/mTOR pathway and EGFR/FAAD proteins. *Int J Oncol.*, vol. 52, no. 1, pp. 189-200.

16. Wang W.-J., Yang W., Ouyang Z.-H., Xue J.-B., Li X.-L., Zhang J., et al. (2018). MiR-21 promotes ECM degradation through inhibiting autophagy via the PTEN/akt/mTOR signaling pathway in human degenerated NP cells. *Biomed Pharmacother.*, vol. 99, pp. 725-734.

17. Medina-Ramirez I., Gonzalez-Garcia M., Palakurthi S., Liu J. (2012). Application of nanometals fabricated using green synthesis in cancer diagnosis and therapy. *Green Chemistry-Environmentally Benign Approaches*. IntechOpen, ISBN 978-953-51-0334-9.

18. Kumar C.S.S.R., Mohammad F. (2011). Magnetic nanomaterials for hyperthermia-based therapy and controlled drug delivery. *Adv Drug Deliv Rev.*, vol. 63, no. 9, pp. 789-808.

19. Kobayashi T., Kakimi K., Nakayama E., Jimbow K. (2014). Antitumor immunity by magnetic nanoparticle-mediated hyperthermia. *Nanomed.*, vol. 9, no. 11, pp. 1715-1726.

20. Austin L.A., Kang B., Yen C.-W., El-Sayed M.A. (2011). Nuclear targeted silver nanospheres perturb the cancer cell cycle differently than those of nanogold. *Bioconjug Chem.*, vol. 22, no. 11, pp. 2324-2331.

21. Chauhan G., Chopra V., Tyagi A., Rath G., Sharma R.K., Goyal A.K. (2017). Gold nanoparticles composite-folic acid conjugated graphene oxide nanohybrids for targeted chemo-thermal cancer ablation: *in vitro* screening and *in vivo* studies. *Europ J Pharm Sci.*, vol. 96, pp. 351-361.

22. Firdhouse M.J., Lalitha P. (2013). Biosynthesis of silver nanoparticles using the extract of *Alternanthera sessilis* – antiproliferative effect against prostate cancer cells. *Cancer Nanotechnol.*, vol. 4, no. 6, pp. 137-143.

23. Garg P., Hazra D.K. (2017). Conjugation of antibodies with radiogold nanoparticles, as an effector targeting agents in radiobioconjugate cancer therapy: Optimized labeling and biodistribution results. *Indian J Nuclear Med.*, vol. 32, no. 4, pp. 296.

24. Ghoneum A., Zhu H., Woo J., Zabinyakov N., Sharma S., Gimzewski J.K. (2014). Biophysical and morphological effects of nanodiamond/nanoplatinum solution (DPV576) on metastatic murine breast cancer cells *in vitro*. *Nanotech.*, vol. 25, no. 46, pp. 465101.

25. Hariri G., Edwards A.D., Merrill T.B., Greenbaum J.M., van der Ende A.E., Harth E. (2013). Sequential targeted delivery of paclitaxel and camp-

tothecin using a cross-linked “nanosponge” network for lung cancer chemotherapy. *Mol Pharm.*, vol. 11, no. 1, pp. 265-275.

26. Hsieh D.-S., Wang H., Tan S.-W., Huang Y.-H., Tsai C.-Y., Yeh M.-K., et al. (2011). The treatment of bladder cancer in a mouse model by epigallocatechin-3-gallate-gold nanoparticles. *Biomater.*, vol. 32, no. 30, pp. 7633-7640.

27. Huang R.-F.S., Wei Y.-J., Inbaraj B.S., Chen B.-H. (2015). Inhibition of colon cancer cell growth by nanoemulsion carrying gold nanoparticles and ly-copene. *Int J Nanomed.*, vol. 10, pp. 2823.

28. Jin H., Hong B., Kakar S.S., Kang K.A. (2008). Tumor-specific nano-entities for optical detection and hyperthermic treatment of breast cancer. *Oxygen Transport to Tissue XXIX*. Springer, pp. 275-284.

29. Komenek S., Luesakul U., Ekgasit S., Vilai-van T., Praphairaksit N., Puthong S., et al. (2017). Nanogold-gallate chitosan-targeted pulmonary delivery for treatment of lung cancer. *AAPS Pharm Sci Tech.*, vol. 18, no. 4, pp. 1104-1115.

30. Lalitha P. (2015). Apoptotic efficacy of biogenic silver nanoparticles on human breast cancer MCF-7 cell lines. *Prog Biomater.*, vol. 4, no. 2-4, pp. 113-121.

31. Lin C.-M., Kao W.-C., Yeh C.-A., Chen H.-J., Lin S.-Z., Hsieh H.-H., et al. (2015). Hyaluronic acid-fabricated nanogold delivery of the inhibitor of apoptosis protein-2 siRNAs inhibits benzo [a] pyrene-induced oncogenic properties of lung cancer A549 cells. *Nanotech.*, vol. 26, no. 10, pp. 105101.

32. Liu J., Zhao Y., Guo Q., Wang Z., Wang H., Yang Y., et al. (2012). TAT-modified nanosilver for combating multidrug-resistant cancer. *Biomater.*, vol. 33, no. 26, pp. 6155-6161.

33. Pan Y.L., Qiu S.Y., Qin L., Cai J.Y., Sun J.S. (2009). Nanogold inhibits angiogenesis and growth of liver cancer: experiment with mice. *Zhonghua yi xue za zhi.*, vol. 89, no. 12, pp. 800-804.

34. Satapathy S.R., Mohapatra P., Das D., Sid-dharth S., Kundu C.N. (2015). The apoptotic effect of plant based nanosilver in colon cancer cells is a p53 dependent process involving ROS and JNK cascade. *Pathol Oncol Res.*, vol. 21, no. 2, pp. 405-411.

35. Sathishkumar G., Gobinath C., Wilson A., Sivaramakrishnan S. (2014). *Dendrophthoe falcata* (Lf) Ettingsh (Neem mistletoe): a potent bioresource to fabricate silver nanoparticles for anticancer effect against human breast cancer cells (MCF-7). *Spectrochim Acta Part A*, vol. 128, pp. 285-290.

36. Wang J., Nantz M.H., Achilefu S., Kang K.A. (2010). FRET-like fluorophore-nanoparticle

complex for highly specific cancer localization. Oxygen transport to Tissue XXXI. Springer, pp. 407-413.

37. Pavlovich E., Volkova N., Yakymchuk E., Perepelitsyna O., Sydorenko M., Goltsev A. (2017). In vitro study of influence of Au nanoparticles on HT29 and SPEV cell lines. *Nanoscale Res Lett.*, vol. 12, no. 1, pp. 494.

38. Kelland L. (2007). The resurgence of platinum-based cancer chemotherapy. *Nat. Rev. Cancer*, vol. 7, no. 8, pp. 573.

39. Shahsavar F., Bozorgmehr M., Mirzadegan E., Abedi A., Mehri Lighvan Z., Mohammadi F., et al. (2016). A novel platinum-based compound with preferential cytotoxic activity against a panel of cancer cell lines. *Anti-Cancer Agents Med Chem.*, vol. 16, no. 3, pp. 393-403.

40. Porcel E., Liehn S., Remita H., Usami N., Kobayashi K., Furusawa Y., et al. (2010). Platinum nanoparticles: a promising material for future cancer therapy? *Nanotech.*, vol. 21, no. 8, pp. 085103.

41. Nekouian R., Khalife N.J., Salehi Z. (2014). Anti human fibronectin-gold nanoparticle complex, a potential nanobiosensor tool for detection of fibronectin in ECM of cultured cells. *Plasmonics*. vol. 9, no. 6, pp. 1417-1423.

42. Bhattacharyya S., Kudgus R.A., Bhattacharya R., Mukherjee P. (2011). Inorganic nanoparticles in cancer therapy. *Pharm res.*, vol. 28, no. 2, pp. 237-259.

43. Rendosova M., Vargova Z., Sabolova D., Imrichova N., Hudecova D., Gyepes R., et al. (2018). Silver pyridine-2-sulfonate complex – its characterization, DNA binding, topoisomerase I inhibition, antimicrobial and anticancer response. *J Inorg Biochem.*, vol. 186, no., pp. 206-216.

44. Ahmad S., Munir S., Zeb N., Ullah A., Khan B., Ali J., Salman S.M., Ali S. (2019). Green nanotechnology: a review on green synthesis of silver

nanoparticles – an ecofriendly approach. *Int J Nanomed.*, vol. 14, pp. 5078-5107.

45. Kathiravan V., Ravi S., Ashokkumar S. (2014). Synthesis of silver nanoparticles from *Melia dubia* leaf extract and their in vitro anticancer activity. *Spectrochim Acta Part A: Mol Biomol Spectr.*, vol. 130, pp. 116-121.

46. Bickford L.R., Agollah G., Drezek R., Yu T.-K. (2010). Silica-gold nanoshells as potential intraoperative molecular probes for HER2-overexpression in *ex vivo* breast tissue using near-infrared reflectance confocal microscopy. *Breast Cancer Res Treat.*, vol. 120, no. 3, pp. 547-555.

47. Lee J., Chatterjee D.K., Lee M.H., Krishnan S. (2014). Gold nanoparticles in breast cancer treatment: promise and potential pitfalls. *Cancer Lett.*, vol. 347, no. 1, pp. 46-53.

48. Kheirollahi A., Hasanvand A., Abbaszadeh S., Momeni Safarabadi A., Moghadasi M. (2019). Pathophysiology and urinary system cancer: an overview of the most important herbal plants and natural antioxidants on kidney and bladder disorders. *Res J Pharm Tech.*, vol. 12, no. 2, pp. 972-980.

49. Nikbakht M., Jha A.K., Malekzadeh K., Askari M., Mohammadi S., Marwaha R. K., Kaul D., Kaur, J. (2017). Aberrant promoter hypermethylation of selected apoptotic genes in childhood acute lymphoblastic leukemia among North Indian population. *Exp Oncol.*, vol. 39, no. 1, pp. 57-64.

50. Haggi, A., Mohammadi S., Heshmati M., Ghavamzadeh A., Nikbakht M. (2017). Anti-vascular endothelial growth factor effects of sorafenib and arsenic trioxide in acute myeloid leukemia cell lines. *Asian Pac J Cancer Prev.*, vol. 18, no. 6, pp. 1655-1661.

51. Ghanadi K., Shayanrad B., Ahmadi S.A.Y., Shahsavar F., Eliasy, H. (2016). Colorectal cancer and the KIR genes in the human genome: a meta-analysis. *Genom Data*, vol. 10, no. c, pp. 118-126.

¹H.A. Nasr, ^{2,3}O.M. Nassar, ^{1,4*}M.H. El-Sayed, ⁵A.A. Kobisi

¹Department of Biology, Northern Border University, Kingdom of Saudi Arabia

²Department of Home Economics, Northern Border University, Kingdom of Saudi Arabia

³Nutrition and Food Sciences Department, Minufiya University, Minufiya, Egypt

⁴Department of Botany and Microbiology, Faculty of Science, Al-Azhar University, Cairo, Egypt

⁵Plant Protection Department, Desert Research Center, El-Mataria, Cairo, Egypt

*e-mail: m_helal2007rm@yahoo.com

Characterization and antimicrobial activity of lemon peel mediated green synthesis of silver nanoparticles

Abstract: For a long time, nanoparticle biosynthetic discipline is still under development and is known to have a big impact on numerous manufactures. Synthesis of nanoparticles by green methods with antimicrobial properties is of great researchers concern in the explored of new pharmaceutical and biomedical products. In this study, synthesis of silver nanoparticles (AgNPs) have been carried out using aqueous extract of lemon peel (*Citrus limon*), which acts as encapsulating cage for the silver nanoparticles. Synthesized AgNPs was monitored by formation of brown color, confirmed by UV/VIS spectra, which showed appearance of a surface plasmon resonance (SPR) band. FT-IR analysis of the bioextract after the addition of silver solution showed strong bands at 1021, 1443, 1634 and 3428 cm^{-1} . Transmission electron microscopy examination of the solution containing AgNPs demonstrated spherical particles within nanorange from 9.3 nm to 20.3 nm with the main diameter of 15.76 nm. The biologically synthesized AgNPs showed a promising antimicrobial activity, where the maximal growth inhibition was recorded for both *Pseudomonas (P.) aeruginosa* and *Escherichia (E.) coli* – 21.5 ± 1.3 and 19.0 ± 0.20 mm, respectively. While the minimum growth inhibition was recorded for Gram positive bacteria *Bacillus subtilis (B.)* and *Staphylococcus (S.) aureus* – 15.0 ± 0.20 and 16.5 ± 1.50 mm, respectively. At the same time weak antifungal activity was observed for both *Aspergillus (A.) flavus* and *Candida (C.) albicans* – 14.0 ± 0.15 and 12.5 ± 0.45 mm, respectively.

Key words: green synthesis, silver nanoparticles, lemon peel extract, antimicrobial activity.

Introduction

In the fast development of nanomaterials in the quest for green, eco-friendly routes for new products often culminates in the utilization of microorganisms [1] and plant biomasses for the manufacture of sustainable nanocomposites [2; 3] and nanoparticles [4-6], which are frequently used in biological approaches [7]. Nanotechnology mainly deals with the fabrication of nanoparticles having various shapes, sizes and managing their chemical and physical parameters for further use in human benefits with their growing applications in various fields [8]. Preparation of metal nano-sized, usually ranging in size from 1 to 100 nm, is amongst the most emerging areas in the field of nanotechnology. Currently, the application of nano materials is becoming increasingly important in order to solve the problems associated with material sciences, including solar energy conversion, photonics [9; 10],

catalysis [11], microelectronics [12], antimicrobial functionalities [13], and water treatment [14]. Many biological routes of AgNPs synthesis have been reported using plant extracts, such as *Citrus aurantium*, *Citrus limon*, *Capsicum annum*, *Brassica oleracea*, *Aloe vera*, *Nigella sativa*, *Pulicaria glutinosa*, *Justicia glauca*, *Mimusops elengi L.*, and *Coffea L.* [15-26].

However, in most cases, a deep characterization of the biomolecule coating is not made. It is known that the reducing agents may include flavonoids, membrane proteins, NAD(P)⁺ reductases, dehydrogenases, citric acid, polyphenols, and secondary metabolites [27], whereas the capping agents may be extracellular proteins, enzymes, peptides, and tannic acids [28]. The AgNPs have various and important applications. Historically, silver has been known having a disinfecting effect and has been found in applications ranging from traditional medicines to culinary items. It has been reported

that AgNPs are non-toxic to human and most effective against bacteria, virus and other eukaryotic micro-organism at low concentrations and without any side effects [29; 30]. Moreover, several salts of silver and their derivatives are commercially manufactured as antimicrobial agents [31]. A small concentration of silver is safe for human cells, but lethal for microorganisms [32]. Antimicrobial capability of AgNPs allows them to be suitably employed in numerous household applications such as textiles disinfection in water treatment, food storage containers, home appliances and in medical devices [33]. The most important application of silver and AgNPs is in medical industry such as tropical ointments to prevent infection against burn and open wounds [34]. Nowadays, biosynthesis of silver nanoparticles (AgNPs) had gained so much attention in developed countries due to development demand of environmental friendly technology for material synthesis. Thus, this study aims to show sustainable alternatives of new antimicrobial products based on nanomaterials by utilizing lemon waste to produce AgNPs that are active toward a number of pathogenic microorganisms.

Materials and methods

Chemicals. Chemicals and reagents used in the following experiments were of analytical grade. Silver nitrate (AgNO_3) salt was purchased from Techno Pharmchem, India. All the media components were from Oxoid, India.

Microbial strains. Antimicrobial activity was assayed against a panel of microorganisms certified by American Type Culture Collection (ATCC) and National Collection of Pathogenic Fungi (NCPF), including three Gram-positive bacteria *Bacillus subtilis* ATCC 6633 and *Staphylococcus aureus* ATCC 6538, and against Gram-negative *Pseudomonas aeruginosa* ATCC 9027 and *Escherichia coli* ATCC 7839, a fungus (yeast) – *Candida albicans* (NCPF-stock laboratory strain) filamentous fungi – *Aspergillus flavus*. Cultures were inoculated into specific broths and incubated at 37 °C for 24 h.

Collection of lemon peel. The lemon *Citrus limon* was purchased from two popular markets at Rafha governorate, Northern Border region in the Kingdom of Saudi Arabia. The collected lemon was washed, air-drying and subjected for peel obtaining in the laboratory under aseptic conditions.

Preparation of lemon peel biological extract. The collected lemon peel was washed and boiled in

distilled water for 10 min at 90°C. 100 g of the lemon peel were crushed in 200 mL of distilled water; resulting extract was filtered through a clean cloth and treated with equal volumes of chilled ethanol. Resulting precipitate was lyophilized into a powder for further experiments.

The green synthesis of silver nanoparticles (AgNPs). AgNPs were synthesized by bioreduction of Ag^+ . 5 mL of the fresh suspension of lemon peel extract (greenish in color) were added to 45 mL 0.002 M AgNO_3 solution in 100 mL conical flasks at the room temperature in darkness for some period. The emulsion color turned to dark brown after adding of 1 mM AgNO_3 and stirring at room temperature.

Characterization of silver nanoparticles (AgNPs) as follows

UV/VIS spectral analysis. The synthesized silver nanoparticles were characterized spectrophotometrically using ultraviolet UV/VIS spectroscopy analyses as function of time at room temperature using Perkin Elmer UV/VIS spectrometer. Samples of aliquots (0.2 ml) of the suspension were diluted with 2 ml deionized water and subsequently measured UV/VIS spectra of the resulting diluents.

Fourier transform infrared spectrometer (FT-IR). FT-IR measurements were carried out in order to obtain information about chemical groups present around AgNPs for their stabilization and conclude the transformation of functional group due to reduction process. The measurements were carried out using JASCO FT-IR-3600 infra-red spectrometer by employing KBr Pellet technique.

Transmission electron microscopy (TEM). The size and morphology of the synthesized nanoparticles were recorded by using TEM model JEOL electron microscopy JEM-100 CX. TEM studies were prepared by drop coating silver nanoparticles onto carbon-coated TEM grids. The Film on the TEM grids were allowed to dry, the extra solution was removed using a blotting paper.

Assay of antimicrobial activity of the synthesized AgNPs. Antimicrobial activity was determined by the disk diffusion method [35], using cell suspensions with concentrations equilibrated to a 0.5 McFarland standard for bacterial and unicellular fungal strains and loopful for the filamentous fungi. After incubation at appropriate incubation conditions, the plates were investigated and the diameters of inhibition zones were recorded.

Statistical analysis. All experiments were performed in triplicate and the values were expressed as mean \pm SD using Microsoft Excel 2016.

Results and discussion

Buzzing of nanotechnology in each and every aspect of science and technology has been booming at a tremendous rate now a day. Nanotechnology has different applications in the field of physical, chemical and medical sciences; it has now started revolutionizing the drug delivery sciences [36].

Biological synthesis of nanoparticles by plant extracts is at present under exploitation as some researchers worked on it [37; 38] and testing for antimicrobial activities [39-41]. For the last two decades, extensive work has been done to develop new drugs from natural products because of the resistance of microorganisms to the existing drugs. Nature has been an important source of a products currently used in medicinal practice [42].

Biosynthesis of silver nanoparticles by lemon peels bioextract. In the present study, synthesis of AgNPs by the lemon peel bioextract was carried out. Silver nitrate used has distinctive properties such as good conductivity, catalytic and chemical stability. The formation of AgNPs was found to be successful as suggested by initial changes in color. It is well known that AgNPs exhibit brown color (Figure 1a, b) in aqueous solution due to excitation of surface plasmon vibrations in AgNPs. It is well known that silver nanoparticles exhibit yellowish-brown color in aqueous solution due to excitation of surface plasmon vibrations in silver nanoparticles [43-45]. Reduction of the silver ion to silver nanoparticles during exposure to the peel extracts was followed by color change and as well as by UV/VIS spectroscopy.

Characterization of the synthesized silver nanoparticles AgNPs. Reduction of the silver ion to

silver nanoparticles during exposure to the peel extract was followed by color change and as well as by UV/VIS spectroscopy. It is generally recognized that UV/VIS spectroscopy could be used to examine size and shape-controlled nanoparticles in aqueous suspensions. UV/VIS spectra that were recorded at different intervals for monitoring the reaction, the appearance of a surface plasmon resonance (SPR) band increased in intensity with time. It also reveals the production of silver nanoparticles within 1 h. The UV/VIS absorption spectra recorded from the silver nanoparticles solution after 1.5 h of reaction (Figure 2). Metallic silver nanocrystals generally show a typical optical absorption peak at approximately 3 keV due to the surface plasmon resonance [46-48]. This result confirmed that the produced nano-structures are pure silver. Therefore, metallic nanoparticles have spectrum in the UV/VIS region [49].



Figure 1 – Differential colouring dependent of AgNPs synthesis.

Note: a – extract of lemon peel (colorless),
b – synthesized AgNPs (brown color)

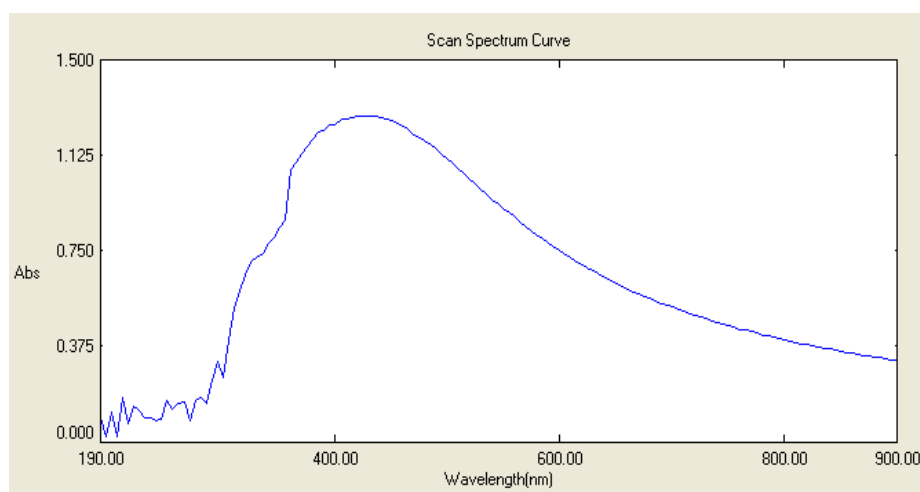


Figure 2 – UV/VIS spectra of reduced Ag ions to AgNPs with lemon peel bioextract

Analysis of FT-IR absorption spectra of the bio-extract after the addition of silver solution revealed the strong bands at 1021, 1443, 1634 and 3428 cm^{-1} . The band at 1021 cm^{-1} corresponded to C-N stretching vibrations of amine. The band at 1443 cm^{-1} cor-

responded to C-H and OH bending and 3428 cm^{-1} was attributed to characteristic of -NH stretching of amide (II) band. The weaker band at 1634 cm^{-1} corresponded to amide I, arisen due to carbonyl stretch in proteins (Figure 3).

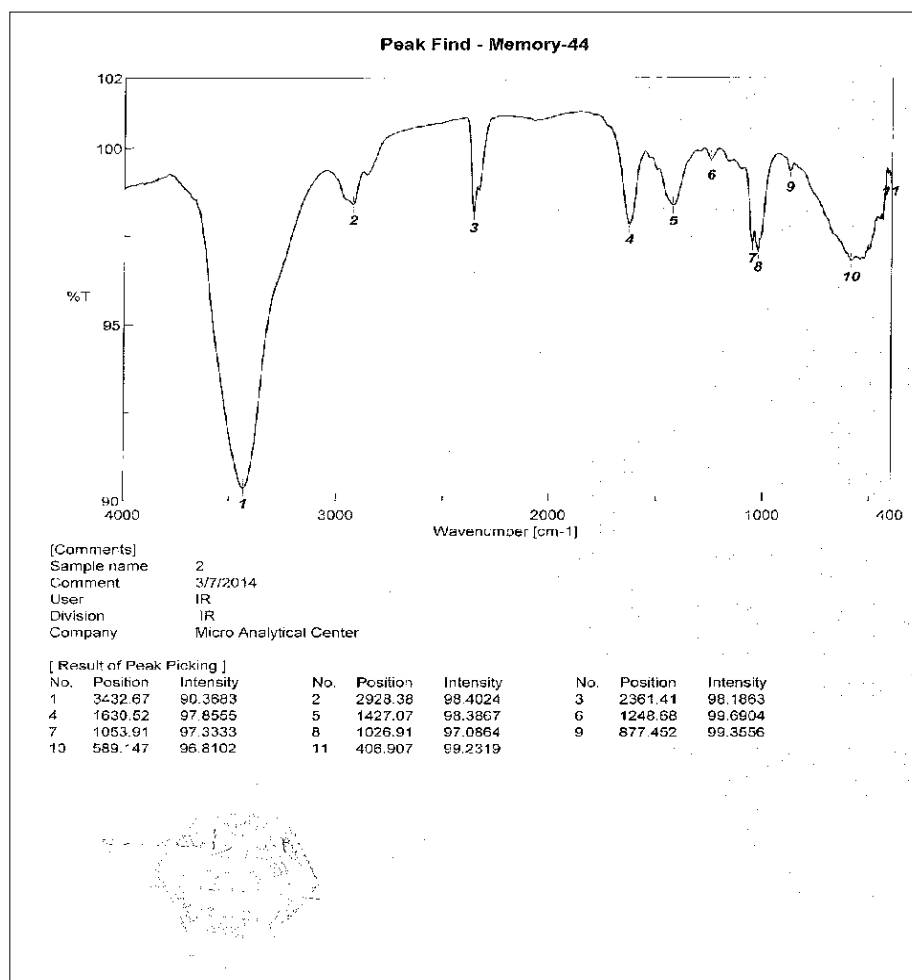


Figure 3 – FT-IR spectra of silver nanoparticles from lemon peel bioextract

FT-IR analysis of the synthesized AgNPs after the addition of silver solution revealed the strong bands at 1021, 1443, 1634 and 3428 cm^{-1} . The positions of these bands were close to that reported formative proteins. The FT-IR results indicate that the secondary structure of proteins was not affected as a consequence of reaction with Ag^+ ions or binding with AgNPs [49].

Transmission electron microscopy (TEM) examination of the solution containing AgNPs demonstrated spherical particles within nanorange from

7.4 nm to 18.5 nm with the main diameter of 11.60 nm (Figure 4).

TEM examination of the solution containing AgNPs demonstrated spherical particles within nanorange from 7.4 nm to 18.5 nm with the main diameter of 11.60 nm. Similar AgNPs sizes synthesized from different sources were obtained various studies [49-51].

Antimicrobial activity of synthesized silver nanoparticles (AgNPs). The biologically synthesized AgNPs showed strong antimicrobial activity against number of the tested microbial strains (Table 1).

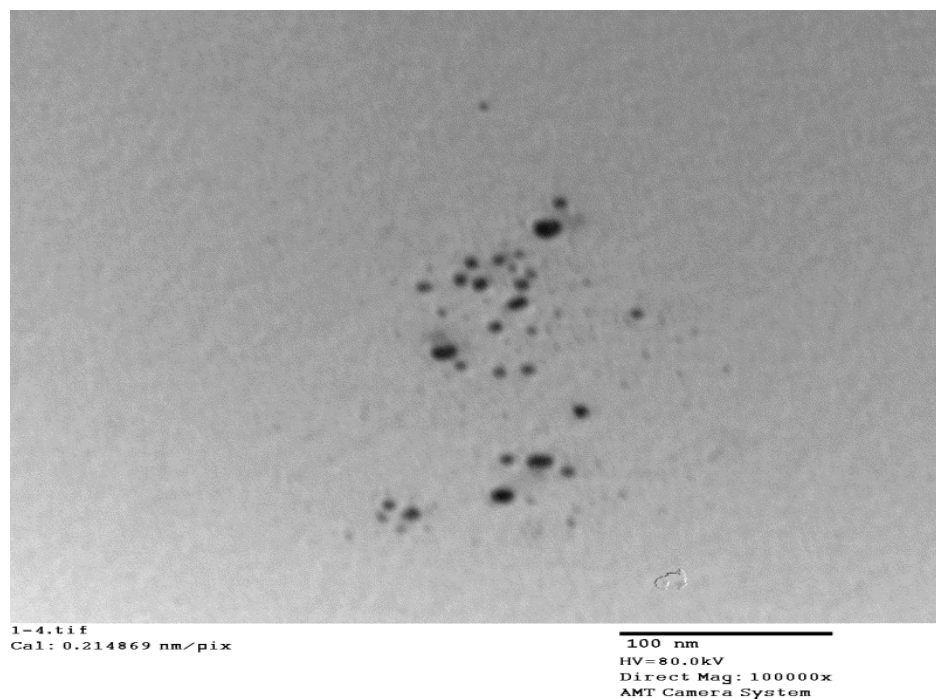


Figure 4 – TEM of the synthesized silver nanoparticles from lemon peel bioextract

Table 1 – Antimicrobial activity of silver nanoparticles from lemon peel

Agent	Mean diameter of inhibition zone (mm)					
	Gram positive bacteria		Gram negative bacteria		Unicellular fungi	Filamentous fungi
	<i>B. subtilis</i> ATCC 6633	<i>S. aureus</i> ATCC 6538	<i>P. aeruginosa</i> ATCC 9027	<i>E. coli</i> ATCC 7839	<i>C. albicans</i>	<i>A. flavus</i>
AgNPs	15.0 ± 0.20	16.5 ± 1.50	21.5 ± 1.3	19.0 ± 0.20	12.5 ± 0.45	14.0 ± 0.15

The maximal growth inhibition was observed in case of Gram-negative bacteria both for *P. aeruginosa* and *E. coli* with 21.5 ± 1.3 and 19.0 ± 0.20 mm, respectively. While the minimum growth inhibition was recorded for Gram-positive bacteria *B. subtilis* and *S. aureus* with 15.0 ± 0.20 and 16.5 ± 1.50 mm, respectively. At the same time weak antifungal activity was observed for both *A. flavus* and *C. albicans* with 14.0 ± 0.15 and 12.5 ± 0.45 mm, respectively.

Biologically synthesized AgNPs showed good antimicrobial activity against Gram-positive, Gram-negative bacteria as well as against unicellular multicellular fungi. Nanomaterials are the leaders in the field of nanomedicine, bionanotechnology and have a great importance in nano toxicology research. Silver exhibits the strong toxicity in various chemical forms to a wide range of microorganism that is very well known and AgNPs have recently been shown to be a promising antimicrobial material [46]. Silver ions

have been known to bind with the negatively charged cell wall resulting in the rupture and consequent denaturation of proteins which leads to cell death [52]. The synthesized AgNPs with smaller size can act drastically on cell membrane and further interact with DNA and causes damage [53]. Other proposed mechanisms include the AgNPs causing depletion of intracellular ATP by rupture of plasma membrane or by blocking respiration in association with oxygen and sulfhydryl (–S–H) groups on the cell wall to form R–S–S–R bonds thereby leading to cell death [54].

Conclusion

Silver nanoparticles synthesized by the green chemistry approach reported in this study using lemon peels extract can be used as an antimicrobial agent in biomedicine and pharmaceuticals. This study demonstrated that synthesized AgNPs have spherical

shape within nanorange of 9.3 nm to 20.3 nm with the main diameter of 15.76 nm and have a promising antibacterial activity, with maximal growth inhibition against both *P. aeruginosa* and *E. coli* of 21.5 ± 1.3 and 19.0 ± 0.20 mm, respectively, as well as antifungal activity against both *A. flavus* and *C. albicans* with mean diameter of inhibition zone of 14.0 ± 0.15 and 12.5 ± 0.45 mm, respectively. Biogenic method used in this study is non-toxic, environmentally friendly, simple, and low-cost.

Acknowledgement

The research was conducted within the framework of the grant No. 7687-SAR-2018-3-9-F from Deanship of Scientific Research, Northern Border University, Arar, Saudi Arabia.

References

- Kiran G., Dhasayan A., Lipton N., Selvin J., Arasu V., Al-Dhabi A. (2014) Melanin-templated rapid synthesis of silver nanostructures. *J Nanobiotechnol.*, vol. 12, no. 1, pp. 1-18.
- Lee V., Hamid B., Zain K. (2014) Conversion of lignocellulosic biomass to nanocellulose: structure and chemical process. *Sci World J.*, vol. 2014, no. 2, pp. 1-20.
- Tian D., Hu J., Bao J., Chandra P., Saddler N., Lu C. (2017) Lignin valorization: lignin nanoparticles as high-value bio-additive for multifunctional nanocomposites. *Biotechnol Biofuels*, vol. 10, no. 192, pp.1-11.
- Singh K., Panghal M., Kadyan, S., Chaudhary U., Yadav P. (2014) Green silver nanoparticles of *Phyllanthus amarus*: as an antibacterial agent against multi drug resistant clinical isolates of *Pseudomonas aeruginosa*. *J Nanobiotechnol.*, vol. 2014, no. 12, pp. 40.
- Ahmed S., Ahmad M., Swami L., Ikram S. (2016) A review on plants extract mediated synthesis of silver nanoparticles for antimicrobial applications: a green expertise. *J Adv Res.*, vol. 7, no. 1, pp.17-28.
- Duman F., Ocoy I., Kup F. (2016) Chamomile flower extract-directed CuO nanoparticle formation for its antioxidant and DNA cleavage properties. *Mater Sci Eng C.*, vol. 60, no. 1, pp. 333-338.
- Jewett C., Patolsky P. (2013) Nanobiotechnology: synthetic biology meets materials science. *Curr Opin Biotechnol.*, vol. 24, no. 4, pp. 551-554.
- Bhyan B., Alam M., Ali S. (2007) Effect of plant extracts on *Okra mosaic* virus incidence and yield related parameters of *Okra*. *J Agric Res.*, vol. 1, no. 1, pp. 112-118.
- Calvo A., Angulo E., Costa-Batllore P., Shiva C., Adelantado C., Vicente A. (2006) Natural plant extracts and organic acids: synergism and implication on piglet's intestinal microbiota. *Biotechnol.*, vol. 5, no. 2, pp. 137-142.
- Cao L., Cheng C., Ma L., Zhao S. (2010) Preparation of silver nanoparticles with antimicrobial activities and the researches of their biocompatibilities. *J Mater Sci Mater M.*, vol. 21, no. 10, pp. 2861-2868.
- Chandan S., Vineet S., Pradeep N., Vikas K., Harvinder S. (2011) A green biogenic approach for synthesis of gold and silver nanoparticles using *Zingiber officinale*. *Digest J Nanomat Biostruc.*, vol. 6, no. 2, pp. 535-542.
- Dastjerdi R., Montazer M., Shahsavan S. (2010) Size-controlled preparation of silver nanoparticles by a modified polyol method, *Colloids Surf. A Physicochem Eng Aspects*, vol. 366, no. 1, pp. 197-202.
- Du L., Niu S., Xu L., Xu R., Fan L. (2009) Antibacterial activity of chitosan tripolyphosphate nanoparticles loaded with various metal ions. *Carbohydr Polym.*, vol. 75, no. 3, pp. 385-389.
- Huang J., Li Q., Sun D., Lu Y., Su Y., Yang X., Wang H., Wang Y., Shao W., He N., Hong J., Chen C. (2007) Biosynthesis of silver and gold nanoparticles by novel sundried *Cinnamomum camphora* leaf. *Nanotech.*, vol. 18, no. 10, pp. 105-109.
- Barros E., Madalossi N., Sigoli A., Mazali O. (2015) Silver nanoparticles: green synthesis, self-assembled nanostructures and their application as SERS substrates. *New J Chem.*, vol. 39, no. 4, pp. 2839-2846.
- Awad M., Hendi A., Ortashi K., et al. (2014) Silver nanoparticles biogenic synthesized using an orange peel extract and their use as an anti-bacterial agent. *Int J Phys Sci.*, vol. 9, no. 3, pp. 34-40.
- Vankar P., Shukla D. (2012) Biosynthesis of silver nanoparticles using lemon leaves extract and its application for antimicrobial finish on fabric. *Appl Nanosci.*, vol. 2, no. 2, pp. 163-168.
- Augustine R., Kalarikkal N., Thomas S. (2014) A facile and rapid method for the black pepper leaf mediated green synthesis of silver nanoparticles and the antimicrobial study. *Appl. Nanosci.*, vol. 4, no. 1, pp. 809-818.
- Demirbas A., Welt B., Ocoy I. (2016) Biosynthesis of red cabbage extract directed Ag NPs and their effect on the loss of antioxidant activity. *Mater Lett.*, vol. 179, no. 3, pp. 20-23.

20. Ocsoy I., Demirbas A., McLamore E., Altinsoy B., Ildize N., Baldemir A. (2017) Green synthesis with incorporated hydrothermal approaches for silver nanoparticles formation and enhanced antimicrobial activity against bacterial and fungal pathogens. *J Mol Liq.*, vol. 238, no. 1, pp. 263-269.
21. Medda S., Hajra A., Dey U., Bose P., Mondal K. (2015) Biosynthesis of silver nanoparticles from *Aloe vera* leaf extract and antifungal activity against *Rhizopus* sp. and *Aspergillus* sp. *Appl Nanosci.*, vol. 5, no. 1, pp. 875-880.
22. Amooaghaie R., Saeri M., Azizi M. (2015) Synthesis, characterization and biocompatibility of silver nanoparticles synthesized from *Nigella sativa* leaf extract in comparison with chemical silver nanoparticles. *Ecotoxicol Environ Saf.*, vol. 120, no. 2, pp. 400-408.
23. Khan M., Khan M., Adil S., et al. (2013) Green synthesis of silver nanoparticles mediated by *Pulicaria glutinosa* extract. *Int J Nanomed.*, vol. 8, no. 3, pp. 1507-1516.
24. Emmanuel R., Palanisamy S., Chen S., et al. (2015) Antimicrobial efficacy of green synthesized drug blended silver nanoparticles against dental caries and periodontal disease causing microorganisms. *Mater Sci Eng C.*, vol. 56, no. 4, pp. 374-379.
25. Prakash P., Gnanaprakasam P., Emmanuel R., Arokiyaraj S., Saravanan M. (2013) Green synthesis of silver nanoparticles from leaf extract of *Mimusops elengi*, Linn. for enhanced antibacterial activity against multi drug resistant clinical isolates. *Colloids Surf B.*, vol. 108, no. 1, pp. 255-259.
26. Dhand V., Soumya L., Bharadwaj S., Chakra S., Bhatt D., Sreedhar B. (2016) Green synthesis of silver nanoparticles using *Coffea arabica* seed extract and its antibacterial activity. *Mat Sci Eng C.*, vol. 58, no. 1, pp. 36-43.
27. Karatoprak G., Aydin G., Altinsoy B., Altinkaynak C., Koşar M., Ocsoy I. (2017) The Effect of *Pelargonium endlicherianum* Fenzl. root extracts on formation of nanoparticles and their antimicrobial activities. *Enzyme Microb Technol.*, vol. 97, no. 1, pp. 21-26.
28. Akhtar M., Panwar J., Yun Y. (2013) Biogenic synthesis of metallic nanoparticles by plant extracts. *ACS Sustainable Chem Eng.*, vol. 1, no. 6, pp. 591-602.
29. Jeong H., Yeo Y., Yi C. (2005) The effect of filler particle size on the antibacterial properties of compounded polymer/silver fibers. *J Mat Sci.*, vol. 40, no. 20, pp. 5407-5411.
30. Kamyar S., Mansor A., Seyed J., Parvaneh S., Parvanh S., Hossein J., Yadollah S. (2012) Investigation of antibacterial properties silver nanoparticles prepared via green method. *Chem Centr J.*, vol. 6, no. 1, pp. 73.
31. Khandelwal N., Singh A., Jain D., Upadhyay K., Verma N. (2010) Green synthesis of silver nanoparticles using *Argimone mexicana* leaf extract and evaluation of their antimicrobial activities. *J Nanomat Biostruct.*, vol. 5, no. 2, pp. 483-489.
32. Krutyakov A., Kudrynskiy A., Olenin Y., Lisichkin V. (2008) Extracellular biosynthesis and antimicrobial activity of silver nanoparticles. *Russ Chem Rev.*, vol. 77, no. 1, pp. 233-236.
33. Marambio-Jones C., Hoek V. (2010) A review of the antibacterial effects of silver nanomaterials and potential implications for human health and the environment. *J Nanopart Res.*, vol. 12, no. 5, pp. 1531-1551.
34. Muhammad A., Farooq A., Muhammad J., Muhammad I., Umer R. (2012) Green synthesis of silver nanoparticles through reduction with *Solanum xanthocarpum* L. berry extract: characterization, antimicrobial and urease inhibitory activities against *Helicobacter pylori*. *Int J Mol Sci.*, vol. 13, no. 8, pp. 9923-9941.
35. Chung Y., Chung Y., Ngeow F., Goh H., Imiyabir Z. (2004) Antimicrobial activities of Malaysian plant species. *Pharm Biol.*, vol. 42, no. 1, pp. 292-300.
36. Jain D., Daima K., Kachhwaha S., Kothari L. (2009) Synthesis of plant-mediated silver nanoparticles using papaya fruit extract and evaluation of their antimicrobial activities. *Digest J Nanomat Biostruct.*, vol. 4, no. 4, pp. 723-727.
37. Palanivel V., Sang-Myung L., Mahudunan L., Kui-Jae L., Byung-Taek O. (2013) Pine cone-mediated green synthesis of silver nanoparticles and their antibacterial activity against agricultural pathogens. *Appl Microbiol Biotechnol.*, vol. 97, no. 1, pp. 361-368.
38. Savage N., Diallo S. (2005) Nanomaterials and water purification. opportunities and challenges. *Nanopart. Res.*, vol. 7, no. 4, pp. 331-342.
39. Savithamma N., Linga M., Rukmini K., Suvarnalatha D. (2011) Antimicrobial activity of silver nanoparticles synthesized by using medicinal plants. *Int J Chem Technol Res.*, vol. 3, no. 3, pp. 1394-1402.
40. Saxena A., Tripathi M., Singh P. (2010) Biological synthesis of silver nanoparticles by using Onion (*Allium cepa*) extract and their antibacterial activity. *J Nanomater Biostruct.*, vol. 5, no. 2, pp. 427-432.
41. Setua P., Chakraborty A., Seth D., Bhatta U., Satyam V., Sarkar N. (2007) Synthesis, optical

properties, and surface enhanced Raman scattering of silver nanoparticles in nonaqueous methanol reverse micelles. *N J Phys Chem C.*, vol. 111, no. 10, pp. 3901-3907.

42. Sharma K., Yngard A., Lin Y. (2009) Silver nanoparticles: Green synthesis and their antimicrobial activities. *Adv Coll Int Sci.*, vol. 145, no. 1-2, pp. 83-96.

43. Shankar, S.S.; A. Rai, et al. (2004) Rapid synthesis of Au, Ag, and bimetallic Au core- Ag shell nanoparticles using *Neem (Azadirachta indica)* leaf broth. *J Coll Interface Sci.*, vol. 275, no. 2, pp. 496-502.

44. Ankamwar B., Chaudhary M., et al. (2005) Gold nanotriangles biologically synthesized using tamarind leaf extract and potential application in vapor sensing. *Synth React Inorg Metal-Org., Nano-Metal Chem.*, vol. 35, no. 1, pp. 19-26.

45. Chandran P., Chaudhary M., et al. (2006) Synthesis of gold nanotriangles and silver nanoparticles using *Aloe vera* plant extract. *Biotech Progress*, vol. 22, no. 2, pp. 577-583.

46. Ip M., Lui L., Poon M., Lung I., Burd A. (2006) Antimicrobial activities of silver dressings: an in vitro comparison. *J. Medical Microb.*, vol. 55, no. 3, pp. 59-63.

47. Bar H., Bhui H., Sahoo G., Sarkar P., De P., Misra A. (2009) Green synthesis of silver nanoparticles using latex of *Jatropha curcas*. *Colloids Surf. A Physicochem Eng Asp.*, vol. 339, no. 1-3, pp. 134-139.

48. Magudapathy P., Gangopadhyay P., Panigrahi K., Nair M., Dhara S. (2001) Electrical transport studies of Ag nanoclusters embedded in glass matrix. *Physica B.*, vol. 299, no. 1-2, pp. 142-146.

49. El-Batal I., Haroun M., Farrag A., Baraka A., El-Sayyad S. (2014) Synthesis of silver nanoparticles and incorporation with certain antibiotic using gamma irradiation. *Brit J Pharm Res.*, vol. 4, no. 11, pp. 1341-1363.

50. Awad A., Hendi A., Khalid O., Ortashi F., Elradi A., Eisa E., Al-lahieb L., Al-Otiby M., Merghani M., Awad A. (2014) Silver nanoparticles biogenic synthesized using an orange peel extract and their use as an anti-bacterial agent. *Int J Phys Sci.*, vol. 9, no. 3, pp. 34-40.

51. Padma S., Dhara S. (2012) Biosynthesis of silver nanoparticles by lemon leaves extract and its application for antimicrobial finish on fabric. *Appl Nanosci.*, vol. 2, no. 2, pp.163-168.

52. Senapati S., Ahmad A., Khan I., Sastry M., Kumar R. (2005) Extracellular biosynthesis of bimetallic Au-Ag alloy nanoparticles. *Small.*, vol. 1, no. 5, pp. 517-520.

53. Pridham G., Anderson P., Foley C., Lindenfesler L., Hesselting W., Benedict C. (1956) A selection of media for maintenance and taxonomic study of *Streptomyces*. *Antibiotics Ann.*, vol. 3, no. 1, pp. 947-953.

54. Lechevalier A., Williams T., Sharpe E., Holt G. (1989) The Actinomycetes: a practical guide to genetic identification of actinomycetes. In: Berge's Manual of Systematic Bacteriology, pp. 2344-3330.

¹M.Kh. Narmuratova , ²Céline Cakir-Kiefer , ^{1*}Zh.B. Narmuratova 

¹Al-Farabi Kazakh National University, Almaty, Kazakhstan

²Université de Lorraine, INRA, URAFPA, Nancy, France

*e-mail: janarka.90b@gmail.com

Isolation and purification of lactoferrin from Kazakhstan mare milk

Abstract: The single chemical composition of mare milk, rich in whey proteins is similar to human milk. Lactoferrin is one of the important compounds contained in whey protein fraction, and has multiple biological functions such as antimicrobial and activation of human and animal immune system. Due to its strong antimicrobial activity, lactoferrin has potential pharmaceutical applications. The present work is mainly focused on the isolation and purification of the lactoferrin from mare's milk. First, the lactoferrin from Kazakhstan mare milk has been purified by gel filtration Sephadex G-100 chromatography in two steps. The column of Sephadex G-100 was eluted with 0.01 M sodium phosphate buffer (pH 6.8). Lactoferrin enriched fractions were detected using UV absorbance at 280 nm and were identified in the first peak. Second, the purity of lactoferrin was checked by 12% SDS-PAGE and the molecular weight of lactoferrin (in the range of 80-82 kDa) was estimated using protein standard, which is recombinant human lactoferrin (expressed in rice, iron saturated, molecular weight 82.4 kDa).

Key words: Kazakhstan mare milk, isolation, whey protein, lactoferrin, purification, analysis.

Introduction

Traditionally, mare milk has been an integral part of the daily diet for centuries in many countries of Central Asia and Eastern Europe. In terms of protein composition, mare milk is close to human milk. It is then a promising alternative to cow's milk for human infant feeding, especially due to its low-fat content, large amount of valuable nutrients with several health benefits [1], high abundance of whey proteins, including lactoferrin, lysozyme and immunoglobulins [2; 3], which have positive effects on the human immune system and infectious diseases [4]. The percentage of whey proteins in mare's milk (39%) [5] is higher than in cow milk (20%), but is lower than in human milk (50%). Cow milk contains the largest amount of caseins. That is why cow milk is defined as casein type milk, while human and mare milk is called albumin type milk [3-5]. The composition of mare milk makes it a beneficial source of nutrients for people.

Lactoferrin is an iron-binding protein of the transferrins family, which plays multifunctional roles in the formation of the innate immune system [6]. Lactoferrin also has ability to bind free iron in biological fluids of mammals [7]. It has been suggested that the

antimicrobial activity of this protein is due to its iron-binding properties, but the exact role of lactoferrin in iron binding in milk is unknown [8]. In the last thirty years, research has discovered several milk proteins and related peptides with interesting antimicrobial properties, particularly lactoferrin, which protects against microbial pathogens, and its antibacterial activity has already been well-described [9]. With the steady increase in the number of multidrug-resistant pathogens, many researchers are looking to alternative medicine instead of classical antibiotics. Indeed, it has become necessary to explore natural resources for new, alternative and/or complementary medicines. In this search for novel antimicrobial agents for the future, lactoferrin, a multifunctional protein that participates in a range of essential physiological processes, offers a new source with potential pharmaceutical applications. In addition, lactoferrin containing antimicrobial fragments are still being explored, through both chemical synthesis and enzymatic digestion, and the peptides have potential applications as pharmaceutical products [10; 11] as recently been described [12].

Kee-Sung et al. (2009) purified lactoferrin from Mongolian mare milk and compared its 20 amino acids N-terminal sequence with mare diferric lacto-

ferrin and bovine lactoferrin. The molecular weight of Mongolian mare milk lactoferrin is 81 kDa [9]. Mare lactoferrin contains 689 amino acid residues, which is similar to bovine lactoferrin [7]. Many studies were performed on isolated milk proteins, which are well described [13-15]. However, in Kazakhstan, the research on isolation and purification of lactoferrin from mare milk has not been studied adequately. The purpose of the current study was to isolate and purify the lactoferrin of whey mare milk by using gel filtration, Sephadex G-100. SDS-PAGE was used to check the level of purity of the lactoferrin enriched fractions.

Materials and methods

Fresh mare milk sample was procured from the local mare dairy farm in Irgelyi village in Almaty region. Temperate grasslands were used to feed horses, because feeding is one of the factors that determine the chemical composition of mare milk. Sephadex G-100 and woman milk lactoferrin marker for determination of protein molecular weight were from Sigma. The molecular weight of human recombinant lactoferrin, expressed in rice, iron saturated, $\geq 90\%$ (SDS-PAGE), is 82.4 kDa.

Sample preparation. Mare milk was stored frozen at 4°C for 30 min and the sample was prepared as follows: defatting (100 mL) was done by centrifugation at $10.000 \times g$ for 30 min at 4°C and filtration. Casein was eliminated by acid precipitation at pH 4.2 with a 1 M HCl solution followed by a centrifugation step ($10.000 \times g$ for 30 min at 20°C).

The pH of the obtained supernatant (containing whey proteins) was adjusted to pH 6.8 with 1 M NaOH and dialyzed (cut-off of dialysis membranes = 6-8 000 Da, SpectraPor; Spectrum Labs Inc., Rancho Dominguez, CA, USA) against ultrapure water for 72 h to remove salts. After dialysis, the whey samples were then kept at -20°C before being used for lactoferrin purification [9; 16].

Isolation and purification of mare lactoferrin.

In order to isolate lactoferrin from the whey proteins, a column of Sephadex G-100 was used. A column was a glass tube (50×2.0 cm) with a dropping funnel on the bottom. That was set vertically in a ring stand. Glass wool was put to the bottom of the column to prevent Sephadex gel from coming out of the column during washing with 0.01 M sodium phosphate buffer. The height of poured gel in the column was 70% of the height of a glass tube. Then the loaded whey proteins (2 mL sample each time) were eluted with 0.01 M sodium phosphate buffer (pH 6.8)

and the flow rate was 0.4-0.5 mL/min. The presence of proteins was measured at 280 nm by a spectrophotometer PD-303 UV (Apel, Japan).

Estimation of lactoferrin concentration. A common and practical expression of the Beer-Lambert law relates the optical attenuation of a material containing a concentration of attenuating species to the optical path length through the sample and absorptivity of the species. This expression is:

$$A = \epsilon lc,$$

where:

A – amount of light absorbed by the sample for a particular wavelength;

ϵ – coefficient of molar extinction;

l – distance that the light travels through the solution;

c – molar concentration of the absorbing species per unit volume.

Estimation of molecular weight (SDS-PAGE). Electrophoresis was performed in Consort EV 265 apparatus with 12% SDS-PAGE with stacking gel (Tris-HCl, pH 6.8) and separation gel (Tris-HCl, pH 8.8). Tris-glycine buffer 5x concentrate (300 mL of 5x Tris-glycine buffer mixed with 1200 mL of distilled water) was used as a running buffer. To provide protein migration in the gel, obtained protein fraction was denatured for with buffer (deionized H₂O, 0.5 M Tris-HCl, pH 6.8, glycerol 50 %, 10 % SDS, 1% bromophenol blue, 2-mercaptoethanol) in the presence of sodium dodecylsulfate in water bath at 100°C 2 min. 10 μ L of eluted fraction was loaded into the each well. The fixation of protein samples in the gel was carried out in 10% trichloroacetic acid solution during 30 min. In order to detect protein a band after electrophoresis, the gel was stained with 0.1% Coomassie Brilliant Blue R-250 for 1 h. The gel was washed with 7% acetic acid for further visualization analyses.

Results and discussion

Chromatography is designed to purify molecules based their size, chemical composition, chemical and physical properties. Size-exclusion chromatography is particularly designed to isolate pure molecules based their molecular weight. Standard markers allow to determine molecular weight of isolated proteins. Gel filtration chromatography has been widely used in the purification of whey proteins. Sephadex G-100 gel filtration chromatography was effective in isolating the major whey proteins [17]. That is why in the present study, lactoferrin was separated by gel filtration

chromatography through Sephadex G-100 column. Whey protein dissolved in 0.01 M sodium phosphate buffer (pH 6.8) was loaded into the column. The protein elution done with the same buffer and the flow rate of 0.4-0.5 mL/min, was monitored by UV absorbance measurement at 280 nm. The elution of the protein was evaluated by the measure of absorbance at 280 nm in a spectrophotometer. After loading samples into a column of gel chromatography large mo-

lecules move through porous beads faster than small molecules. Consequently, large molecules elute first, then small molecules are washed out from the gel. Prepared Sephadex G-100 gel may be used several times only if it is protected from degradation due to contamination with microorganisms. The results of gel filtration are shown on the Figure 1. The lactoferrin enriched fractions were loaded second time in order to get pure lactoferrin.

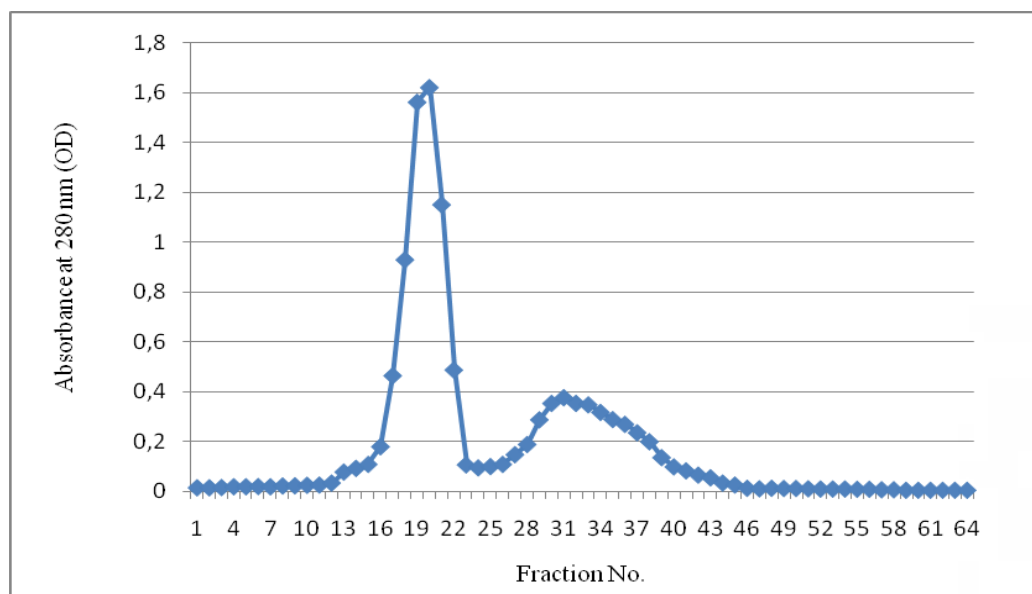


Figure 1 – Purification of lactoferrin from mare's whey protein on Sephadex G-100

Figure 1 shows that two protein peaks appeared in the eluted fractions 15-25 and 28-42, however a strong peak was observed between 15-25 fractions. In order to check purity, samples which showed the highest level of lactoferrin (fractions 17-22 and fractions 33-35) were selected.

Gel filtration has also been useful in the isolation of whey proteins, to examine the purity of commercial preparations of whey proteins [16], to separate glycopeptides of immunoglobulins, and to study the composition of whey proteins from other species [15-19].

Further amino acid composition of lactoferrin is identified. According to the information received from the ProtParam software (<https://web.expasy.org/cgi-bin/protparam/protparam>), The amino acid sequence of the lactoferrin from mare's milk consists of 708 amino acids; the theoretical molecular weight is 77.361 Da, the theoretical pI is 8.36 and the molar extinction coefficient at 280 nm is $81425 \text{ M}^{-1}\text{cm}^{-1}$. Amino acid composition of lactoferrin is presented

in Table 1.

The total number of negatively charged residues (Asp + Glu): 77. The total number of positively charged residues (Arg + Lys): 86.

Estimation of lactoferrin purity and molecular weight by SDS-PAGE. In order to determine required protein samples from fractions SDS-PAGE is used. Before loading samples into the gel of SDS-PAGE, the samples were denatured with buffer. Due to differences in charge, size and shape, proteins have different movement ability in the gel of SDS-PAGE. In order to detect protein bands after electrophoresis, the gel was stained with 0.1% Coomassie Brilliant Blue R-250. The single band of isolated lactoferrin from 17-22 fractions obtained on performing SDS-PAGE. Molecular weight was determined by applying the purified lactoferrin on 12% SDS-PAGE. According to Figure 2, lactoferrin enriched fractions gave different results, while the quantity of loaded samples was the same (10 μL). The protein concentration was determined for selected fractions by measuring the

absorbance A at 280 nm and by applying the Beer – Lambert formula.

Table 1 – Amino acid composition of mare’s milk lactoferrin

Amino acid composition		
Ala (A)	74	10.5%
Arg (R)	37	5.2%
Asn (N)	35	4.9%
Asp (D)	34	4.8%
Cys (C)	35	4.9%
Gln (Q)	29	4.1%
Glu (E)	43	6.1%
Gly (G)	52	7.3%
His (H)	10	1.4%
Ile (I)	13	1.8%
Leu (L)	69	9.7%
Lys (K)	49	6.9%
Met (M)	4	0.6%
Phe (F)	30	4.2%
Pro (P)	36	5.1%
Ser (S)	50	7.1%
Thr (T)	31	4.4%
Trp (W)	9	1.3%
Tyr (Y)	20	2.8%
Val (V)	48	6.8%

The protein concentrations are approximately:
 for 17th fraction: 5.7 μ M;
 for 18th fraction: 11.5 μ M;
 for 19th fraction: 19 μ M;
 for 20th fraction: 20 μ M;
 for 21th fraction: 14 μ M;
 for 22nd fraction: 6 μ M

Figure 2 shows the molecular weight of mare’s milk lactoferrin approximately in the range of 80-82 kDa.

According to the type of animal and carbohydrate content, molecular weight of lactoferrin differs slightly. Jolles *et al.* purified lactoferrin from E. Wettstein mare’s milk by Sephadex G-100 filtration and estimated its molecular mass as 81 kDa [17]. In the present study the molecular weight is 82 kDa on SDS–PAGE 12%. It was similar to the mass of Mongolian mare milk lactoferrin, which was characterized corresponding to a molecular mass of 82 kDa [9]. Konuspayeva *et al.* used gel permeation chromatography on Sephadex G-200 to purify lactoferrin from camel colostrum whey and checked its purity by polyacrylamide gel electrophoresis (12.5%) [18].

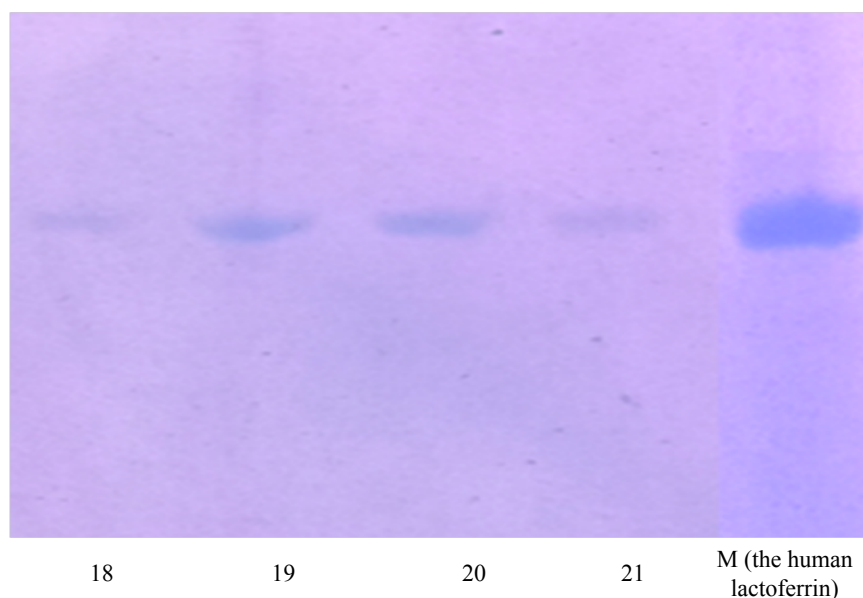


Figure 2 – SDS-PAGE 12% of lactoferrin isolated from mare’s milk whey through a column of Sephadex G-100: fractions 18-21 were loaded. Note: the molecular weight of the isolated bands of lactoferrin, is approximately 80-82 kDa; M – protein standard marker (the human lactoferrin with a molecular weight of 82.4 kDa)

Many researchers used SDS–PAGE to confirm the presence or for characterization of lactoferrin [19-24]. The purity of isolated lactoferrin was confirmed by SDS–PAGE. As a result, a single band of lactoferrin was obtained. The results of the present study were similar to other studies. Younghoon et al. checked the purity of caprine lactoferrin using SDS–PAGE [20]. The purity of isolated lactoferrin from defatted bovine colostrums was also confirmed on the SDS–PAGE gel [21]. Zainab et al. used SDS–PAGE to confirm lactoferrin purity which was isolated from goat colostrums whey [13] and cow's milk by using Sephadex G-50 [22]. Vijayan et al. employed SDS–PAGE to confirm the molecular weight of Malabari goat's colostrum lactoferrin, which was determined as 80 kDa [23]. Further, Annabelles et al. confirm the molecular weight of goat milk lactoferrin by SDS–PAGE as 78 kDa [24].

In depth research on protein properties requires purification homogeneous protein bands from samples. Isolation and purification proteins are the first and important step of protein investigation in biochemical and biomedical studies. Protein isolation methods are designed based on protein size, charge, and polarity. Moreover, these mentioned protein characteristics determine the richness and abundance of proteins. Every protein purification method allows to isolate and further purify desired proteins. In this study, size exclusion chromatography is applied to isolate pure mare's lactoferrin. Column gel filtration for isolation of lactoferrin has some advantages. First, it is convenient to isolate and classify proteins regarding their molecular weight and size. Second, the determination of molecular weight of isolated protein samples is possible by applying standard or specific markers. Sephadex G-100, which is used in this study, allows isolating proteins in a particular molecular weight. Then, in order to determine required protein samples from fractions SDS–PAGE is used. The results show that a single band of lactoferrin is isolated, and further, molecular weight of lactoferrin is determined with standard protein marker 80-82 kDa.

Conclusion

Chromatographic methods have been employed extensively in extracting many individual components of the casein and whey fractions of milk of different animals. Gel filtration, a column chromatography based on Sephadex and ion exchange chromatography are probably more frequently used than any other separation procedures. These chromatographic methods are very effective in isolating and

purifying whey lactoferrin. The results of the present study showed the effectiveness of gel filtration chromatography (Sephadex G-100) in isolation of single band lactoferrin from mare whey.

References

1. Markiewicz-Keszycka M., Wójtowski J., Kuczynska B., Puppel K., Czyzak-Runowska G., Bagnicka E., Strzalkowska N., Jozwik A., Krzyzewski J. (2013) Chemical composition and whey protein fraction of late lactation mare's milk. *Int Dairy J.*, vol. 31, pp. 62-64.
2. Karav S., Salcedo J., Frese S.A., Barile D. (2018) Thoroughbred mare's milk exhibits a unique and diverse free oligosaccharide profile. *FEBS Open Bio*, vol. 8, pp. 1219-1229.
3. Pecka E., Dobrzanski Z., Zachwieja A., Szulc T., Czyz K. (2012) Studies of composition and major protein level in milk and colostrum of mares. *Anim Sci J.*, vol. 93, pp. 162-168.
4. Jastrzebska E., Wadas E., Daszkiewicz T., Pietrzak-Fiecko R. (2017) Nutritional value and health-promoting properties of mare's milk – a review. *Czech J Anim Sci.*, vol. 62, No 12, pp. 511-518.
5. Čagalj M., Brezovečki A., Mikulec N., Antunac N. (2014) Composition and properties of mare's milk of Croatian Coldblood horse breed. *Mljekarstvo*, vol. 64 (1), pp. 3-11.
6. Ismail A.B., El Hafez S.M.A., Mahmoud M.B., Elaraby A-K. A., Hassan H.M. (2013) Development of new strategy for non-antibiotic therapy: dromedary camel lactoferrin has a potent antimicrobial and immunomodulator effects. *Adv Infect Dis.*, vol. 3, pp. 231-237.
7. Uniacke-Lowe T., Huppertz T., Fox. F. P. (2010) Equine milk proteins: Chemistry, structure and nutritional significance. *Int Dairy J.*, vol. 20, pp. 609-629.
8. Detha A., Saputra A., Ola A. (2019) Antimicrobial activity of whey mare's milk against *Salmonella enteritidis*. *Journal of Physics: Conference Series*, no. 1146, pp. 1-4.
9. Kee-Sung K., Ji-Sun K., Mi-Soon S., Hae-Won N., Sang-Dong L., Duvjir S., Alimaa J. (2009) Purification and characterization of Mongolian mare lactoferrin. *Korean J Food Sci Ani Resour.*, vol. 29, no. 2, pp. 164-167.
10. Bruni N., Capucchio M. T., Biasibetti E., Pessione E., Cirrincione S., Giraud L., Corona A., Dosio F. (2016) Antimicrobial Activity of Lactoferrin-Related Peptides and Applications in Human and Veterinary Medicine. *Molecules*, vol. 21(6), 752.

11. Théolier J., Fliss I., Jean J. (2014) Hammami, R. Antimicrobial peptides of dairy proteins: From fundamental to applications. *Food Rev Int.*, vol. 30, pp. 134–154.
12. Rastogi N., Nagpal N., Alam H., Pandey S., Gautam L., Sinha M., Shin K., Manzoor N., Viridi J.S., Kaur, P. et al. (2014) Preparation and antimicrobial action of three tryptic digested functional molecules of bovine lactoferrin. *PLoS ONE*, vol. 9, e90011.
13. Zainab H. Abbas, Kifah S. Doosh, Nahi Y. Yaseen (2015) Isolation, purification and characterization of lactoferrin from goat colostrum whey. *Pak J Nutr.*, vol. 14, pp. 517-523.
14. Niaz B., Zahoor T., Randhawa Muhammad A., Jamil A. (2017) Isolation of lactoferrin from camel milk through fast protein liquid chromatography and its antagonistic activity against: *Escherichia coli* and *Staphylococcus aureus*. *Pak J Zool.*, vol. 49, pp. 1307-1313.
15. Nicolása P., Ferreirab María L., Lassallea V. (2019) A review of magnetic separation of whey proteins and potential application to whey proteins recovery, isolation and utilization. *J Food Eng.*, vol. 246, pp. 7-15.
16. Parkar R. D., Jadhav N. R., Pimpliskar R. M. (2016) Extraction and characterization of lactoferrin from commercial milk. *Int J Pharm Res.*, vol. 6, no. 2, pp. 34-36.
17. Armstrong McD J., Hopper K.E., McKenzie H.A., Murphy W.H. (1970) On the column chromatography of bovine whey proteins. *Biochim Biophys Acta*, vol. 2014, pp. 419-426.
18. Jolles J., Donda A., Amiguet, Jolles P. (1984) Mare lactotransferrin: purification, analysis and N-terminal sequence determination. *FEBS letters*, vol. 176, no. 1, pp. 185-188.
19. Konuspayeva G., Faye B., Loiseau G., Levieux D. (2007) Lactoferrin and immunoglobulin contents in camel's milk (*Camelus bactrianus*, *Camelus dromedarius*, and Hybrids) from Kazakhstan. *J Dairy Sci.*, vol. 90, pp. 38-46.
20. Younghoon, K., J. Mae, S.H. Kyoung, Y.I. Jee, O. Sejong and H.K. SAE. (2009) Anticancer activity of lactoferrin isolated from caprin colostrums on human cancer cell lines. *Int J Dairy Techn.*, vol. 62, pp. 277-281.
21. Yafei, L., W. Xuewan, W. Mianbinand, Z. Wanping. (2011) Simultaneous isolation of lactoferrin and Lactoperoxidase from bovine colostrums by SPEC 70 SLS Cation Exchange Resin. *Int J Environ Res.*, vol. 8, pp. 3764-3776.
22. Moradian, F. (2014) Lactoferrin Isolation, purification and Antimicrobial Effects. *J Med Bio-Eng.* vol. 3, pp. 203-206.
23. Vijayan S., Radhakrishnan U., Eldho L., Jayavardhanan K. K. (2017) Isolation and purification of lactoferrin from colostrum of Malabari goats. *J Exp Biol Agric Sci.*, vol. 5, no. 4, pp. 550-555.
24. Le Parc A., Dallas D.C., Duaut S., Leonil J., Martin P., Barile D. (2014) Characterization of goat milk lactoferrin N-glycans and comparison with the N-glycomes of human and bovine milk. *Electrophor.*, vol. 35, pp. 1560-1570.

^{1*}Ayşe Gul Sarıkaya, ²Serap Canıs

¹Bursa Technical University, Faculty of Forestry,
Forest Engineering Department, Bursa, Turkey

²Isparta Regional Forestry Directorate, Isparta, Turkey

*e-mail: aysegul.sarikaya@btu.edu.tr

Volatile components of leaf and flowers of natural mountain sage (*Sideritis* spp.) taxa from Davraz Mountain, Isparta-Turkey

Abstract: This study was conducted to volatile components of Natural Mountain Sage (*Sideritis* spp.) in Davraz Mountain of Isparta, Turkey. For this aim, samples of *Sideritis condensata* (Boiss. & Heldr.) subsp. *condensata*, *S. hispida* P. H. Davis, *S. libanotica* Labill. subsp. *linearis* ve *S. perfoliata* L. taxa, which grow naturally in Davraz Mountain, were collected and examined in terms of volatile constituents and their percentiles. As result, 45 different volatile constituents were identified regarding the leaves and flowers of the samples of *Sideritis condensata* (Boiss. & Heldr.) subsp. *condensata* and β -Pinene, 3-Octanole and Limonene were determined as main components. Also, 42 different volatile components were identified for *S. hispida* P. H. Davis and (E)-2-Hexenal, β -Myrcene and Caryophyllene were found as main components. 40 different volatile constituents were identified, regarding the leaves and flowers of the samples of *S. libanotica* Labill. subsp. *linearis*. (E)-2-Hexenal, 3-Octanole and Limonene were main components for this taxa. 37 different volatile components were identified for *S. perfoliata* and α -Pinene, β -Pinene and Limonene were found as main components.

Key words: *Sideritis*, Davraz Mountain, Volatile components, Isparta, Turkey.

Introduction

Medicinal and aromatic plants, have been used for many purposes; as a source of tea, spices, condiment, cosmetics and volatile oils. The group of medicinal and aromatic plants, particularly those which are rich with respect to volatile constituents and oil extracts, place a significant importance. Volatile components (essences, etheric oils) and aromatic extracts, are frequently used by fragrance and taste industries, in manufacturing perfumes, food additives, cleaning products, cosmetics and drugs; also as a source of aroma chemicals, or as the starting material for synthesis reaction regarding nature identical, semi-synthetic, and useful aroma chemicals. In particular, there has been a large increase in the demand for volatile components, to be used in aromatherapy applications that have shined out in recent years [1; 2].

Turkey has a significant importance in terms of production and trade of medicinal and aromatic plants. Particularly Isparta province in Turkey, has become one of the most important production centers as of medicinal and aromatic herbs. In accordance with the floristic research conducted in terms of the

flora, regarding Isparta province, located at the intersection of the Mediterranean and Iranian-Turanian regions with regard to floral region, it is known that a total of 2280 different plant taxa are distributed, 190 of which have high medicinal, aromatic and perfume values and 160 of which have high spice values [3].

The cosmopolitan *Lamiaceae* family, which usually consists of fragrant, one or perennial herbaceous, rarely encountered as shrubs or trees, contains 546 species, 45 genera, and a total of 731 taxa [4]. The genus *Sideritis*, a member of the *Lamiaceae*, constitute of one or perennial herbs or small bushes, about 20-90 cm high, pilous or tomentose, with leaves in full edges or dentated, its bracteoles in the form of leaves, calyx, tubular or bell-shaped, with 5-10 nerved, 5 petals, its corolla usually yellow, sometimes white or red, and have a broad distribution in subtropical and middle regions [4,5].

Sideritis L. genus has more than 150 taxa, mostly encountered in the Mediterranean Region. This genus is represented by 46 species and 55 taxa, 42 of which are considered to be endemic [4,6]. Since Turkey is one of two main genetic centers of *Sideritis* L. genus, its endemic rate (79.5%) is quite high [7]. The genus *Sideritis*, is used extensively, colloquially as

a herbal tea, due to its calmative, anti-inflammatory, antispasmodic, carminative, analgesic, sedative, cough suppressant and anticonvulsant features, against stomach pains, coughs caused by cold, and various diseases such as digestive complaints [8].

Davraz Mountain, which is located within the boundaries of Isparta province, in the Lakes District of Mediterranean Region, is rich in botany and also a natural area that contains rich populations of rare, endangered and endemic plant species. In this study that was conducted in Davraz Mountain, samples of *Sideritis condensata* (Boiss. & Heldr.) subsp. *condensata*, *Sideritis hispida* P. H. Davis, *Sideritis libanotica* Labill. subsp. *linearis* ve *Sideritis perfoliata* L. taxa, which grow naturally in Davraz Mountain, were col-

lected and examined in terms of volatile constituents and their percentiles. Studies have been conducted on the volatile components of mountain sage (*Sideritis*) species, in different regions of Turkey. By the way, volatile components of leaf and flowers of *Sideritis* taxa from Davraz Mountain were detected for the first time by this study.

Material and methods

Davraz Mountain is located within the C3 frame throughout the gridding system prepared based on Turkish flora. The research material consists of *Sideritis* L. samples which were collected from Davraz between 2017 and 2018 (Figure 1).

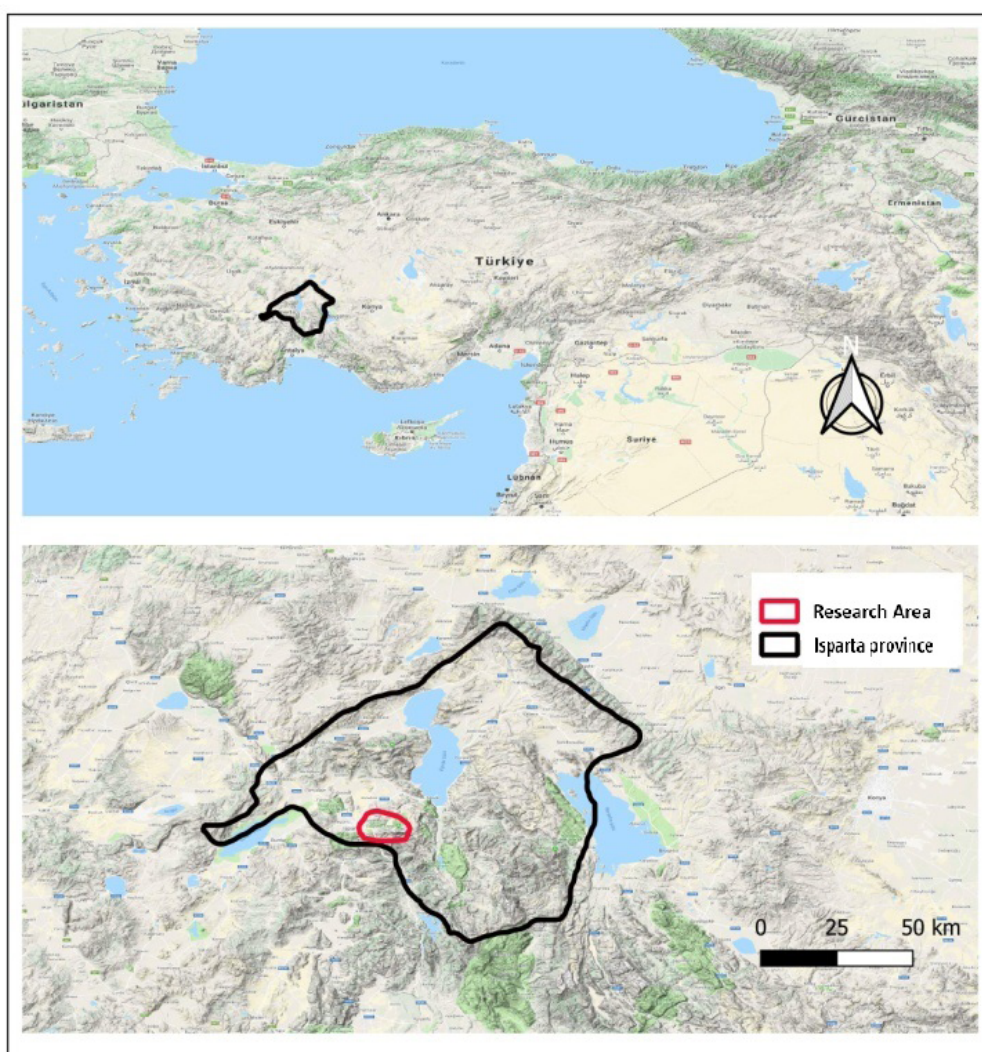


Figure 1 – Research area

The samples were collected from the field were taken to the Forest Botany laboratory of the Faculty of Forestry in Isparta University of Applied Sciences. Leaf and flower samples pertaining to another bulk of the plant samples collected from the research area, were transferred to the laboratory on the same day, at once, in paper packages and without being exposed to sunlight. Plant samples were dried at room temperature (25°C). Volatile constituents of leaves and flowers were examined through Headspace-Solid Phase Micro Extraction (HS-SPME) technique combined with gas chromatography/mass spectrometry (GC/MS). Grounding on Solid Phase Micro Extraction technique, 2 g of the leaves and floral samples, collected from each sample were placed in a 10 mL vial, with the mouth sealed with a silicone lid, and then stored at 60°C temperature for 30 min. The SPME apparatus was passed through the headspace, with a fused silica fiber of 75 µm, coated with Carboxen/Polydimethylsiloxane (CAR/PDMS) and then injected directly into the capillary column of the Shimadzu 2010 Plus GC-MS device (Restek Rx-5 Sil MS 30 m x 0.25 mm, 0.25 µm). The device was connected to the same brand, mass selector detector, which was operated in Hand mode (70 eV). Helium with a flow rate of 1.61 mL per minute was used as the carrier gas. Injection and detection temperatures were set at 250°C. Retention Indices (RI) of volatile constituents were calculated in accordance with alkane standard mixtures C7-C30, under the above mentioned chromatographic conditions. Wiley, NIST Tutor and FFNSC libraries were used to identify volatile constituents.

Since the percentiles determined in the study with respect to each volatile components and their fields, could not meet the pre-requisites of parametric tests in determining statistical data, non-parametric tests were used. Kruskal-Wallis Test was used as a non-parametric test in order to determine the difference between species.

Results and discussion

The leaves and flowers of *Sideritis condensata* (Boiss. & Heldr.) subsp. *condensata*, were collected from three different sampling sites: Büyükhacılar (1015 m), Çobanisa (1068 m) and Darideresi (1113 m). The above-ground parts, including flowers, leaves and stems, are consumed as a herbal tea, upon brewing in boiled water for 5-10 min. It has been found out to be used colloquially as a pain relief, remedy against stomach pain, and as appetizer. Using Solid Phase Micro Extraction (HS-SPME) technique,

combined with gas chromatography/mass spectrometry (GC/MS), 45 different volatile constituents were identified regarding the leaves and flowers of the samples of *Sideritis condensata* (Boiss. & Heldr.) subsp. *condensata* collected from the 1st sample area, 40 different volatile constituents were identified regarding the leaves and flowers of the samples collected from the 2nd sample area, and 39 from the 3rd sample area respectively, making up a total of 62 different volatile constituents, their main components and their percentages were identified respectively as follows: β-Pinene (11.44%, 11.44%, 12.29%), 3-Octanole (11.83%, 11.90%, 11.73%), Limonene (15.31%, 14.37%, 14.52%), Caryophyllene (13.55%, 12.04%, 17.31%). It was observed upon examining the classes of volatile components that, monoterpene and sesquiterpene hydrocarbons were high in all three sample areas.

The leaves and flowers of *Sideritis hispida* P. H. Davis, were collected from three different sampling sites: Akdoğan (1128 m), Büyükhacılar (1033 m) and Yazısöğüt (989 m). The above-ground parts, including flowers, leaves and stems, are consumed as a herbal tea, upon brewing in boiled water. It has been found out to be used colloquially as a pain relief, intestinal regulator and antitussive. Using Solid Phase Micro Extraction (HS-SPME) technique, combined with gas chromatography/mass spectrometry (GC/MS), 42 different volatile components were identified regarding the leaves and flowers of the samples of *Sideritis hispida* P. H. Davis, collected from the 1st sample area, 40 different volatile constituents were identified regarding the leaves and flowers of the samples collected from the 2nd sample area, and 44 from the 3rd sample area respectively, making up a total of 46 different volatile constituents, their main components and their percentages are identified respectively as follows: (E)-2-Hexenal (10.22%, 13.04%, 12.03%), β-Myrcene (35.08%, 36.54%, 35.86%), Caryophyllene (10.07%, 11.78%, 11.26%), p-Cymene (9.64%, 8.80%, 8.11%). It was observed upon examining the classes of volatile components that, monoterpene and sesquiterpene hydrocarbons together with aromatic alcohol, were high in all three sample areas.

The leaves and flowers of *Sideritis libanotica* Labill. subsp. *linearis* were collected from three different sample areas: Direkli (930 m), Büyükhacılar (1354 m) and Sav (1152 m). The above-ground parts, including flowers, leaves and stems, are consumed as a herbal tea, upon brewing in boiled water for 5-10 minutes.

Table 1 – Volatile components of leaf and flowers of taxa *Sideritis* L.

R.T.	Components	<i>S. condensata</i> subsp. <i>condensata</i>			<i>S. hispidula</i>			<i>S. libanotica</i> subsp. <i>linearis</i>			<i>S. perfoliata</i>			Formula	Category
		1. Site	2. Site	3. Site	1. Site	2. Site	3. Site	1. Site	2. Site	3. Site	1. Site	2. Site	3. Site		
1.	2-Methylpropanal	*	*	*	0.09	0.11	0.15	0.24	0.27	0.22	*	*	*	C ₄ H ₈ O	AA
2.	Acetic acid	1.70	*	*	0.50	0.59	0.61	1.37	1.36	2.07	0.70	0.11	0.91	C ₂ H ₄ O ₂	FA
3.	2-Butanal	*	*	0.23	2.33	1.90	1.10	0.68	0.55	*	0.15	0.36	*	C ₄ H ₈ O	AAI
4.	3-Methyl butanal	0.19	*	*	*	*	*	0.21	0.17	0.54	*	*	*	C ₅ H ₁₀ O	AA
5.	Butanal	*	*	*	*	*	*	0.31	0.19	0.33	*	*	*	C ₄ H ₈ O	AA
6.	1-Penten-3-one	*	*	*	*	*	*	*	*	*	0.33	0.03	*	C ₅ H ₈ O	AAI
7.	2-Pentanone	1.98	1.50	*	*	*	*	0.36	*	*	*	*	0.41	C ₅ H ₁₀ O	AA
8.	3-Pentanone	1.05	*	*	*	*	*	0.43	0.19	0.48	*	*	*	C ₅ H ₁₀ O	AA
9.	Pentanal	*	*	*	*	*	*	*	0.55	*	*	*	*	C ₅ H ₁₀ O	AAI
10.	2-ethyl-Furan	0.51	0.89	0.56	1.45	1.52	1.65	1.92	1.20	1.98	0.18	0.15	0.27	C ₆ H ₈ O	AA
11.	(E)- 3-Penten-2-one	*	*	*	0.71	0.87	0.75	*	*	*	*	0.09	*	C ₅ H ₈ O	AAI
12.	3-Methyl-1-butanol	0.59	*	*	*	*	*	0.29	*	*	*	*	*	C ₅ H ₁₂ O	AA
13.	1-Butanol	0.90	*	*	*	*	*	0.23	*	*	*	*	*	C ₄ H ₁₀ O	AA
14.	(E)-2-Pentenal	*	*	0.20	0.73	0.62	0.79	0.72	0.66	0.54	0.75	0.07	0.30	C ₅ H ₈ O	AAI
15.	1-Pentanol	*	*	*	*	*	*	*	*	*	0.21	*	*	C ₅ H ₁₂ O	AAI
16.	(Z)-3-Hexenal	*	*	*	*	*	*	*	*	*	0.24	*	*	C ₆ H ₁₀ O	AA
17.	4.596 Hexanal	0.18	0.53	0.47	1.21	1.64	1.45	0.33	0.84	0.75	0.96	0.13	0.56	C ₆ H ₁₂ O	AA
18.	6.085 (E)-2-Hexenal	1.96	3.59	3.22	10.22	13.04	12.03	18.84	19.32	22.24	0.29	0.51	0.13	C ₆ H ₁₀ O	AA
19.	6.180 cis-3-Hexene-1-ol	0.72	0.61	0.69	0.52	0.32	0.42	2.01	2.08	2.18	0.22	0.06	0.38	C ₆ H ₁₂ O	AA
20.	6.522 (E)- 2-Hexen-1-ol	*	*	0.49	*	*	*	0.65	0.43	0.46	0.28	*	0.74	C ₆ H ₁₂	AA
21.	6.646 n-Hexanol	0.23	0.28	0.41	*	0.46	0.52	0.22	0.48	0.52	0.22	0.03	0.64	C ₆ H ₁₄ O	AA
22.	7.267 2-Heptanone	0.64	*	*	*	*	*	0.19	*	*	*	*	0.16	C ₇ H ₁₄ O	AA
23.	7.676 n-Heptanal	*	*	*	*	0.37	0.21	*	*	*	0.20	*	*	C ₇ H ₁₄ O	AA
24.	7.970 Sorbaldehyde	0.19	*	0.32	2.03	2.14	2.04	0.18	0.89	0.72	0.23	0.08	0.74	C ₈ H ₈ O	AA
25.	8.495 α-Thujene	0.63	0.50	*	0.80	0.84	0.57	0.57	0.44	*	0.23	0.47	0.20	C ₁₀ H ₁₆	MH
26.	8.734 α-Pinene	5.65	4.06	6.05	0.95	0.62	0.66	3.92	3.85	2.56	41.83	51.02	41.92	C ₁₀ H ₁₆	MH
27.	9.172 Benzene	*	*	*	*	*	*	*	*	*	*	*	0.54	C ₆ H ₆	AH
28.	9.365 Camphene	*	*	*	*	*	*	*	*	*	*	0.22	0.16	C ₁₀ H ₁₆	MH
29.	9.676 (Z)-2-Heptenal	*	*	*	0.76	*	0.74	*	*	*	0.22	0.05	*	C ₇ H ₁₂ O	AA
30.	9.788 Benzaldehyde	0.91	1.42	0.43	0.84	0.70	0.58	0.20	0.75	0.03	0.19	0.09	0.41	C ₇ H ₆ O	AAI

Continuation of table 1

R.T.	Components	<i>S. condensata</i> subsp. <i>condensata</i>			<i>S. hispida</i>			<i>S. tibanoica</i> subsp. <i>linearis</i>			<i>S. perfoliata</i>			Formula	Category	
		1. Site	2. Site	3. Site	1. Site	2. Site	3. Site	1. Site	2. Site	3. Site	1. Site	2. Site	3. Site			
31.	9.807	Methyl 2-hexenoate	1.09	*	*	*	*	*	*	*	*	*	*	C ₇ H ₁₂ O ₂	EC	
32.	10.268	β-Phellandrene	0.42	0.32	0.22	0.41	0.56	0.67	0.47	0.46	0.26	0.28	0.37	0.62	C ₁₀ H ₁₆	MH
33.	10.400	β-Pinene	11.44	11.44	12.29	0.95	0.80	0.75	4.10	5.09	5.70	11.46	11.30	12.47	C ₁₀ H ₁₆	MH
34.	10.445	Vinyl amyl ketone	0.32	0.32	*	*	*	*	0.34	0.28	0.29	0.19	*	0.81	C ₈ H ₁₄ O	AAI
35.	10.647	3-Octanol	11.83	11.90	11.73	1.63	1.34	1.45	22.19	19.11	20.87	5.65	4.00	4.68	C ₈ H ₁₆ O	AAI
36.	10.766	6-Methyl-5-hepten-2-one	*	*	*	0.33	0.52	0.42	*	0.38	*	*	*	*	C ₈ H ₁₄ O	AAI
37.	10.802	3-Octanone	2.58	2.74	0.81	*	0.56	0.54	1.65	*	1.64	*	*	*	C ₈ H ₁₄ O	AAI
38.	10.943	β-Myrcene	4.43	5.18	2.26	35.08	36.54	35.86	4.62	3.99	2.95	1.70	2.00	1.52	C ₁₀ H ₁₆	MH
39.	11.186	2,4-Heptadienal	*	*	*	2.32	2.72	2.35	0.75	0.70	1.44	0.19	0.22	0.21	C ₇ H ₁₀ O	AA
40.	11.347	Decane	*	*	*	0.18	0.27	0.21	*	*	*	*	*	*	C ₁₀ H ₂₂	AH
41.	11.440	Octanal	*	0.45	*	*	*	*	*	0.34	0.50	0.34	0.09	0.32	C ₈ H ₁₆ O	AA
42.	11.498	Phellandrene	*	*	*	*	*	*	*	*	*	*	0.45	*	C ₁₀ H ₁₆	MH
43.	11.543	Hex-3(Z)-enyl acetate	*	*	*	*	*	*	0.23	0.28	0.22	*	*	0.20	C ₈ H ₁₄ O ₂	FA
44.	11.640	δ-3-Carene	*	*	*	*	*	0.21	*	*	*	*	0.31	*	C ₁₀ H ₁₆	MH
45.	11.923	α-Terpinene	*	*	*	0.59	0.53	0.55	*	0.25	*	0.29	0.15	*	C ₁₀ H ₁₆	MH
46.	12.255	p-Cymene	1.43	0.27	*	9.64	8.80	8.11	1.20	1.09	0.75	0.44	0.34	0.44	C ₁₀ H ₁₄	MH
47.	12.414	Limonene	15.31	14.37	14.52	2.83	2.49	2.41	14.70	13.73	10.77	11.90	11.12	10.71	C ₁₀ H ₁₆	MH
48.	12.632	1,8-Cineole	0.38	0.14	*	*	*	*	*	0.49	0.30	0.24	*	*	C ₁₀ H ₁₈ O	OM
49.	12.725	cis-OCimene	0.23	0.79	0.44	0.25	0.36	0.28	1.23	0.79	1.22	*	1.74	1.06	C ₁₀ H ₁₆	MH
50.	12.801	Oct-3(E)-en-2-one	*	*	*	0.22	*	*	*	*	*	*	*	*	C ₈ H ₁₄ O	AAI
51.	12.943	Benzeneacetaldehyde	*	*	0.22	0.22	0.30	0.25	*	*	*	*	*	*	C ₈ H ₈ O	OC
52.	13.163	β-OCimene	*	0.91	0.46	1.04	1.41	1.12	0.66	*	*	*	0.39	0.80	C ₁₀ H ₁₆	MH
53.	13.544	γ-Terpinene	*	*	*	0.42	0.37	0.22	*	0.50	0.26	0.46	0.26	*	C ₁₀ H ₁₆	MH
54.	14.039	E,E-3,5-octadien-2-one	*	*	*	0.47	*	*	*	*	*	0.88	0.03	*	C ₈ H ₁₂ O	AAI
55.	14.593	α-Terpinolene	*	*	*	*	*	*	*	0.27	0.43	*	0.92	0.15	C ₉ H ₁₈ O	AAI
56.	15.138	Furan, 3-(4-methyl-3-pentenyl)	*	*	*	0.12	0.55	0.33	*	*	*	*	*	*	C ₁₀ H ₁₄ O	OM
57.	15.246	Dodecane	*	*	*	0.73	0.25	0.58	*	*	*	*	*	*	C ₁₂ H ₂₆	AH
58.	15.265	Linalool	3.13	0.59	0.31	*	*	*	0.64	1.31	0.79	0.76	0.18	1.74	C ₁₀ H ₁₈ O	OM
59.	15.389	Nonanal	*	0.22	*	0.29	*	0.40	*	0.37	0.78	0.56	*	*	C ₉ H ₁₈ O	AAI
60.	15.928	Octanoic acid	1.38	*	*	*	*	*	*	*	*	*	*	*	C ₈ H ₁₆ O ₂	FA
61.	16.297	Alloocimen	*	1.36	*	*	*	*	*	*	*	*	0.20	0.58	C ₁₀ H ₁₆	MH

Continuation of table 1

R.T.	Components	<i>S. condensata</i> subsp. <i>condensata</i>			<i>S. hispidata</i>			<i>S. libanotica</i> subsp. <i>linearis</i>			<i>S. perfoliata</i>			Formula	Category
		1. Site	2. Site	3. Site	1. Site	2. Site	3. Site	1. Site	2. Site	3. Site	1. Site	2. Site	3. Site		
62.	18.719	<ethyl->Octanoate	0.18	*	*	*	*	*	*	*	*	*	*	C ₁₀ H ₂₀ O ₂	FA
63.	18.824	Isopentyl cyclobutanecarboxylate	*	*	*	*	*	*	*	*	*	*	0.36	C ₈ H ₁₄ O ₂	FA
64.	18.852	α -Terpineol	0.23	*	*	*	*	0.28	0.26	0.23	*	*	*	C ₁₀ H ₁₈ O	OM
65.	19.285	Decanal	*	*	*	*	*	*	0.31	0.22	0.25	*	*	C ₁₀ H ₂₀ O	OM
66.	19.692	β -Cyclocitral	*	*	*	*	*	*	*	0.21	*	*	*	C ₁₀ H ₁₆ O	OM
67.	20.776	Pentyl hexanoate	0.20	*	*	*	*	*	*	*	*	*	*	C ₁₁ H ₂₂ O ₂	FA
68.	20.785	Methyl 2,4-decadienoate (2E,4Z)	0.95	*	*	*	*	*	*	*	*	*	*	C ₁₁ H ₁₈ O ₂	FA
69.	22.715	Carvacrol	*	*	*	*	*	0.57	*	*	*	*	*	C ₁₀ H ₁₄ O	OM
70.	24.476	α -Cubebene	0.30	1.00	0.61	*	*	*	*	*	*	*	*	C ₈ H ₁₄	SH
71.	25.091	Cyclosativene	*	*	0.49	0.36	0.20	*	*	*	*	*	0.31	C ₈ H ₁₄	SH
72.	25.334	α -Copaene	6.14	6.73	5.06	3.64	0.38	0.63	0.41	1.61	*	*	1.68	C ₈ H ₁₄	SH
73.	25.605	β -Bourbonene	2.77	1.33	2.16	1.74	0.53	1.60	1.69	1.52	*	*	1.26	C ₈ H ₁₄	SH
74.	25.813	β -Elemene	0.43	1.12	0.75	*	*	*	*	*	*	*	*	C ₈ H ₁₄	SH
75.	26.001	Nepeialactone	*	*	*	*	*	*	0.78	*	*	*	*	C ₁₀ H ₁₆ O ₂	FA
76.	26.905	Caryophyllene	13.55	12.04	17.31	10.07	11.78	12.10	10.32	12.17	12.11	10.49	*	C ₁₅ H ₂₄	SH
77.	27.453	Aromadendrene	*	*	0.41	*	*	*	*	*	*	*	*	C ₁₅ H ₂₄	SH
78.	27.688	Cadinna-1(6),4-diene<10betaH->	*	0.16	0.52	*	*	*	*	*	*	*	*	C ₁₅ H ₂₄	SH
79.	27.934	(E)- β -Farnesene	0.42	1.38	1.66	*	*	*	*	*	*	*	*	C ₁₅ H ₂₄	SH
80.	28.003	α -Humulene	0.20	0.43	0.37	0.17	0.34	0.42	*	0.24	0.10	0.16	*	C ₁₅ H ₂₄	SH
81.	28.228	β -Cubebene	*	0.55	0.73	*	*	*	0.18	*	*	*	*	C ₁₅ H ₂₄	SH
82.	28.661	α -Amorphene	*	0.61	0.82	*	*	*	*	*	*	0.15	*	C ₁₅ H ₂₄	SH
83.	28.822	Curcumene	*	*	0.22	*	*	*	*	0.70	*	*	*	C ₁₅ H ₂₂	SH
84.	28.867	Germaerene-D	1.12	4.81	4.26	0.23	*	0.71	0.65	*	*	0.38	*	C ₁₅ H ₂₄	SH
85.	29.189	Viridiflorene	*	0.96	*	*	*	*	*	*	*	*	*	C ₁₅ H ₂₄	SH
86.	29.323	Germaerene B	*	*	*	*	*	*	*	*	*	*	*	C ₁₅ H ₂₄	SH
87.	29.326	γ -Curjumenene	0.20	0.85	2.77	*	*	*	*	*	*	*	*	C ₁₅ H ₂₄	SH
88.	29.883	γ -Cadinene	0.18	0.80	0.99	*	*	*	*	*	*	0.22	*	C ₁₅ H ₂₄	SH
89.	30.059	δ -Cadinene	0.87	2.60	4.19	0.68	0.50	0.62	0.45	0.33	*	0.21	*	C ₁₅ H ₂₄	SH
90.	30.617	α -Muurotene	*	0.25	0.35	*	*	*	*	*	*	*	*	C ₁₅ H ₂₄	SH
91.	32.035	Caryophyllene oxide	0.26	*	*	1.99	1.83	1.97	*	*	*	*	*	C ₁₅ H ₂₄ O	OS

Continuation of table 1

	R.T.	Components	<i>S. condensata</i> subsp. <i>condensata</i>			<i>S. hispidata</i>			<i>S. libanotica</i> subsp. <i>linearis</i>			<i>S. perfoliata</i>			Formula	Category
			1. Site	2. Site	3. Site	1. Site	2. Site	3. Site	1. Site	2. Site	3. Site	1. Site	2. Site	3. Site		
92.	32.101	2-ethyl-Hexanol	*	*	*	*	*	*	*	*	*	*	*	*	C ₈ H ₁₈ O	AA
TOTAL			100	100	100	100	100	100	100	100	100	100	100	100		
Number of Components			45	40	39	42	40	44	40	43	41	42	37	41		
AA: Aromatic alcohol			9.14	7.85	6.16	18.60	22.32	21.56	27.04	27.23	31.26	3.38	1.10	4.35		
AAI: Aromatic aldehyde			15.64	16.6	13.4	7.55	6.51	6.58	26.19	22.79	25.73	8.91	4.89	5.60		
AH: Aromatic hydrocarbon			*	*	*	0.91	0.52	0.79	*	*	*	*	*	0.54		
EC: Ester compound			1.09	*	*	*	*	*	*	*	*	*	*	*		
FA: Fatty acids methyl ester			4.41	*	*	0.50	0.59	0.61	2.07	2.10	3.33	0.70	0.11	1.47		
MH: Monoterpen hydrocarbon			39.54	39.20	36.24	53.22	53.65	51.41	31.34	29.51	24.24	68.78	81.26	71.44		
OC: Other component			*	*	0.22	0.22	0.30	0.25	*	*	*	*	*	*		
OM: Oxygenated monoterpen			0.26	*	*	1.99	1.83	1.97	*	*	*	*	*	*		
OS: Oxygenated seskiterpen			3.74	0.73	0.31	0.12	0.55	0.33	0.64	3.15	1.92	1.66	0.43	1.74		
SH: Seskiterpen hydrocarbon			26.18	35.62	43.67	18.88	13.73	16.50	12.72	15.22	13.52	16.57	12.21	14.86		

It has been found out to be used colloquially as a pain relief, as a remedy against stomach pain, as an intestinal regulator, carminative, diuretic, cough suppressant and appetizer. Using Solid Phase Micro Extraction (HS-SPME) technique, combined with gas chromatography/mass spectrometry (GC/MS), 40 different volatile constituents were identified, regarding the leaves and flowers of the samples of *Sideritis libanotica* Labill. subsp. *linearis* collected from the 1st sample area, 43 different volatile constituents were identified regarding the leaves and flowers of the samples collected from the 2nd sample area, and 41 from the 3rd sample area respectively, making up a total of 54 different volatile constituents, their main components and their percentages are identified respectively as follows (E)-2-Hexenal (18.84%, 19.32% and 22.24%), 3-Octanole (22.19%, 19.11% and 20.87%), Limonene (14.70%, 13.73% and 10.77%), Caryophyllene (10.82%, 12.10% and 10.32%). It was observed upon examining the classes of volatile components that, monoterpene hydrocarbons together with aromatic alcohol and aromatic aldehydes were high in all three sample areas.

The leaves and flowers of *Sideritis perfoliata* L. were collected from three different sample areas: Yazısöğüt (1010 m), Büyükhacılar (1365 m) and Sav (1089 m). The above-ground parts, including flowers, leaves and stems, are consumed as a herbal tea, upon brewing in boiled water. It has been found out to be used colloquially as a pain relief, as a remedy against stomach pain, as an intestinal regulator, carminative, and cough suppressant. Using Solid Phase Micro Extraction (HS-SPME) technique, combined with gas chromatography/mass spectrometry (GC/MS), 42 different volatile constituents were identified, regarding the leaves and flowers of the samples of *Sideritis perfoliata* L. collected from the 1st sample area, 37 different volatile components were identified regarding the leaves and flowers of the samples collected from the 2nd sample area, and 41 from the 3rd sample area respectively, making up a total of 59 different volatile constituents, their main components and percentages are identified respectively as follows: α -Pinene (41.83%, 51.02% and 41.92%), β -Pinene (11.46%, 11.30% and 2.47%), Limonene (11.90%, 11.12% and 10.71%), Caryophyllene (12.17%, 12.11% and 10.49%). It was observed upon examining the classes of volatile constituents that, monoterpene and sesquiterpene hydrocarbons were high in all three sample areas.

There is no statistically significant difference regarding the fields of collection, of volatile constituents pertaining to leaves and flowers of *Sideritis*

condensata (Boiss. & Heldr.) subsp. *condensata*, *S. hispida* P. H. Davis, and *S. libanotica* Labill. subsp. *linearis*. As a result of Kruskal-Wallis test, applied to find out the proportions of the classes of volatile constituents pertaining to leaves and flowers of *Sideritis condensata* (Boiss. & Heldr.) subsp. *condensata*, the difference between the median of the sites 2 and 3 was found to be statistically significant ($p_2=0.004 < 0.05$, $p_3=0.006 < 0.05$). No statistically significant difference was found between the median of the sites 2 and 3 regarding the volatile constituents pertaining to leaves and flowers of *S. hispida* P. H. Davis, as a result of Kruskal-Wallis test, applied to find out the proportions of the fields. The difference between the median of the site 1, was found to be statistically significant regarding the leaves and flowers of *S. libanotica* Labill. subsp. *linearis* ($p=0.043 < 0.05$) whereas the difference between the median of the site 2 was found to be statistically significant ($p=0.000 < 0.05$), as a result of Kruskal-Wallis test, applied to find out the proportions of the sites of volatile constituents pertaining to leaves and flowers of *S. perfoliata* L.

Sideritis L. taxa, which is colloquially called as “mountain tea”, is used as a herbal tea, upon brewing for 5-10 min in boiled hot water. It has been found out to be used as a pain relief, as a remedy against stomach pains, as a cough suppressant, carminative, intestinal regulator, diuretic and appetizer.

The leaves and flowers regarding 4 different natural *Sideritis* taxa, which are distributed in Mount Davraz, were collected from three different sample areas. Using Solid Phase Micro Extraction (HS-SPME) technique, combined with gas chromatography/mass spectrometry (GC/MS), 62 different volatile constituents were identified, regarding the leaves and flowers of the samples of *Sideritis condensata* (Boiss. & Heldr.) subsp. *condensata*, 46 different volatile constituents were identified regarding the leaves and flowers of the samples of *Sideritis hispida* P. H. Davis, 54 different volatile constituents were identified regarding the leaves and flowers of the samples of *Sideritis libanotica* Labill. subsp. *linearis* and 59 as of *Sideritis perfoliata* L. respectively.

The main components of the volatile constituents as of *Sideritis condensata* (Boiss. & Heldr.) subsp. *condensata* were identified as β -Pinene, 3-Octanol, Limonene, Caryophyllene; the main components of the volatile constituents as of *S. hispida* P. H. Davis were identified as (E)-2-Hexenal, β -Myrcene, Caryophyllene, p-Cymene; the main components of the volatile components as of *S. libanotica* Labill. subsp. *linearis* were identified as (E)-2-Hexenal, 3-Octa-

anol, Limonene, Caryophyllene and the main components of the volatile constituents as of *S. perfoliata* were identified as α -Pinene, β -Pinene, Limonene and Caryophyllene, respectively. The Caryophyllene component was identified among the main compo-

nents in each of the 4 different, natural *Sideritis* taxa that were widely distributed in Davraz Mountain. The Limonene component was encountered among the main components in the other 3 taxa except for *S. hispida* P. H. Davis.

Table 2 – Kruskal-Wallis test as a result of *Sideritis* L.

<i>Sideritis condensata</i> (Boiss. & Heldr.) subsp. condensata		1. Site	2. Site	3. Site
	Chi-Square	4,955	15,126	14,628
	df	4	4	4
	Asymp. Sig.	,292	,004	,006
<i>Sideritis hispida</i> P. H. Davis		1. Site	2. Site	3. Site
	Chi-Square	2,120	3,448	1,697
	df	3	3	3
	Asymp. Sig.	,548	,328	,638
<i>Sideritis libanotica</i> Labill. subsp. linearis		1. Site	2. Site	3. Site
	Chi-Square	11,468	4,318	2,855
	df	5	5	5
	Asymp. Sig.	,043	,505	,722
<i>Sideritis perfoliata</i> L.		1. Site	2. Site	3. Site
	Chi-Square	,578	22,862	7,404
	df	4	4	4
	Asymp. Sig.	,966	,000	,116

Ezer and Abbasoğlu [9], has identified the volatile oil components pertaining to the four types of *Sideritis*, 3 of which are endemically distributed in Turkey through GC and GC/MS (gas chromatography/mass spectrometry). α -pinene and β -pinene were found as the main constituents in *S. congesta* and *S. argyrea*. β -caryophyllene and α -pinene were found as the main constituents in *S. condensata*. Limonene was found as the main constituents in *S. perfoliata*. The results of the study differ from the results of this thesis study in terms of *S. condensata*. β -caryophyllene and α -pinene were found as the main constituents in *S. condensata*, with respect to the study conducted by Ezer and Abbasoğlu [9], whereas the main constituents were found as β -Pinene, 3-Octenol, Limonene and Caryophyllene in our study. Ezer and Abbasoğlu [9] has determined the main constituent of *S. perfoliata* as limonene. This result supports the results of our study. In our study, α -Pinene, β -Pinene, and Caryophyllene were also determined among the main components in *S. perfoliata*.

Kirimer et al. [10] reported the volatile oil constituents pertaining to six samples of *Sideritis condensata* Boiss, endemically present in Turkey through GC

and GC/MS. They have determined Germacrene-D and hexadecanoic acid as main components. However, the result of the study differs with that of the results of our study. In our study, the main components were divergently reported as β -Pinene, 3-Octenol, Limonene, and Caryophyllene. What's more, the main components of *S. perfoliata*, in our study were reported as α -Pinene, β -Pinene, and Caryophyllene.

Özkan et al. [11] reported the volatile oil constituents pertaining to *Sideritis condensata*, *S. pisidica* and *S. perfoliata*, making use of GC and GC/MS. The main components of *S. condensata* were determined as carvacrol, germacrene-D, β -pinene and β -caryophyllene, the main components of *S. pisidica* were determined as α -bisabolol, sabinene, α -pinene and β -caryophyllene, whereas the main components of *S. perfoliata* were determined as α -bisabolol, myrcene, β -caryophyllene and germacrene-D. The result of this study differs with the result of this thesis. The main components of *S. condensata* were determined as carvacrol, germacrene-D, and β -pinene in the study of Özkan et al. [11] where as the main components in *S. condensata* as of our study is found out to be β -Pinene, 3-Octanol, Limonene, and Caryophyllene.

However, β -Pinene component was identified as the main component in both studies. The main components in *S. perfoliata* as of the study conducted by Özkan et al. (2005) were determined as α -bisabolol, myrcene, β -caryophyllene and germacrene-D, whereas the main components of *S. perfoliata* in our study were found out to be α -Pinene, β -Pinene, Limonene, and Caryophyllene.

Krimer et al. [12] has reported the volatile oil constituents pertaining to *Sideritis hispida* P. H. Davis, which is endemically widespread in Turkey, making use of GC and GC/MS. They have identified 63 different constituents, where β -caryophyllene and carvacrol were defined as main components. The result of their study differs with the result of this thesis. In our study the main components of *S. hispida* were reported as (E)-2-Hexenal, β -Myrcene, Caryophyllene, and p-Cymene.

In a study conducted by Özderin [13] on natural tea herbs and their volatile oil constituents as of Muğla-Ula Region, the main components of *Sideritis libanoitica* Labill subsp. *linearis* were reported as myrcene, linalool, β pinene, α -cadino and caryophyllene. The result of their study differs with the result of this thesis. However, the caryophyllene component was determined among the main components, in both studies.

Conclusion

This study determines the volatile constituents and their percentiles regarding the leaves and flowers pertaining to *Sideritis condensata* (Boiss. & Heldr.) subsp. *condensata*, *S. hispida* P. H. Davis, *S. libanotica* Labill. subsp. *linearis* and *S. perfoliata*, widely encountered in Davraz Mountain. Results are important to reveal the economic value of the plants in the region, which are widely consumed as natural herbal tea, and to provide a perception of conscious consumption.

Moreover, *Sideritis* tea is widely consumed colloquially as a pain relief, remedy against stomach pains, as a cough suppressant, carminative, intestinal regulator, diuretic and appetizer. These and similar studies should be upgraded in order to ensure people to consume *Sideritis* more consciously.

Acknowledgements

We express our sincere appreciation to Suleyman Demirel University, Coordinatorship of Scien-

tific Research Projects for their financial support by project numbered as 5032-YL1-17.

References

1. Başer K.H.C. (2000). Uçucu yağların parlak geleceği. Tıbbi ve Aromatik Bitkiler Bülteni Sayı: 15, Anadolu Üniversitesi Tıbbi ve Aromatik Bitki ve İlaç Araştırma Merkezi, Eskişehir (in Turkish)
2. Weiss E.A. (1997). Essential Oil Crops. The Journal of Agricultural Science, no. 129, pp. 121-123.
3. Özçelik H., Serdaroğlu H. (2000). Isparta Florasına Ön Hazırlık. Süleyman Demirel Üniversitesi Fen Bilimleri Enstitüsü Dergisi, vol. 1, no. 4, pp. 135-154. (in Turkish)
4. Davis P.H. (1982). Flora of Turkey and East Aegean Islands 7, Edinburg University Press, 948 p., Edinburg.
5. Seçmen Ö., Gemici Y., Görk G., Bekat L., Leblebici E. (2011). Tohumlu Bitkiler Sistematığı, 9. Baskı, 361 s.. Ege Üniversitesi Basımevi, İzmir (in Turkish)
6. Güner A. (2012). Türkiye Bitkileri Listesi, Damarlı Bitkiler. Nezahat Gökyiğit Botanik Bahçesi Yayınları, 1290 s., İstanbul. (in Turkish)
7. Başer K.H.C. (2002). Aromatic biodiversity among the flowering plant taxa of Turkey. *Pure Appl. Chem.*, 74, 527-545.
8. Kirimer N., Tabanca N., Tümen G., Duman H., Başer K.H.C. (1999). composition of the essential oils of four endemic *Sideritis* species from Turkey. *Flav. Fragr. J.*, no. 14, pp. 421-425.
9. Ezer N., Abbasoğlu U. (1996). Antibacterial activity of essential oils of some *Sideritis* species growing in Turkey. *Fitoterapia*, vol. 5, pp. 474-475.
10. Kirimer N., Kürkcüoğlu M., Özek T., Başer K.H.C. (1996). Composition of Essential Oil of *Sideritis condensata* Boiss. et Heldr. *Flav. Fragr. J.*, vol. 11, pp. 315-320.
11. Özkan G., Sağdıç O., Özcan M., Özçelik H., Ünvers A. (2005). Antioxidant and antibacterial activities of Turkish endemic *Sideritis* extracts. *Grasasy Aceites*, vol. 1, pp. 16-20.
12. Kirimer N., Özek T., Başer K.H.C., Tümen G. (2011). Essential oil of *Sideritis hispida* P. H. Davis, an endemic species from Turkey. *J. Essent. Oil Res.*, vol. 6, no. 4, pp. 435-436.
13. Özderin S. (2010). Muğla-Ula Yöresi'nin Doğal Çay Bitkileri ve Uçucu Yağ Bileşenleri. Süleyman Demirel Üniversitesi, Fen Bilimleri Enstitüsü, Yüksek Lisans Tezi, 92s. (in Turkish)

¹*O. Bulgakova^{ib}, ¹A. Kussainova^{ib}, ²N. Kalibekov^{ib}, ²D. Serikbaiuly^{ib},
³T. Zinoveva^{ib}, ¹A. Aripova^{ib}, ¹R. Bersimbaev^{ib}

¹L.N. Gumilyov Eurasian National University, Institute of Cell Biology and Biotechnology, Kazakhstan

²National Research Oncology Center, Nur-Sultan, Kazakhstan

³Multidisciplinary regional hospital of Akmola region, Kokshetau, Kazakhstan

*e-mail: ya.summer13@yandex.kz

The plasma levels of hsa-miR-19b-3p, hsa-miR-125b-5p and hsa-miR-155b-5p in NSCLC patients

Abstract: Lung cancer is one of the leading causes of cancer deaths worldwide. Presently for lung cancer patients various treatments are available, such as surgery, chemotherapy and radiotherapy. Nevertheless the 5 year overall survival remains still low. As many modern studies show, microRNAs can be novel and reliable biomarkers to predict the prognosis of lung cancer. Therefore, the aim of this study was to investigate the expression levels of hsa-miR-19b-3p, hsa-miR-125b-5p and hsa-miR-155b-5p in plasma of patients with non-small cell lung cancer (NSCLC) to clarify the relationships of free-circulating microRNAs expression with clinical factors and prognosis of NSCLC patients. Total RNA was extracted from blood samples of 49 NSCLC patients before treatment, 37 NSCLC patients after platinum-based chemotherapy and 50 healthy controls. The relative expression levels of microRNAs were evaluated by real time-polymerase chain reaction (RT-PCR). Kaplan-Meier method was used to analyze the survival curve. Plasma hsa-miR-19b-3p, hsa-miR-125b-5p and hsa-miR-155b-5p expression levels in NSCLC patients were significantly upregulated compared with those in healthy individuals (all $P \leq 0.01$). In plasma of NSCLC patients the expression level of hsa-miR-155b-5p significantly decreased in response to chemotherapy ($P < 0.01$). NSCLC patients with high plasma hsa-miR-19b-3p and hsa-miR-155b-5p expression levels had a shorter overall survival than patients with low expression levels of these microRNAs ($P = 0.005$). Thus, the free-circulating hsa-miR-19b-3p and hsa-miR-155b-5p levels may serve as promising prognostic biomarkers in patients with NSCLC and hsa-miR-155b-5p can be used as biomarker for monitoring of effectiveness of antitumor therapy.

Key words: free-circulating microRNA, non-small cell lung cancer, hsa-miR-19b-3p, hsa-miR-125b-5p, hsa-miR-155b-5p, overall survival.

Introduction

MicroRNAs are a class of small non-coding endogenous RNAs with a length of 21-25 nucleotides that play an important role in the post-transcriptional regulation of gene expression by targeting mRNA followed by translation repression. MicroRNAs are involved in the pathogenesis of numerous diseases, including autoimmune, neurodegenerative diseases and cancer. Recently, the study of the level of free-circulating miRNAs has an increasingly widespread practical application in the diagnosis, prevention and treatment of various diseases [1]. Many studies have shown that microRNAs participate in tumorigenesis and progression of various types of cancer, including lung [2; 3]. Lung cancer is one of the leading causes of cancer deaths worldwide [4]. Unfortunately, to

date, 100% sensitive and specific biomarkers for lung cancer have not been found. Moreover, some cancer-specific biomarkers were also found in plasma of healthy people [5]. Perhaps the development of microRNA-based panels would be effective for the early diagnosis of lung cancer.

Therefore, the purpose of this study was to assess the predictive value of free-circulating microRNAs hsa-miR-19b-3p, hsa-miR-125b-5p and hsa-miR-155b-5p for diagnosis, prognosis and effectiveness of antitumor therapy in NSCLC patients.

Materials and methods

Patients. A total of 86 blood samples of NSCLC patients and 50 blood samples of healthy individuals collected between 2015 and 2018 from Astana On-

cology Center and Akmola region Oncology Hospital. All cases were newly diagnosed, previously untreated and histologically confirmed. Clinical stage was classified according to the sixth edition of the tumor-node-metastases (TNM) classification of the International Union Against Cancer.

49 samples were obtained before anticancer treatment, including surgery, chemotherapy and radiotherapy. 37 samples were obtained from patients after a course of platinum-based chemotherapy. The treatment was carried out in accordance with the Clinical Protocol for the Diagnosis and Treatment of Lung Cancer, recommended by the Expert Council of the Republican State Health Service at the Republican Center for the Development of Health Care of the Ministry of Health and Social Development of the Republic of Kazakhstan dated October 30, 2015 (Protocol No. 14) [6].

The study was approved by the Ethical Committee of the Astana Medical University, Kazakhstan (Astana, Kazakhstan; approval no. 4).

All participants were informed about the purpose and procedures, and their written informed were obtained.

RNA extraction from blood. A 10 ml sample of whole peripheral blood was collected from each subject into EDTA containing tubes. Blood was centrifuged at 3,000 x g for 10 min and supernatant stored in aliquots at -80°C. Total RNA from 200 µL plasma was isolated using the miRCURY RNA Isolation Kit – Biofluids (#300112, EXIQON, Vedbaek, Denmark) in accordance with the protocol.

microRNAs analysis by qPCR. The expression levels of microRNAs were determined by evaluating the level of fluorescence emitted by SYBR GREEN tracer. MiRCURY LNA™ UNIVERSAL RT microRNA PCR LNA™ kit, including microRNAs specific primers hsa-miR-19b-3p (#204450, Exiqon, Denmark), hsa-miR-125b-5p(#205713, Exiqon, Denmark), hsa-miR-155-5p(#204308, Exiqon, Denmark) was used to amplify microRNAs according to the manufacturer's instructions. cDNAs were prepared using Universal synthesis Kit (#203301, EXIQON, Vedbaek, Denmark) according to the manufacturer's instructions. Real-time PCR amplification was performed in the CFX96 Touch™ Real-Time PCR Detection System (Bio-Rad). Each reaction was carried out using 4 µL of cDNA, 1 µL of PCR primer mix and 5 µL SYBR-Green PCR Master mix (#203403, EXIQON, Vedbaek, Denmark) in a final 10 µL volume. The qRT-PCR was performed at 95°C for 10 min for one cycle, then 95°C for 10 sec with 60°C for 60 sec for 40 cycles. Gene expression was nor-

malized to RNU6B (#203907, EXIQON, Vedbaek, Denmark). All reactions were carried out in triplicate, and the 2^{-ΔΔCt} method was used to quantify the relative microRNA amount [7].

Statistical Analysis. Differences in microRNA levels between NSCLC patients and healthy control were compared using a paired Student's t-test. Kaplan-Meier method was used to analyze the survival curve. P value < 0.05 considered as significant. These statistical analyses were performed using GraphPad Prism 7.0 (Graphpad software Inc., CA, USA).

Results and discussion

Study design. The study included 50 volunteers without pulmonary pathologies and acute/chronic inflammatory diseases (control), among them 11 women and 39 men. The average age in the group was 47 years. The group consisted of 8 smokers, 41 non-smokers and 1 former smoker. The group of lung cancer patients included 86 people, among them 16 women and 70 men. The average age in the group was 65 years. The lung patients group consisted of 34 smokers, 33 non-smokers and 19 former smokers.

The group of lung cancer was consisted of 20 patients with pathologic stage I NSCLC, 32 patients with stage II, 25 patients with stage III and 9 patients with pathologic stage IV NSCLC.

Comparison of two groups ("Lung cancer" and "Control") by sex, age and smoking status presented in Table 1.

Table 1 – Characteristics of the subject participating in the study

	Lung cancer (n=86)	Control (n=50)	P
Male	70(81%)	39 (78%)	0.12
Female	16 (19%)	11(22%)	
Age ≤60	30 (35%)	21 (42%)	0.35
Age >60	56 (65%)	29 (58%)	
Non-smokers	33 (34%)	41 (82%)	0.36
Smokers	34 (39%)	8 (16%)	
Former Smokers	19 (27%)	1(2%)	

NSCLC patients were divided into two experimental groups: lung cancer before treatment and lung cancer after treatment, depending on the presence/absence of chemotherapy. The first group consisted of 49 people; the second group consisted of 37 people.

Comparison of the experimental groups “Lung cancer after treatment” and “Lung cancer before treatment” are shown in Table 2.

Table 2 – Comparative characteristic of the experimental groups “Lung cancer before treatment” and “Lung cancer after treatment”

	Lung cancer after treatment (n=37)	Lung cancer before treatment (n=49)	P
Male	31(84%)	39(80%)	0.78
Female	6 (16%)	10(20%)	
Age ≤60	18 (27%)	14(8%)	0.51
Age >60	27 (73%)	45(92%)	
Non-smokers	9 (24%)	24(49%)	0.52
Smokers	21 (57%)	13(27%)	
Former Smokers	7 (19%)	12(24%)	

The level of relative expression of free-circulating microRNA hsa-miR-19b-3p in lung cancer patients

The results showed that the level of expression of hsa-miR-19b-3p in patients with lung cancer before treatment was 6.5 times higher than in healthy people ($p < 0.0001$). Similar data were obtained by analyzing the expression of hsa-miR-19b-3p in the plasma samples of patients with lung cancer after treatment. In this group, the level of hsa-miR-19b-3p was 6.9

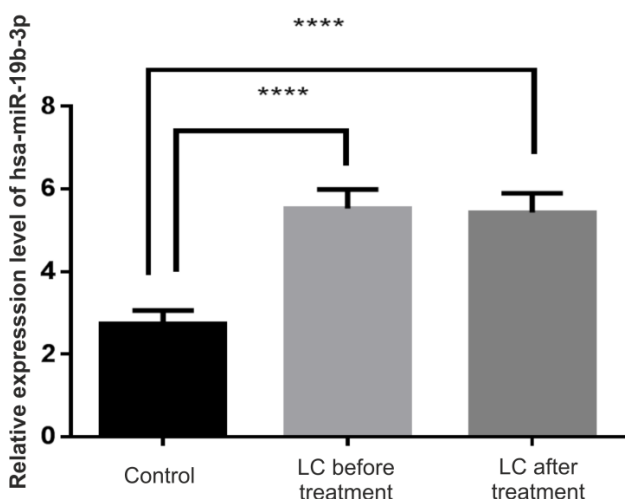


Figure 1 – Relative expression level of hsa-miR-19b-3p in patients with lung cancer before and after treatment compared to control

times higher compared with the control ($p < 0.0001$) (Figure 1). There was no difference in expression of hsa-miR-19b-3p in both groups of lung cancer patients.

The level of relative expression of free-circulating microRNA hsa-miR-125b-5p in lung cancer patients

The relative expression level of hsa-miR-125b-5p in plasma samples of lung cancer patients before treatment was 4 times higher than that in plasma samples of healthy individuals ($p < 0.001$). The results showed no differences in the expression level of hsa-miR-125b-5p in plasma of lung cancer patients after treatment and healthy people from the control group. Comparison of the expression level of hsa-miR-125b-5p in blood plasma of lung cancer patients showed that the expression level was almost 2 times lower after treatment than in lung cancer patients before treatment (Figure 2).

The level of relative expression of free-circulating microRNA hsa-miR-155-5p in lung cancer patients

In plasma of patients with lung cancer before treatment, the expression level of hsa-miR-155-5p was 2 times higher compared to the control group ($p < 0.001$). Difference in the level of hsa-miR-155-5p expression between the lung cancer patients after treatment and healthy individuals was not detected. A twofold decrease in the level of free-circulating hsa-miR-155-5p was observed in plasma samples of lung cancer patients after treatment compared to patients before treatment ($p < 0.01$) (Figure 3).

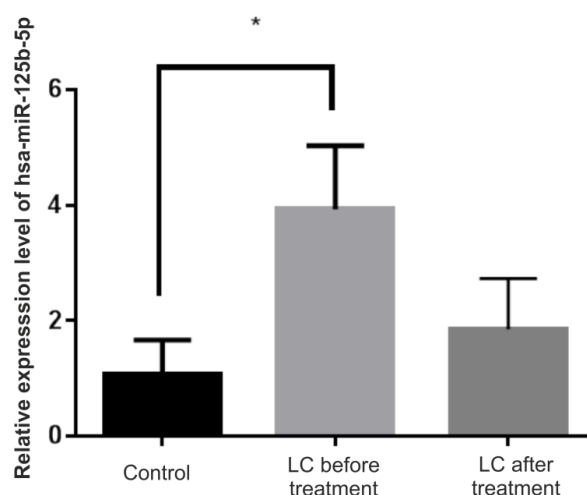


Figure 2 – Relative expression level of hsa-miR-125b-5p in lung cancer patients before and after treatment compared to control

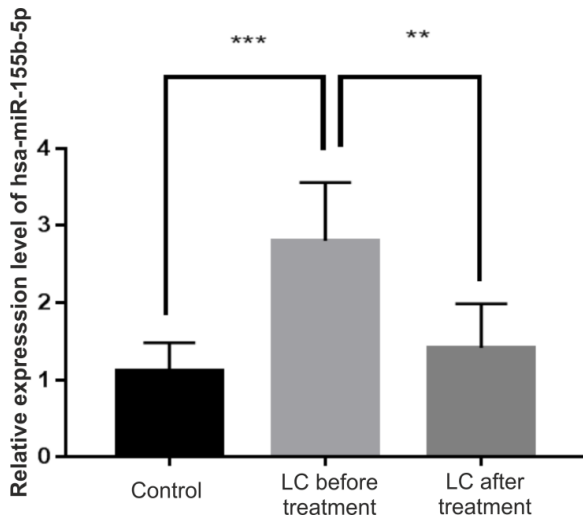


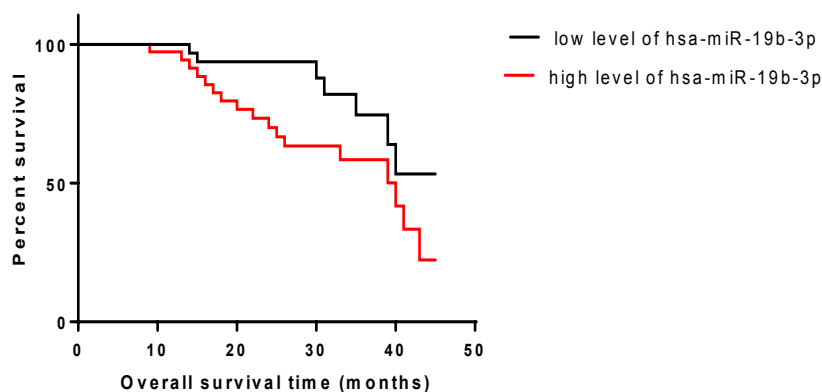
Figure 3 – Relative expression level of hsa-miR-155b-5p in lung cancer patients before and after therapy compared to control

Survival of lung cancer patients according to the expression levels of free-circulating microRNA hsa-miR-19b-3p, hsa-miR-125b-5p, hsa-miR-155-5p

Univariate analysis revealed that patients with high expression of hsa-miR-19b-3p had shorter survival time than those with low expression (HR = 2.33, 95% CI: 1.04-5.230, $p = 0.02$) (Figure 4A). Plasma level of hsa-miR-125b-5p was not associated with survival in lung cancer patients ($p = 0.2$). High expression level of hsa-miR-155b-5p was significantly associated with worse survival in lung cancer patients (HR = 2.78, 95% CI: 1.32-5.88, $P = 0.005$) (Figure 4D).

Then combination of plasma hsa-miR-19b-3p and hsa-miR-155b-5p was analyzed. Using the low-risk group (low hsa-miR-19b-3p and hsa-miR-155b-5p expression) as a reference, patients with high hsa-miR-19b-3p and hsa-miR-155b-5p expression had 2.14- (95% CI: 1.147 to 4.092, $p=0.005$) increased risk of death.

A



B

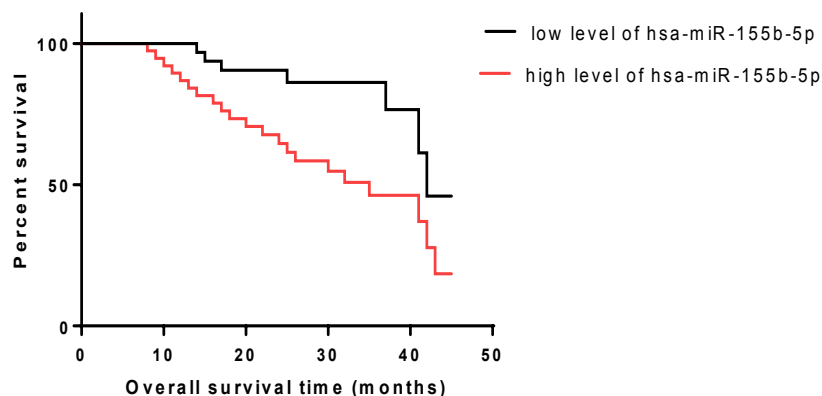


Figure 4 – Kaplan-Meier survival curves of lung cancer patients according to the expression levels of free-circulating microRNA hsa-miR-19b-3p (A) and hsa-miR-155-5p (B)

Despite the accuracy of diagnostic methods used in modern pathology has dramatically improved, the early diagnosis of lung cancer remains challenging. Unique microRNA expression profiles have been observed in various cancer types at different stages, suggesting their potential as diagnostic and prognostic biomarkers. In addition, there is a requirement to new sensitive and specific prognostic markers which can be used to determine the effectiveness of chemotherapy and the individual response of the patient to the treatment.

microRNAs can modulate the expression of multiple genes, playing essential roles in many cellular processes, and thus microRNAs can directly influence the development and progression of many types of cancer [1]. Unique microRNA expression profiles have been observed in various cancer tumors [1], suggesting their potential as diagnostic and prognostic biomarkers. The miR-19 family (miR-19a and miR-19b) are key oncogenic components of the miR-17-92 cluster [8]. It was shown that miR-19b enhances the proliferation and apoptosis resistance of cancer cells by the epidermal growth factor receptor (EGFR) signaling pathway [9]. Moreover, overexpression of miR-19b observed in human cancer cells can diminish p53 protein levels [10].

In our study we have shown aberrant expression level of hsa-miR-19b-3p in plasma of NSCLC patient. Our data are consistent with other studies [11; 12]. Considering these results, hsa-miR-19b-3p might serve as an oncogene, and play a crucial role during tumor development of lung cancer. However, it is interesting that the expression of hsa-miR-19b-3p remained at the same level in the group after platinum-based chemotherapy.

Based on the altered this microRNA expression in plasma of NSCLC patients, we further analyzed the clinical value of hsa-miR-19b-3p in lung cancer prognosis. According to the Kaplan–Meier survival analysis, we observed that patients with high hsa-miR-19b-3p expression had a shorter survival time than those with low expression, suggesting that overexpression of hsa-miR-19b-3p might be closely correlated with poor overall survival of lung cancer patients.

There are a lot of controversial data about role of hsa-miR-125b in human cancer. Thus, Gong et al. shown that miR-125b may promote apoptosis by suppressing the anti-apoptotic molecules of the Bcl-2 family [13]. On the other hand, it was demonstrated, that miR-125b is an important negative regulator of p53 and p53-induced apoptosis [14; 15]. There is the same situation in the question about a role of miR-125b as biomarkers for diagnosis of lung cancer.

Different studies have shown that miR-125b is up-regulated [16] or down-regulated [17] in lung cancer. Our results are consistent with the data from other authors on the role of hsa-miR-125b as an oncomiR since over-expression of this microRNA is observed in plasma blood samples of lung cancer patients. The trend of down-regulation of hsa-miR-125b in NSCLC patients after treatment was found ($p=0.06$). There was no significant relationship between high expression levels of blood free-circulating hsa-miR-125b and patient survival prognosis. Li et al. had shown that miR-125b promoted tumor metastasis in NSCLC patients [18]. In our study we could not find correlation between metastasis progression and the expression level of hsa-miR-125b (data not shown).

Many studies had shown that altered expression of miR-155 was associated with various physiological and pathological processes, including hematopoietic lineage differentiation [19], immune response [20], inflammation [21] and tumorigenesis [22]. Furthermore, Lv et al. [23] found that miR-155 drives therapy resistance mechanisms in human lung cancer A549/dox cells. Our results demonstrated overexpression of hsa-miR-155b-5p in blood plasma of NSCLC patients compared to control. Moreover, high hsa-miR-155b-5p expression level was found to be correlated with poor survival in lung cancer patients. Our data suggest that hsa-miR-155b-5p can be promising biomarker for monitoring of effectiveness of antitumor therapy. Because, the significant decrease in the level of free-circulating hsa-miR-155-5p was observed in NSCLC patients after treatment compared to patients before treatment. Our data are consistent with the results of Van Roosbroeck [24], who showed, that combined treatment of miR-155 inhibitor and cisplatin significantly reduced viability of lung cancer cells.

Conclusion

Present study showed that plasma levels of hsa-miR-19b-3p, hsa-miR-125b-5p and hsa-miR-155b-5p were associated with lung cancer and could be useful for further development of microRNA-based panels for early diagnosis of NSCLC. Free-circulating hsa-miR-19b-3p and hsa-miR-155b-5p can be used as prognostic biomarkers for NSCLC patients. Plasma levels of hsa-miR-155b-5p may serve as biomarker for NSCLC patients receiving platinum-based chemotherapy. Further studies are needed to investigate the role of hsa-miR-125b-5p as biomarker for monitoring of effectiveness of antitumor therapy in NSCLC.

Acknowledgements

We thank the Astana Oncology Center (Astana city) and Akmola Region Oncology Hospital (Kokshetau city) for their help in collection of samples.

References

- Izzotti A., Carozzo S., Pulliero A., Zhabayeva D., Ravetti J.L., Bersimbaev R. (2016) Extracellular MicroRNA in liquid biopsy: applicability in cancer diagnosis and prevention. *Am. J. Cancer Res.*, vol. 6, pp. 1461-1493.
- Wu K.L., Tsai Y.M., Lien C.T., Kuo P.L., Hung A.J. (2019) The Roles of MicroRNA in Lung Cancer. *Int. J. Mol. Sci.*, vol. 20, p. 1611.
- Bulgakova O., Zhabayeva D., Kussainova A., Pulliero A., Izzotti A., Bersimbaev R. (2018) miR-19 in blood plasma reflects lung cancer occurrence but is not specifically associated with radon exposure. *Oncol. Lett.*, vol. 15, pp. 8816-8824.
- Siegel R., Ma J., Zou Z., Jemal A. (2014) Cancer statistics. *CA Cancer J. Clin.*, vol. 64, pp. 9-29.
- Zamay T.N., Zamay G.S., Kolovskaya O.S., et al. (2017) Current and Prospective Protein Biomarkers of Lung Cancer. *Cancers*, vol. 9, p. 155.
- Kazakh Research Institute of Oncology and Radiology. <https://onco.kz/klinicheskie-protokola-diagnostiki-i-lechenie-zlokachestvennyh-novoobrazovaniy/>
- Livak and Schmittgen (2001) Analysis of relative gene expression data using real-time quantitative PCR and the 2- $\Delta\Delta$ Ct method. *Methods*, vol. 25, pp. 402-408.
- Zhang X., Li Y., Qi P., Ma Z. (2018) Biology of MiR-17-92 Cluster and Its Progress in Lung Cancer. *Int J Med Sci.*, vol. 15, pp. 1443-1448.
- Baumgartner U., Berger F., Hashemi Gheini A., Burgener S.S., Monastyrskaya K., Vassella E. (2018) miR-19b enhances proliferation and apoptosis resistance via the EGFR signaling pathway by targeting PP2A and BIM in non-small cell lung cancer. *Mol. Cancer*, vol. 17, p. 44.
- Fan Y., Yin S., Hao Y., Yang J., Zhang H., Sun C., Ma M., Chang Q., Xi J.J. (2014) miR-19b promotes tumor growth and metastasis via targeting TP53. *RNA*, vol. 20, pp. 765-772.
- Zaporozhchenko I.A., Morozkin E.S., Skvortsova T.E., Ponomaryova A.A., Rykova E.Y., Cherdynseva N.V., Polovnikov E.S., Pashkovskaya O.A., Pokushalov E.A., Vlassov V.V., Laktionov P.P. (2016) Plasma miR-19b and miR-183 as Potential Biomarkers of Lung Cancer. *PLoS One*, vol. 11, e0165261.
- Lu S., Kong H., Hou Y., Ge D., Huang W., Ou J., Yang D., Zhang L., Wu G., Song Y., Zhang X., Zhai C., Wang Q., Zhu H., Wu Y., Bai C. (2018) Two plasma microRNA panels for diagnosis and subtype discrimination of lung cancer. *Lung Cancer*, vol. 123, pp. 44-51.
- Gong J., Zhang J.P., Li B., Zeng C., You K., Chen M.X., Yuan Y., Zhuang S.M. (2013) MicroRNA-125b promotes apoptosis by regulating the expression of Mcl-1, Bcl-w and IL-6R. *Oncogene*, vol. 32, pp. 3071-3079.
- Le M.T., Teh C., Shyh-Chang N., Xie H., Zhou B., Korzh V., Lodish H.F., Lim B. (2009) MicroRNA-125b is a novel negative regulator of p53. *Genes Dev.*, vol. 23, pp. 862-876.
- Yuxia M., Zhennan T., Wei Z. (2012) Circulating miR-125b is a novel biomarker for screening non-small-cell lung cancer and predicts poor prognosis. *J. Cancer Res. Clin. Oncol.*, vol. 138, pp. 2045-2050.
- Zhang Y., Huang S. (2015) Up-regulation of miR-125b reverses epithelial-mesenchymal transition in paclitaxel-resistant lung cancer cells. *Biol. Chem.*, doi: <https://doi.org/10.1515/hsz-2015-0153>.
- Yu X., Wei F., Yu J., Zhao H., Jia L., Ye Y., Du R., Ren X., Li H. (2015) Matrix Metalloproteinase 13: A Potential Intermediate Between Low Expression of microRNA-125b and Increasing Metastatic Potential of Non-Small Cell Lung Cancer. *Cancer Genet.*, vol. 208, pp. 76-84.
- Li Q, Han Y, Wang C, Shan S, Wang Y, Zhang J, Ren T (2015) MicroRNA-125b promotes tumor metastasis through targeting tumor protein 53-induced nuclear protein 1 in patients with non-small-cell lung cancer. *Cancer Cell Int.*, doi: 10.1186/s12935-015-0233-x.
- Van Roosbroeck, K., Calin, G.A (2016) MicroRNAs in chronic lymphocytic leukemia: miRacle or miRage for prognosis and targeted therapies? *Semin Oncol.*, vol. 43, pp. 209-214.
- Alivernini S, Gremese E, McSharry C, Tolusso B, Ferraccioli G, McInnes IB, Kurowska-Stolarska M (2018) microRNA-155 – at the critical interface of innate and adaptive immunity in arthritis. *Front. Immunol.*, doi: 10.3389/fimmu.2017.01932.
- Mahesh G., Biswas R. (2019) MicroRNA-155: a master regulator of inflammation. *J. Interferon Cytokine Res.*, vol. 39, pp. 321-330.
- Chen S., et al. (2015) Host miR155 promotes tumor growth through a myeloid-derived suppressor cell-dependent mechanism. *Cancer Res.*, vol. 75, pp. 519-531.
- Lv L., et al. (2016) Effect of miR-155 knock-down on the reversal of doxorubicin resistance in human lung cancer A549/dox cells. *Oncol Lett.*, vol. 11, pp. 1161-1166.
- Van Roosbroeck, K., et al. (2017) Combining anti-Mir-155 with chemotherapy for the treatment of lung cancers. *Clin Cancer Res.*, vol. 23, pp. 2891-2904.

¹*G.A. Yestemirova , ¹Z.B. Yessimsiitova , ²M.P. Danilenko 

¹Al-Farabi Kazakh National University, Almaty, Kazakhstan

²Ben-Gurion University of the Negev, Beer-Sheva, Israel

*e-mail: gulfira.yestemirova@gmail.com

Current progress in the study of acute myeloid leukemia

Abstract. In recent years the rate of malignant diseases has been growing rapidly around the world. The Republic of Kazakhstan, according to international statistics, refers to the countries with moderately high cancer incidence and mortality. Every year approximately thirty thousand Kazakhstani people are diagnosed with cancer. In 2018, 35,753 patients were registered in the country, of which 44.3% were men and 55.7% were women. Cancer mortality over the same period amounts to about 15,000 lives. The cancer incidence rate increased by 8% from 181.2 (in 1999) to 195.7 per 100,000 population in 2019 [1]. Blood cancers are relatively rare diseases but, nevertheless, in Kazakhstan about 7,000 patients with hematopoietic malignancies are currently registered. Therefore, our knowledge of recent advances in hemato-oncology is highly relevant for successful therapy of these malignancies. In this review we provide information on the subtypes, symptoms, diagnosis and treatment of acute myeloid leukemia (AML) – one of the most aggressive blood cancer.

Key words: acute myeloid leukemia, cancer, anemia, FLT3, flavopyridol, HDAC inhibitor, PAP, targeted therapy.

Cancer is a major health problem facing the entire world, and Kazakhstan is not the exception. Currently, according to Kazakhstan statistics, blood cancer is one of the ten most common oncological diseases. There is a tendency for a slight increase in the incidence over the past ten years. The situation in the rest of the world is similar. One possible explanation is the improvement in diagnostic methods. Lymphomas and leukemias are most common in the industrialized countries, such as the USA, Switzerland and other European countries. Low rates of these cancers are recorded in Asian countries. In Kazakhstan, metrics are lower than in European countries. Chronic lymphocytic leukemia is more common in the Caucasian race. But it is also found among Asians and Kazakhs. There is also a tendency towards a “rejuvenation” of the blood cancer which has faced an epidemiological crisis due to an increase in the country’s population. Totally, 6 741 new cases of leukemia were registered in Kazakhstan during the 2003-2012 period. The mean age of patients with leukemia was 48.5. The age-standardized incidence rates for leukemia among men and women were 5.3 and 3.6, respectively ($p < 0.001$) [2].

It is known that cancer of the blood or hemoblastosis is a serious disease that can arise in men, women and even children, during the course of which

blood-forming organs are affected. Malignant neoplasms which occur in the bone marrow are called leukemias. In addition to leukemias hemoblastoses include diseases such as hematosarcomas and lymphomas, which are extra-bone marrow growths of blast cells. Over time, tumor cells in hematosarcomas and lymphomas can spread to the bone marrow [3]. The causes of hemoblastoses are chemical carcinogenic agents, radiation or inherited genetic and epigenetic aberrations. Various carcinogens, acting on the hematopoietic cell genome, cause the transformation of its normal genetic program into a program for the formation of malignant neoplasms [4].

Acute myeloid leukemia (AML) is an aggressive clonal oncohematological disease associated with damage to the genetic material in hematopoietic stem and/or progenitor cells. Genetic and epigenetic transformation results in an appearance of immature myeloid blast cells which lack the ability to differentiate and are characterized by rapid uncontrolled proliferation. This leads to suppression of normal hematopoiesis due to replacement of normal bone marrow blast cells with leukemic blasts. There are several subtypes of AML, including monoblastic leukemia, acute promyelocytic leukemia, monocytic leukemia, megakaryocytic leukemia and erythroblastic leukemia and there are also mixed acute leukemia forms (Figure 1).

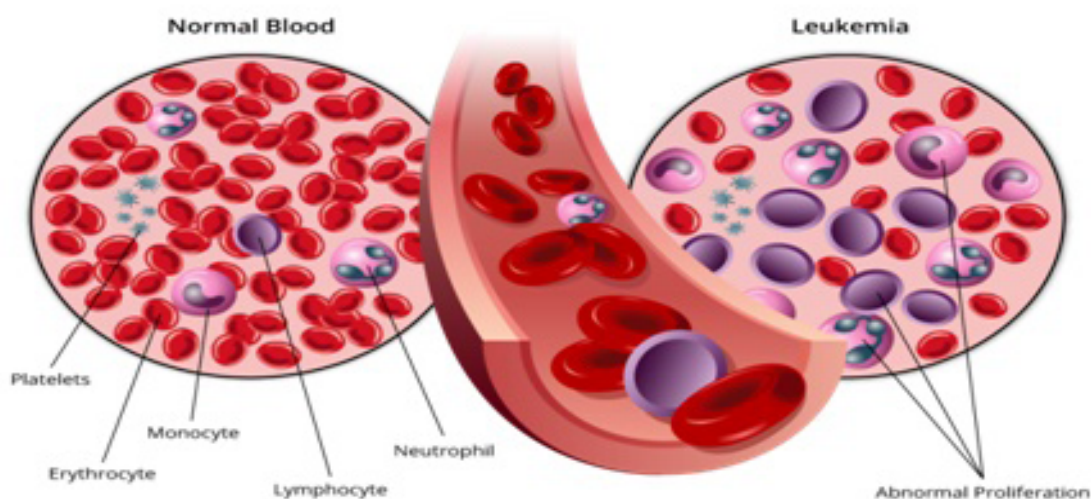


Figure 1 – General scheme for blood changes during leukemia (<https://westcancercenter.org>)

Laboratory tests, including cytomorphological, immunological and genetic analyses are employed to diagnose specific AML subtypes.

The fact that the pathogenesis of acute leukemia is associated with genetic breakdowns is often confirmed by the discovery of various chromosomal aberrations, translocations, deletions, inversions, etc. In most cases, the specific cause of AML remains unknown. However, there are several predisposing factors that significantly increase the risk of developing this disease. The clearly proven relationship between chemotherapy and/or radiotherapy for other tumors and an increased risk of acute leukemia, made many research groups study other possible leukemogenic factors, such as low doses of radiation, various chemicals, smoking, and electromagnetic waves. For instance, clear dose dependence has been proven between smoking and the risk of developing acute leukemia, that is especially evident for people over 60 years of age. A number of reports suggest that about 20% of AML are due to smoking. Prolonged exposure of the human body to benzene has a leukemogenic effect, but at low concentrations of this substance, which people most often encounter in the workplace, the relationship with an increased risk of AML is not proven.

In studying the effects of continual low-dose radiation, evidence has not yet been obtained in favor of an increase in the incidence of acute leukemia. For the first time, the relationship between previous chemotherapy or radiation treatment of other tumor diseases and an increased risk of AML was observed in patients cured of lymphogranulomatosis. It has been shown that not so much the cumulative dose as the

dose intensity of the exposure is associated with an increase in the incidence of AML. The risk of developing secondary AML is highest between 2 and 9 years after completion of previous chemotherapy. In 85% of cases, secondary leukemia occurs within up to 10 years from the end of treatment [5; 6]. Children and adolescents with a specific congenital or acquired immunodeficiency, certain chromosomal abnormalities, diseases Down syndrome, Fanconi anemia, have a high predisposition to get sick with develop one of the forms of myeloid leukemia.

In the course of leukemogenesis, when diseased cells displace healthy ones, anemia, various infectious complications and frequent bleeding are observed. These are the first symptoms that can speak of acute leukemia. Other symptoms, such as fatigue, general weakness, sickness, fever, abdominal pain, loss of appetite are very often observed. Enlarged lymph nodes are noted. If leukemia cells enter the central nervous system, then cranial nerves can be paralyzed and breathing becomes difficult [7; 8]. AML, like all other types of leukemia, is a systemic malignant disease, that is, from the bone marrow it rapidly spreads into the bloodstream, lymphoid tissues and other organs. If acute leukemia is not treated, then death occurs in a few weeks or months.

Among all forms of cancer in children and adolescents, AML accounts for about 4.2% cases. According to German medical statistics, about 80 children and adolescents aged 0 to 14 years with a diagnosis of AML are registered annually in the Children's Cancer Register (Mainz), and the total number of patients with leukemia under the age of 18 is approximately 100 people a year [9; 10]. However, this

disease primarily targets older individuals and the median age of AML patients in general is about 68.

Carcinogenesis can be induced by chemical agents that are part of the food, and compounds used in various fields of industry. More than 1,500 organic and inorganic chemical compounds are potentially carcinogenic. Physical carcinogens include radioactive substances containing ^{32}P , ^{131}I , ^{90}Sr and other isotopes, x-rays and ultraviolet radiation. DNA – the main target of carcinogenic agents – is exposed either to their direct action or through mediators of carcinogenesis, including free radicals of oxygen, lipids and other organic and inorganic substances. Oncogenic viruses can also cause the development of blood cancers. For instance, the Epstein – Barr virus leads to the development of Burkitt's lymphoma, the human T-cell leukemia virus type I leads to T-lymphocytic leukemia. Retroviruses, adenoviruses and adeno-associated viruses can integrate into the human blood-forming cell genome and cause their oncogenic transformation. By the type of viral nucleic acid, oncogenic viruses are divided into DNA- and RNA-containing. Some oncoviral genes can play the role of promoters of cellular proto-oncogenes [11].

The mainstream treatment of AML is intensive chemotherapy with drugs that block cell growth or induce cytotoxicity. One such drug cannot kill all tumor cells, thus modern therapeutic approaches employ combinations of different cytostatics, cytotoxic agents and/or targeted drugs that act on cancer cells in different ways. Using these approaches it becomes possible, in some cases, to completely kill leukemia cells throughout the body so that the bone marrow can again earn as a hematopoietic organ. The initial stage of AML management is induction chemotherapy when a particularly intensive treatment is carried out in order to kill a maximum of leukemia cells within a short time. The next stage is consolidation therapy, which aims at destroying those leukemic cells that could survive the induction stage. The standard drug combination used in induction chemotherapy of AML is cytarabine and one of anthracyclines. Yet, the clinical outcomes remain to be poor, especially for those patients who are older or carry other higher-risk diseases. In recent years, extensive research has led to the development and characterization of novel agents which target AML by diverse mechanisms [12]. Among these are targeted therapeutics such as kinase inhibitors and oligonucleotide constructs. These aim to suppress the production or activity of oncogenic proteins, such as FLT3 and BCL2, and thus disrupt related signaling cascades essential for leukemogenesis and blast cell

proliferation. Other agents, e.g., flavopiridol target myeloid blasts by suppression of cyclin-dependent kinases and interference with nucleotide synthesis. Another class of novel therapeutics includes histone deacetylase inhibitors, which cause growth arrest and apoptosis through histone acetylation and resultant conformational changes [13].

Bone marrow/hematopoietic stem cell transplantation is a method of choice in various hematological, oncological and autoimmune diseases in which, after intensive immunosuppressive therapy with high doses of cytostatic drugs, immunosuppressants, the patient is injected with pre-harvested bone marrow or peripheral blood hematopoietic stem/progenitor cells. The patients most in need of this method of treatment are those suffering from highly aggressive lymphomas, which make up 70% of all forms of lymphomas and leukemias. As a rule, these are young, potentially fit people. According to preliminary estimates, the need for about 1000 hematopoietic stem cell transplants arises annually in the Republic of Kazakhstan [14].

This review presents an overview of preclinical and clinical studies of selected promising small molecule compounds that are currently tested for a potential antileukemic activity. Differential therapy is an alternative or complementary treatment for AML, which aims at causing maturation of poorly differentiated leukemic blasts. The physiological form of vitamin D, 1,25-dihydroxyvitamin D_3 (1,25D3) is a steroid-like hormone with pleiotropic properties. These include important contributions to the control of cell proliferation, survival and differentiation, as well as the regulation of immune responses. This hormone also has a role in normal hematopoiesis, enhancing monocyte-macrophage differentiation. It also has antiproliferative and prodifferentiation effects against various myeloid leukemia cell lines and AML blasts *ex vivo*. Nevertheless, hematopoiesis in mice with vitamin D receptor (VDR) deletion is essentially normal, indicating that in mammals the vitamin D pathway appears to have a nonessential but perhaps a contributory role in blood formation [15].

Clinical trials with 1,25D3 have been performed for the treatment of preleukemia/myelodysplastic syndrome and AML, but the 1,25D3 doses effective *in vitro* caused severe hypercalcemia *in vivo*. Numerous vitamin D analogs with reduced calcemic activity have been synthesized which exhibit increased ability to induce cell differentiation and to inhibit proliferation of leukemic cells in preclinical model systems. Although such analogs have also been tested in trials, either alone or combined with other

agents, the therapeutic outcomes were inconclusive and hypercalcemia remained the major issue. The reasons for the unimpressive results of most clinical studies of the therapeutic effects of vitamin D derivatives (VDDs) in leukemia and related diseases may include the lack of a precise rationale for the conduct of these studies. Further, clinical trials to date have generally used extremely heterogeneous patient populations and, in many cases, small numbers of patients, generally without controls [16]. The available or new VDDs combined with other differentiating or antiproliferative agents, each working through different pathways, are expected to demonstrate synergistic activity and offer improved therapy for AML [15].

There is evidence that vitamin D₂ is less toxic than vitamin D₃ in animals. Recently, the research group led by M. Danilenko has determined the differentiation effects of several novel analogs of 1 α ,25-dihydroxyvitamin D₂ (1,25D₂), including PRI-1916 and PRI-1917, in which the extended side chains of their previously reported precursors (PRI-1906 and PRI-1907, respectively) underwent further 24Z (24-*cis*) modification [17]. Using four human AML cell

lines representing different stages of myeloid maturation (KG-1a, HL60, U937, and MOLM-13), it was found that the potency of PRI-1916 was slightly higher or equal to that of PRI-1906 while PRI-1917 was significantly less potent than PRI-1907. It was also demonstrated that 1,25D₂ was a less effective differentiation agent than 1,25D₃ in these cell lines. Irrespective of their differentiation potency, all the vitamin D₂ derivatives tested were less potent than 1,25D₃ in transactivating the DR3-type vitamin D response elements (VDREs).

The data presented in Table 1 and Figure 3 demonstrate that PRI-1907 has much higher differentiation efficiency than PRI-1906 in all used AML cell lines. However, the effect of the new 24Z modification on the activities of PRI-1906 and PRI-1907 was different. Thus, the activity of PRI-1916 was slightly higher or equal to the effectiveness of PRI-1906, which contains naturally occurring alkyl branches at C-25. On the other hand, it was found that the activity of PRI-1917 in four cell lines was consistently lower compared to PRI-1907 containing homologated chains on C-25 (Table 1).

Table 1 – Comparative differentiation-inducing potencies of vitamin D derivatives in acute myeloidleukemia (AML) cells

Compounds	HL60	U937	MOLM-13	KG-1a
1.25D ₃	4.58 ± 0.34	1.97 ± 0.19	1.45 ± 0.09	8.65 ± 0.42
1.25D ₂	8.71 ± 0.62 *	4.31 ± 0.66 *	1.86 ± 0.15	32.29 ± 4.52 **
PRI-1906	4.88 ± 0.02	2.51 ± 0.28	1.67 ± 0.10	4.72 ± 0.97
PRI-1916	3.45 ± 0.07 *	2.87 ± 0.43	1.19 ± 0.08	5.85 ± 1.24
PRI-1907	0.42 ± 0.06	0.56 ± 0.08	0.19 ± 0.02	1.27 ± 0.04
PRI-1917	3.90 ± 0.15 ##	2.92 ± 0.51 ##	0.57 ± 0.04 #	4.87 ± 0.42 #

Cells were incubated with the indicated agents or vehicle ($\leq 0.2\%$ ethanol) for 96 h. The expression of CD14 and CD11b was determined by flow cytometry. EC₅₀ values (nM) were calculated by non-linear regression analysis of the dose-response curves for the CD14⁺CD11b⁺ double-positive cell population. The percentage of the double-positive CD14⁺CD11b⁺ cell population is presented on Figure 2.

Plant polyphenols have been shown to potentiate the differentiation of AML cells induced by low, non-toxic concentrations of 1,25D₃ and other VDDs. The enhanced antileukemic effects of these combinations may constitute the basis for the development of novel approaches for differentiation therapy of AML. Stud-

ies conducted by M. Danilenko's laboratory have shown that carnosic acid (CA), curcumin and silibinin (SIL) synergistically enhanced 1,25D₃-induced differentiation of myeloblastic HL60 cells. However, in promonocytic U937 cells, only CA caused potentiation while SIL attenuated 1,25D effect [18]. The enhanced effect of 1,25D+CA was accompanied by increases in both the VDR and retinoid X receptor alpha (RXR α) protein levels and transactivation in both cell lines. Similar increases were observed in HL60 cells treated with 1,25D + SIL. In U937 cells, however, SIL inhibited 1,25D-induced VDRE transactivation concomitant with downregulation of RXR α at both transcriptional and posttranscriptional levels.

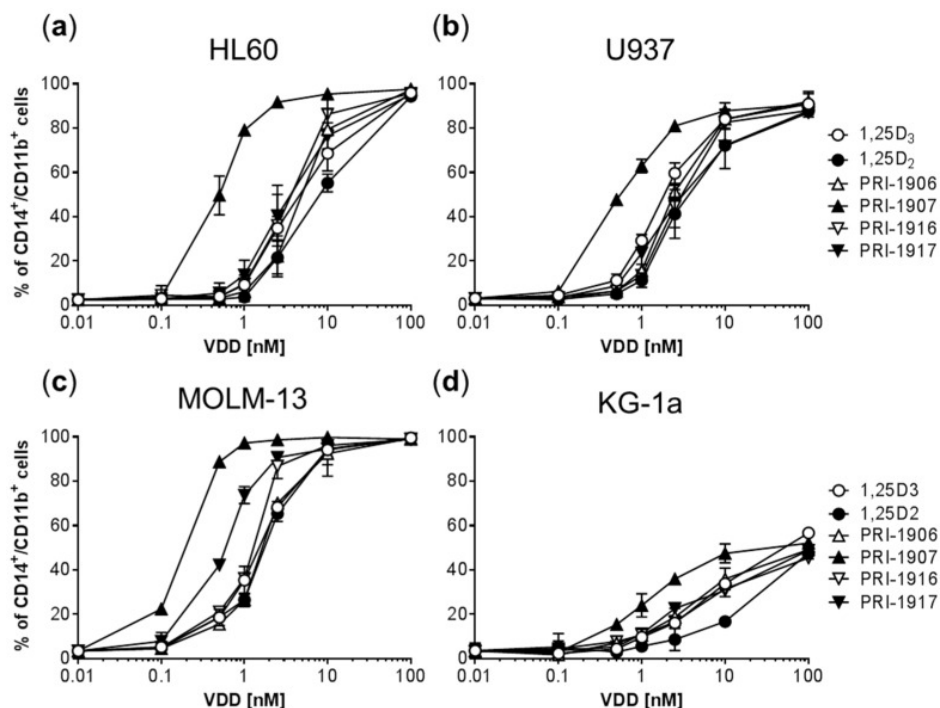


Figure 2 – Comparison of the differentiation-inducing effects of different vitamin D derivatives on AML cells (a–d). The data are the means \pm SD of at least four independent experiments; *, $p < 0.05$ vs. 1,25D3; **, $p < 0.01$ vs. 1,25D3; #, $p < 0.05$ vs. PRI-1907; ##, $p < 0.01$ vs. PRI-1907 [17]

How the above phytochemicals modulate VDDs effects in different subtypes of AML cells is not yet fully understood. However, it has been demonstrated that the transcription factor Nrf2 and the Nrf2//anti-oxidant response element (Nrf2//ARE) signaling pathway mediate the differentiation-enhancing effects of plant polyphenols [19]. Particularly the inhibitory effects of SIL on 1,25D3-induced differentiation of U937 cells correlated with the inability of SIL, with or without 1,25D3, to activate the Nrf2//ARE pathway in these cells. These results suggest that opposite effects of SIL on 1,25D3-induced differentiation of HL60 and U937 cells may be determined by cell-type-specific signaling and transcriptional responses to this polyphenol resulting in differential modulation of RXR α expression [18]. Interestingly, similar to 1,25D3, both 1,25D2 and its analogs could strongly cooperate with CA in inducing cell differentiation and inhibition of G1-S cell cycle transition [17]. Most recently, it has been demonstrated that activators of Nrf2 other than polyphenols, including clinically approved drug dimethyl fumarate, can also markedly potentiate the antileukemic effects of VDDs on AML cells both *in vitro* and *in vivo* [21].

Besides their differentiation-enhancing activity, VDD/CA combinations can also potentiate the cyto-

toxic effects of chemotherapeutics. Thus, it has been found that the combination of the clinically approved vitamin D₂ analog doxercaliferol and CA (D2/CA) significantly increases the extend of AML cell death caused by a low concentration of arabinosylcytosine (AraC) [21, 22]. Notably, although AraC-induced cytotoxicity was accompanied by the increased generation of intracellular reactive oxygen species (ROS), the enhancement of cell death by D2/CA was accompanied by a decrease in ROS levels and by activation of VDR-dependent signaling pathway leading to ASK1-mediated apoptosis.

Plant-derived phenolic compounds are capable of cooperating with one another against different types of malignant cells. Particularly, studies by M. Danilenko's laboratory have demonstrated that curcumin (CUR) or methyl 4-hydroxycinnamate (MHC) can uniquely synergize with CA at non-cytotoxic concentrations of each agent, producing massive apoptotic cell death in different AML cell lines [23, 24]. The CUR+CA combination also demonstrated a marked antileukemic effect *in vivo* [24]. Importantly, these combinations did not affect normal hematopoietic cells. Mechanistically, MHC+CA- and CUR+CA-induced apoptosis was mediated solely by the disruption of cellular Ca²⁺ homeostasis. Ac-

tivation of caspase cascade in combination-treated AML cells resulted from sustained elevation of cytosolic Ca^{2+} (Ca^{2+}_{cyt}) and was not preceded by endoplasmic reticulum stress or mitochondrial damage. The CUR+CA-induced Ca^{2+}_{cyt} rise did not involve excessive influx of extracellular Ca^{2+} but, rather, occurred due to massive Ca^{2+} release from intracellular stores concomitant with inhibition of Ca^{2+}_{cyt} extrusion through the plasma membrane. Collectively, these results provide the mechanistic and translational basis for further characterization of MHC+CA and CUR+CA combinations as a prototypes of novel Ca^{2+} -targeted pharmacological tools for the treatment of AML [25, 26].

The socio-economic problem of blood cancer is currently extremely relevant, taking into account not only the high mortality rate, but also the disability of patients, the huge material costs during treatment. Therapy of AML still remains a challenge. As survival of patients has not changed significantly over the years, and new strategies are urgently needed. Some anticancer agents, such as flavopiridol, have shown promising results in commercially developed AML clinical trials. Others, such as those that target individual signaling proteins, are already approved by the United States Food and Drug Administration (FDA) and the European Medicines Agency (EMA) for the treatment of different AML subtypes. In addition, we describes novel promising approaches based on the use of combinations of natural agents, which deserve further detailed discussion beyond the scope of our review. Future therapeutic modalities in AML include immunomodulation with vaccines as well as targeting leukemic microenvironment, leukemia stem cells, and oncogenic fusion proteins or transcription factors involved in leukemogenesis. Overall, it is hoped that continued progress in expanding new approaches will soon provide useful additions to AML therapy and will significantly improve its currently poor prognosis.

References

1. Howlader N., Noone A.M., Krapcho M., Miller D., Brest A., Yu M., Ruhl J., Tatalovich Z., Mariotto A., Lewis D.R., Chen H.S., Feuer E.J., Cronin K.A. (eds). SEER Cancer Statistics Review, National Cancer Institute, 2019.
2. Igissinov N., Kulmirzayeva D., Moore M.A., Igissinov S., Baidosova G., Akpolatova G., Bukeyeva Z., Omralina Y. (2014) Epidemiological assessment of leukemia in Kazakhstan, 2003- 2012. *Asian Pac J Cancer Prev.*, vol. 15, no. 16, pp. 6969-6972.
3. Shinkevich D.S., Mikhailova E.A., Parovichnikova E.N., Troitskaya V.V. (2015) Clinical and morphological manifestations of hemoblastosis in the maxillofacial region. Tactics of surgical dental care for patients with hemoblastoses. *Rus dent.*, vol. 8, no. 2, pp. 19-28.
4. Kumar V., Abbas A.K., Aster J.C. (2015) Robbins and Cotran pathologic basis of disease. Neoplastic proliferation of white cells, 9th ed., Philadelphia: Elsevier, pp. 586-622.
5. Savchenko V.G. (2012) Program treatment of diseases of the blood system. Moscow: Practice, pp. 155-245.
6. Savchenko V.G., Parovichnikova E.N. (2001) Acute leukemia. In: Clinical Oncohematology, Moscow: Medicine, pp. 156-207.
7. Swerdlow S.H., Campo E., Pileri S.A., et al. (2016) The 2016 revision of the World Health Organization classification of lymphoid neoplasms. *Blood*, vol. 127, no. 20, pp. 2375-2390.
8. Arber D.A., Orazi A., Hasserjian R., et al. (2016) The 2016 revision to the World Health Organization classification of myeloid neoplasms and acute leukemia. *Blood*, vol. 127, no. 20, pp. 2391-2405.
9. Campana D., Pui C.H. (2014) Childhood leukemia. In: Niederhuber JE, Armitage J.O., Doroshow J.H., Kastan M.B., Tepper J.E., eds. *Abeloff's Clinical Oncology*. 5th ed., Philadelphia, PA: Elsevier Saunders, 96.
10. Dahl G.V., Weinstein H.J. Acute myeloid leukemia in children (2005) In: Hoffman R., Benz E.J., Shattil S.J., Furie B., Cohen H.J., Silberstein L.E., McGlave P., eds. *Hematology: Basic principles and practice*. 4th ed., Philadelphia, Pa. Elsevier, pp. 1121-1133.
11. Litvitsky P.F., Zhevak T.N. (2016) Hemoblastoses. Leukemia of lymphoid origin. Questions of modern pediatrics, vol. 15, no. 5, pp. 457-470.
12. Bohl S.R., Bullinger L., Rucker F.G. (2019) New targeted agents in acute myeloid leukemia: new hope on the rise, *Int J Mol Sci.*, vol. 20, p. 1983.
13. Fathi A.T., Grant S., and Karp J.E. (2010) Exploiting cellular path-ways to develop new treatment strategies for AML. *Cancer Treatment Reviews*, vol. 36, no. 2, pp. 142-150.
14. The Ministry of Health of the Republic of Kazakhstan, the Kazakhstan Research Institute of Oncology and Radiology. Comprehensive plan to combat cancer in the Republic of Kazakhstan for 2018-2022. 42 p.
15. Studzinski G.P., Gocek E., Coffman F., Danilenko M. (2018) Effects of vitamin D deriva-

tives on differentiation, cell cycle, and apoptosis in hematological malignancies. 4th ed., vol. 2: Health, Disease and Therapeutics, pp. 761-799.

16. Studzinski G.P., Harrison J., Wang X., Sarkar S., Kalia V., Danilenko M. (2015) Vitamin D control of hematopoietic cell differentiation and leukemia. *J Cell Biochem.*, vol. 116, no. 8, pp. 1500-1512.

17. Nachliely M., Sharony E., Rao Bolla N., Kutner A., Danilenko M. (2016) Prodifferentiation activity of novel vitamin D₂ analogs PRI-1916 and PRI-1917 and their combinations with a plant polyphenol in acute myeloid leukemia cells. *Int J of Mol Sci.*, vol. 17, no. 7, p. 1068.

18. Danilenko M., Wang Q., Wang X., Levy J., Sharoni Y. and Studzinski G.P. (2003) Carnosic acid potentiates the antioxidant and prodifferentiation effects of 1 α ,25-dihydroxyvitamin D₃ in leukemia cells, but does not promote elevation of basal levels of intracellular calcium. *Cancer Res.*, vol. 63, pp. 1325-1332.

19. Bobilev I., Novik V., Levi I., Shpilberg O., Levy J., Sharoni Y., Studzinski G.P., Danilenko M. (2011) The Nrf2 transcription factor is a positive regulator of myeloid differentiation of acute myeloid leukemia cells. *Cancer Biol Ther.*, vol. 11, pp. 317-329.

20. Nachliely M., Trachtenberg A., Khalfin B., Nalbandyan K., Cohen-Lahav M., Yasuda K., Sakaki T., Kutner A., Danilenko M. (2018) Dimethyl fumarate and vitamin D derivatives cooperatively enhance

VDR and Nrf2 signaling in differentiating AML cells in vitro and inhibit leukemia progression in a xenograft mouse model. *J Steroid Biochem Mol Biol.*, vol. 188, pp. 8-16.

21. Wang X., Dawod A., Nachliely M., Harrison JS., Danilenko M., Studzinski G.P. (2019) Differentiation agents increase the potential AraC therapy of AML by reactivating cell death pathways without enhancing ROS generation. *J Cell Physiol.*, vol. 235, no. 1, pp. 573-586.

22. Studzinski G.P., Harrison J.S., Wang X., Sarkar S., Kalia V., Danilenko M. (2015) Vitamin D control of hematopoietic cell differentiation and leukemia. *J Cell Biochem.*, vol. 116, no. 8, pp. 1500-1512.

23. Trachtenberg A., Muduli S., Sidoryk K., Cybulski M., Danilenko M. (2019) Synergistic cytotoxicity of methyl 4-hydroxycinnamate and carnosic acid to acute myeloid leukemia cells via calcium-dependent apoptosis induction. *Front Pharmacol.*, vol. 10, no. 507, pp. 1-7.

24. Pesakhov S., Nachliely M., Barvish Z., Aqaq N., Schwartzman B., Voronov E., Sharoni Y., Studzinski G.P., Fishman D., Danilenko M. (2016) Cancer-selective cytotoxic Ca²⁺ overload in acute myeloid leukemia cells and attenuation of disease progression in mice by synergistically acting polyphenols curcumin and carnosic acid. *Oncotarget*, vol. 7, no. 22, pp. 1-7.

^{1*}A. Ryskaliyeva, ²Z. Krupova, ³C. Henry, ⁴B. Faye, ⁵G. Konuspayeva, ¹P. Martin

¹INRA, UMR GABI, AgroParisTech, Université Paris-Saclay, Elancourt, France

³INRA, MICALIS Institute, Plateforme d'Analyse Protéomique

Paris Sud-Ouest (PAPPSO), Université Paris-Saclay, Jouy-en-Josas, France

⁴CIRAD, UMR SELMET, Montpellier Cedex 5, France

⁵Research and Production Enterprise "Antigen" Co. Ltd, Almaty region, Kazakhstan

*e-mail: alma.ryskali@gmail.com

Comprehensive proteomic analysis of camel milk-derived extracellular vesicles

Abstract: Extracellular vesicles were recovered by optimized density gradient ultracentrifugation from milk of *Camelus (C.) dromedarius*, *C. bactrianus* and hybrids reared in Kazakhstan, visualized by transmission electron microscopy and characterized by nanoparticle tracking analysis. Purified extracellular vesicles had a heterogeneous size distribution with diameters varying between 25 and 170 nm, with average yield of $9.49 \times 10^8 - 4.18 \times 10^{10}$ particles per milliliter of milk. Using a comprehensive strategy combining classical and advanced proteomic approaches an extensive LC-MS/MS proteomic analysis was performed of EVs purified from 24 camel milks (*C. bactrianus*, n=8, *C. dromedarius*, n=10, and hybrids, n=6). A total of 1,010 unique proteins involved in different biological processes were thus identified, including most of the markers associated with small extracellular vesicles, such as CD9, CD63, CD81, HSP70, HSP90, TSG101 and ADAM10. Camel milk-derived EV proteins were classified according to biological processes, cellular components and molecular functions using gene-GO term enrichment analysis of DAVID 6.8 bioinformatics resource. Camel milk-derived EVs were mostly enriched with exosomal proteins. The most prevalent biological processes of camel milk-derived EV proteins were associated with exosome synthesis and its secretion processes (such as intracellular protein transport, translation, cell-cell adhesion and protein transport, and translational initiation) and were mostly engaged in molecular functions such as Poly(A) RNA and ATP binding, protein binding and structural constituent of ribosome. Proteomic studies of camel milk and sub-fractions thereof, such as casein, whey, or the milk fat globule membrane (MFGM) have revealed a plethora of bioactive proteins and peptides beneficial for developing immune and metabolic systems (Casado et al., 2008; Kussmann and Van Bladeren, 2011). By contrast, camel milk-derived EVs are still a largely uncharted proteomic terrain, although we know that milk-derived EVs carry cell origin-specific cargo and transport both bioactivity and information between cells (de la Torre Gomez et al., 2018).

Key words: milk, camel, exosomes, extracellular vesicles, proteome, tetraspanins.

Introduction

Milk is usually considered as a complex biological liquid in which supramolecular structures (casein micelles and milk fat globules) are found beside minerals, vitamins and soluble proteins (whey proteins) as well as cells. In addition to these components, it was recently shown that milk contains also extracellular vesicles that are released by cells as mediators of intercellular communication. Indeed, cell communicate with neighboring cells or with distant cells through the secretion of extracellular vesicles [1]. Phospholipid bilayer-enclosed extracellular vesicles (EVs) are naturally generated and released from several cell domains of life (*Bacteria*, *Archaea*, *Eukarya*)

into the extracellular space under physiological and pathological conditions [2]. EVs are commonly classified according to their sub-cellular origin into three major subtypes, such as microvesicles, exosomes, and apoptotic bodies. Contents of vesicles vary a with respect to mode of biogenesis, cell type, and physiologic conditions [3]. Exosomes represent the smallest population among EVs ranging in size from 30 to 150 nm in diameter [4]. They are generated inside multivesicular bodies in the endosomal compartment during the maturation of early late endosomes and are secreted when these compartments fuse with the plasma membrane [5]. Found in all biofluids exosomes harbor different cargos as a function of cell type and physiologic state [3].

Milk is the sole source of nutrients for the newborn and very young offspring, as well as being an important means to transfer immune components from the mother to the newborn of which the immune system is immature [6]. Milk is therefore thought to play an important role in the development of the immune system of the offspring [7]. Milk is also a source of delivers molecules, via exosomes and/or microvesicles, acting on immune modulation of neonates due to their specific proteins, mRNA, long non-coding RNA and miRNA contents. Exosomes have come in the limelight as biological entities containing unique proteins, lipids, and genetic material. It was shown that the RNA contained in these vesicles could be transferred from one cell to another, through an emerging mode of cell-to-cell communication [8]. RNAs conveyed by exosomes are translated into proteins within transformed cells (mRNA), and/or are involved in regulatory functions (miRNA). For this reason, exosomes are recognized as potent vehicles for intercellular communication, capable for transferring messages of signaling molecules, nucleic acids, and pathogenic factors [9].

Over the last decade, exosomes were widely explored as biological nanovesicles for the development of new diagnostic and therapeutic applications as a promising source for new biomarkers in various diseases [10]. For example, exosomes secreted by dendritic cells have been shown to carry MHC-peptide complexes allowing efficient activation of T lymphocytes, thus displaying immunotherapeutic potential as promoters of adaptive immune responses [11]. Recently, cell culture studies showed that bovine milk-derived exosomes act as a carrier for chemotherapeutic/chemopreventive agents against lung tumor xenografts *in vivo* [12]. Nevertheless, their physiological relevance has been difficult to evaluate because their origin, biogenesis and secretion mechanisms remained enigmatic.

Despite a significant number of publications describing the molecular characteristics and investigating the potential biological functions of milk-derived exosomes [13; 14], there are only one dealing with exosomes derived from camel milk [15]. These authors report for the first time isolation and characterization using proteomic (SDS-PAGE and western blot analysis) and transcriptomic analyses exosomes from dromedary milk at different lactation stages. However, there is no comprehensive investigation on exosomal protein variations and variability in composition between individual camels. Milk-derived EVs from Bactrian and hybrid milks have never been ex-

plored before. Therefore, to gain insight into the protein diversity of camel milk-derived EVs, we herein provide results of isolation and in-depth morphological and protein characterization of milk-derived EVs from *C. dromedarius*, *C. bactrianus* and hybrids from Kazakhstan using a comprehensive strategy combining classical (SDS-PAGE) and advanced proteomic approaches (LC-MS/MS).

Materials and methods

Milk sample collection and preparation. Raw milk samples were collected during morning milking on healthy dairy camels belonging to two species: *C. bactrianus* (n=72) and *C. dromedarius* (n=65), and their hybrids (n=42) at different lactation stages, ranging between 30 and 90 days postpartum. Camels grazed on four various natural pastures at extreme points of Kazakhstan: Almaty (AL), Shymkent (SH), Kyzylorda (KZ), and Atyrau (ZKO). Whole-milk samples were centrifuged at 3,000 g for 30 min at 4°C (Allegra X-15R, Beckman Coulter, France) to separating fat from skimmed milk. Samples were quickly frozen and stored at -80°C (fat) and -20°C (skimmed milk) until analysis.

Selection of milk samples for analysis. In total 24 camel milk samples (*C. bactrianus*, n=8, *C. dromedarius*, n=10, and hybrids, n=6) were selected for isolation of camel milk-derived EVs, based on lactation stages and number of parities of each camel group composed by the species and grazing regions. It should be emphasized that data available on animals: breed, age, lactation stage and calving number, were estimated by a local veterinarian, since no registration of camels in farms is maintained. Six samples of camel milk-derived EVs (*C. bactrianus*, n=2, *C. dromedarius*, n=2, and hybrids, n=2) were selected randomly for transmission electron microscopy (TEM) with negative staining (uranyl acetate). Then, 15 milk samples including the 6 examined by TEM (*C. bactrianus*, n=5, *C. dromedarius*, n=5, and hybrids, n=5) were analyzed by SDS-PAGE and LC-MS/MS analysis using a QExactive (Thermo Fischer Scientific, USA) Mass Spectrometer after a tryptic digestion of excised gel bands.

Isolation of camel milk-derived EVs. First, skimmed milk samples (40-45 mL) were incubated at 37°C for 30 min in a water bath to enhance free β -casein adsorption to casein micelles. Then, acetic acid was added to the total volume of milk, to obtain a final concentration of 10% and thus acidified milk was incubated at 37°C for 5 min for precipitation of

caseins. Finally, 1M sodium acetate was added to obtain a final concentration of 10% for salting out at RT for 5 min, followed by centrifugation at 1,500 g for 15 min at 20°C (Beckman Coulter, Allegra X-15R Centrifuge, France). After being passed through sterilized vacuum-driven filtration system Millipore Steritop, 0.22 µm, the supernatant, namely the filtrated whey, was concentrated by centrifugation at 4,000 g and 20°C using Amicon 1,000K ultracentrifuge tube until to obtain 3 mL of concentrate remaining. The retentate thus obtained was ultra-centrifuged for pelleting the EVs at 33,000 g for 1h10 at 4°C (Beckman Coulter, Optima XPN-80, 50TI rotor, France). Next, the pellet was suspended in 500 µL of PBS and added to pre-prepared 11 mL of sucrose gradient 5-40% and ultra-centrifuged at 34,000 g for 18h at 4°C (Beckman Coulter, Optima XPN-80, SW41 rotor, France). In total, 12 fractions of 1 mL were collected. Fractions previously demonstrated to be enriched in exosomes (10, 11 and 12) were finally suspended into 50 µL of PBS and stored at -80°C, until further analyses.

Transmission electron microscopy (TEM). The EVs were analyzed as whole-mounted vesicles deposited on EM copper/carbon grids during 5 min and contrasted 10 sec in 1% uranyl acetate. Grids were examined with Hitachi HT7700 electron microscope operated at 80kV (Elexience – France), and images were acquired with a charge-coupled device camera (AMT).

Nanoparticle tracking analysis. The size distribution and concentration of EVs were measured by NanoSight (NS300) (Malvern Instruments Ltd, Malvern, Worcestershire, UK) according to manufacturer's instructions. A monochromatic laser beam at 405 nm was applied to the diluted suspension of vesicles. Sample temperature is fully programmable through the NTA software (version 3.2 Dev Build 3.2.16). A video of 30 sec was taken with a frame rate of 30 frames/s and particle movement was analyzed by NTA software.

Proteomic analysis. To estimate the concentration of total EVs, the Coomassie Blue Protein Assay was used [43]. Absorbance at 595 nm was measured using the UV-Vis spectrophotometer (UVmini-1240, Shimadzu, France). The reference standard curve was done with 1 mg/mL commercial bovine serum albumin (BSA, Thermo Fischer Scientific, USA).

In order to identify proteins, mono dimensional electrophoresis (1D SDS-PAGE) followed by trypsin digestion and LC-MS/MS analysis, was used. Ten µg of each individual skimmed camel milk sample were loaded onto 4-15% Mini-PROTEAN® TGX™

Precast Gels (Bio-Rad, Marne-la-Coquette, France) and subjected to electrophoresis. Samples were prepared with Laemmli Lysis-Buffer (Sigma-Aldrich, USA) with β-mercapto ethanol and denatured at 100°C for 15 min. Separations were performed in a vertical electrophoresis apparatus (Bio-Rad, Marne-la-Coquette, France). After a short migration (0.5 cm) of samples, gels were stored at -80°C until LC-MS/MS analysis.

Reduction of disulfide bridges of proteins was carried out by incubating at 37°C for one hour with dithiothreitol (DTT, 10 mM, Sigma, USA), meanwhile the alkylation of free cysteinyl residues with iodoacetamide (IAM, 50 mM, Sigma, USA) at RT for 45 min in total obscurity. After gel pieces were washed twice, first, with 100 µL 50% ACN/50 mM NH₄HCO₃ and then with 50 µL ACN, they were finally dried. The hydration was performed at 37°C overnight using digestion buffer 400 ng lys-C protease + trypsin. Hereby, peptides were extracted with 50% ACN/0.5% TFA and then with 100% ACN. Peptide solutions were dried in a concentrator and finally dissolved into 70 µL 2% ACN in 0.08% TFA.

The identification of peptides was obtained using UltiMate™ 3,000 RSLC nano System (Thermo Fisher Scientific, USA) coupled to a QExactive (Thermo Fischer Scientific, USA) mass spectrometer.

Four µL of each sample were injected at a flow rate of 20 µL/min on a precolumn cartridge (stationary phase: C18 PepMap 100, 5 µm; column: 300 µm x 5 mm) and desalted with a loading buffer 2% ACN and 0.08% TFA. After 4 min, the precolumn cartridge was connected to the separating RSLC PepMap C18 column (stationary phase: RSLC PepMap 100, 2 µm; column: 75 µm x 150 mm). Elution buffers were A: 2% ACN in 0.1% formic acid (HCOOH) and B: 80% ACN in 0.1% HCOOH. The peptide separation was achieved with a linear gradient from 0 to 35% B for 34 min at 300 nL/min. One run took 42 min, including the regeneration and the equilibration steps at 98% B.

Peptide ions were analyzed using Xcalibur 2.1 with the following machine set up in CID mode: 1) full MS scan in QExactive with a resolution of 15,000 (scan range [m/z] = 300-1,600) and 2) top 8 in MS/MS using CID (35% collision energy) in Ion Trap. Analyzed charge states were set to 2-3, the dynamic exclusion to 30 s and the intensity threshold was fixed at 5.0 x 10².

Raw data were converted to mzXML by MS convert (ProteoWizard version 3.0.4601). Uni-ProtKB Cetartiodactyla database was used (157,113

protein entries, version 2015), in conjunction with contaminant databases were searched by algorithm X!TandemPiledriver (version 2015.04.01.1) with the software X!TandemPipeline (version 3.4) developed by the PAPPSO platform (<http://pappso.inra.fr/bioinfo/>). The protein identification was run with a precursor mass tolerance of 10 ppm and a fragment mass tolerance of 0.5 Da. Enzymatic cleavage rules were set to trypsin digestion (“after R and K, unless P follows directly after”) and no semi-enzymatic cleavage rules were allowed. The fix modification was set to cysteine carbamide methylation and methionine oxidation was considered as a potential modification. Results were filtered using inbuilt X!TandemParser with peptide E-value of 0.05, a protein E-value of -2.6 and a minimum of two peptides.

Bioinformatics and functional enrichment analysis. Functional enrichment analyses on camel milk-derived EV protein was performed using online software for gene annotation “The Database for Annotation, Visualization and Integrated Discovery (DAVID)” version 6.8 (<https://david.ncifcrf.gov/home.jsp/>), as described by [16].

Ethics statements. All animal studies were carried out in compliance with European Community regulations on animal experimentation (European Communities Council Directive 86/609/EEC) and with the authorization of the Kazakh Ministry of Agriculture. Milk sampling was performed in appropriate conditions supervised by a veterinary accredited by the French Ethics National Committee for Experimentation on Living Animals. No endangered or protected animal species were involved in this study. No specific permissions or approvals were required for this study except for the rules of afore-mentioned European Community regulations on animal experimentation, which were strictly followed.

Results and discussion

Isolation of camel milk-derived EVs. EVs are complex and delicate systems requiring optimized isolation and characterization adapted to each fluid type of origin [41], which may be achieved by a variety of methods, including ultracentrifugation, filtration, immunoaffinity isolation and microfluidics techniques [17]. Choice of method should be guided by the required degree of EVs purity and concentration. General protocols to isolate EVs from cell culture supernatants and body fluids involve steps of differential ultracentrifugation and further purification on a sucrose density gradient [18]. Commercially pro-

duced kits for exosome isolation are nowadays available; however, they are not adapted to milk samples. Due to highly variable composition between different body fluids and even within milks of different species, special optimization steps are required. Isolating milk-derived EVs is complicated by milk composition that differs significantly across species, lactation stage, physiological and health status of individuals. In addition, the recovery of purified exosomes from milk for subsequent analysis requires, according to research objectives, to increase sample volume that is not compatible with classical protocols.

In our study, for milk-derived EVs isolation, the “gold standard method”, including differential ultracentrifugation with sucrose density gradient, was performed (Krupova et al., unpublished results). However, to achieve efficient and quantitative recovery of EVs from camel milk, commonly used protocol was modified. First, milk fat, cells and cellular debris were removed by differential ultracentrifugation. The resuspended pellet was loaded on top of a sucrose gradient and ultra-centrifuged to allow for the separation and concentration of EVs. After ultracentrifugation, individual fractions were collected, and EVs enriched fractions (10 to 12) were pooled.

Morphology of isolated camel milk-derived EVs. The method comprising differential ultracentrifugation with density gradient ultracentrifugation was described as being suitable for efficient isolation and purification of higher quality EVs with intact native morphology [19]. To visualize and characterize the morphology and size distribution of camel milk-derived EVs, TEM and NTA analyses were performed. In all 6 milk samples analyzed, a high abundance of homogenous population of EVs enriched in spherical exosomes with average yield of $9.49 \times 10^8 - 4.18 \times 10^{10}$ particles per milliliter was observed. The average sizes varied between 25 and 170 nm in diameter. A classical EV-like morphology has been noticed with no significant differences between *C. dromedarius*, *C. bactrianus* and hybrids samples (Figure 1).

Results confirmed that we have isolated both higher purity and higher quality EVs with intact morphological structures. Based on earlier observations described for dromedary milk [15] and on milk of other species, such as bovine [13], porcine [20], equine [21] and human [22], obtained characteristics for *Camelus* milk appear common to EVs across species. So, we can conclude that the method of differential ultracentrifugation with sucrose density gradient ultracentrifugation resulted in efficient and reliable isolation of camel milk-derived EVs.

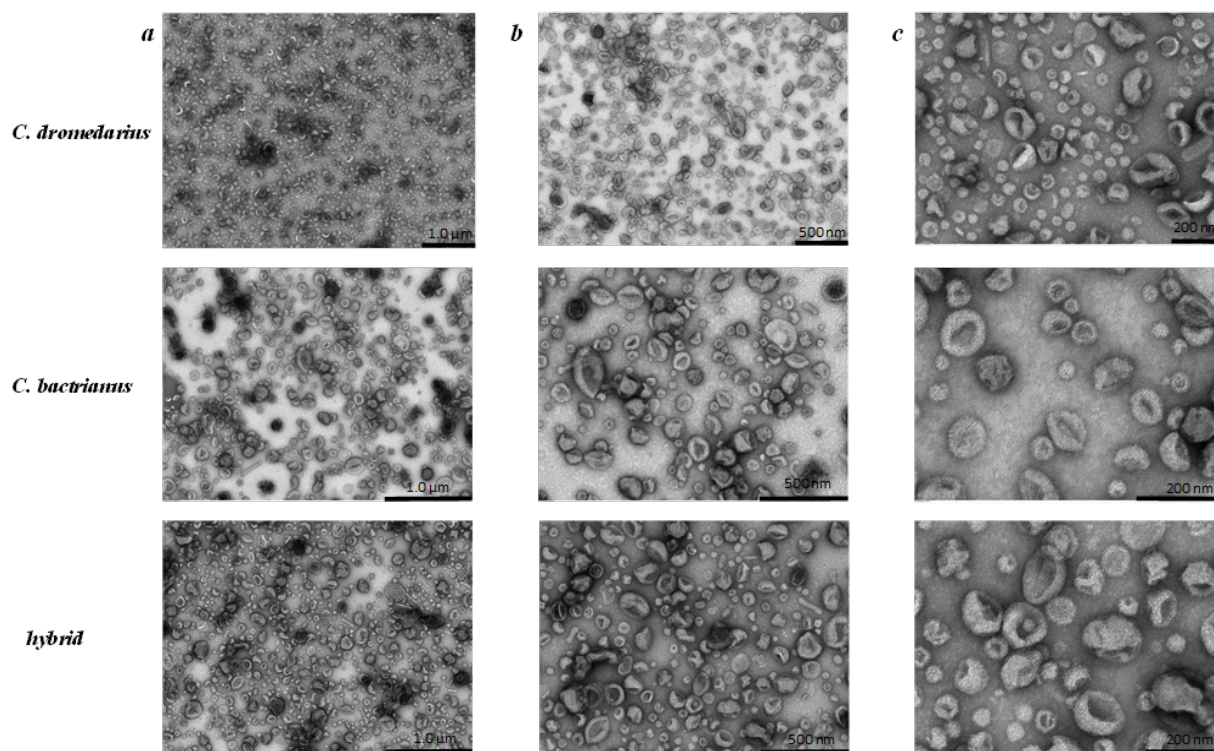


Figure 1 – Representative electron micrographs of *C. dromedarius*, *C. bactrianus* and hybrid camel milk-derived EVs. Scale bar represents: a) 1 μm , b) 500 nm, c) 200 nm.

In-depth proteomic analysis of camel milk-derived EVs. Apart from the morphology, specific protein composition enables to characterize EVs. To identify the proteins present in camel milk-derived EVs, extensive analyses involving trypsin digestion, LC-MS/MS (Q Exactive, Thermo Fisher Scientific, USA) and database searches were performed. Recently, using a similar approach, a total of 1,963 proteins were identified in human milk-derived EVs [14], and 2,107 unique proteins were described in bovine milk-derived EVs [23]. Here, from EV samples derived from 15 camel milks (*C. bactrianus*, $n=5$, *C. dromedarius*, $n=5$, and hybrids, $n=5$), a total of 1,010 functional groups of proteins (proteins belonging to a same group share common peptides) were detected (S1). About 890 proteins were common between the three camel (Figure 2a), while there are several proteins indicated as unique to *C. bactrianus* (31), *C. dromedarius* (5), and hybrids (12). Using UniprotKB taxonomy Cetartiodactyla (SwissProt + Trembl) database, proteins were identified as authentically matching with proteins in *Camelus* protein databases (*C. dromedarius*, *C. bactrianus*, and *C. ferus*), and with the other mammalian species such as, *Lama glama*, *Lama guanicoe*, *Bos taurus*, *Bos mutus*, *Sus scrofa* and *Ovis aries* protein databases and others.

Including the major exosomal protein markers identified, the higher number of low abundant and several differentially expressed proteins enhance the opportunity for revealing the crucial proteins, which can affect exosome synthesis and secretion pathways. By comparison, the proteome of camel milk-derived EVs identified in this study is relatively larger compared to the camel milk proteome reported in a previous study [24]. A total of 391 functional groups of proteins have been identified from 8 camel milk samples using a less sensitive LC-MS/MS (LTQ Orbitrap XLTM Discovery, Thermo Fisher Scientific), of which 235 proteins were observed as common across camel species. We cannot exclude that there may be several reasons for the significant difference in the number of proteins identified in camel milk-derived EVs, comparatively to previously published data on camel milk proteome. First and foremost the instruments (Q Exactive vs LTQ Orbitrap), since the Q Exactive analyzer was reported to provide significant improvement over the Orbitrap mass spectrometers [25] in terms of sensitivity. Comparing the proteomes between camel milk and camel milk-derived EVs, 222 proteins were identified as common (Figure 2, b), the list of which are provided as a supplementary data (S2¹).

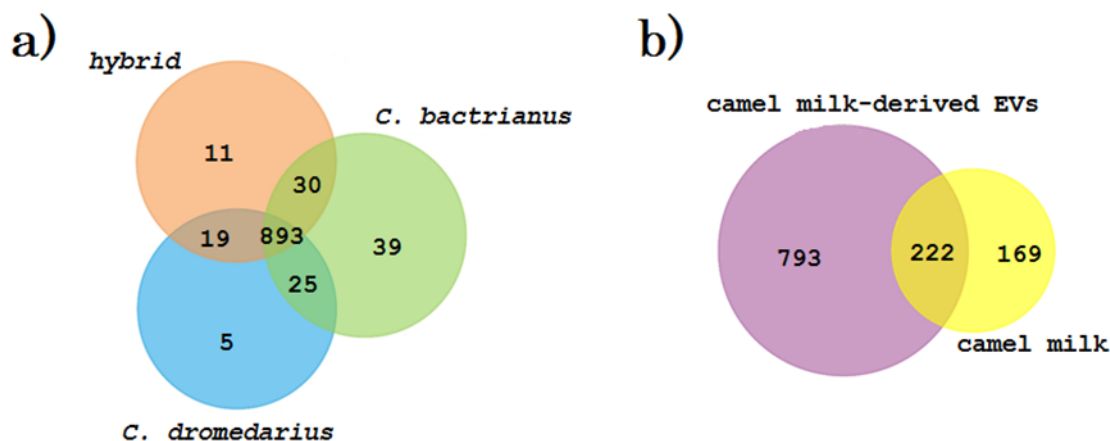


Figure 2 – Общее название. **a)** Venn diagram comparing proteins identified in *C. dromedarius*, *C. bactrianus* and hybrids milk-derived EVs. The diagram illustrates common and unique EV proteins between the three species **b)** Venn diagram comparing proteins identified in camel milk-derived EVs and proteins detected in camel milk reported in our previous study [24]

To get more insight into the subcellular origin of proteins identified, gene-GO term enrichment analysis was performed using DAVID bioinformatics resources 6.8. This analysis helps to understand the function of proteins and addresses them into different biological pathways [26]. In total 890 and 235 common proteins expressed in camel milk-derived EVs and camel milk, respectively, have been classified according to cellular components. However, despite the limitations of the gene annotations not all camel proteins have been annotated, therefore only 517 exosomal and 96 milk proteins could be converted to DAVID gene IDs. Thereby, 463 exosomal and 84 milk proteins matched to GO terms under the cellular components' headings. As shown in Figure 3, both milk-derived EVs and milk samples were mostly enriched with extracellular exosomal proteins (31.09% vs 35.41%, respectively), the specific subset of cellular proteins that are targeted specifically to exosomes. These results coincide with data reported previously on human milk and milk-derived EVs, where a high percentage of proteins linked to GO terms like “exosomes” [14]. The next biggest group represented a large number of cytoplasmic proteins (19.58% EVs vs 14.58% milk) found in milk-derived EVs and nucleus proteins (13.24% EVs vs 15.62% milk) in camel milk. Cytoplasmic proteins might originate from “cytoplasmic crescents”, which are trapped between the membrane layers of the MFGM during the budding process when the fat globule leaves the epithelial cell [27]. Thus, the MFGM can reflect dynamic changes within the MEC and may provide a “snapshot” of mammary gland biology, under specific pathophysiological conditions. About 13.24% and 12.50% were

reported to be membrane proteins identified in camel milk-derived EVs and milk samples. Membrane trafficking proteins represent Rab proteins, which belong to the Ras superfamily of small GTPase. Function of these proteins is central regulation of vesicle budding, motility and fusion. They play a role in endocytosis, transcytosis and exocytosis processes [26]. In addition, some membrane proteins from intracellular organelles such as cytosol, mitochondrion and Golgi apparatus were highly expressed in camel milk-derived EVs.

Next, we classified proteins expressed in camel milk-derived EVs according to biological processes, molecular functions, and KEGG pathways. Camel milk-derived EV proteins observed were involved in twenty-six GO biological process terms (Figure 4). The most prevalent biological processes of camel milk-derived EV proteins were associated with exosome synthesis and its secretion processes, such as intracellular protein transport (5.57%), translation (3.45%), cell-cell adhesion and protein transport (3.26%), and translational initiation. Exosomes are increasingly recognized as mediators of intercellular communication due to their capacity to merge with and transfer a repertoire of bioactive molecular content (cargo) to recipient cells [11]. In addition, EV proteins were mostly engaged in cellular functions such as Poly(A) RNA and ATP (9.60%) binding, protein binding and structural component of ribosome (3.65%). About 3.84% proteins are associated with GTP binding function (Figure 4), regulating membrane-vesicle trafficking process. Proteins expressed in camel milk-derived EVs were categorized into 34 different KEGG pathways.

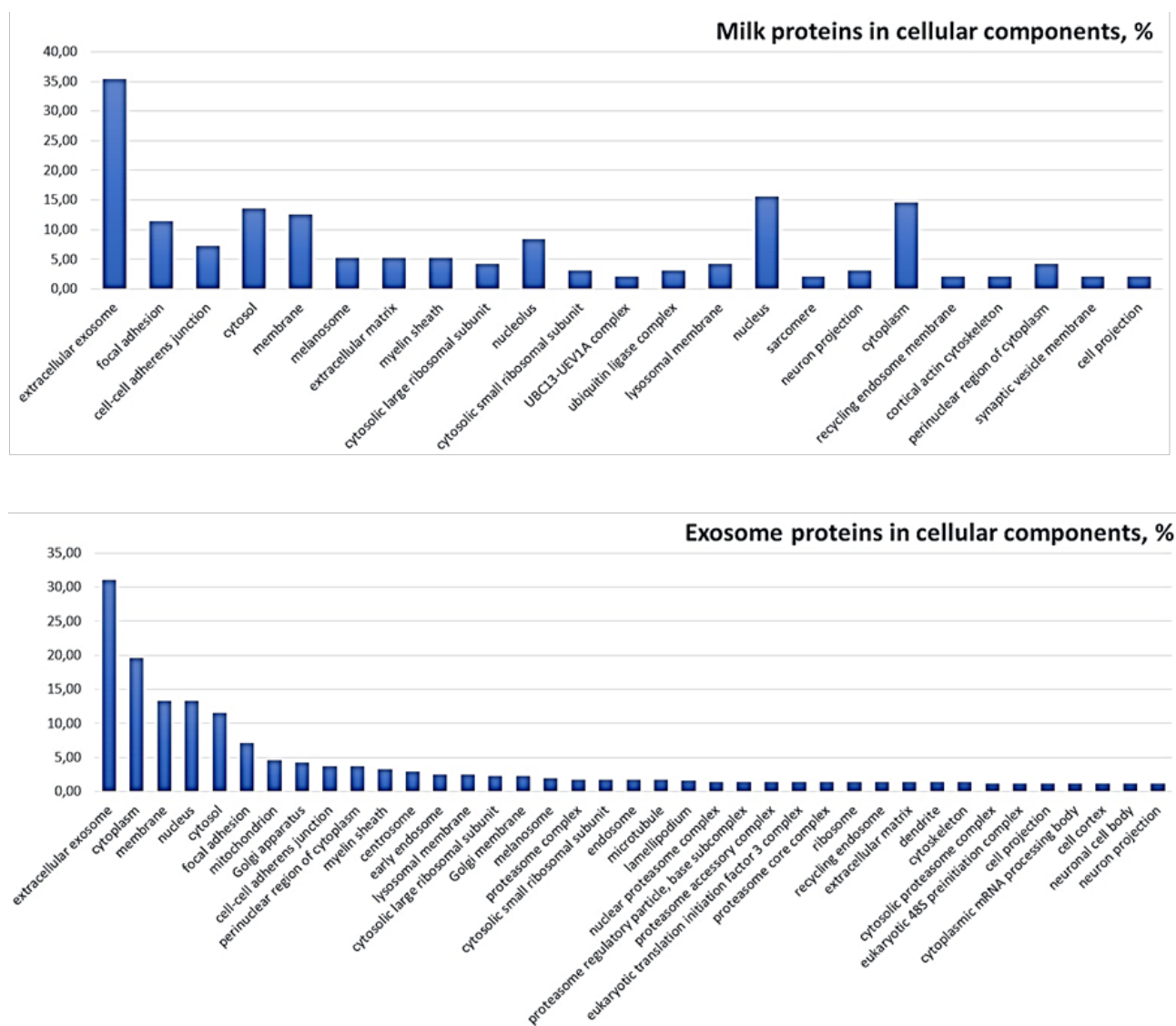


Figure 3 – Functional annotations of camel milk and milk-derived EV proteins classified into cellular components using DAVID bioinformatics resources 6.8

As shown in Table 1, camel milk-derived EV proteins were mostly associated with endocytosis (5.57%), Epstein-Barr virus infection (4.03%), ribosome (3.84%), proteasome (3.45%), RNA transport and viral carcinogenesis (2.50%) KEGG pathways. It is known that exosomes display a wide variety of immuno-modulatory properties. This is highlighted by findings showing that exosomes secreted by Epstein-Barr virus (EBV)-transformed B cells are able to stimulate CD4⁺ T cells in an antigenic-specific manner [11].

Exosomes are a rich source of potential milk biomarkers. Isolation of EVs from milk is complicated by the high lipid content of milk [17]. Lipids are released in milk as fat globules (MFGs) by mammary epithelial cells. These MFGs are droplets of lipids surrounded by a complex phospholipid trilayer con-

taining proteins and glycoproteins [28], and thus are a type of EVs. MFGs are largely heterogeneous in size, and their buoyant densities are different from those of EVs. Because of their plasma membrane origin, vesicular nature, and high abundance in milk, however, MFGs may be co-isolated with other EVs populations present in milk [23]. As expected, camel milk-derived EVs analyzed were mostly enriched with MFGM-enriched proteins associated with milk, such as fatty acid synthase (FAS), MFG-E8 (also termed lactadherin), butyrophilin (BTN) and xanthine dehydrogenase. FAS, BTN and MFG-E8 are negative co-stimulatory molecules inhibiting anti-tumor immune responses, which have become novel target pathways for cancer- and immunotherapy development [29-31].

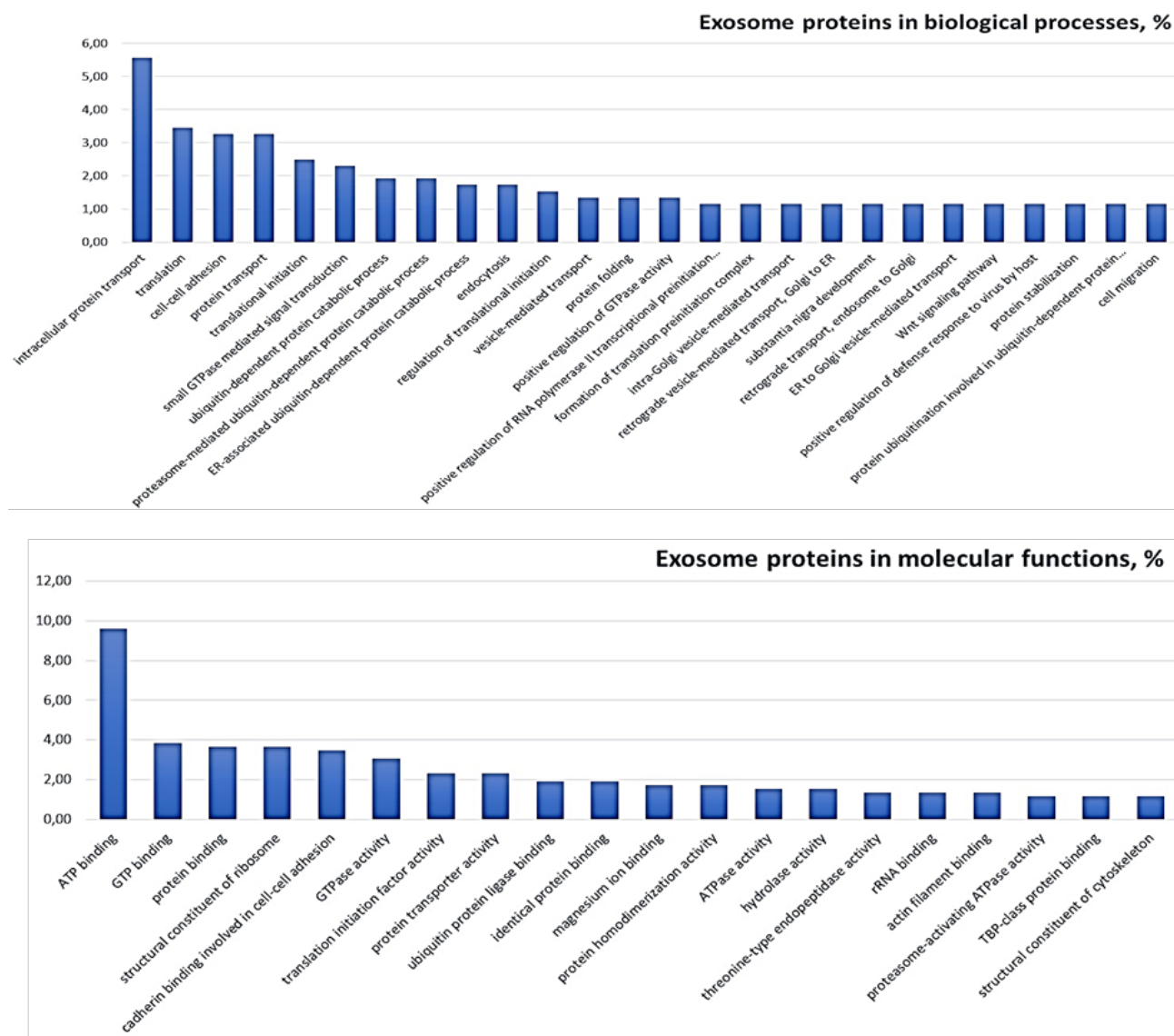


Figure 4 – GO enrichment analysis of camel milk-derived EV proteins classified into biological processes and molecular functions using DAVID bioinformatics resources 6.8

Table 1 – KEGG pathway analysis of camel milk-derived EVs

KEGG pathway term	%	PValue	Fold enrichment
Endocytosis	5.57	8.0E-11	4.32
Epstein-Barr virus infection	4.03	8.7E-8	4.23
Ribosome	3.84	1.1E-9	5.77
Proteasome	3.45	4.1E-16	15.14
RNA transport	2.69	2.2E-4	3.41
Bacterial invasion of epithelial cells	2.11	2.5E-5	5.53
Tight junction	2.11	2.7E-3	3.11
Vasopressin-regulated water reabsorption	1.92	1.9E-6	8.41
Synaptic vesicle cycle	1.92	2.9E-5	6.14

Continuation of table 1

KEGG pathway term	%	PValue	Fold enrichment
Adherens junction	1.92	5.4E-5	5.69
Salmonella infection	1.73	1.3E-3	4.19
Fc gamma R-mediated phagocytosis	1.34	2.2E-2	3.19
Legionellosis	1.15	1.5E-2	4.07
mTOR signaling pathway	1.15	1.7E-2	3.93
Biosynthesis of amino acids	1.15	4.1E-2	3.14
Endocrine and other factor-regulated calcium reabsorption	0.96	2.2E-2	4.61
Collecting duct acid secretion	0.77	3.1E-2	5.73

Camel milk-derived EVs analyzed were highly enriched with ubiquitous, cell-specific and cytosolic proteins, including proteins associated with the endosomal pathway, involved in mechanisms responsible for exosome biogenesis. All populations of EVs analyzed expressed in abundance the small Rab GTPases, such as RAB1A, RAB11B, RAB5C, RAB18, RAB2A, RAB7A and RAB21. Rab GTPases are key regulators of intracellular membrane trafficking, from the formation of transport vesicles to their fusion with membranes. Additionally, exosomes derived from all camel milk analyzed were significantly enriched with certain multifunctional proteins, such as Alix (programmed cell death 6 interacting protein PDCD6IP) and TSG101 (tumor susceptibility gene 101). These Endosomal Sorting Complexes required for Transport (ESCRT) protein components of vesicular trafficking process are believed to be a specific exosome-segregated biomarker during its biogenesis [15, 32]. Recently, it was reported that syndecan-syntenin-ALIX is an important regulator of membrane trafficking and heparan sulphate-assisted signaling, which influences pathological processes, including cancer, the propagation of prions, inflammation, amyloid deposition and neurodegenerative disease [33]. Moreover, HSP70 and HSP90 proteins implicated in innate immune responses and antigen presentation [34], involved in signal transduction protein kinases and 14-3-3 proteins, and metabolic enzymes such as peroxidases, pyruvate kinases, and α -enolase were also observed in camel milk-derived EVs. Cell membrane proteins, such as MHC I and MHC II, demonstrating vesical nature of the analyzed materials, were identified as well in all camel milk-derived EVs analyzed, as well as, cytosolic proteins such as tubulin, actin, and actin-binding proteins were highly expressed.

As a consequence of their endosomal origin, most of exosomes are composed of proteins in-

involved in membrane transport and fusion, in multivesicular body biogenesis, in processes requiring heat shock proteins, integrins and tetraspanins [35]. While some of the proteins that are found in the proteome of many exosomal membrane preparations may merely reflect the cellular abundance of the protein, others are specifically enriched in exosomes and can therefore be defined as exosome-specific marker proteins. Apart from providing nourishment to the offspring, these proteins play a role in intercellular communication via transfer of biomolecules between cells. However, it is currently unknown whether exosomes found in milk originate from immune cells present in milk, from mammary epithelial cells, from circulating cells coming from elsewhere in the body or from bacterial species present in the mammary gland under mild permanent infection (sub-clinical mastitis).

Available proteomic studies define specific markers of the EVs (membrane and cytosolic proteins) and a specific subset of cellular proteins that are targeted specifically to exosomes, the functions of some of them still remain unknown [36]. This is particularly interesting in relation to their possible involvement in human diseases. The knowledge of exosome proteomics can help not only in understanding their biological roles but also in supplying new biomarkers [37]. Among the membrane proteins most enriched in exosomes are tetraspanins, which play a critical role in exosome formation and are involved in morphogenesis, fission and fusion processes [38]. Recently CD9, CD63, and CD81 tetraspanins have been defined as novel markers characterizing heterogeneous populations of EVs subtypes [39], the presence of which, including CD82 and TSPAN14 proteins, were confirmed in camel milk-derived EVs. However, some exosome samples analyzed were devoid of CD63. The absence of this tetraspanin in secreted exosomes by some cell types was previously re-

ported, and the necessity of analyzing instead either CD81- or CD9-bearing EVs was reported [39].

Even in the case of markers with strong evidence for EVs subtype specificity, the presence of such markers does not rule out that other types of vesicles are present in a preparation simultaneously [17]. Not only the desired populations must be confirmed as present; contaminants must be demonstrated to be absent. The purity of the exosomes isolated is highly variable due to the presence of contaminating particles, vesicles and molecules such as proteins and/or nucleic acids as well as other cellular components [40], which may co-purify in vesicle preparations and confound analysis [41, 17]. Minimizing contamination in the isolation of exosomes is vital in providing reliable information upon which to base new paradigms [40]. It was reported that exosomes isolated by differential ultracentrifugation with density gradient ultracentrifugation method can be used to examine the relationship of EV proteins to physiological or disease status of the host without any involvement or contamination of other free proteins in milk [19]. Density gradients add stringency by efficiently separating particles of different density, which allows removing contaminating non-vesicular particles. Thus, the purity of the camel milk-derived vesicles isolated from contaminations with other multivesicular bodies has been examined and confirmed by the absence of microvesicle surface markers such as p-selectin and CD40, an endoplasmic reticulum marker calnexin, mitochondrial protein mitofilin, and an ER-associated protein GP96. Even though, we have applied a filtration step of the milk supernatant prior to the EVs pelleting step, camel milk-derived EVs were contaminated with caseins, the expression of which have been also detected previously in dromedary [15], human [14] and bovine milk exosomes [23].

Conclusion

Using an optimized isolation protocol, we obtained milk-derived exosomes originating from 15 camel (*C. dromedarius*, *C. bactrianus* and hybrids) milk samples that satisfied the typical requirements for exosomal morphology, size and protein content. LC-MS/MS analyses allowed identifying a thousand of different proteins that represents to our knowledge, the first comprehensive proteome of camel milk-derived EVs that appears wider than the milk proteome. As mentioned previously in other species camel milk-derived EVs contain proteins also present in other milk components. This is particularly the case for lactadherin/MFG-E8, Ras-related proteins

or CD9 that have been reported to occur in MFG. Our results strongly suggest that milk-derived exosomes have different cellular origin. Indeed, besides exosomes originating from mammary epithelial cells there are milk-derived exosomes from immune cells. If we consider that milk-derived exosomes also carry microRNAs, these vesicles have to be recognized as another important bioactive component of milk that might be involved in transmitting signals from the mother to the newborn but also represents a source of factors potentially responsible for the properties attributed to camelids milk and its health value.

Acknowledgments

The study was carried out within the Bolashak International Scholarship of the first author, funded by the JSC «Center for International Programs» (Kazakhstan). This work was supported in part by the grant for Scientific Research project named “Proteomic investigation of exosomes from milk of *Camelus bactrianus* and *Camelus dromedarius*” #AP05134760 from the Ministry of Education and Science of the Republic of Kazakhstan, which is duly appreciated. The authors thank all Kazakhstani camel milk farms for rendering help in sample collection, as well as PAPPSO, @BRIDGE, and MIMA2 platforms at INRA (Jouy-en-Josas, France) for providing necessary facilities and technical support. We are grateful to Christine Longin for assistance with TEM analysis.

References

1. Tkach M., Théry C. (2016) Communication by extracellular vesicles: where we are and where we need to go. *Cell*, vol. 164, no. 6, pp. 1226-1232. <https://doi.org/10.1016/j.cell.2016.01.043>.
2. Delcayre A., Helen S., Le Pecq J.-P. (2005) Dendritic cell-derived exosomes in cancer immunotherapy: exploiting nature's antigen delivery pathway. *Exp R Antic Ther.*, vol. 5, no. 3, pp. 537-547. <https://doi.org/10.1586/14737140.5.3.537>.
3. Abels E.R., Breakefield O. (2016) Introduction to extracellular vesicles: biogenesis, rna cargo selection, content, release, and uptake. *Cell Mol Neurobiol.*, vol. 36, no. 3, pp. 301-312, <https://doi.org/10.1007/s10571-016-0366-z>.
4. Hromada C., Mühleder S., Grillari J., Heinz R., Holnthoner W. (2017) Endothelial extracellular vesicles-promises and challenges. *Front Physiol.*, 8: 275, <https://doi.org/10.3389/fphys.2017.00275>.
5. van der Pol E., Boing A.N., Harrison P.,

- Sturk A., Nieuwland R. (2012) Classification, functions, and clinical relevance of extracellular vesicles. *Pharm R.*, vol. 64, no. 3, pp. 676-705, <https://doi.org/10.1124/pr.112.005983>.
6. Kelleher S.L., Lonnerdal B. (2001) Long-term marginal intakes of zinc and retinol affect retinol homeostasis without compromising circulating levels during lactation in rats. *J Nutr.*, vol 131, no. 12, pp. 3237-3242.
7. Hanson, Lars Å. (2007) Session 1: Feeding and infant development breast-feeding and immune function – Symposium on ‘Nutrition in early life: new horizons in a new century’. In: Proceedings of the Nutrition Society. <https://doi.org/10.1017/S0029665107005654>.
8. Colombo M., Graça R., and Clotilde T. (2014) Biogenesis, secretion, and intercellular interactions of exosomes and other extracellular vesicles. *Ann R Cell Dev Biol.*, vol. 30, no. 1, pp. 255-289. <https://doi.org/10.1146/annurev-cellbio-101512-122326>.
9. Kabani M., Ronald M. (2016) More than Just Trash Bins? Potential roles for extracellular vesicles in the vertical and horizontal transmission of yeast prions. *Cur Gen.*, vol. 62, no. 2, pp. 265-270, <https://doi.org/10.1007/s00294-015-0534-6>.
10. Kanada M., Bachmann M.H., Hardy J.W., Frimannson D.O., Bronsart L., Wang A., Sylvester M.D., et al. (2015) Differential fates of biomolecules delivered to target cells via extracellular vesicles. *Proc Natl Acad Sci.*, 201418401. <https://doi.org/10.1073/pnas.1418401112>.
11. Keller S., M. P. Sanderson, A. Stoeck, P. Altevogt (2006) Exosomes: from biogenesis and secretion to biological function. *Immunol L.* <https://doi.org/10.1016/j.imlet.2006.09.005>.
12. Munagala R., Farrukh A., Jeyaprakash J., R. C. Gupta. (2016) Bovine Milk-Derived Exosomes for Drug Delivery. *Canc L.* vol. 371, no. 1, pp. 48-61. <https://doi.org/10.1016/j.canlet.2015.10.020>.
13. Reinhardt T.A., Randy E.S., Brian J.N., Lippolis J.D. (2013) Bovine milk proteome: quantitative changes in normal milk exosomes, milk fat globule membranes and whey proteomes resulting from *Staphylococcus aureus* mastitis. *J of Prot.*, vol. 82, pp. 141-154, <https://doi.org/10.1016/j.jprot.2013.02.013>.
14. Herwijnen M.J.C. van, Marijke I. Z., Soenita G., Nolte E., Hoen N.M., Garssen J., Stahl B., Altelaar A.F., Frank M., Redegeld A., Marca H.M. Wauben. (2016) Comprehensive proteomic analysis of human milk-derived extracellular vesicles unveils a novel functional proteome distinct from other milk components. *Mol and Cell Prot.*, <https://doi.org/10.1074/mcp.M116.060426>.
15. Yassin A.M., Marwa I.A., Hamid O.A., Amer F.H., Warda M. (2016) Dromedary milk exosomes as mammary transcriptome nano-vehicle: their isolation, vesicular and phospholipidomic characterizations. *J of Adv Res.*, vol. 7, no. 5, pp. 749-756. <https://doi.org/10.1016/j.jare.2015.10.003>.
16. Huang D.W., Sherman B.T., Lempicki R.A. (2009) Systematic and integrative analysis of large gene lists using DAVID Bioinformatics resources. *Nat Prot.*, vol. 4, no. 1, pp. 44-57. <https://doi.org/10.1038/nprot.2008.211>.
17. Witwer K.W., Buzás E.I., Bemis L.T., Bora A., Lässer C., Lötvall J., Nolte-t Hoen E.N., et al. (2013) Standardization of sample collection, isolation and analysis methods in extracellular vesicle research. *J of Extr Ves.*, <https://doi.org/10.3402/jev.v2i0.20360>.
18. Zonneveld M.I., Brisson A.R., van Herwijnen M.J.C., Tan S., van de Lest C.H.A., Redegeld F.A., Garssen J., Wauben M.H.M., Nolte-t Hoen E.N. (2014) Recovery of Extracellular Vesicles from Human Breast Milk Is Influenced by Sample Collection and Vesicle Isolation Procedures. *J of Extr Ves.*, <https://doi.org/10.3402/jev.v3.24215>.
19. Yamada T., Inoshima Y., Matsuda T., Ishiguro N. (2012) Comparison of methods for isolating exosomes from bovine milk. *J of Vet Med Sci.*, vol. 74, no. 11, pp. 1523-1525. <https://doi.org/10.1292/jvms.12-0032>.
20. Chen T., Xie M.Y., Sun J.J., Ye R.S., Cheng X., Sun R.P., Wei L.M., et al. (2016) Porcine milk-derived exosomes promote proliferation of intestinal epithelial cells. *Sci Rep.*, vol. 6, <https://doi.org/10.1038/srep33862>.
21. Sedykh S. E., Purvinish L.V., Monogarov A.S., Burkova E.E., Grigor'eva A.E., Bulgakov D.V., Dmitrenok P.S., Vlassov V.V., Ryabchikova E.I., Nevinsky G.A. (2017) Purified horse milk exosomes contain an unpredictable small number of major proteins. *Bioch Open*, vol. 4, pp. 61-72. <https://doi.org/10.1016/j.biopen.2017.02.004>.
22. Admyre C., Johansson S.M., Qazi K.R., J.-J.r Filen, Lahesmaa R., Norman M., Neve E.P.A., Scheynius A., Gabrielsson S. (2007) Exosomes with immune modulatory features are present in human breast milk. *J Immun.*, vol. 179, no. 3, pp. 1969-1978, <https://doi.org/10.4049/jimmunol.179.3.1969>.
23. Reinhardt T.A., Lippolis J.D., Nonnecke B.J., Sacco R.E. (2012) Bovine milk exosome proteome. *J of Prot.*, vol. 75, no. 5, pp. 1486-1492. <https://doi.org/10.1016/j.jprot.2011.11.017>.
24. Ryskaliyeva A., Henry C., Miranda G., Faye B., Konuspayeva G., Martin P. (2018) Combining different proteomic approaches to resolve complexity of the milk protein fraction of dromedary, bac-

- trian camels and hybrids, from different regions of Kazakhstan. *PLoS ONE*, vol. 13, no. 5, <https://doi.org/10.1371/journal.pone.0197026>.
25. Michalski A., Damoc E., Hauschild J.-P., Lange O., Wiegand A., Makarov A., Nagaraj N., Cox J., Mann M., Horning S. (2011) Mass spectrometry-based proteomics using Q exactive, a high-performance benchtop quadrupole orbitrap mass spectrometer. *Mol and Cell Prot.*, <https://doi.org/10.1074/mcp.M111.011015>.
26. Lu J., van Hooijdonk T., Boeren S., Vervoort J., Hettinga K. (2014) Identification of lipid synthesis and secretion proteins in bovine milk. *J of Dair Res.*, vol. 81, no. 1, pp. 65-72, <https://doi.org/10.1017/S0022029913000642>.
27. McManaman J.L., Neville M.C. (2003) Mammary physiology and milk secretion. *Adv Drug Del Rev.*, vol. 55, no. 5, pp. 629-641, [https://doi.org/10.1016/S0169-409X\(03\)00033-4](https://doi.org/10.1016/S0169-409X(03)00033-4).
28. Lopez C., Ménard O. (2011) Human milk fat globules: polar lipid composition and in situ structural investigations revealing the heterogeneous distribution of proteins and the lateral segregation of sphingomyelin in the biological membrane. *Coll and Surf B: Biointerfaces*, <https://doi.org/10.1016/j.col-surf.2010.10.039>.
29. Kuhajda F.P. (2000) Fatty-acid synthase and human cancer: new perspectives on its role in tumor biology. *Nutrition*, vol. 16 no. 3, pp. 202-208, [https://doi.org/10.1016/S0899-9007\(99\)00266-X](https://doi.org/10.1016/S0899-9007(99)00266-X).
30. Cubillos-Ruiz J.R., Conejo-Garcia J.R. (2011) It never rains but it pours: potential role of butyrophilins in inhibiting anti-tumor immune responses. *Cell Cyc.*, vol. 10, no. 3, pp. 368-369. <https://doi.org/10.4161/cc.10.3.14565>.
31. Neutzner M., Lopez T., Feng X., Bergmann-Leitner E.S., Leitner W.W., Udey M.C. (2007) MFG-E8/Lactadherin promotes tumor growth in an angiogenesis-dependent transgenic mouse model of multistage carcinogenesis. *Canc Res.*, vol. 67, no. 14, pp. 6777-6785, <https://doi.org/10.1158/0008-5472.CAN-07-0165>.
32. Samuel M., Chisanga D., Liem M., Keerthikumar S., Anand S., Seng Ang C., Adda C.G., Versteegen E., Jois M., Mathivanan S. (2017) Bovine milk-derived exosomes from colostrum are enriched with proteins implicated in immune response and growth. *Sci Rep.*, vol. 7, no. 1, <https://doi.org/10.1038/s41598-017-06288-8>.
33. Baietti M.F., Zhang Z., Mortier E., Melchior A., Degeest G., Geeraerts A., Ivarsson Y., et al. (2012) Syndecan-Syntenin-ALIX regulates the biogenesis of exosomes. *Nat Cell Biol.*, vol. 14, no. 7, pp. 677-685, <https://doi.org/10.1038/ncb2502>.
34. Srivastava P. (2002) Interaction of heat shock proteins with peptides and antigen presenting cells: chaperoning of the innate and adaptive immune responses. *An Rev of Im.*, vol. 20, no. 1, pp. 395-425, <https://doi.org/10.1146/annurev.immunol.20.100301.064801>.
35. Simons M., Raposo G. (2009) Exosomes-vesicular carriers for intercellular communication. *Cur Op in Cell Biol.*, vol. 21, pp. 575-581. <https://doi.org/10.1016/j.ceb.2009.03.007>.
36. Théry C., Zitvogel L., Amigorena S. (2002) Exosomes: composition, biogenesis and function. *Nat Rev Immun.*, vol. 2, no. 8, pp. 569-579, <https://doi.org/10.1038/nri855>.
37. Raimondo F., Morosi L., Chinello C., Magni F., Pitto M. (2011) Advances in membranous vesicle and exosome proteomics improving biological understanding and biomarker discovery. *Prot.*, vol. 11, no. 4, pp. 709-720, <https://doi.org/10.1002/pmic.201000422>.
38. Rana S., Zöller M. (2011) Exosome target cell selection and the importance of exosomal tetraspanins: a hypothesis. *Bioch Soc Trans.*, vol. 39, no. 2, pp. 559-562. <https://doi.org/10.1042/BST0390559>.
39. Kowal J., Arras G., Colombo M., Jouve M., Morath J.P., Primdal-Bengtson B., Dingli F., Loew D., Tkach M., Théry C. (2016) Proteomic comparison defines novel markers to characterize heterogeneous populations of extracellular vesicle subtypes. *Proc of the Nat Acad of Sci.*, vol. 113, no. 8, pp. E968-77, <https://doi.org/10.1073/pnas.1521230113>.
40. Vaswani K., Koh Y.Q., Almughlliq F.B., Peiris H.N., Mitchell M.D. (2017) A method for the isolation and enrichment of purified bovine milk exosomes. *Repr Biol.*, vol. 17, no. 4, pp. 341-348, <https://doi.org/10.1016/j.repbio.2017.09.007>.
41. la Torre G., C. de R. V. Goreham, Bech Serra J.J., Nann T., Kussmann M. (2018) 'Exosomics' – a review of biophysics, biology and biochemistry of exosomes with a focus on human breast milk. *Front in Gen.*, vol. 9, no. 92. <https://doi.org/10.3389/fgene.2018.00092>.
42. Mathivanan S., Ji H., Simpson R.J. (2010) Exosomes: extracellular organelles important in intercellular communication. *J of Prot.*, vol. 73, no. 10, pp. 1907-1920, <https://doi.org/10.1016/j.jprot.2010.06.006>.
43. Bradford M.M. (1976) A rapid and sensitive method for the quantitation of microgram quantities of protein using the principle of protein dye binding. *Anal Bioch.*, vol. 72, pp. 248-254. [https://doi.org/10.1016/0003-2697\(76\)90527-3](https://doi.org/10.1016/0003-2697(76)90527-3).

¹M.I. Tulepov , ¹F.Yu. Abdrakova , ^{1*}L.R. Sassykova , ¹Z.A. Mansurov ,
¹A. Kuznetsov , ¹I.A. Pustovalov , ¹G.A. Spanova , ¹D.M. Tolep , ²B. Elouadi 
¹Institute of Combustion Problems, 172, Bogenbai, Batyr St., 050000, Almaty, Kazakhstan
²Université De La Rochelle, Technoforum, 23 ave. Albert Einstein,
BP 33060 – 17031, La Rochelle, France
*e-mail: larissa.rav@mail.ru

Modeling of the explosion of pyroxylin or combustion of the pyrotechnic composition

Abstract: Considering the blow force as the given parameter during the combustion of pyrotechnic compositions, it is possible to calculate the mass of a necessary charge of pyrotechnic formulation. By this cause, a special interest is the model of an explosion or burning of the pyrotechnic composition, in which is possible at high degree of accuracy to calculate the mass of the pyrotechnic charge. This will lower the percentage of accidents when dealing with pyrotechnics. The aim of the work is formulation of the physical and mathematical model of explosion or combustion of pyrotechnic composition on the basis of laws of conservation of momentum and energy. The calculation formulas were checked on a concrete example – pyroxylin and compared with data from reference books and the Internet. The analysis of a calculated formula for a pyroxylin showed that in the course of explosion the main contribution to destruction of the chosen objects is made by a potential energy of gases (about 88%), and only 12% by a kinetic energy of incandescent gases, but when calculating force of explosion it needs to be considered.

Key words: explosion, combustion, pyroxylin, energy, momentum, the physical and mathematical model of explosion or combustion of pyrotechnic composition.

Introduction

Combustion explosive gas (or fluid) mixtures or individual explosives is a homogeneous combustion. Pyrotechnic compositions are the mechanical mixtures of the solid, finely crushed components – on degree of homogeneity are in the middle between the condensed fuel and individual substances (or homogeneous mixtures). Combustion of pyrotechnic compositions is carried out by a heat transfer from a reaction zone, to layers in which there is a preparation for combustion process. Inflaming of pyrocompositions also is based on the same principle. For emergence of combustion it is necessary to create local temperature increase in composition; it is reached by usually immediate impact on composition of hot gunpowder gases or use of special flammable formulations. When the pyrocomposition is put in action by a fire impulse and its combustion takes place in open space, its burning rate is small (usually a few mm/s). If the combustion occurs in an enclosed space, or if used in as an initiator a detonator cap, it may be an explosion (which speed is measured in hundreds, and sometimes thousands of m/s) [1-8].

There are many ways of calculation and choice of necessary explosive, for carrying out blasting, production of pyrotechnic devices, etc. These are chemical ways where calculations are carried out through an explosive decomposition reaction; physical ways where many researchers solve this problem as a problem only of thermal explosion. Explosion modeling assumes the solution of this problem, through the laws of conservation of energy and momentum, that allows to see visually the role introduced by each component in the reaction equations of conservation of energy and momentum [9-13].

In the solution of the equation the blow force necessary for destruction of this material is especially highlighted, using it as the given parameter, it is possible to specify enough the mass of a necessary charge of pyrotechnic formulation [14-18].

Therefore, a special interest is the model of an explosion or burning of the pyrotechnic composition, in which is possible at high degree of accuracy to calculate the mass of the pyrotechnic charge. This will lower the percentage of accidents when dealing with pyrotechnics, when dealing with

pyrotechnics that may arise on fault of the manufacturer, as well as to reduce the percentage of systematic deviation from the intended accuracy of blasting and other work associated with the pyrotechnic compositions.

The aim of the work is formulation of the physical and mathematical model of explosion or combustion of pyrotechnic composition on the basis of laws of conservation of momentum and energy.

Experimental

Physical and mathematical modeling of chemical and physical reactions is a way to describe a physical and chemical phenomena, using the equations of mathematical physics, usually under the terms of an approximation to the real phenomenon. Physical and mathematical model is necessary for the study of chemical and physical phenomena in the laboratory, i.e. on the equipment, which is created with the specified parameters, and which reproduces the studied physical phenomenon [19-21]. If there are difficulties with reproduction and the description of the physical phenomenon, because of complexity of a physical task, then usually use similarity of the phenomena in which the solution of a task considerably becomes simpler, and the resulting mathematical decision for the description of the studied physical phenomenon is used.

For burning modeling, or explosion of pyrotechnic formulation, it is necessary to use the conservation equations:

$$\frac{d}{dt} \sum_{i=1}^n (m_i \cdot \vec{v}_i) = 0 \quad (1),$$

where $n=1,2,3,4,5,\dots$

The equation (1) is the law of conservation of momentum, m_i, \vec{v}_i – the weight and speed of the i -th component of system, before and after the explosion.

$$\frac{d}{dt} \sum_{i=1}^n E_i = 0 \quad (2),$$

where E^i – the total energy of the system, and the equation (2) is the law of conservation of energy.

Let's transform, the equation of conservation of momentum, for this purpose use differentiation in private derivatives, on variable coordinates \vec{r} , t – radius of the vector, and of time

$$\begin{aligned} \frac{d}{dt} \sum_{i=1}^n (m_i \cdot \vec{v}_i) &= \sum_{i=1}^n m_i \cdot \left(\frac{\partial}{\partial t} \vec{v}_i + \frac{\partial \vec{r}}{\partial t} \cdot \frac{\partial}{\partial \vec{r}} \vec{v}_i \right) + \\ &+ \sum_{i=1}^n \vec{v}_i \cdot \left(\frac{\partial}{\partial t} m_i + \frac{\partial \vec{r}}{\partial t} \cdot \frac{\partial}{\partial \vec{r}} m_i \right) = 0 \end{aligned} \quad (3)$$

The two parts of the equation (3) can be equalized and rewritten as:

$$\begin{aligned} \sum_{i=1}^n m_i \cdot \left(\frac{\partial}{\partial t} \vec{v}_i + \frac{\partial \vec{r}}{\partial t} \cdot \frac{\partial}{\partial \vec{r}} \vec{v}_i \right) &= \\ = - \sum_{i=1}^n \vec{v}_i \cdot \left(\frac{\partial}{\partial t} m_i + \frac{\partial \vec{r}}{\partial t} \cdot \frac{\partial}{\partial \vec{r}} m_i \right) \end{aligned} \quad (4)$$

If to add variables as multipliers, under a sign of private derivatives, then we will obtain the equation (4) in a semi-logarithmic form:

$$\begin{aligned} \sum_{i=1}^n \left(\frac{\partial}{\partial t} \ln(\vec{v}_i) + \frac{\partial \vec{r}}{\partial t} \cdot \frac{\partial}{\partial \vec{r}} \ln(\vec{v}_i) \right) &= \\ = - \sum_{i=1}^n \left(\frac{\partial}{\partial t} \ln(m_i) + \frac{\partial \vec{r}}{\partial t} \cdot \frac{\partial}{\partial \vec{r}} \ln(m_i) \right) \end{aligned} \quad (5)$$

Let's group in the equation (5) parts identical on derivatives and we will highlight a derivative in the right part of equation (5) $\frac{\partial \vec{r}}{\partial t}$:

$$\begin{aligned} \sum_{i=1}^n \left(\frac{\partial}{\partial t} \ln(\vec{v}_i) + \frac{\partial}{\partial t} \ln(m_i) \right) &= \\ = - \frac{\partial \vec{r}}{\partial t} \cdot \sum_{i=1}^n \left(\frac{\partial}{\partial \vec{r}} \ln(\vec{v}_i) + \frac{\partial}{\partial \vec{r}} \ln(m_i) \right) \end{aligned} \quad (6)$$

So multiply private derivatives on equal in brackets:

$$\begin{aligned} \sum_{i=1}^n \left(\frac{\partial}{\partial t} \ln(\vec{v}_i) + \frac{\partial}{\partial t} \ln(m_i) \right) \partial t &= \\ = - \sum_{i=1}^n \left(\frac{\partial}{\partial \vec{r}} \ln(\vec{v}_i) + \frac{\partial}{\partial \vec{r}} \ln(m_i) \right) \partial \vec{r} \end{aligned} \quad (7)$$

As private derivatives with different variables are partitioned on the different sides of the equation (7) and in each part differentiation on one variable is made, it is possible on properties of private derivatives, to pass from private derivatives to differentials:

$$\begin{aligned} \sum_{i=1}^n \left(\frac{d}{dt} \ln(\vec{v}_i) + \frac{d}{dt} \ln(m_i) \right) dt &= \\ = - \sum_{i=1}^n \left(\frac{d}{d\vec{r}} \ln(\vec{v}_i) + \frac{d}{d\vec{r}} \ln(m_i) \right) d\vec{r} \end{aligned} \quad (8)$$

Let's make reduction in both members of equation and will integrate the equation (8):

$$\begin{aligned} & \sum_{i=1}^n \int (dL_n(\bar{v}_i) + dL_n(m_i)) = \\ & = - \sum_{i=1}^n \int (dL_n(\bar{v}_i) + dL_n(m_i)) \end{aligned} \quad (9)$$

For convenience of transformation, the constants obtained at integration have presented in the logarithmic form:

$$\begin{aligned} & \sum_{i=1}^n L_n(\bar{v}_i * m_i) + L_n C_1 = \\ & = - \sum_{i=1}^n L_n(\bar{v}_i * m_i) + L_n C_2 \end{aligned} \quad (10)$$

Let's raise the right and left member of equation in degree on the basis of a constant of Napier:

$$\begin{aligned} & \exp \left[\sum_{i=1}^n L_n(C_1 * \bar{v}_i * m_i) \right] = \\ & = \exp \left[\sum_{i=1}^n L_n \left(\frac{C_2}{\bar{v}_i * m_i} \right) \right] \end{aligned} \quad (11)$$

As we have no determining factors for the constants obtained in case of integration, will continue transformations of the equation, and we will determine constants according to the energy conservation law in an integrated type:

$$C_1 * \sum_{i=1}^n \bar{v}_i * m_i = \frac{C_2}{\sum_{i=1}^n \bar{v}_i * m_i} \quad (12)$$

Let's take out constants to the right side of the equation:

$$\sum_{i=1}^n (\bar{v}_i * m_i)^2 = \frac{C_2}{C_1} \quad (13)$$

We will reduce the degree of the left side of the equation (13):

$$\sum_{i=1}^n (\bar{v}_i * m_i) = \sqrt{\frac{C_2}{C_1}} \quad (14),$$

where $C_1 \neq 0$, on the problem statement $C_2 = 0$

Law of conservation of momentum in an integrated form is obtained:

$$\sum_{i=1}^n (\bar{v}_i * m_i) = 0 \quad (15)$$

Since, in the course of the explosion involved three components of the system (an explosive, gases produced at the chain reaction, and solid residues), that for our case $n=3$

$$\bar{v}_1 * m_1 = -\bar{v}_2 * m_2 - \bar{v}_3 * m_3 \quad (16),$$

where $|\bar{v}_1| = |\bar{v}_2| = |\bar{v}_3|$

$$m_1 = m_2 + m_3 \quad (17),$$

where m_1 is weight of explosive charge, m_2 is resulting gases mass, m_3 is the cooling solid product of the explosion. In order to find the sought variable – volume of gases produced during the flow of the chain reaction it is necessary to present the mass through density and the occupied substance volume

$$\rho_1 * V_1 = \rho_2 * V_2 + \rho_3 * V_3 \quad (18)$$

Let's transfer a required variable to the left side of the equation (18):

$$\rho_2 * V_2 = \rho_1 * V_1 - \rho_3 * V_3 \quad (19)$$

After simple mathematical transformations, we obtain an equation that determines the desired value:

$$V_2 = \frac{\rho_1 * V_1 - \rho_3 * V_3}{\rho_2} = \frac{m_1 - m_3}{\rho_2} \quad (20),$$

where ρ_1 is stoichiometric density of the explosive charge, ρ_2 is density the produced gases at an actual temperature, ρ_3 is the density of the combustion residue.

V_1, V_2, V_3 are the corresponding volumes.

Since V_2 is the volume of gases, and is searched at N.C. (normal conditions), then at solution of the problem it is necessary volume of gases result to the real conditions, i.e. to a temperature equal to about 2500 K, for pyroxylin, and to the selected volume V (pressing of a pyroxylin by volume V is possible), p_1, p_2 – the atmospheric pressure and $v_1 = v_2$.

For the analysis of the obtained specified value the volume of gases needs to be given to N.C., then it is necessary to use the state equations for gases:

$$\begin{cases} P_2 * V'_2 = \nu_2 * R * T'_2 \\ P_2 * V_2 = \nu_2 * R * T_2 \end{cases} \quad (21)$$

$$V'_2 = \frac{\rho_1 * V_1^{-\rho_3} * V_3 * T'_2}{\rho_2} = \frac{m_1^{-m_3} * T'_2}{\rho_2} \quad (22),$$

where T'_2 is a temperature of normal conditions (293,16 K), T_2 is a temperature of incandescent gas (2,500 K for pyroxylin).

For the projectile having the volume of V we can lead the equation (20) to a form, it will help to estimate the value of pressure of gases upon projectile walls, as characterizes explosion:

$$\begin{cases} P * V = \nu_2 * R * T_2 \\ P_2 * V_2 = \nu_2 * R * T_2 \end{cases} \quad (23)$$

$$P * V = P_2 * \frac{\rho_1 * V_1^{-\rho_3} * V_3}{\rho_2},$$

$$P * V = P_2 * \frac{m_1^{-m_3}}{\rho_2} = P_2 * \frac{m_2}{\rho_2} \quad (24),$$

in this equation is considered the pressure P and temperature T in real conditions, the formation of gas in the projectile, in a chain reaction.

Transform the energy balance equation:

$$\sum_{i=1}^n E_i = \sum_{i=1}^n (E_{ki} + \dot{I}_i) \quad (25),$$

the total energy is the sum of kinetic and potential energy.

To obtain the necessary equations substitute the equation (25) into equation (2):

$$\frac{d}{dt} \sum_{i=1}^n E_i = \sum_{i=1}^n \left(\frac{\partial}{\partial t} E_{ki} + \frac{\partial \vec{r}}{\partial t} * \frac{\partial}{\partial \vec{r}} E_{ki} \right) + \sum_{i=1}^n \left(\frac{\partial}{\partial t} \Pi_i + \frac{\partial \vec{r}}{\partial t} * \frac{\partial}{\partial \vec{r}} \Pi_i \right) = 0 \quad (26)$$

Since potential energy change with time and kinetic energy on radius to a vector is equal to zero, the equation (26) is given to a form:

$$\frac{d}{dt} \sum_{i=1}^n E_i = \sum_{i=1}^n \left(\frac{\partial}{\partial t} E_{ki} + \frac{\partial \vec{r}}{\partial t} * \frac{\partial}{\partial \vec{r}} \dot{I}_i \right) = 0 \quad (27)$$

Multiply the left and right side of the equation (27) on the partial derivative, by time

$$\sum_{i=1}^n \left(\frac{\partial}{\partial t} E_{ki} + \frac{\partial \vec{r}}{\partial t} * \frac{\partial}{\partial \vec{r}} \dot{I}_i \right) \partial t = 0 \quad (28).$$

Reduce by a multiplier present an expression to the total differentials

$$\sum_{i=1}^n (dE_{ki} + d\dot{I}_i) = 0 \quad (29)$$

Integrate the equation (29)

$$\sum_{i=1}^n \int_0^{E_{ki}} dE_{ki} + \sum_{i=1}^n \int_0^{\dot{I}_i} d\dot{I}_i = 0 \quad (30)$$

We obtain the equation of the energy balance in the integral form:

$$\sum_{i=1}^n E_{ki} + \sum_{i=1}^n \dot{I}_i = 0 \quad (31)$$

As in the model system are involved three bodies – an explosive gas, solid residue, then $n = 3$.

$$\sum_{i=1}^3 E_{ki} + \sum_{i=1}^3 \dot{I}_i = 0 \quad (32)$$

Let's consider work which is made by potential force at expansion of the formed gases

$$\delta A = \vec{F} * d\vec{r} = P * dV \quad (33),$$

where P is defined from a formula (24).

On the other hand

$$\vec{F} * d\vec{r} = - \frac{d\varphi}{d\vec{r}} * d\vec{r} = -d\varphi$$

Then potential can be presented in the form

$$\varphi = -P * \int_V dV = P * V, \quad A = \vec{F} * \vec{r} \quad (34),$$

where S is the surface area of the projectile.

Then the equation of balance taking into account the potential energy, the equation (34)

$$q * m_1 = \frac{m_2}{\mu_2} * \frac{3}{2} * R * T + P * V + c * m_3 * (T_2 - T'_2) \quad (35),$$

where q is the specific heat of combustion.

Substitute the formula (24) in the (35) and obtain:

$$\begin{aligned} q * m_1 - c * m_3 * (T_2 - T'_2) &= \\ &= \frac{m_2}{\mu_2} * \frac{3}{2} * R * T_2 + P_2 * \frac{m_2}{\rho_2} \end{aligned} \quad (36),$$

m_3 via m_1 it is possible to express via a ratio:

$$m_3 = k * m_1 \quad (37)$$

Then the equation (36) can be transformed to a form:

$$m_1 = m_2 * \frac{\left[\frac{3 * R * T_2}{2 * \mu_2} + \frac{P_2}{\rho_2} \right]}{\left[q - c * k * (T_2 - T'_2) \right]} \quad (38)$$

So, a formula of the choice of mass of a charge, with respect to these conditions, have obtained, here the most important parameter is the mass of gases which can be determined by the power of the explosion needed, for example, blasting operations, according to the formula (34), into which is necessary to substitute the formula (24)

$$A = \bar{F} * \bar{r} = P_2 * \frac{m_2}{\rho_2} \quad (39),$$

here \bar{F} is an impact force in Newtons, necessary for material destruction, \bar{r} is the radius vector which is carried out from the beginning of coordinates to a point of application of force.

Now we will transform the equation (39)

$$m_2 = A * \frac{\rho_2}{P_2} \quad (40)$$

Then we can transform a formula (38)

$$m_1 = A * \frac{\rho_2}{P_2} * \frac{\left[\frac{3}{2 * \mu_2} * R * T_2 + \frac{P_2}{\rho_2} \right]}{\left[q - c * k * (T_2 - T'_2) \right]} \quad (41)$$

Results and Discussions

Let's carry out the analysis of the obtained decision on the basis of pyroxylin. It is well known that pyroxylin is a product of the complete esterification of cellulose with nitric acid (trinitrocellulose). Pyroxylin is an explosive used in the manufacture of smokeless powder [22]. For this mathematical analysis it is necessary to know which gases and the solid residue, their quantity are formed as explosion derivatives, or burning, usually for different pyrotechnic formulations they are different and also have different volume in relation to unit of mass [14-16].

For smokeless gunpowder the composition of gases has the following contents in relation to the total amount of gases: H_2O – 16%, H_2 – 20%, N_2 – 11%, CO – 37%, C_2H_4 – 1%, CO_2 – 15%, with a density of 1.214 kg/m³ (under normal conditions) and with a molar weight of 23.6 kg/mol. The solid residue usually for pyroxylin is equal to from 0.1 to 0.5% by weight of the charge [17-19]. The specific heat of combustion of pyroxylin $q = 2,5$ MJ/kg, the combustion temperature is $T = 2500$ K, temperature of NC (normal conditions, the environment) $T' = 293,16$, and $P_2 = 101$ kPa, $R = 8.314$ J/(kmol·K) – the universal gas constant [5, 9, 20-27].

To check the estimated formula (20) it is necessary to set the charge weight $m_1 = 0,001$ t, knowing other parameters it is possible to calculate V is the volume of gases, when burning gunpowder, for this purpose in a formula (20), density of gases is led to real conditions

$$\begin{aligned} V_2 &= \frac{m_1 - m_3}{\rho_2} * \frac{T}{T'} = \frac{0,999 * m_1}{\rho_2} * \frac{T}{T'} = \\ &= \frac{0,999 * 0,001 * 293,16}{1,214} = 9,65 * 10^{-5} \text{ m}^3 \end{aligned} \quad (42)$$

To compare the obtained results with literary data, it is necessary the volume of gases under real conditions of $T = 2500$ K, to lead to water freezing temperature $T = 273,16$ K

$$V'_2 = V_2 * \frac{T}{T_0} = 1,1 * 10^{-4} * \frac{2500}{273,16} = \quad (43),$$

$$= 0,883 * 10^{-3} \text{ m}^3$$

that within 2.0% of an error of measurement is in the range of literary data [19].

The objective of this work is the calculation of the charge of pyrotechnic substances (pyroxylin), depending on the required force of the explosion, as well as the volume of the projectile. The formula (41) obtained in the research allows to calculate the required weight of the charge m_i , depending on the work A of the thermodynamic system, or force from the explosion \vec{F} , at the chosen value of radius vector \vec{r} , i.e. of the selected parameters of impact by explosion (the main direction of the explosion force, the distance).

The analysis of a formula (41) can be carried out on a concrete example, by means of a function graph, fig.1, and $m_1 = f(\vec{F}, \vec{r})$, fig.2.

In fig.1 dependence of mass of a charge of a pyroxylin on the work made by gases at expansion is obtained. The function graph is presented by direct proportionality, it allows to count rather precisely the mass of pyrotechnic formulation, excepting various kinds of accidents.

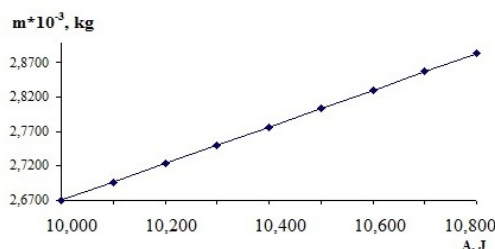


Figure 1 – The dependence of the charge weight from the explosion force

In the fig.2 the same dependence, but in three-dimensional form is set, here serve as parameters force making work (explosion) and radius the vector having the direction to a point of application where a surface area is the work made by force of expansion of incandescent gases. Analysis of the formula (41) showed that during the explosion a major contribution to the destruction of objects makes the potential energy of gas, about 88%, and only 12% makes the kinetic energy of incandescent gases. Of course, when calculating force of explosion it needs to be considered. The energy

introduced by solid residue, on cooling, is very small – about 0.05% and so it, in the calculations, may be neglected [28-32]. Unfortunately, in some references calculated formulas are obtained either for kinetic, or for a potential component of a calculated formula of explosion, that is the contribution made by both components of a calculated formula is underestimated.

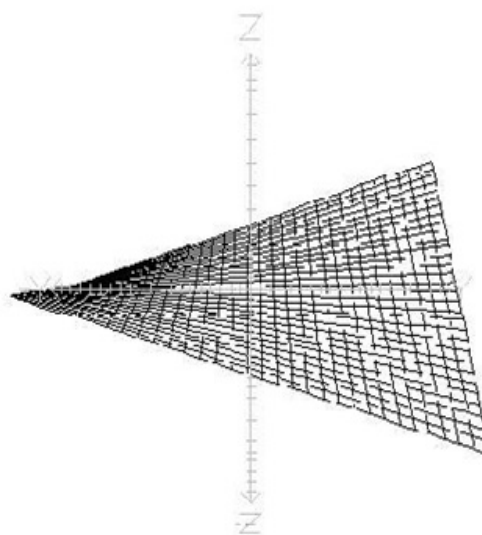


Figure 2-The dependence of weight of a charge from a force and radius vector

Conclusions

The physical and mathematical model of explosion or combustion of pyrotechnic composition on the basis of laws of conservation of momentum and energy is obtained. Calculation formulas were checked on a concrete example – pyroxylin and compared with data from reference books and the Internet. This model, or calculated formula of a method, is intended for use, at manufacture of pyrotechnic substances, and also when carrying out blasting on mineral deposits, etc. It was showed that in the course of explosion the main contribution to destruction of the chosen objects is made by a potential energy of gases (about 88%), and only 12% by a kinetic energy of incandescent gases, but when calculating force of explosion it needs to be considered.

References

1. Beck M.W., Brown M.E., *Combustion and Flame*, 1986, 66(1), 67.

2. Shu-gang C., Yan-bao L., Yan-ping W., *J. Min. Technol.*, 2008, 18, 0172–0176.
3. Coleman P.J., *Journal of Safety Research*, 2007, 38, 523-533.
4. Riba S. J., Lesaoana M., Sigauke C., Makwela M. R., *Journal of Geology and Mining Research*, 2011, 3(1), 188-192.
5. Tulepov M.I., Baiseitov D.A., Gabdrashova Sh.E., Sassykova L.R., Kazakov Y.V., Tursynbek S., Toshtay K., Pustovalov I.O., Abdrakova F.Y., Mansurov Z.A., Dalton A.B., *Rasayan J. Chem.*, 2017, 10(4), 1145-1150.
6. Sullivan M.J., Stewart W.F., Belanger D.L., *SPE Annual Technical Conference and Exhibition Dallas, Texas*, 2000. <http://dx.doi.org/10.2118/62979-MS>.
7. Sullivan M.J., Belanger D.L., Stewart W.F., *SPE Reservoir Evaluation & Engineering*, 2002, 5, 60-67. <http://dx.doi.org/10.2118/76643-PA>.
8. Banahene A.O., Pepe D.C., Lueck W.R., *SPE Rocky Mountain Petroleum Technology Conference, Keystone, Colorado*, 2001. <http://dx.doi.org/10.2118/71075-MS>.
9. Tulepov M. I., Mansurov Z.A., Kazakov Y.V., Abdrakova F.Y., Sultanova Z.L., Rakhova N. M., Madiyev S.S., Golovchenko O.Y., Sassykova L.R., Tolep D.M., Chikhradze N., Chikhradze M.N., *Oriental Journal of Chemistry*, 2018, 34(6), 3037-3043. <http://dx.doi.org/10.13005/ojc/350103>.
10. Bondarev E.A., *SPE Russian Oil and Gas Technical Conference and Exhibition, Moscow, Russia*, 2006. <http://dx.doi.org/10.2118/104331-MS>.
11. Tulepov M., Baiseitov D., Sassykova L., Kazakov Y., Gabdrashova Sh., Mansurov Z., Dalton A., *Journal of Chemical Technology & Metallurgy*, 2018, 53(2), 281-288.
12. Gürocak H.B., *International Journal of Mechanical Engineering Education*, 1998, 26(3), 210-222.
13. Abdelhamid T. S., Everett J. G., *Journal of Construction Engineering & Management*, 2000, 126(1), 52.
14. Lu Kai-Tai, Yang Ching-Chyuan, *Propellants, Explosives, Pyrotechnics*, 2008, 33(5), 403-410.
15. Dem'yanenko D. B., Dudyrev A. S., Efanov V. V., Strakhov G., Tsinbal M. N., *Solar System Research*, 2013, 47(7), 508-512.
16. Podkopaev S., Sakhno S., *J of Donetsk Mining Institute*, 2018, 1, 61-68. <https://doi.org/10.31474/1999-981x-2018-1-61-68>.
17. Sari M., Duzgun H.S.B., Karpuz C., Selcuk A.S., *Saf. Sci.*, 2004, 42, 675-690.
18. Haslam R. A., Hide S. A., Gibb A. G. F., Gyi D. E., Pavitt T., Atkinson S., Duff A. R., *Applied Ergonomics*, 2005, 36(4), 401–415.
19. Soares A.C., Ferreira F.H., Vargas E.A., *SPE Reservoir Evaluation & Engineering*, 2002, 5(6), SPE-80614-PA, <https://doi.org/10.2118/80614-PA>.
20. Baiseitov D.A., Tulepov M. I., Tursynbek S., Sassykova L.R., Nazhipkyzy M., Gabdrashova Sh.E., Kazakov Y.V., Pustovalov I.O., Abdrakova F.Y., Mansurov Z.A., Dalton A.B., *Rasayan Journal of Chemistry*, 2017, 10(2), 344-348.
21. Bououdina M., Guo Z.X., *Materials Science and Engineering: A*, 2002, 332(1-2), 210-222.
22. Wildlife Toxicity Assessments for Chemicals of Military Concern. Edited by: Marc A. Williams, Gunda Reddy, Michael J. Quinn, Jr. Mark S. Johnson, Elsevier, 2015, 722p. <https://doi.org/10.1016/C2013-0-13473-3>.
23. Saleh J.H., Cummings A.M., *Safety Science*, 2012, 49(6), 767-777.
24. Montgomery Y. C., Focke W.W., Kelly Ch., *Propellants, Explosives, Pyrotechnics*, 2017, 42(11), 1289-1295.
25. Baiseitov D., Tursynbek S., Tulepov M., Sassykova L., Nazhipkyzy M., Gabdrashova Sh., Kazakov Y., Pustovalov I., Abdrakova F., Mansurov Z., Dalton A., *Journal of Chemical Technology & Metallurgy*, 2018, 53(3), 543-548.
26. Tulepov M. I., Gabdrashova Sh. E., Rakhova N. M., Sassykova L. R., Baiseitov D. A., Elemesova Zh., Korchagin M. A., Sendilvelan S., Pustovalov I. O., Mansurov Z.A., *Rasayan J. Chem.*, 2018, 11(1), 287-293.
27. Whiffen B.W., A pyrotechnic delay ignition system for a submarine launched marine signal, 1987. <https://doi.org/10.21236/ada188715>
28. Pletcher J.L., *SPE Reservoir Evaluation & Engineering*, 2002, 5(1), SPE-75354-PA. <https://doi.org/10.2118/75354-PA>
29. Winsdor C. R., *International Journal of Rock Mechanics and Mining Sciences*, 1997, 34(6), 919-951.
30. Gabdrashova Sh., Tulepov M., Pustovalov I., Sassykova L., Rakhova N., Spanova G., Hamzina B., Elouadi B., Kazakov Yu., *Journal of Chemical Technology and Metallurgy*, 2019, 54(3), 650-656.
31. Focke W.W., Tichapondwa Sh.M., Montgomery Y.C., Grobler J.M., Kalombo M. L., Review of Gasless Pyrotechnic Time Delays, *Propellants Explos. Pyrotech.*, 2019, 44, 55–93. <https://doi.org/10.1002/prop.201700311>
32. Mccollum J., Pantoya M. L., Iacono S. T., *ACS Appl. Mater. Interfaces*, 2015, 7, 18742–18749.

^{1,3*}A.N. Gurin , ²Patrick Riss , ¹Ye.T. Chakrova , ^{1,3}I.V. Matveyeva 

¹RSE Institute of Nuclear Physics, Ministry of Energy
of the Republic of Kazakhstan, Kazakhstan

²University of Oslo, Oslo, Norway

³Al-Farabi Kazakh National University, Almaty, Republic of Kazakhstan

*e-mail: gurenandrey@mail.ru

Quality control test for ¹⁷⁷Lu-DOTAELA

Abstract. This article provides a brief overview of ¹⁷⁷Lu-DOTAELA (¹⁷⁷Lu-1,4,7,10-tetraazacyclododecane-1,4,7,10-tetraacetic acid – 4-[[[(1R)-2-[5-(2-fluoro-3-methoxyphenyl)-3-[[2-fluoro-6-(trifluoromethyl)phenyl] methyl]-4-methyl-2,6 dioksopirimidin-1-yl]-1-phenylethyl] amino] butanoic acid) quality control based on practical experience. Over the past few years, radionuclide ¹⁷⁷Lu has attracted considerable attention and demonstrated great perspectives in the scientific, commercial and clinical communities for application in various therapeutic procedures. Requirements for quality control of radiopharmaceuticals can be found in volume 3 of the State Pharmacopoeia of the Republic of Kazakhstan (SF RK) which is the main regulative document in our country, in the absence of specific monographs and articles in the national Pharmacopoeia it is allowed to use and refer to the Pharmacopoeia of other countries (USA, Japan, UK and Europe). The main requirements for radiopharmaceuticals: pH; radionuclide identification; radiochemical purity; residual solvents; chemical purity; sterility and bacterial endotoxins; checking the integrity of the filter membrane. It should also be noted that there are differences in the quality requirements of some monographs of radiopharmaceuticals in the Pharmacopoeia of different countries. Considering above, during development of the quality control procedure we have to use several regulatory sources. The solution to this problem can be the harmonization of Pharmacopoeia of the Member-States of the Eurasian Economic Union. The process of testing the methodology of quality control is time-consuming and includes many tasks, especially in the area of new radiopharmaceuticals development.

Key words: ¹⁷⁷Lu-DOTAELA, radiopharmaceutical, test, quality control (QC), pharmacopoeia, nuclear medicine.

Introduction

The active substance of the radiopharmaceutical being developed for treatment of triple negative breast cancer is a complex of the radioactive isotope of lutetium ¹⁷⁷Lu and the non-peptide antagonist gonadotropin-releasing hormone (GnRH) elagolix (¹⁷⁷Lu-DOTAELA). Receptors for triple negative breast cancer show expression of gonadotropin-releasing hormone (GnRH) in more than 50% of cases [1]. Elagolix, marketed under the Orilissa brand, which is used to treat pain associated with endometriosis in women. It is also developed for treatment of hysteromyoma and heavy menstrual bleeding in women.

The aim of this work is to highlight the process of developing the quality control procedure, using the example of the developed ¹⁷⁷Lu-DOTAELA radiopharmaceutical, which is intended for treatment of triple negative breast cancer.

Materials and methods

Quality control ¹⁷⁷Lu-DOTAELA

Quality control of radiopharmaceuticals is one of the most important production stages with the special requirements, established in volume 3 of the State Pharmacopoeia of the Republic of Kazakhstan [2], including in the Pharmacopoeia of the USA [3], Great Britain [4] and Europe [5]. The IAEA also published a draft document entitled “Quality Control in the Production of Radiopharmaceuticals” [6]. If we compare the monograph of the same drug in different countries, you can find some differences. The reason for the differences may be the use of different standards. There are tests listed in the BF, but not specified in the GF RK, for example the measurement of radioactivity or USP and BP do not require a test for integrity of the membrane filter.

Table 1 Quality control tests to be performed regularly for the radiopharmaceutical ¹⁷⁷Lu-DOTAELA (Fig. 1).

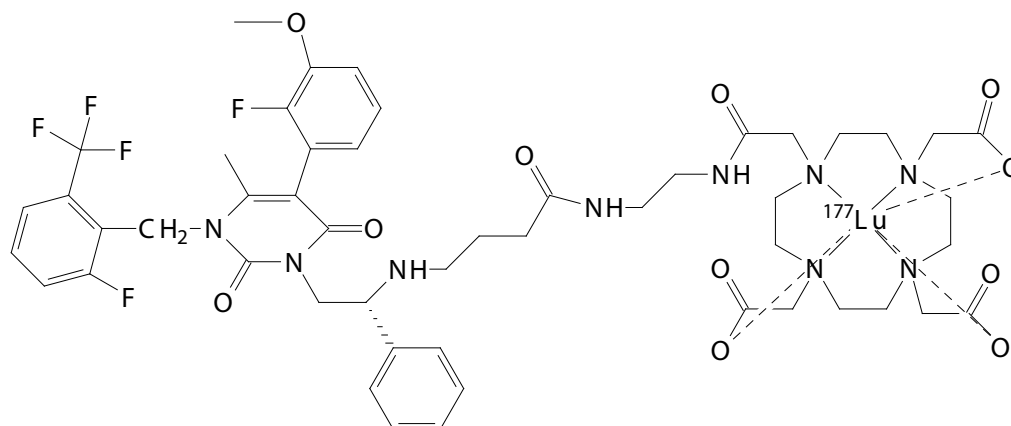


Figure 1 – Structural formula of ^{177}Lu -DOTAELA

Table 1-Quality control analysis ^{177}Lu -DOTAELA

Test	Method	Requirements
Identification ^{177}Lu -DOTAELA	HPLC (SP RK I, vol. 1, 2.2.29)	The relative retention time of ^{177}Lu -DOTAELA should differ by no more than 3 % from the retention time of the non-radioactive Lu-DOTAELA complex.
Identification ^{177}Lu	Gamma spectrometry	The ^{177}Lu gamma spectrum of the test solution should have characteristic lines with energies of 0.113 and 0.208 MeV
pH	Potentiometry (SP RK I, vol. 1, 2.2.3)	from 4.5 to 8.5
Transparency	SP RK I, v. 1, 2.2.1	Transparent compared to <i>water P</i>
Color	SP RK I, v. 1, 2.2.2	The color of the drug should not be more intense <i>than the color of the solution of comparison Y7</i>
Mechanical inclusions	SF RK I, v. 1, 2.9.20	Mechanical inclusions should be absent.
Sodium chloride	Direct titration	8 to 10 mg
Radionuclide impurities	Gamma spectrometry	The content of gamma-emitting radionuclide impurities should not exceed a total of 0.1% of total radioactivity.
Radiochemical purity	Chromatography on paper (SP RK I, vol. 1, 2.9.26)	Minimum 95%
Residual Solvents	Gas chromatography (SP RK I, vol. 1, 2.2.28)	Ethanol content should be maximum 50 mg/V
Sterility	Direct culture inoculation (SP RK I, v. 2, 2.6.1)	Sterile
Bacterial endotoxins	Turbidimetric kinetic method (SP RK I, v. 1, 2.6.14)	Should not exceed 175/V ME/ml

Results and discussion

Visual analysis methods

If the Pharmacopoeia monographs for radiopharmaceuticals do not specify the test methods, the tests such as transparency, chromaticity and mechanical inclusions are included and mandatory.

In the developed radiopharmaceutical ^{177}Lu -DOTAELA, there should be no mechanical im-

purities, and it should also be transparent and colorless.

Identity (radionuclidic and radiochemical)

In most cases, the radionuclide and radiochemical identification test is the same test as that for determining the radionuclide and radiochemical purity. In turn, radionuclide identification can be confirmed either by obtaining the gamma spectrum or by measuring the half-life of the product [7].

The half-life measurement can be performed by measuring the same test solution at 2 or more time points. The half-life is calculated using the half-life equation. The SP RK does not specify the time interval between each measurement, but it should be long enough for half-life estimation.

In the SP RK, there are no guidelines for determining radiochemical identification, and according to BP, it can be determined by HPLC or planar chromatography. The planar chromatography method is easy to reproduce, and it is as accurate and reliable as HPLC. However, planar chromatography may require longer time. It should be noted that the results of planar chromatography may vary depending on different grades of plates, chromatographic paper. It is therefore important to use the same grade and freshly prepared mobile phase, if possible. In case when the number of theoretical plates changes with a new batch number (from the same grade), the Rf values shall be confirmed according to the validation process.

Thus, for the tested preparation ^{177}Lu -DOTAELA, the gamma spectrum of ^{177}Lu of the test solution should have a characteristic line with the energy of 0.113 and 0.208 MeV, and the relative retention time of ^{177}Lu -DOTAELA on the chromatogram, obtained by the HPLC method, should differ by maximum 3% from the retention time of the non-radioactive Lu-DOTAELA complex.

pH

The pH of the injection solutions should be as close to the physiological pH as possible. Some laboratories use pH paper to determine the pH of the tested solution, while others use pH meters. It should be noted that the pH indicator paper should be checked using the standard buffer solutions, showing the color change for each pH unit, and the pH value, measured with the pH paper, is approximate.

Residual solvent

Determination of residual solvents is always based on the technological scheme of the drug preparation process. In case of ^{177}Lu -DOTAELA at the purification stage, ethanol is used in the product elution and preconditioning of the Sep-Pak C18 cartridge. Typically, radiopharmaceutical monographs do not specify a method for determining the residual solvents, although the description implies that gas chromatography should be used. The flame-ionization detector is used to determine the residual solvents. Analysis for residual solvents takes only few minutes and 4 minutes for measuring ethanol in ^{177}Lu -DOTAELA. Many laboratories accept ethanol limits of 0.05% or 5 mg/ml, as required by the Pharmacopoeia.

Radionuclidic purity

Radionuclide impurities can form during the production and decay of the radionuclide. Potential radionuclide impurities may be indicated in monographs, and their characteristics are given in General Section 5.7, Table of physical characteristics of radionuclides, mentioned in the European Pharmacopoeia.

In most cases, to establish the radionuclide purity of a radiopharmaceutical, it is necessary to determine the authenticity of each available radionuclide and its radioactivity. Typically, the most common method of evaluation of gamma and X-ray emitters radionuclide purity is gamma-spectrometry. The content of gamma-emitting radionuclide impurities in ^{177}Lu -DOTAELA in total should not exceed 0.1% of total radioactivity. Due to the fact that the build-up of ^{177}Lu is made by "direct" method, which is accompanied by formation of the long-lived isomer $^{177\text{m}}\text{Lu}$ ($T_{1/2} = 160$ days). In order to reduce the radiation load for the patient and reduce waste activity, the content of $^{177\text{m}}\text{Lu}$ in the final product is limited.

Sterility

Sterility should be tested by incubating the tested sample for 14 days at 25 and 37 °C. US FDA recommends the use of a temporary "window" for the analysis of radiopharmaceuticals for sterility, since greater activity in the hours after synthesis can lead to false results. In many cases, the 24-hour window may not be sufficient. Some enterprises send their samples to other microbiological laboratories for sterility testing. The manufacturers shall establish their own protocols in this case.

Bacterial endotoxins

The most common technique for determining the bacterial endotoxins is gel thrombin method, which requires application of amoebocyte lysate (*Limulus*). When lysate is added to the solution containing bacterial endotoxins, turbidity, precipitation or gelation of the mixture occurs. The analysis usually takes from 25 to 60 minutes.

Spectrophotometric methods are also used to determine the level of bacterial endotoxins. This method is based on changing the color of the substrate due to formation of an enzyme that results from the interaction of endotoxins and lysate. The proenzyme is activated by gram-negative bacterial endotoxins in the lysate, and the concentration of bacterial endotoxins affects the duration of this activation reaction. The cleavage of substrates is activated by a proenzyme, which acts as an enzyme. As a result, there is a change in color of the substrate, which is detected by the spectrophotometric method. The time taken

before the appearance of color change is inversely proportional to the concentration of endotoxin. The endotoxin concentration can be determined by extrapolating the sample reaction time to a standard curve based on the standards containing the known concentrations of endotoxin [8, 9].

The appearance of turbidity by the method of gel-thrombus in the sample can also be the indicator of endotoxins concentration, which is using spectrophotometry. The time of turbidity appearance is inversely proportional to the concentration of endotoxins. The value of endotoxin can be determined by extrapolating the reaction time of the sample to a standard curve constructed using the standards with the known endotoxin concentrations [10]. The appearance of turbidity may be influenced by the presence of polysaccharides such as beta-glucans. Currently, proper methods are being developed to reduce such impacts [11].

Conclusion

Recently, there has been a great interest in development of new radiopharmaceuticals for diagnosis and therapy. Availability of new radiopharmaceuticals and the regulatory framework for application and approval of new medicines creates a new vector for development of nuclear medicine. Synthesis, quality control and production regulation of radiopharmaceuticals such as ^{18}F -FDG, ^{177}Lu -DOTATATE can become the models in development of new radiopharmaceuticals. Volume 3 of the State Pharmacopoeia of Kazakhstan contains some monographs of radiopharmaceuticals, which indicates a positive trend of harmonization with the European Pharmacopoeia. This article provides a brief overview of the quality control of ^{177}Lu -DOTAELA and for those interested in the development of radiopharmaceuticals. However, this article provides only an overview. The interested readers are encouraged to search for more information.

Acknowledgments

The authors sincerely express their gratitude for the support provided to the University of Oslo, Oslo,

Norway, providing DOTAELA substance throughout the course of the work.

The works were carried out under support of G.2018 [No. AP05134384].

References

1. Mazen Jamous, Uwe Haberkorn and Walter Mier. (2013). Synthesis of Peptide Radiopharmaceuticals for the Therapy and Diagnosis of Tumor Diseases. *Molecules*, 3379-3409
2. State Pharmacopoeia of the Republic of Kazakhstan, Volume 3, "Zhibek Zholy" Almaty (2014).
3. The United States Pharmacopoeia, 25th ed, and The National Formulary, 20th ed. Rockville, MD: United States Pharmacopoeia Convention Inc, 2002: 752-3.
4. Monographs: Radiopharmaceutical preparation. British Pharmacopoeia 2000. London: British Pharmacopoeia Commission, 2000.
5. European Pharmacopoeia. 4 edition. Strasbourg, France: European Directorate for the Quality of the Medicines, 2002: 1361-8.
6. Quality control in the production of radiopharmaceuticals / International Atomic Energy Agency. Vienna: International Atomic Energy Agency, 2018. | Series: IAEA TECDOC; no. 1856
7. Hung JC. Comparison of various requirements of the quality assurance procedures for (18) F-FDG injection. *J Nucl Med* 2002; 43 (11): 1495-506.
8. Iwanaga S, Morita T, Harada T, et al. Chromogenic substrates for horseshoe crab clotting enzyme. Its application for the assay of bacterial endotoxins. *Haemostasis* 1978; 7 (2-3): 183-8.
9. Roth RI, Levin J, Behr S. A modified Limulus amoebocyte lysate test with increased sensitivity for detection of bacterial endotoxin. *J Lab Clin Med* 1989; 114 (3): 306-11.
10. Yokota M, Kambayashi J, Tanaka T, et al. A simple turbidimetric time assay of the endotoxin in plasma. *J Biochem Biophys Methods* 1989; 18 (2): 97-104.
11. Kambayashi J, Yokota M, Sakon M, et al. A novel endotoxin specific assay by turbidimetry with Limulus amoebocyte lysate containing beta-glucan. *J Biochem Biophys Methods* 1991; 22 (2): 93-100

¹*Sh. Nazarkulova , ¹M. Burkitbayev ,
¹N. Nursapina , ²O. Mokhodoeva 

¹al-Farabi Kazakh National University, al-Farabi av., 71, Almaty, Kazakhstan

²Vernadsky Institute of Geochemistry and Analytical Chemistry, Russian Academy of Sciences, Moscow, Russia
e-mail: Sholpan.Nazarkulova@kaznu.kz

Species of uranium of the Kamyshanovskoe deposit (Kyrgyzstan)

Abstract: On the territory of Southern Kazakhstan and its adjacent territory of Kyrgyzstan, there is a unique world-wide Betpakdala-Shu-Ili Province, where up to 15% of the world uranium reserves are concentrated. Technological work on the extraction and processing of uranium ores in these deposits began in the middle of the last century, while until the mid-80s mining was carried out by mining in mines and open pits, and from the mid-80s the method of sulfuric acid leaching was used.

Object of this investigation is Kamyshanovskoe uranium deposit, which is located on the territory of Republic of Kyrgyzstan (about 22 km of its capital – Bishkek city). The natural gamma-emitted radionuclides were determined by gamma-spectrometry measurements (“Ortec” HPGe detector) in a core sample collected from the Kamyshanovskoe uranium peat deposit (0-37 cm depth). The results show U isotopes concentration peak at 12 cm, while the concentrations of its progenies are roughly constant down the profile. Thermo-gravimetry analysis (NETZSCH STA 449 F3A-0372-M) showed, the main part of potentially mobile phases (organic matter, clay and carbonates) was located at the surface.

Solid speciation of uranium has been examined in peat samples collected at the Kamyshanovskoe deposit using sequential extraction. Sequential extraction was carried out using the protocol employed by A. Tessier and et al. In all filtrates natural uranium isotopes were measured by a high resolution alpha-spectrometer (“Alpha-analyst”, Canberra) after appropriate radiochemical preparation, consisting of extraction by 30% tributyl phosphate in toluene and electrodeposition on a steel disk with a mixture of 25% solution of ammonium chloride and saturated solution of ammonium acetate as electrolyte solution. Sequential extraction of peat samples clearly showed that most of uranium is in reversibly bound fractions obtained by treatment with ammonium acetate, hydroxylamine with hydrochloric acid and distilled water, indicating high mobilization potential of uranium in this peat.

Key word: uranium isotopes, peat, Kamyshanovskoe deposit, species of uranium isotopes, sequential extraction, thermo-gravimetry analysis

Introduction

The territories of Southern Kazakhstan and adjacent territory of Kyrgyzstan are known as unique uranium provinces. Different sources of uranium are concentrated here. Uranium-238 and its decay products, due to potential toxicity, became important theme in environmental investigations [1].

Nowadays the determination of total content of radionuclides became less informative in comparison with data of chemical compounds, which radionuclides are involved in; as hazard of radionuclides depend on their bioavailability and eco-toxicity, which are in strong depend from their chemical forms, or

speciation [2]. It is possible to name several interactions, controlling mobilization of uranium in solution. Among them are dissolution, complex formation, and desorption-sorption at the water-rock interface [3-4].

This paper focuses primarily on determination of species of uranium isotopes of the Kamyshanovskoe deposit. In this study, solid speciation of uranium has been examined in peat samples collected at the Kamyshanovskoe deposit using sequential extraction. Sequential extraction was carried out using the protocol employed by A. Tessier and et al. (1979). The obtained data will give basis for prediction of behaviour of uranium isotopes in environment depending on changing conditions.

Materials and methods

2.1 Object description

On the territory of Southern Kazakhstan and its adjacent territory of Kyrgyzstan, there is a unique world-wide Betpakdala-Shu-Ili Province, where up to 15% of the world uranium reserves are concentrated. Technological work on the extraction and processing of uranium ores in these deposits began in

the middle of the last century, while until the mid-80s mining was carried out by mining in mines and open pits, and from the mid-80s the method of sulfuric acid leaching was used.

Object of this investigation is Kamyshanovskoe uranium deposit. This uranium peat deposit is located on the territory of Republic of Kyrgyzstan and about 22 km of its capital – Bishkek city. Figure 1 presents the map of the investigated area.



Figure 1 – Location of the Kamyshanovskoe uranium deposit.

The deposit was formed as a result of ground and surface water filtration through peat-bearing materials of Kendyktas mountains following uranium sorption onto organic-rich minerals. The area (1.5 km²) of Kamyshanovskoe deposit is flat and covered by canes.

The adjacent territory is strongly applied by agriculture. Agricultural techniques can be an additional reason of uranium release to solution [5]. One of the biggest rivers of the region, Shu river, is located close to the deposit. Hence, uranium isotopes and decay products can migrate on long distances.

2.2 Sampling and sample pre-treatment

The core was collected by manually driving polyvinylchloride (PVC) tubes, with a diameter of 10 cm, into the peat. The core was promptly transferred to the laboratory. Then, the core was sectioned at 1 cm intervals. The slices were dried at ambient temperature, sieved through 1 mm sieve and homogenized.

2.3 Gamma-ray spectrometry

Gamma-ray spectrometry was done for investigation of uranium-series radionuclides, such as U-238 (measured via ²³⁴Th), Ra-226, Pb-210. The slices were sealed to obtain equilibrium of ²²⁶Ra with its proge-

nies to determine their activities by gamma spectrometry. The gamma spectrometric measurements were done by an “Ortec” HPGe detector and the spectra were analysed by “GammaVision-32” programme.

2.4 Thermo-gravimetry analysis

The thermo-gravimetry analysis was done for determination of content of moisture, organic matter, water in clay materials, carbonate dioxide of carbonates. The determination was done by NETZSCH STA 449 F3A-0372-M and analysed by NETZSCH Proteus programme. The determination is based on destruction of main soil components under different temperatures and measuring of mass changing (Table 1) [6].

Table 1 – The temperatures of thermo-gravimetry analysis

Step	Temperature	Component
1	105	moisture
2	350	organic matter
3	600	water of clay materials
4	850	carbon dioxide of carbonates

2.5 Sequential extraction

Uranium speciation in soils was determined by sequential extractions [7]. The analytical procedure

is used for the sequential chemical extractions partitioning uranium into seven fractions is presented in Table 2.

Table 2 – The reactants and conditions of sequential extractions

Step	Soil fractions	Corresponding minerals	Used reactant	Procedure
1.	Water soluble	-	MilliQ-water	Shaken for 2 h; centrifuged at 5000 rpm for 30 min
2.	Exchangeable	-	1M NH ₄ Ac (pH 8.2)	Shaken for 2 h; centrifuged at 5000 rpm for 30 min
3.	Bound to carbonates	Carbonates (calcite, etc.)	1M NH ₄ Ac (pH 5.0)	Shaken for 2 h; centrifuged at 5000 rpm for 30 min
4.	Bound to Fe-/Mn-oxides	Oxides of iron and manganese (goethite, hematite, perrolusite)	0.04M NH ₂ OH·HCl in 25% (v/v) HOAc	85 °C; shaken for 5 h; centrifuged at 5000 rpm for 30 min
5.	Bound to organic matter	Organic substances (humus, etc.)	0.02 M HNO ₃ and 30% H ₂ O ₂	85 °C; pH 2 shaken for 5 h; centrifuged at 5000 rpm for 30 min
6.	Strongly bound	Clay minerals (chlorite, kaolinite, etc.)	7 M HNO ₃	85 °C; pH 2 shaken for 6h; centrifuged at 5000 rpm for 30 min
7.	Residual	Terrigenous minerals (quartz, spar, mica)	HF-HClO ₄	Decompose

The procedure was done with samples of 1.0-1.5 g of initial weight and after each extraction step, samples were centrifuged for 25 minutes at 5000 rpm and supernatants were filtered (0.45 μm). The ratio of solid:liquid was 1:20.

2.6 Alpha-particle spectrometry

In all filtrates natural uranium isotopes were measured by a high resolution alpha-spectrometer (“Alpha-analyst”, Canberra) after appropriate radiochemical preparation, consisting of co-precipitation of radionuclides with iron hydroxide, extraction by

30% tributyl phosphate (TBP) in toluene and electro-deposition on a steel disk with a mixture of 25% solution of NH₄Cl and saturated solution of (NH₄)₂C₂O₄ as electrolyte solution [8].

Results and discussion

3.1 Concentrations of gamma-emitting radionuclides

The concentration of profiles of ²³⁸U, ²²⁶Ra, ²²⁸Ra, ²²⁸Th, ²¹⁰Pb and ⁴⁰K are shown in Figure 2.

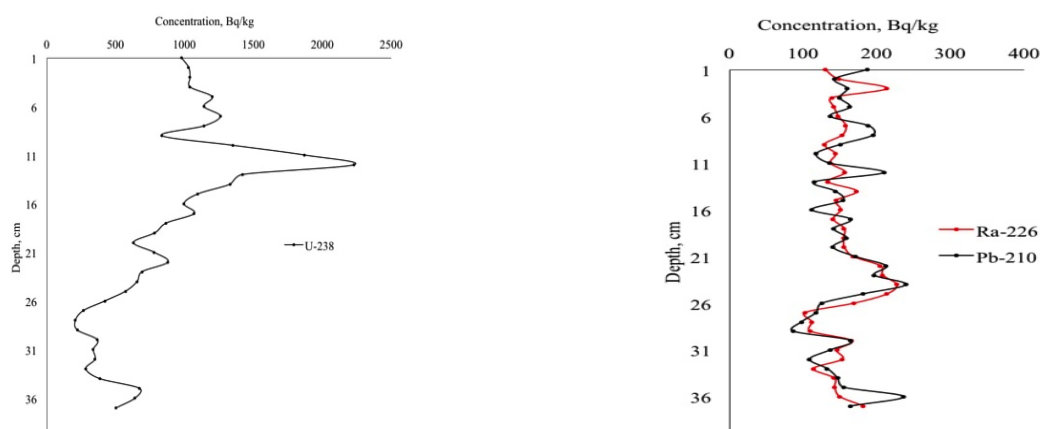


Figure 2 – The uranium series radionuclide’s specific activity profiles (Bq kg⁻¹, dry weight) in peat core.

Concentrations of ^{226}Ra and ^{210}Pb are roughly constant with two small peaks found at 3 cm and 27 cm. By contrast, the ^{238}U profile showed a rather constant value down to about 8 cm and then a considerable increase with a maximum at 12 cm. This suggests that uranium migrated

down the core with surface waters and accumulated in the depth where the maximum was observed.

3.2 Results of thermo-gravimetry analysis

Thermograms of selected core slice samples are presented at the Figure 3.

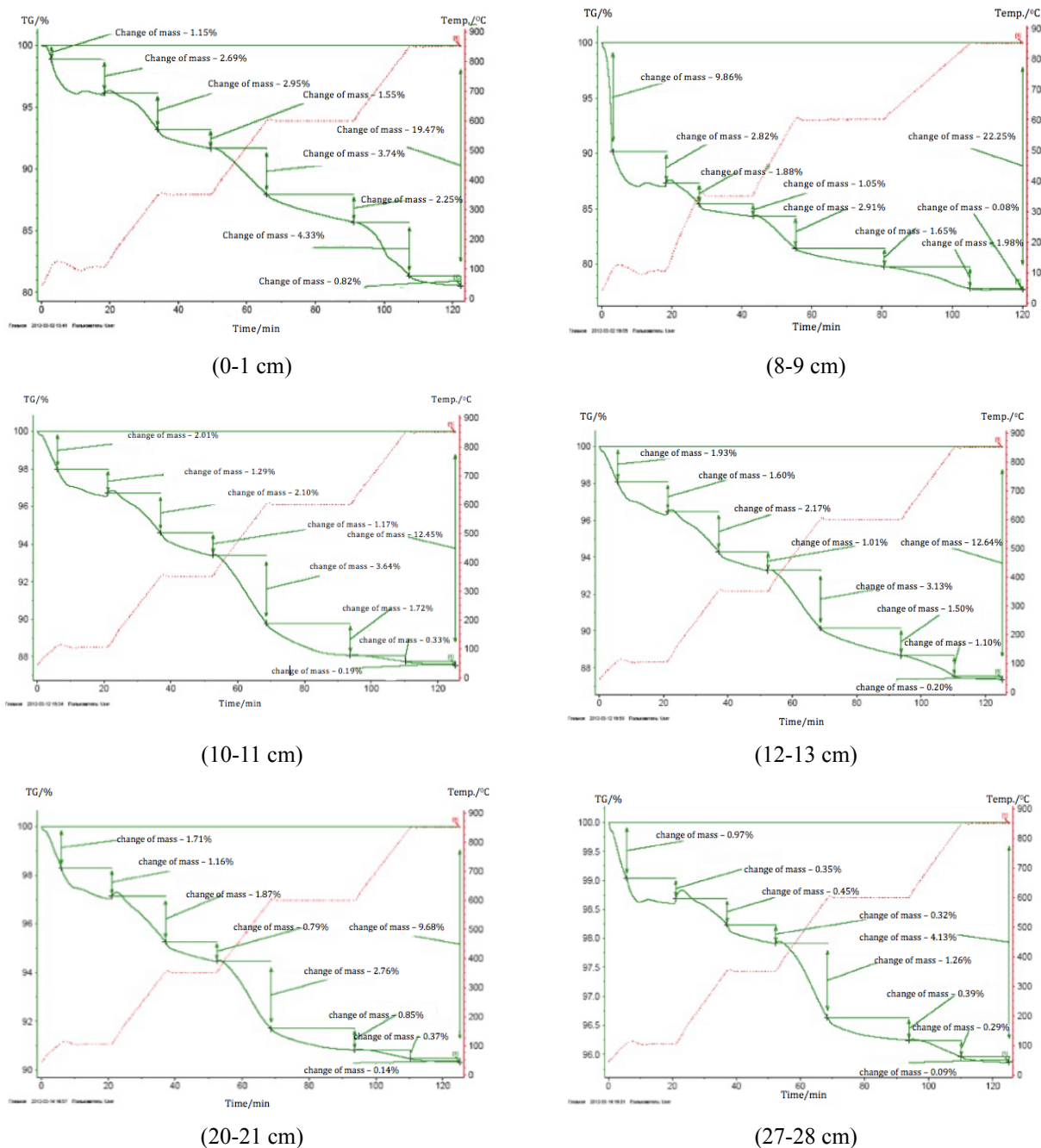


Figure 3 – The thermo-gravimetry analysis of core profiles

The results of thermo-gravimetry analysis showed the decreasing of organic matter down the investigated profiles with maximum amount of organic matter (20.2

mg/g) at the surface (0-1 cm depth). At the depth 8-12 cm, 19-20 and 27-28 cm the concentration of organic matter is 14, 11.8 and 3.1 mg/g, respectively (Table 2).

Table 2 – The results of thermo-gravimetry analysis of the core.

Depth, (cm)	Moisture, (%)	Organic matter,		Clay, (%)	Carbonates, (%)	Total loss of mass, (%)
		(%)	mg/g			
0-1	3.84	4.5	20.21	5.99	5.15	19.47
8-9	12.68	2.94	13.06	4.56	2.06	22.24
10-11	3.3	3.27	14.6	5.36	0.52	12.45
12-13	3.53	3.18	14.16	4.63	1.3	12.64
20-21	2.87	2.66	11.8	3.64	1.23	9.68
27-28	2.09	0.77	3.13	1.67	0.38	4.13

According to results of thermo-gravimetry analysis, the main part of potentially mobile phases (organic matter, clay and carbonates) are located at the surface.

Radionuclides bound to solid samples (soil, peat materials, rock and other) can be desorbed to the liquid phase by changes in soil pH, temperature or oxidation-reduction potential, as well as by the decomposition of soil organic matter, leaching processes, etc. Moreover, the biological availability of metals also depends on the genesis (i.e., source spe-

cific characteristics) of the fallout or contamination involved.

3.3 Uranium speciation

The sequential extraction results obtained for the Kamyshanovskoe peat deposit, given in Figure 4, clearly show that most of uranium is in the reversibly bound fractions (in form of carbonates, bound with oxides of iron and manganese and organic fraction), obtained by treatment with NH_4Ac , $\text{NH}_2\text{OH}\cdot\text{HCl}$ and H_2O_2 , indicating high mobilization potential of uranium in this peat.

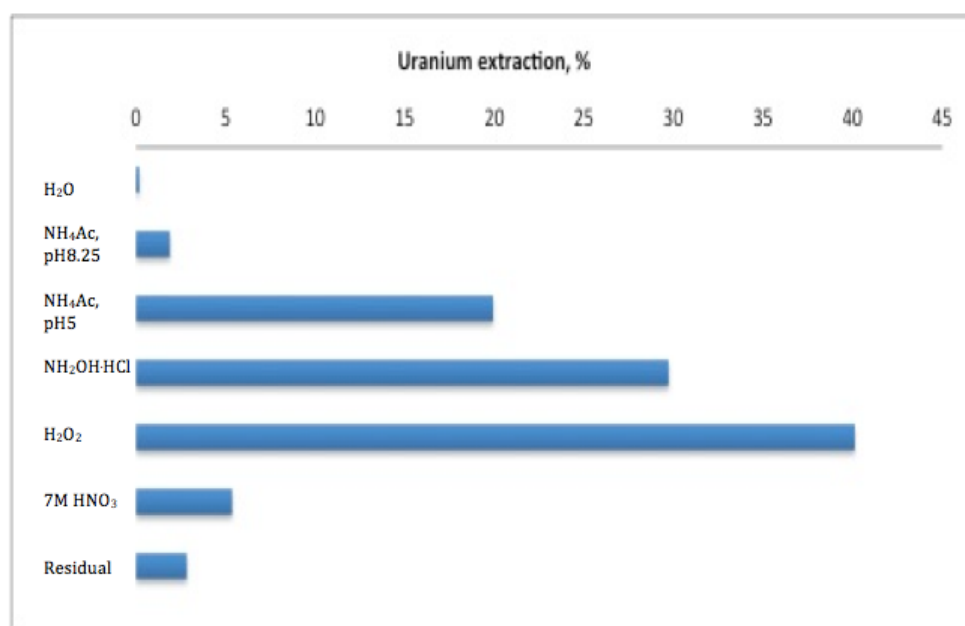


Figure 4 – The partitioning of uranium in soils from Kamyshanovskoe deposit upon sequential extraction analysis

Conclusion

The obtained results of analysing of peat core from the Kamyshanovskoe uranium deposit show a significant variation of uranium series concentrations with depth. The concentrations of main elements are higher than mainly for this region. The uranium concentration in the peat is an order of magnitude higher than the corresponding values of its progenies (^{226}Ra , ^{210}Pb). The highest concentration of ^{238}U was obtained at the at the depth of 12 cm.

Thermo-gravimetry analysis showed, that the main part of potentially mobile phases (organic matter, clay and carbonates) were located at the surface.

Data on the solid partitioning of uranium in peat from the Kamyshanovskoe deposit reveal that about 90 % of uranium was found in potentially mobile forms, indicating potential mobility and availability for plant and other organism uptake.

Acknowledgement

This work was funded under the International Science and Technology Center (ISTC) project (ChuRad Project, Contract K-1474).

References

1. Steffanowski J, Banning A (2017) Uraniferous dolomite: a natural source of high groundwater uranium concentrations in northern Bavaria, Germany. *Environ. Earth. Sci.* 76:508
2. Perez-Moreno SM, Gazquez MJ, Perez-Lopez R, Bolivar JP (2018) Validation of the BCR sequential extraction procedure for natural radionuclides. *Chemosphere* 198:397-408.
3. Liu B, Peng T, Sun H, Yue H (2017) Release behavior of uranium in uranium mill tailings under environmental conditions. *Journal of Environmental Radioactivity* 171:160-168.
4. Tricca A, Porcelli D, Wasserburg GJ (2000) Factors controlling the groundwater transport of U, Th, Ra, and Rn. *J. Earth Syst. Sci.* 109: 95-108.
5. Banning A, Pawletko N, Röder J, Kübec C, Wisotzky F (2017) Ex situ groundwater treatment triggering the mobilization of geogenic uranium from aquifer sediments. *Science of the Total Environment* 587:371–380
6. Alvarado JS, Neal TJ, Smith LL, Erickson MD (1996) Microwave dissolution of plant tissue and the subsequent determination of trace lanthanide and actinide elements by inductively coupled plasma-mass spectrometry. *Analytical Chemica Acta* 322:11-20.
7. Tessier A, Campbell PGC, Bisson M (1979) Sequential extraction procedure for the speciation of particulate trace metals. *Analytical Chemistry* 51 (7):844-85.
8. Burkitbayev M, Uralbekov B, Nazarkulova Sh, Matveyeva I, Vintro LL (2012) Uranium series radionuclides in surface waters from the Shu river (Kazakhstan). *J. Environ. Monit.* 14:1190-1195.

¹A.K. Bopi , ¹A.A. Kudaibergen , ¹M.A. Dyusebaeva , ²Y. Feng , ^{1*}J. Jenis 

¹ Al-Farabi Kazakh National University, Faculty

of Chemistry and Chemical Technology, al-Farabi ave. 71, Almaty, Kazakhstan

²Griffith Institute for Drug Discovery, Griffith university, QLD 4111, Brisbane, Australia

*e-mail: janarjenis@mail.ru

Chemical composition of hexane and chloroform extracts from *Artemisia scopaeformis*

Abstract: Research in the field of medicinal products, especially medicinal plants, has been constantly expanding recently. However, to date, health research has not been widely disseminated. This article focus on the analysis of hexane and chloroform extracts of *Artemisia scopaeformis* by Gas Chromatography and Mass Spectroscopy (GC-MS) technique. Detailed chemical constituents of *A. scopaeformis* collected in Kazakhstan were investigated for the first time. The quantitative and qualitative analysis of bioactive constituents of the medicinal plant have been made. *A. scopaeformis* hexane extract contained 4 compounds: methyleugenol (33.87%), hexadecanoic acid, ethyl ester (41.02%), butyl 4,7,10,13,16,19-docosahexaenoate (11.55%), hexasiloxane, 1,1,3,3,5,5,7,7,9,9,11,11-dodecamethyl- (13.56%). The chloroform extract of *A. scopaeformis* contained 5 compounds: fluorene, 2,7-bis(1-hydroxyethyl)- (24.28%), p-dimethylaminobenzylidene p-anisidine (14.59%), 3-acetoxy-5-methyl-2-nitro- terephthalic acid, 4-isopropyl ester 1-methyl ester (11.74%), 3,4-diacetyl-2-methyl-4H-thieno [3,2-b] pyrrole-5-carboxylic acid, methyl ester (17.35%), 4H-1,2,4-triazole-3-thiol, 4-(2-fluorophenyl)-5-(1-methylethyl) – (32.04%). The resulting compounds have significant biological properties: antimicrobial, antioxidant, anti-inflammatory.

Key words: *Artemisia scopaeformis*, GC-MS, hexane, chloroform, bioactive constituents, extract.

Introduction

Currently, there is a tendency in the world to increase interest in consuming a wide range of phytochemicals based on environmentally friendly plant materials. In recent decades, there has been an increase in their use not only in the countries of Asia and Africa, where they have been traditionally used for many centuries, but also in Europe, the USA and other countries of the world community. At the same time, not only medicinal plants and fees, but also various galenical and newgalenic preparations, individual biologically active compounds isolated from plants are used as herbal medicines [1]. A report from the World Health Organization disclosed that almost 80% of the world's population relies on nonconventional drug-treatment, particularly of herb, in their primary healthcare [2]. However, despite significant progress is being made in the disclosure of the chemical composition and bioactivities of herbal medicines, their exact biological functions and regulation mechanisms largely remain to be clarified. Medicinal plants with the ancient history of human

use have been considered one of the important and reliable sources to discover promising therapeutic agents in a number of cases, including cancer chemopreventive drugs [3-5].

The *Asteraceae* family includes over 24,000 species, combined in about 1,200 genera. 224 genera and more than 3,500 species grow in the CIS, more than 140 genera and about 790 species of the family are found in the flora of Kazakhstan. The rich chemical composition of the family determines their use as insecticidal and medicinal sources. The genus *Artemisia* unites over 500 species, distributed mainly in the temperate zone of the northern hemisphere. Wormwood species are most often found in the steppes, others grow in semi-deserts and deserts [6-8]. It is known that the pharmacological properties of plants of the genus *Artemisia* are associated with the content of essential oils, terpenoids, flavonoids, coumarins, caffeoylquinic acids and sesquiterpene lactones in them. At the same time, of particular interest are phenolic compounds, in particular flavonoids with a wide spectrum of biological activity [9, 10]. In practical medicine, *Artemisia* species are often used to treat

diseases of the gastrointestinal tract, as a choleric, laxative, diuretic, anti-inflammatory, wound healing [11]. In traditional medicine – as an anti-cancer, anti-inflammatory, wound healing, sedative, choleric, metabolic regulating, diaphoretic, detoxification, bacteriological and fungistatic, antiviral, protistocidal, anthelmintic; with pulmonary tuberculosis and lymph nodes [12]. Currently, sesquiterpene lactones are considered as a promising source of new drugs due to the possibility of easy cultivation of these plants and a high content of lactones in a number of plant species. According to their physicochemical properties, mono – and sesquiterpenes belong to the group of essential oils that have been studied in more detail by the example of *A. princeps*. Unfortunately, to date, drugs based on sesquiterpene lactones produced by pharmaceuticals are insignificant. Some interesting sesquiterpenes lactones including effective antimalarial principle – artemisinin were identified in dichloromethane, chloroform and methanol extracts of perennial herb *A. herba alba*. *Artemisia annua* L. is the main raw material for artemisinin. Medicines based on artemisinin and its derivatives are widely used as new treatments for malaria – a disease that takes at least a million lives annually. It is also important that artemisinin and related compounds showed cytotoxic activity, which allows them to be used in anti-cancer therapy. In addition to artemisinin, *A. annua* is appreciated for the essential oil, which is used in perfumes and cosmetics. The antibacterial effect of essential oils is due to the presence of oxygen-containing compounds (camphor, various acids). Essential oil contains a large number of components of biological value, such as artemisia ketone, 1,8-cineole, borneol, etc. [13]. One of the promising types for use in medical practice is Pontian wormwood (*Artemisia pontica* L.), the essential oil of which has a pronounced anti-inflammatory, wound healing, analgesic effect. Total complexes from *A. absinthium* have an antitoxic effect (in case of mercuric chloride poisoning); exhibit antibacterial, antifungal, antiviral and protistocidal activity. All of the above types of wormwood, being essential oil crops, find their application in various areas of human activity, and most often in cooking, the production of alcoholic and soft drinks, medical supplies and dosage forms. In this regard, wormwood is without exaggeration one of the most studied medicinal plants. [14].

Based on the foregoing, a research of the chemical composition of representatives of the genus *Artemisia*, growing in Kazakhstan, seems to be an urgent task.

Artemisia scopaeformis is an endemic plant that grows in the desert zone on clay and sandy soils, along the margins of meadow. In Kazakhstan, it grows in the Chu-Ili Mountains and Karatau [15]. In our study, constituents in the hexane and chloroform parts of the medicinal plant *Artemisia scopaeformis*, which were grown in the Almaty region of Kazakhstan, were first identified by GC-MS. Over the past 15–20 years in the field of pharmacognosy, qualitative changes have occurred in the technical capabilities of studying the chemical composition of medicinal plants and herbal remedies. This was facilitated by the enrichment of this science with modern spectral and other physicochemical methods. GC-MS method can provide accurate results. It gives a high degree of specificity, good sensitivity and permits the simultaneous determination of a wide range of compounds from phenolic compounds to terpenes in complex matrices. It provides complementary data to LC-MS analysis comprising small polar chemicals such as organic acids, sugars, amino acids, sugar alcohols and many more. GC-MS results can also be recommended for rapid screening of the chemical composition of the main groups of biologically active substances of plant materials used in the development and creation of new herbal medicines [16].

Materials and methods

Plant material. The aerial part of *Artemisia scopaeformis* was collected in Almaty region of Kazakhstan, in 2018. The air dried aerial parts of plant *A. scopaeformis* were cut into small pieces and preserved at room temperature.

Extraction and isolation. The air-dried aerial parts of *A. scopaeformis* (100 g) were pulverised then extracted with 70% ethyl alcohol (1:1) three times (seven days each time) at room temperature. After evaporation of the solvent under reduced pressure, the residues were mixed and suspended in water and then successively partitioned with hexane and chloroform to afford the corresponding extracts. The obtained hexane and chloroform extracts were analyzed by GC-MS method.

Experimental part. The constituents from hexane and chloroform extracts of the medicinal plant were analyzed by using GC-MS method. GC-MS analysis was performed on Agilent 7890A-5975C GC-MS (Gas Chromatograph coupled to Mass Spectrometer) with a HP-5MS fused silica capillary column (30m x 2.5mm; 0.25 µm film thickness). Helium (99.999%) was used as a carrier gas, the column temperature was flashed from 50°C (held for 10min) to 300°C

at 10°C/min. The latter temperature maintained for 40 min. The injector temperature was 310°C. Injection volume was 1µl with the split ratio 5:1. Mass spectra: electron impact (EI+) mode, 70 eV. Mass spectra were recorded over scan range 30-1000 a.m.u.

Identification of the compounds: Interpretation on mass spectrum GC-MS was carried out using the database of National Institute Standard and Technology (NIST) having more than 62,000 patterns. The spectrum of the unknown component was compared with the spectrum of the known components existed in the NIST library. The Name, Molecular weight and Structure of the components of the test materials were ascertained. Percentage composition was computed from GC peak areas on HP-5MS column without applying correction factors.

Results and discussion

The constituents of hexane and chloroform extracts from the aerial parts of *A. scopaeformis* were

analyzed by GC-MS. GC-MS technology is recognized as the “gold standard” in identifying chemicals in simple and complex mixtures. Besides, the technology is able to recognize substances at a trace level that is unattainable with other technologies. This method allows to selectively and with high sensitivity to determine various types of compounds.

GC-MS chromatogram of the hexane extract from aerial part of *Artemisia scopaeformis* (Fig.1) clearly shows 4 peaks indicating the presence of 4 phytochemical compounds. The identification of the resulting phytochemical compounds was based on the peak area, retention time and molecular formula. The active substances with their retention time, molecular formula, molecular weight and concentration (%) are presented in Table 1 and Fig 1. Analysis of the chloroform extract from *A. scopaeformis* revealed 5 compounds in the studied samples (Fig.2). Detailed data of compounds are shown in Table 2. Their relative contents were determined by area normalization.

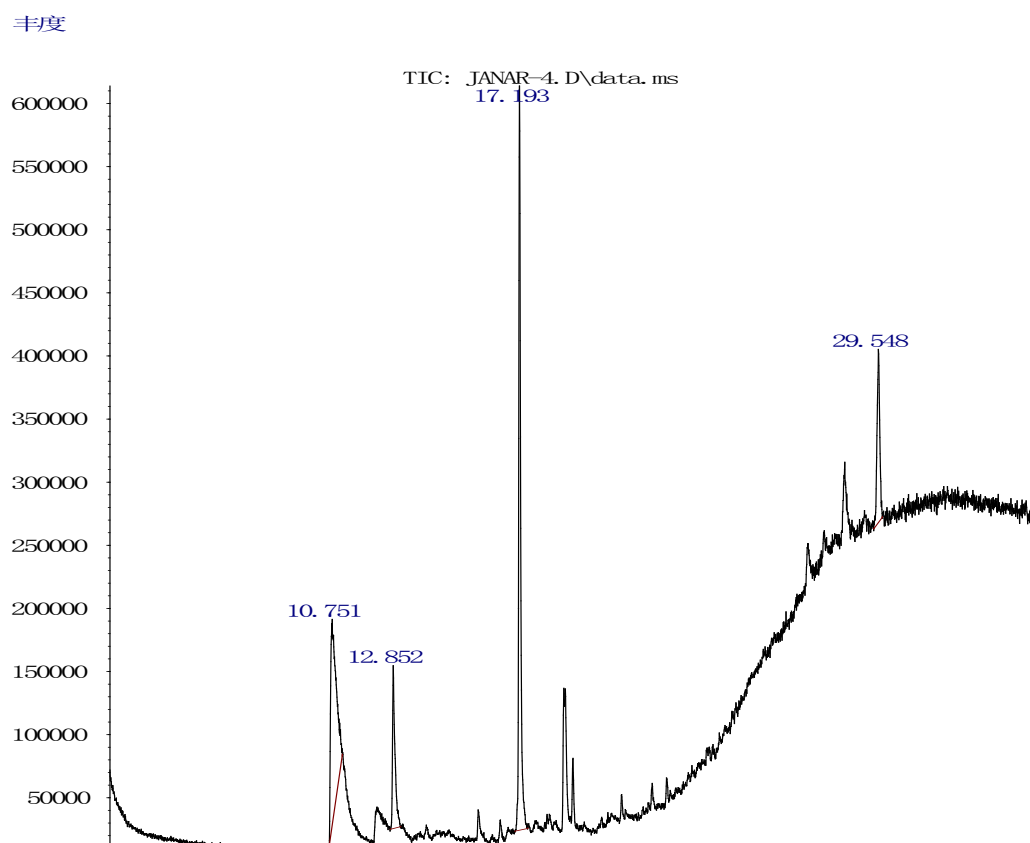


Figure 1 – GC-MS Chromatogram of hexane extract of *Artemisia scopaeformis* plant.

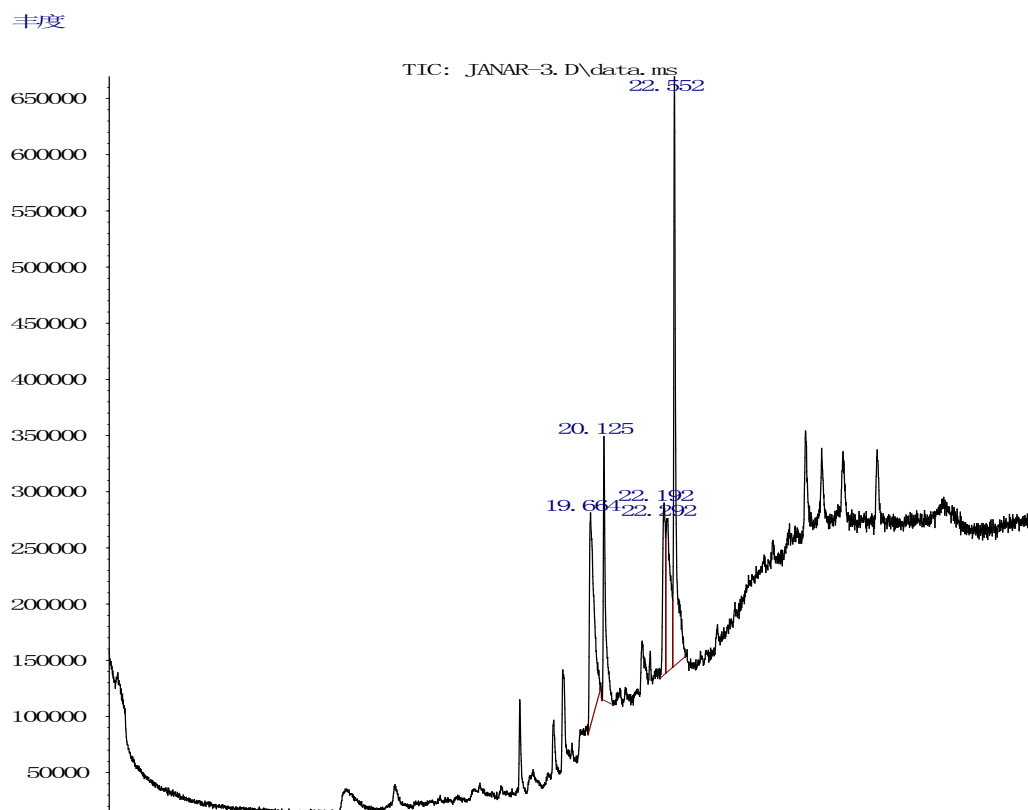
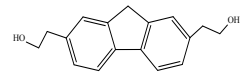
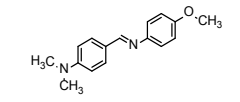
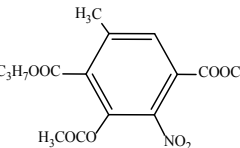
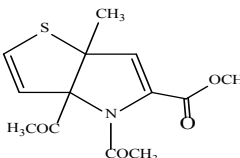
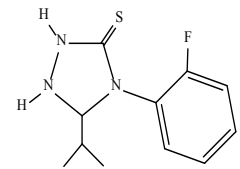


Figure 2 – GC-MS Chromatogram of chloroform extract of *Artemisia scopaeformis* plant

Table 1 – Constituents identified in hexane extract of *Artemisia scopaeformis*.

Peak No	Constituents	t_R (min)	Molecular Formula	Structure	MW	Content (%)
1	Methyleugenol	10.75	$C_{11}H_{14}O_2$		178	33.87
2	Butyl 4,7,10,13,16,19-docosahexanoate	12.857	$C_{26}H_{40}O_2$		384	11.55
3	Hexadecanoic acid, ethyl ester	17.198	$C_{18}H_{36}O_2$		284	41.02
4	Hexasiloxane, 1,1,3,3,5,5,7,7,9,9,11,11-dodeca-methyl-	29.55	$C_{12}H_{38}O_5Si_6$		430	13.56

Table 2 – Constituents identified in chloroform extract of *Artemisia scopaeformis*.

Peak No	Constituents	t _R (min)	Molecular Formula	Structure	MW	Content (%)
1	Fluorene, 2,7-bis(1-hydroxyethyl)-	19.661	C ₁₇ H ₂₀ O ₂		254	24.28
2	p-Dimethylaminobenzylidene p-anisidine	20.128	C ₁₆ H ₁₈ N ₂ O		254	14.59
3	3-Acetoxy-5-methyl-2-nitro-terephthalic acid, 4-isopropyl ester 1-methyl ester	22.193	C ₁₅ H ₁₇ NO ₈		339	11.74
4	3,4-Diacetyl-2-methyl-4H-thieno[3,2-b]pyrrole-5-carboxylic acid, methyl ester	22.295	C ₁₃ H ₁₃ NSO ₄		279	17.35
5	4H-1,2,4-Triazole-3-thiol, 4-(2-fluorophenyl)-5-(1-methylethyl)-	22.55	C ₁₀ H ₁₄ N ₃ SF		237	32.04

The GC-MS analysis of hexane extract revealed the presence of 4 compounds: methyleugenol (33.87%), hexadecanoic acid, ethyl ester (41.02%), butyl 4,7,10,13,16,19-docosahexaenoate (11.55%), hexasiloxane, 1,1,3,3,5,5,7,7,9,9,11,11-dodecamethyl- (13.56%), main contents of them were methyleugenol and hexadecanoic acid, ethyl ester. The principal chemical constituents of chloroform extract were found to be fluorene, 2,7-bis(1-hydroxyethyl)- (24.28%), p-dimethylaminobenzylidene p-anisidine (14.59%), 3-acetoxy-5-methyl-2-nitroterephthalic acid, 4-isopropyl ester 1-methyl ester (11.74%), 3,4-diacetyl-2-methyl-4H-thieno[3,2-b]pyrrole-5-carboxylic acid, methyl ester (17.35%), 4H-1,2,4-triazole-3-thiol, 4-(2-fluorophenyl)-5-(1-methylethyl)- (32.04%). Almost one third (34.13%) of the extract consists of the substance 4H-1,2,4-triazole-3-thiol, 4-(2-fluorophenyl)-5-(1-methylethyl)-.

Identified compounds have been found to possess a wide range of biological activities. Their various activities are also mentioned in Table 3. These properties determine the use of the plant for antimicrobial, antioxidant, anti-inflammatory and pesticidal and

other activities. The major component of hexane extract from *A. scopaeformis*, namely the hexadecanoic acid, ethyl ester (41.02%), have been reported to have antioxidant, hypocholesterolemic, nematocidal, antifungal, hemolytic, flavor, pesticide, lubricant activities [17]. Hexadecanoic acid, ethyl ester is also found in plant extracts from *Artemisia austro-yunnanensis*, *Artemisia frigida* Willd *Carbonisatus* [18]. The other compound, methyleugenol (33.87%) is an aromatic terpene, which is a colorless oily liquid with a faint pleasant odor. This substance is an integral part of many essential oils, such as: citronella, laurel, pink, pine and fennel oils. Citronella oil, unlike most other essential oils, has a rather limited list of beneficial properties. Moreover, its main advantage is the ability to scare away all kinds of insects. Many studies show that the oil has quite good antifungal properties. Methyleugenol refers to insect-attracting substances. A mixture of methyleugenol with parathion and pyrolane are effective in controlling insects. It is also used as a flavouring agent in jellies, baked goods, soft drinks, chewing gum, sweets, puddings, condiments and ice cream. In addition methyleugenol is also being applied as a fragrance ingredient in per-

fumes (0.3–0.8%), creams and lotions (0.01–0.05%), toiletries and detergents (0.02–0.2%). The presence of methyleugenol in the plants of *Artemisia dracunculus L.*, *A. scoparia*, *A. capillaris* was also detected. [19]. Methyleugenol is reported as relaxant, antispasmodic, anesthetic, antinociceptive active principal and can be used as insecticide [20]. Hexasiloxane, 1,1,3,3,5,5,7,7,9,9,11,11-dodecamethyl- (13.56%) is a plasticizer compound, it may be act as an antimicrobial, antiseptic, antifouling drug, hair conditioning agent, skin-conditioning agent-emollient and solvent, whereas p-dimethylaminobenzylidene p-anisidine (14.59%) can be represented as an antihistaminic, analgesic drug [21]. Several studies have attributed the antidiabetic, anti asthma and anticancer activities to butyl 4,7,10,13,16,19-docosahexaenoate (11.55%) shows [22]. It should be noted that 4H-1,2,4-triazole-3-thiol, 4-(2-fluorophenyl)-5-(1-methylethyl)- (32.04%) has antitubercular properties. Its antimicrobial and antioxidant activities have also

been demonstrated. Antioxidants have the ability to stabilize free radicals, which leads to cytoprotection from the harmful effects of free radicals. Antioxidants have the ability to stabilize free radicals, which leads to cytoprotection from the harmful effects of free radicals [23].

Thus, as a result of a qualitative analysis of the aerial parts of the plant *A. scopaeformis*, the presence of the main biologically active substances, which determine the pharmacological effect and nutritional value of the studied plant, was established. It is obvious that the plant contains complexes of antioxidant, antifungal, antimicrobial, and also anti-inflammatory effects. Nowadays, the anti-inflammatory properties of medicinal plants and preparations from them are not widely used, differing, perhaps, with a slightly less pronounced effect, but with better tolerance and less toxicity. In this regard, the search for new effective anti-inflammatory herbal preparations is relevant.

Table 3 – Reported activities of the identified bioactive compounds from *A. scopaeformis*

№	Compound	Activity	References
1	Butyl 4,7,10,13,16,19-docosahexaenoate	Antidiabetic, anti asthma, anticancer, anti heart disease	[22]
2	4H-1,2,4-Triazole-3-thiol, 4-(2-fluorophenyl)-5-(1-methylethyl)-	Antioxidant, antitubercular and antimicrobial	[23]
3	Methyleugenol	Relaxant, antispasmodic, anesthetic, flavouring agent, insecticide, shows antinociceptive effect	[24, 25]
4	Hexadecanoic acid, ethyl ester	Antifungal, antioxidant, aypocholesterolemic nematicide, aesticide, antiandrogenic flavour, hemolytic, 5-Alpha reductase inhibitor, potent antimicrobial activity Antimicrobial, antiseptic, hair conditioning agent, skin-conditioning agent-emollient, solvent	[26]
5	Hexasiloxane, 1,1,3,3,5,5,7,7,9,9,11,11-dodecamethyl-	Antimicrobial, antiseptic, hair conditioning agent, skin-conditioning agent-emollient, solvent	[27]
6	p-Dimethylaminobenzylidene p-anisidine	Analgesic, anti-inflammatory activity	[28]

Conclusion

Thus, using GC-MS, the chemical composition of the plant *Artemisia Scopaeformis*, growing in the Almaty region of Kazakhstan, was first studied. Among this study, there are 4 compounds were identified from hexane extract of *A. scopaeformis*. From chloroform extract of *A. scopaeformis*, 5 compounds were separated. GC-MS analysis is the first step in identifying and understanding the nature of medicinal plants. Isolation of a individual phytochemical constituent and further study of its biological activity will definitely yield fruitful results. It could be con-

cluded that *A. scopaeformis* contains various bioactive compounds. Though, further studies are needed to determine its bioactivity and toxicity profile.

References

1. Kennedy D. O., Wightman E. L. (2011) Herbal extracts and phytochemicals: plant secondary metabolites and the enhancement of human brain function. *Adv. Nutr.*, vol. 2, pp. 32-50.
2. Chan K. (2003) Some aspects of toxic contaminants in herbal medicines. *Chemosphere*, vol. 52(9), pp. 1361-1371.

3. Cragg G. M., Newman D. J. (2009) Nature: a vital source of leads for anticancer drug development. *Phytochem. Rev.*, vol. 8, pp. 313-331.
4. Joshi R. K., Satyal P., Setzer W. N., (2016) Himalayan aromatic medicinal plants: a review of their ethnopharmacology, volatile phytochemistry, and biological activities. *Medicines*, vol. 3, pp. 6-11.
5. Giang P. M., Binh N. T., Matsunami K., Son P. T. (2014) Three new eudesmanes from *Artemisia Japonica*. *Nat. Prod. Res.*, vol. 28, pp. 631-635.
6. Choi E., Park H., Lee J., Kim G., (2013) Anticancer, anti-obesity, and anti-inflammatory activity of *Artemisia* species in vitro. *J. Tradit. Chin. Med.*, vol. 33, pp. 92-97.
7. Brown G. D. (2010) The biosynthesis of artemisinin (Qinghaosu) and the phytochemistry of *Artemisia annua* L. (Qinghao), *Molecules*, vol. 15, pp. 7603-7698.
8. Baitenov M. S. (2001) Flora of Kazakhstan, Almaty: Gylym, vol. 2.
9. Kazakhstan State Pharmacopeia (2008), pp. 592-609.
10. Manzoor A. Rather, Bilal A. Dar, Wajahat A. Shah, Anil Prabhakar, Kushal Bindu, Javid A. Banday, Mushtaq A. Qurishi (2017) Comprehensive GC-FID, GC-MS and FT-IR spectroscopic analysis of the volatile aroma constituents of *Artemisia indica* and *Artemisia vestita* essential oils. *Arabian Journal of Chemistry*, vol. 10, pp. 3756-3780.
11. Muzichkina R.A., Abilov Zh.A., Korulkin D.Yu. (2010) Basics of Chemical Natural Compounds. Almaty.
12. Burasheva G.Sh., Eskalieva B.K., Kipchakbayeva A.K. (2016) Medical plants of Kazakhstan. Almaty.
13. Xu-Dong Zhou, Chen Zhang, Shan He, Bin Zheng, Ke-Wu Zeng, Ming-Bo Zhao, Yong Jiang, Peng-Fei Tu (2017) New terpenoids and thiophene derivatives from the aerial parts of *Artemisia sieversiana*. *Bioorganic & Medicinal Chemistry Letters*, vol. 27, pp. 5441-5445.
14. Sharmila K., Padma P.R. (2013). Anticancer activity of *Artemisia vulgaris* on hepatocellular carcinoma (HepG2) cells. *Int. J. Pharm. Pharm. Sci.*, vol. 5, pp. 479-483.
15. Nysanbaev A (1998) «Kazakhstan» National Encyclopedia, I: 328. Kazakh Encyclopedia reduction, Almaty. ISBN 5- 89800-123-9.
16. Anjali R., Rasika T., Amruta T., Vedavati P., Nirmala D. (2009) GC-MS study of a steam volatile matter from *Mimusops elengi*. *International Journal of Chem Tech Research*, vol.1, pp. 158-61.
17. Jegadeeswari P, Nishanthini A, Muthukumaraswamy S, Mohan VR. (2012) GC-MS analysis of bioactive components of *Aristolochia krysagathra* (Aristolochiaceae). *J Curr Chem Pharm Sci.*, vol. 2, pp. 226-236.
18. Upgade A, Anusha B. (2013) Characterization and medicinal importance of phytoconstituents of *Carica papaya* from down south Indian region using gas chromatography and mass spectroscopy. *Asian J Pharm Clinical Res.*, vol. 6(4), pp. 101-106.
19. Muzychkina R.A., Korulkin D.Yu. (2006) Bio-Active Plant Substances. Extraction, Separation and Analysis, Almaty: Atamura, p. 438.
20. Suparmi S., Junico Ginting A., Siti M., Weseling S. (2019) Levels of methyleugenol and eugenol in instant herbal beverages available on the Indonesian market and related risk assessment. *Food and Chemical Toxicology*, vol. 125, pp. 467-478.
21. Kokate CK, Purohit AP, Gokhale SB. (2001) Carbohydrate and derived Products, drugs containing glycosides, drugs containing tannins, lipids and protein alkaloids. Text book of Pharmacognosy, vol.7, pp. 133-166.
22. Ramasamy M., Balasubramanian U. (2012) Identification of bioactive compounds and antimicrobial activity of marine clam *Anadara granosa* (linn.). *Int. J. of Scie. and Nat.*, vol. 3(2), pp. 263-266.
23. Ozdemir A., Turan-Zitouni G., Asim Kaplancikli Z., Chevallet P. (2007) Synthesis of some 4-arylidenamino-4H-1,2,4- triazole-3-thiols and their antituberculosis activity. *Journal of Enzyme Inhibition and Medicinal Chemistry*, vol. 22(4), pp. 511-516.
24. Sell A.B., Carlini E.A. (1976) Anesthetic Action of Methyleugenol and Other Eugenol Derivatives. *Pharmacology*, vol. 14, pp. 367-377.
25. Yano S., Suzuki Y., Yuzurihara M., Kase Y., Takeda S., Watanabe S., et al. (2006) Antinociceptive effect of methyleugenol on formalin-induced hyperalgesia in mice. *European Journal of Pharmacology*, vol. 553(1-3), pp. 99-103.
26. Ajayi G.O., Olagunju J.A., Ademuyiwa O., Martins O.C. (2011) GC- MS analysis and phytochemical screening of ethanolic root of *Plumbago zeylanica* (Linn.). *J. Med. Plants Res.*, vol. 5(9), pp. 1756-1761.
27. Kumaradevan G., Damodaran R., Mani, P., Dinesh-kumar G., Jayaseelan T. (2015) Phytochemical Screening and GC-MS Analysis of Bioactive Components of Ethanol Leaves Extract of *Clerodendrum phlomidis* (L.). *Amer. J. of Biol. and Pharm. Res.*, vol. 2(3), pp. 142-148.
28. Kumar J., Rai A., Raj V. (2017) A Comprehensive Review on the Pharmacological Activity of Schiff Base Containing Derivatives. *Organic & Medicinal Chemistry International Journal*, vol. 1(3), pp. 11-25.

^{1*}A.B. Rakhym , ¹U.Zh. Bekturganova , ^{1,2}G.A. Seilkhanova , ³A. Csavdari 

¹Al-Farabi Kazakh National University, Almaty, Kazakhstan

²Center for Physical and Chemical Research and Analysis Methods, Almaty, Kazakhstan

³Babes-Bolyai University, Cluj-Napoca, Romania

e-mail: akmaral.rahym@gmail.com

Chamotte clay sorbent for the extraction of lead and cadmium ions from aqueous solutions

Abstract: Nowadays the problem of wastewater pollution by heavy metal (HM) ions is extremely urgent. HM are harmful for health and environment, they are not biodegradable and can accumulate in plants and body. Clay minerals are known for their high adsorption capacity towards heavy metal ions. There are many research studies on appliance of different types of clays for wastewater treatment. Chamotte clay is a white heat-treated kaolin clay with stone properties, resistant to aggressive media, which contains highly dispersed hydroaluminosilicates. The clay does not require additional purification after secondary use. It is used in industry in large quantities, though wastes of clay are needed to be utilized. In current work chamotte clay wastes are offered to be used as a sorbent for lead (II) and cadmium (II) ions extraction. The choice of the ions is based on the high toxicity and abundance of these metals in wastewaters. Polyvinylpyrrolidone (PVP) was used as a modifier to increase adsorption capacity of the clay. The extraction degree of ions by initial chamotte clay reaches $(97 \pm 7.2) \%$ and $(67 \pm 6.0) \%$ for Pb^{2+} and Cd^{2+} respectively. The modification with PVP increases the extraction degree of Cd^{2+} to $(86.0 \pm 6.4) \%$. The initial and modified clay was characterized by scanning electron microscopy, energy dispersive spectroscopy and Fourier transform infrared spectroscopy methods. The adsorption process was carried out under static conditions at $pH = 6$ and $T = 298 K$, initial concentration of the metal ions was 10 mg/l . The optimal mass for the sorption of lead and cadmium ions was also determined during the study and is equal to 1 g per 100 cm^3 of solution. The use of chamotte clay as the basis for the development of sorbents helps reducing the cost of cleaning water bodies, and also allows solving the problem of wastes disposal.

Key words: adsorption, chamotte clay, polyvinylpyrrolidone, heavy metal ions, wastewater treatment

Introduction

Large industrial production is characterized by the formation of effluents containing heavy metal ions (HM). Heavy metals are natural components of the earth's crust. They cannot be degraded or destroyed [1-3]. However, due to large emissions as a result of industrialization and urbanization, HMs pose a great threat. Unlike organic pollutants that are capable of biodegradation, heavy metals do not decompose into harmless end products and have global consequences for both the human body and the environment [4]. According to studies [5, 6], some TM ions are nutrients for the physiological functions of humans in small doses, but in large quantities they have a negative effect on health.

Many methods are known to reduce the concentration of pollutants or to completely purify water from heavy metal ions (HM), but many of them are

expensive. One of the most effective and low-cost methods for the neutralization of HM ions is sorption [7]. The sorption method makes it possible to purify water from HM ions with high efficiency, approximating the concentration of contaminants to maximum acceptable concentration (MAC) and general sanitary standards.

There is a shortage of clean drinking water existing in some regions of Kazakhstan [8]. One of these regions is the village of Alatau Batyr. The local population is forced to drink low-quality water containing TM ions. During the experiment, a number of water samples were taken and their composition was studied. As it turned out, the water in the region needs to be treated as TM ions in high concentrations, which do not meet sanitary standards, were found in the samples.

In recent years, the use of industrial waste as secondary products has been of great interest [9].

The use of industrial waste as an adsorbent solves 2 problems: 1) purification of water from pollution; 2) wastes disposal. For the first time, secondary commodities of refractory material chamotte clay (ChC) were used for water purification. ChC is a white heat-treated kaolin clay with a stone properties, resistant to aggressive media, which contains highly dispersed hydroaluminosilicates. The clay does not require additional purification after secondary use. It can be used in industry in large quantities [10, 11].

Polyvinylpyrrolidone (PVP) was chosen as a modifier. The choice of modifier is based on the availability and safety of this compound. The presence of the lactone cycle in PVP macromolecule ensures its good solubility in water [12]. The high molecular weight PVP compound is chemically stable and capable of complexation due to the presence of potential nitrogen monoxide donors in its structure. The binding of PVP increases pores on the clay surface, thereby improving its sorption properties [13, 14]. The adsorbing properties of polyvinylpyrrolidone allow it to be used as part of detoxifying agents. It is used in medicine as a stabilizer of emulsions and suspensions [14].

Experimental part

Materials and methods.

In this work, chamotte clay (the Ukrainian deposit Teplosvet Inzhiniring, LLC, Kiev) was selected as an object of the study and polyvinylpyrrolidone 10000 (AppliChem GmbH) – as a modifier. To prepare model solutions for studying the adsorption properties of the obtained sorbents, chemically pure grade salts of $\text{Pb}(\text{NO}_3)_2$ and CdCl_2 (Laborfarm) were used. The residual concentrations of Pb^{2+} and Cd^{2+} ions were determined by atomic absorption spectroscopy on a 'Shimadzu 6200' (Japan) instrument.

The obtained samples were studied by physico-chemical methods of analysis, which included FTIR – spectroscopy (Spectrum 65, Perkin Elmer, USA), scanning electron microscopy (SEM) (Zeiss Supra 40VP instrument) to determine particle size and topography, elemental analysis by EDAX (energy dispersive spectroscopy) method to study chemical composition (Quanta FEG 250 scanning electron microscope, FEI, USA)

Composite sorbents obtainment.

The process of obtaining composite material consisted of the following steps:

1) A weighed portion of ChC (20 g) was poured into 100 ml of a 1% PVP solution (these objects did not need preliminary treatment). The resulting mix-

ture was stirred using a dynamic stirrer for 1 hour, then left for 24 hours.

2) the drying process was carried out at T368–373K for 3-4 hours. The resulting sorbent was subjected to grinding to obtain a homogeneous powder mass.

Adsorption experiments.

A portion of the obtained sorbent was added to a 10 mg/l aqueous solution containing lead or cadmium ions at a temperature of (296 ± 2) K. At certain time intervals, samples were taken, filtered, and the content of heavy metal ions was determined. The degree of extraction of the studied ions was calculated by the Formula 1:

$$E = (C_0 - C_e) / C_0 * 100\%, \quad (1)$$

where E is the degree of extraction of metal ions,%;
 C_0 and C_e – initial and equilibrium concentrations of metal ions, respectively, mg/l.

Results and discussion

The technical characteristics of the chamotte clay used in the current work are presented in Table 1 [15].

Table 1 – Technical characteristics of the ChC [15]

Specifications	Values
Average grain size	2 mm
Moisture absorption	from 2% to 20%
Humidity	not more than 5%
Refractoriness	from 1550°C to 1850°C

The technical characteristics of ChC are especially important, since with prolonged storage or upon expiration (3 years) it loses its unique properties [16].

The structure of the modifier for creating the sorbent (PVP) is shown in Figure 1. The presence of the lactone cycle in the polymer macromolecule ensures solubility in water. PVP molecules in aqueous solutions are static tangles that bind molecules that results ability to complexation with ChC [17].

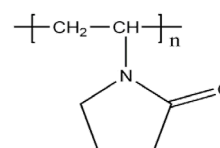


Figure 1 – Molecular structure of PVP

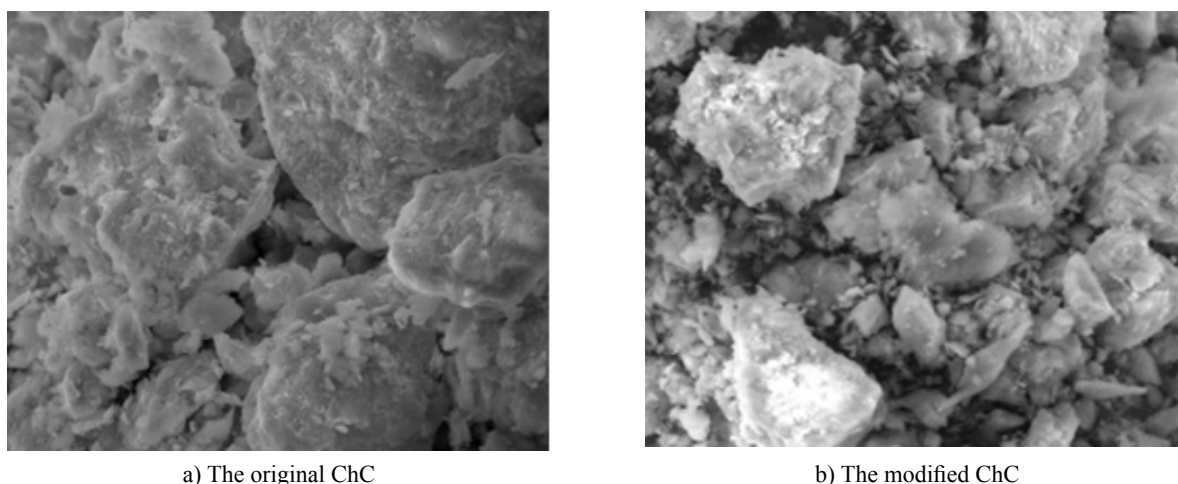


Figure 2 – Fragments of SEM images of Chamotte clay and its modified form (at zoom 20000x)

Figure 2 shows microphotographs of the initial and modified with polyvinylpyrrolidone ChC obtained by scanning electron microscopy (SEM). As it is known, SEM is widely used to study the microstructure of various objects [18]. From figure 2a it follows that the sample of secondary raw materials has a dense structure, represented by hydroaluminosilicates of various shapes and sizes. As a result of the modification of ChC by the PVP polymer, the surface structure of clay changes (2b). As it can be seen from Figure 2b, the ChC sample becomes more uniform after modification, the sizes of hydroaluminosilicates are enlarged, which leads to an increase in its porosity and hence, sorption activity increases. It can be

observed that the addition of the PVP polymer affects the porosity of the hydroaluminosilicates in ChC structure.

Table 2 presents the results of elemental analysis of chamotte clay obtained by energy dispersive spectroscopy (EDS). The qualitative and quantitative composition of ChC was established. As can be seen from Table 2, the main components of ChC are oxygen, aluminum and silicon, since the clay is an aluminosilicate material. Also it contains significant doses of carbon, (which is part of the clay in the form of magnesium and calcium carbonates) and such metals as potassium, sodium and magnesium. The last contribute to the formation of fusibility and are found in the form of soluble salts.

Table 2 – Data of elemental analysis of chamotte clay

Raw materials	The content of the element, wt. %						
	O	Si	Al	C	K	Mg	Na
Chamotte clay	43.22	26.62	22.40	6.71	0.86	0.50	0.44

To confirm the presence of a modifier in the sample, the initial and modified chamotte clay was studied by FTIR spectroscopy. The results of the analysis are presented in figures 3-4. Narrow absorption bands of weak intensity are observed in ChC spectra. The IR spectrum of the sample shows a weak band at 1027 cm^{-1} , corresponding to stretching vibrations of Si – O – Si tetrahedra of the silicon-oxygen skeleton, which are clearly manifested in the spectrum of chamotte clay [19]. The observed intense absorp-

tion bands at 468.40 cm^{-1} , 540.20 cm^{-1} and 519 cm^{-1} can be attributed to deformation vibrations of Me-O type groups related to alkaline-earth metals. Absorption bands in the region of 695 cm^{-1} and 1448 cm^{-1} indicate that calcite impurities are present in the composition. The band 797.15 cm^{-1} is due to the Si – O – Mg bond in the octahedral positions of kaolinite. The intense absorption band of the deformation vibrations of water molecules bound by OH groups is in the range of $1832\text{--}3697\text{ cm}^{-1}$ [20].

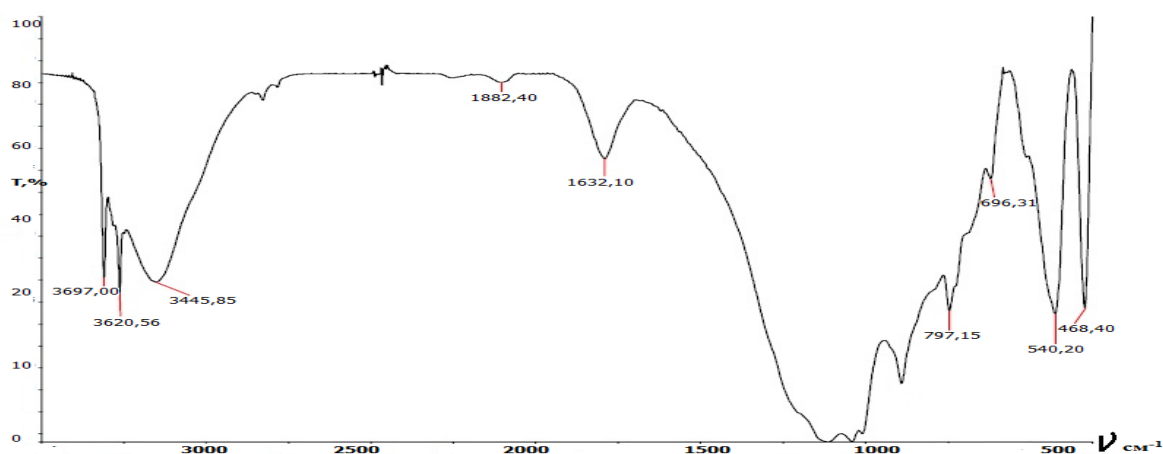


Figure 3 – IR spectrum of ChC

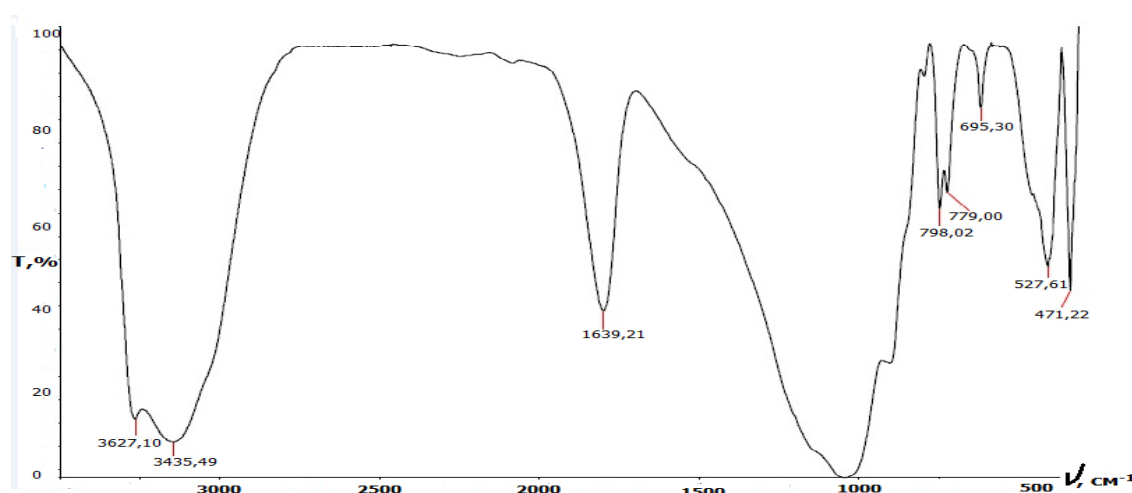


Figure 4 – IR spectrum of ChC + PVP

The IR spectrum of modified clay has absorption bands with wave numbers corresponding to stretching vibrations of $-\text{CH}_2-$ and C-N bonds due to the possible formation of a complex compound of PVP and clay. The stretching vibrations of the $-\text{CH}_2-$ group are located in the range of $1480\text{--}1440\text{ cm}^{-1}$, and the C-N bonds are between the absorption bands of $2260\text{--}2240\text{ cm}^{-1}$, which characterize PVP [21]. This indicates the presence of PVP or its complex compounds in the sorbent. It was found that the band at 1027 cm^{-1} , which is responsible for the stretching vibrations of Si – O bonds, remains unchanged; therefore, the modification does not affect the silicon content in the samples [22].

The research results presented in Figure 5 show that the extraction of lead ions by the initial clay reaches $(97 \pm 7.2)\%$, and the degree of extraction of cadmium from the aqueous solution reaches only $(67$

$\pm 6.0)\%$. Therefore, the activation of ChC by PVP is effective, since the degree of extraction of cadmium ions by modified sorbent reaches $(86 \pm 6.4)\%$. Also it was found during the experiment that the degree of extraction of lead and cadmium ions at the beginning sharply increases and then reaches equilibrium within 30 minutes. The adsorption ability of sorbents towards identically charged metal ions depends on the radius of the ion and charge density [23]. Between two ions of the same charge, ions with a large radius exhibit higher sorption ability, because they are less prone to the formation of a hydration shell, which reduces the forces of electrostatic attraction. Since lead has a larger ionic radius (0.112 nm) compared to cadmium ions (0.099 nm), it should be sorbed better, which corresponds the results of the study. The highest degree of recovery is $(97 \pm 7.2)\%$ for lead ions and $(86 \pm 6.4)\%$ for cadmium ions.

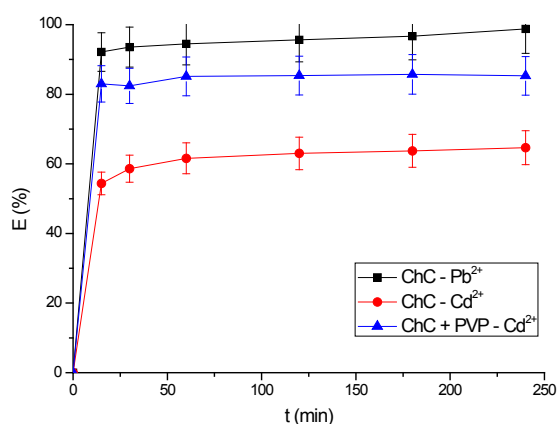


Figure 5 – Dependence of the degree of extraction of Cd²⁺, Pb²⁺ ions (T = 298K, pH = 6, C = 10 mg/l) on time

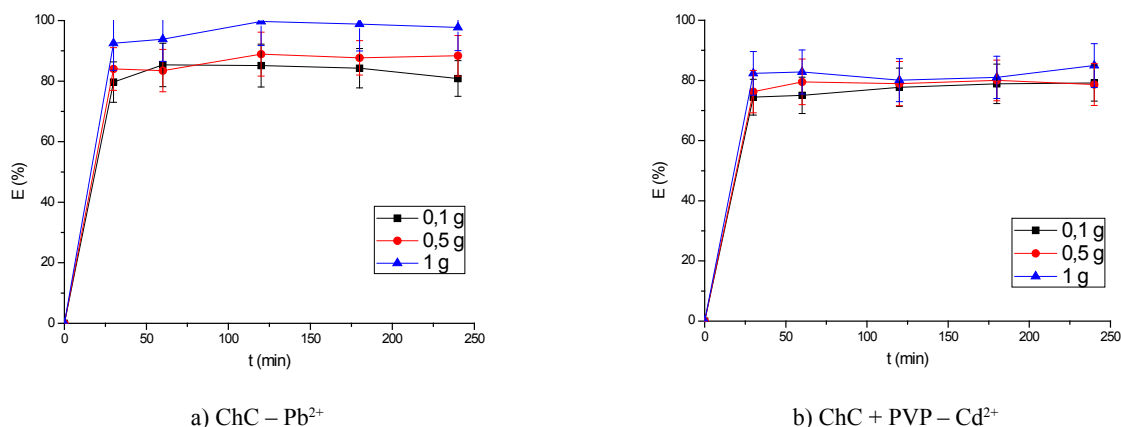


Figure 6 – Dependence of the degree of extraction of Pb²⁺ (a) and Cd²⁺ (b) ions with different masses of ChC(a) and ChC+PVP (b) on time (T = 298 K, pH = 6, C = 10 mg/l)

As the results presented in Fig. 6 show, the efficiency of extracting HM ions from solution increases with a raise in sorbent mass. It was found that the optimal sorbent mass required for the most complete extraction of metal ions was 1 g per 100 cm³ of a metal salt solution for both cadmium and lead.

Conclusion

It was found that the degree of extraction of Pb²⁺ ions by ChC reaches (97.0 ± 7.2)%, while for Cd²⁺ ions it shows a lower efficiency – (86.0 ± 6.4)%. This is probably due to the fact that lead ions have a larger ionic radius (0.112 nm) compared to cadmium ions (0.099 nm). Based on the analysis of the physicochemical characteristics of ChC, it was found that the imposition of polyvinylpyrrolidone significantly increases the sorption ability towards Cd²⁺ ions. The

optimal mass for the sorption of lead and cadmium ions – 1 g per 100 cm³ of solution was also determined during the study at T = 298 K and pH = 6. The use of chamotte clay as the basis for the development of sorbents helps reducing the cost of cleaning water bodies, and also allows solving the problem of wastes disposal.

References

- 1 Fu F., Wang Q. (2011) Removal of heavy metal ions from wastewaters: A review. *J Env Man.*, Vol. 92, pp. 407-418. doi:10.1016/j.jenvman.2010.11.011
- 2 Khan F., Khan M., Samad A., Noor Y., Rashid M., Jan B. (2015) In-situ stabilization of heavy metals in agriculture soils irrigated with untreated wastewater. *J. Geochemical Explor.*, Vol. 159, pp. 1-7. doi:10.1016/j.gexplo.2015.07.002

- 3 Klimenko T.V. (2013) Ochistka stochnyih vod ot ionov tyazhelyih metallov (Wastewater treatment from heavy metal ions). *Sovremennyye nauchnyie issledovaniya i innovatsii (Modern scientific research and innovation)*, No.11 [Electronic resource]. URL: <http://web.snauka.ru/issues/2013/11/28484> (accessed: 03.03.2016). (in Russian)
- 4 Boskabady M., Marefati N., Farkhondeh T., Shakeri F., Farshbaf A., Boskabady M.H. (2018) The effect of environmental lead exposure on human health and the contribution of inflammatory mechanisms, a review. *Env. Int.*, Vol.120, pp, 404-420. doi: 10.1016/j.envint.2018.08.013
- 5 Vodyanitsky Yu.N. (2012) Standards for the contents of heavy metals and metalloids in soils. *Eurasian Soil Science*. Vol.45, Is. 3, pp. 321-328.
- 6 Jan A. T., Azam, M., Siddiqui K., Ali A., Choi I., Mohd Q, Haq R. (2015) Heavy Metals and Human Health: Mechanistic Insight into Toxicity and Counter Defense System of Antioxidants. *Int J Mol Sci.*, Vol.16, Is.12, pp. 29592–29630. doi: 10.3390/ijms161226183
- 7 Kostin A.V., Mostalygina L.V., Bukhtoyarov O.I. (2012) Izuchenie mehanizma sorbtzii ionov medi i svintsa na bentonitovoy gline (Studying the mechanism of sorption of copper and lead ions on bentonite clay). *Sorbtsionnyie i hromatograficheskie protsessy (Sorption and chromatographic processes)*, Vol.12, Is. 6, pp.949-957. (in Russian)
- 8 Balykbaeva A. S. (2017) Zagryaznenie vodnyih resursov Kazakhstana i metody ochistki vodyi (Water pollution of Kazakhstan and methods of water treatment). Oku-Zaman.
- 9 Shishakina O.A., Palamarchuk A.A. (2019) Obzor napravleniy utilizatsii tehnogennyih othodov v proizvodstve stroitelnyih materialov (Overview of directions for the utilization of industrial wastes in the production of building materials). *Mezhdunarodnyiy zhurnal prikladnyih i fundamentalnyih issledovaniy (International Journal of Applied and Basic Research)*. No. 4, pp.-198-203. (in Russian)
- 10 Omotoyinbo, Ajibade J., Leke O. (2008). Working Properties of Some Selected Refractory Clay Deposits in South Western Nigeria. *J Min and Mat Char and Eng.*, Vol.7, Is. 3. doi: 10.4236/jmmce.2008.73018.
- 11 Sharshenbekkyzy A., Kochkorova Z.B., Murzubraimov B.M. (2017) Issledovanie vozmozhnosti polucheniya prirodnoy kaolinovoy glinyi Choko-Bulakskogo mestorozhdeniya (Study of the possibility of obtaining natural kaolin clay of the Choko-Bulakskoye deposit). *Izvestiya Vuzov Kyrgyzystana (University news of Kyrgyzstan)*. Vol.7, pp.74-77. (in Russian)
- 12 Masimov E.A., Shirinov N.Z., Bagirov T.O. (2016) The effect of the molecular weight of polyvinylpyrrolidone on the phase diagram of a water-two-phase system of dextran-polyvinylpyrrolidone. *Int J App and B Res*. No. 12 (part 1), pp. 95-98.
- 13 Evtyukhov, S.A., Berezgon V.G. (2003) Study of the sorption properties of natural aluminosilicates (clay, loam, sandy loam, zeolite). *Rus J Appl Chem.*, Vol. 76, Is. 9. – S. 1454-1457.
- 14 Nikiforova, T.E., Kozlov, V.A., Gagina, A.N. (2010) Sorption of copper ions by cellulose sorbents modified with a dichlorotriazine compound and polyvinylpyrrolidone. *Russ J Appl Chem.*, Vol. 83, Is.10, pp. 1774-1780. doi: 10.1134/S1070427210100083
- 15 Santos, Flavia D., Leyvison Rafael V. Da Conceição, Annie Ceron, and Heizir F. De Castro (2017) Chamotte clay as potential low cost adsorbent to be used in the palm kernel biodiesel purification. *Applied Clay Science*, Vol.149 (9), pp. 41-50. doi:10.1016/j.clay.2017.09.009
- 16 Vladimirov V.S., Galagan A.P., Ilyukhin M.A., Karpukhin I.A., Moisis S.E., Moisis E.S. (2002) Novyye ognepornyie i teploizolyatsionnyie materialy i tehnologii ih proizvodstva (New refractory and heat-insulating materials and technologies for their production). *Nauchno-tehnicheskii i proizvodstvennyiy zhurnal "Novyye ogneporyi" (Scientific-technical and production journal "New refractories")*. No. 1, pp. 87-88. (in Russian)
- 17 Vartepyan R. Sh., Khozina E.V., Chalykh A.E. et.al. (2003) Issledovanie molkulyarnoy podvizhnosti smesi polietilenglikol/polivinilpirrolidon metodami impulsnogo YaMR (Study of the molecular mobility of a mixture of polyethylene glycol / polyvinylpyrrolidone by pulsed NMR). *Coll J.*, Vol. 65, Is. 6, pp. 748-755. (in Russian)
- 18 Goldstein, J., Newbury Dale, Michael Joseph, Ritchie Nicholas, Scott John, Joy David (2018) Scanning Electron Microscopy and X-Ray Microanalysis. doi:10.1007/978-1-4939-6676-9.
- 19 M.V. Volkenstein, L. A. Gribov, M. A. Elyashevich, B. I. Stepanov (1972) Molecular Vibrations. Moscow, Nauka.
- 20 G.S. Koptev, Yu.A. Pentin, (1977) Calculation of molecular vibrations. Ed. Moscow State University.
- 21 Prech E., Bulmann F., Affolter K. (2006) Opredelenie stroeniya organicheskikh veschestv. (Determination of the structure of organic substances). Moscow, Mir. (in Russian)
- 22 Nakamoto K. (1991) Infrakrasnyie spektryi neorganicheskikh i koordinatsionnyih soedineniy (Infrared spectra of inorganic and coordination sequences). Moscow, Mir. (in Russian)
- 23 Telkhozhayeva Madina, Seilkhanova Gulziya, Rakhym, A., Imangaliyeva Ainur, Akbayeva Dina. (2018). Sorption of lead and cadmium ions from aqueous solutions using modified zeolite. *Chem Bull KazNU*, Is.1, pp. 16-22. doi:10.15328/cb980.

¹*R.K. Nadirov , ²M.D. Turan , ¹G.A. Karamyrzayev 

¹Al-Farabi Kazakh national university, Almaty, Kazakhstan

²Firat University, Elazığ, Turkey

*e-mail: nadirov.rashid@gmail.com

Copper ammonia leaching from smelter slag

Abstract: Copper smelter slag can be considered as an important source for using in the copper hydrometallurgy. Ammonia leaching seems to be attractive for processing copper slag. Under the influence of ammonia, copper, which is part of the minerals of copper, forms soluble ammonia complexes, while iron precipitates as insoluble compounds. In the present work, the possibility of leaching the copper smelter slag (1.26 wt.% Cu) of the Balkhash smelter using NH_4OH solutions was considered. The effect of experimental factors (leaching duration, reagent concentration, temperature, stirring rate, as well as a solid-to-liquid ratio) on the extraction of copper into solution was studied. It was found that the extraction of copper into solution increases with increasing temperature (in the studied range 298 – 333 K), pulp density (up to 10 pct) and stirring rate (up to 800 rpm). The concentration of NH_4OH almost does not affect on the level of copper extraction in the range of 1-4 M. The following experimental conditions provide the recovery of 65% of Cu into ammonia solution: 1M NH_4OH , $T = 333$ K, particle size 90% < 200 mesh, solid-to-liquid ratio 10 pct, stirring rate 800 rpm, and leaching duration 180 min, 65% of copper is extracted into the solution. Shrinking core model with mixture kinetics was used to describe the process of ammonia leaching of copper from smelter slag. The activation energy and pre-exponential factor for the reactions of copper dissolution were calculated to be 16.2 ± 0.7 kJ/mol and 0.138 ± 0.001 min⁻¹, respectively. The relatively low value of the activation energy indicates that the rate of the overall leaching process is controlled mainly by the processes of mass transfer rather than by the rate of chemical reactions of copper dissolution.

Key words: copper smelter slag, ammonia leaching, shrinking core model, copper dissolution, ammonia complexes of copper.

Introduction

Being the solid waste by-product of copper pyrometallurgical production, the copper smelter slag contains a significant amount of valuable metals, primarily, copper and zinc [1-5]. This slag is usually dumped directly, or used as ballast or additive in building or road industry [6-8]. Considering the environmental and economic aspects, it is critical to find ways to recover valuable metals from the slag. However, this task is not easy to implement, because copper slag consists of a matrix of fayalite (Fe_2SiO_4) and includes minor components of target valuable metals.

Hydrometallurgy is considered as the promising way to recover such metals from the copper slag [9-14]. Among other hydrometallurgical processes, sulfuric acid leaching is recognized as the most convenient process for this because of the producing huge amount of acid on the metallurgical plants. However, using this process leads to the dissolution of iron pre-

sents in the slag that causes problems in the subsequent treatment of the leachate. In addition, sulfuric acid solutions are highly corrosive.

Ammonia leaching is being proposed for using in copper metallurgy as an alternative to sulfuric acid leaching [15-19]. The main advantages of ammonia leaching of copper- and zinc-containing sources are as follows: (i) raw material with high carbonation can be leached by ammonia solutions; acidic leaching can not be used for processing these types of material due to high consumption of acid (ii) equipment corrosion are eliminated (iii) complexation capacity of iron with ammonia is very low, and iron, leached, precipitates in the form of insoluble compounds. Thus, ammonia leaching has a suitable selective capacity for the non-ferrous metals to the iron (iv) unlike acids, ammonia does not react with alumina silicates, and ferrosilicates (v) the residual ammonia in the soil after leaching can act as fertilizers. The main disadvantage of ammonia leaching is the high evaporation capacity of ammonia.

Despite the fact that ammonia hydrometallurgy has been developing for a long time, there is a very limited number of works devoted to ammonium leaching of non-ferrous metals from metallurgical slag [20-24]. In the present paper, we attempted to use ammonia leaching to extract copper from copper smelting slag sample of the Balkhash copper smelter (Central Kazakhstan). The aim of the work was to investigate the influence of experimental factors on the copper extraction from the smelter slag into the solution during ammonia leaching, as well as to determine the conditions that provide an acceptable level of copper recovery.

Materials and Methods

Slag sample. Copper smelter slag, used in this research, was obtained from copper smelter plant of «Kazakhmys Smelting» (Balkhash, Central Kazakhstan). The major phases of the slag sample were identified by X-ray powder diffractometry (XRD) as (Fe₂SiO₄), ferrosilite (FeSiO₃), and magnetite (Fe₃O₄). The copper-containing minor phases were chalcocite (Cu₂S), chalcopyrite (CuFeS₂), covellite (CuS), and cuprite (Cu₂O). Zinc was mainly presented in the form of its ferrite (ZnFeO₂). The chemical composition of the slag sample determined by ICP-AES (Perkin Elmer, Optima 8000) after complete microwave-assisted dissolving in nitric acid was, wt. %: Fe 14.72, Si 40.28, Zn 2.73, Cu 1.26, Al 1.32, S 0.97, Ca 0.83.

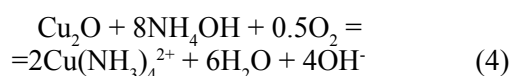
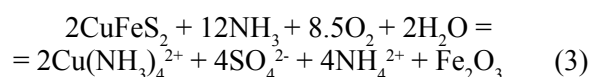
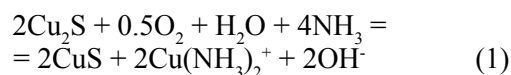
Crushed, ground, and sieved (-0.074 mm) slag sample was used for the leaching experiments.

Leaching experiment. The leaching tests were performed in a 1-L flask. The slag sample (20 g) was placed in the flask filled with an ammonia-ammonium aqueous solution with pre-determined concentrations of NH₄OH, as well as a liquid-to-solid ratio. The flask was stirred at 500 min⁻¹ at a predetermined temperature with continuous air bubbling (300 mL×min⁻¹). After leaching, quantitative analysis of metal ions (Fe, Cu, Zn) in the leachate was performed by using ICP-AES (Perkin Elmer, Optima 8000). All experiments were repeated 3 times.

Variable parameters. The following parameters were varied during the experiments to determine the conditions that provide the highest copper recovery into solution (limit values are shown in brackets): concentration of NH₄OH (1-4 M), temperature (298 – 333 K), leaching duration (40-240 min), and liquid-to-solid ratio (6-20 pct).

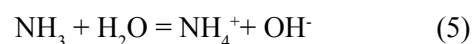
Results and Discussion

Leaching behavior of copper-containing phases. Copper minerals of the slag react with aqueous ammonia in the presence of oxygen with the formation of ammonia complexes of copper (Eqs.1-4):



According to the Eh-pH diagram for the copper-ammonia-water system, Cu(I) and Cu(II) complexes with ammonia are ionic species stable in alkaline aqueous media [22]. In the solutions with an ammonia concentration of 0.01 to 5 M, the complex Cu(NH₃)₄²⁺ predominates.

Complexation of copper ions can only happen with NH₃ and not with NH₄⁺ ions. Therefore, the conditions should be maintained to shift the equilibrium between NH₃ and NH₄⁺ to the left side in the Eq.5:



Obviously, increasing the pH of the medium (i.e., increasing the concentration of hydroxyl ions) is desirable for rising the free ammonia concentration. Once the pH is greater than 9.25, NH₃ is the dominant species in the system.

Effect of temperature. The leaching tests were performed at 298, 318 and 333 K while NH₄OH concentration, S:L ratio, and stirring rate were set at 1M, 10 g: 1 L (10 pct) and 800 rpm, respectively. Fig.1 demonstrates that comparatively higher Cu recovery was obtained as the reaction temperature increased.

At a temperature of 333 K, copper recovery into solution reached 62% after 4 hours of leaching. A further increase in temperature is impractical due to the loss of ammonia in the environment. As has been demonstrated by Liu et al. [24], copper (II) oxide easily reacts with ammonia at ambient temperature with the formation of a soluble copper complex. Apparently, it is precisely due to the leaching of Cu₂O that the presence of dissolved copper in the solution is ensured at 298 K.

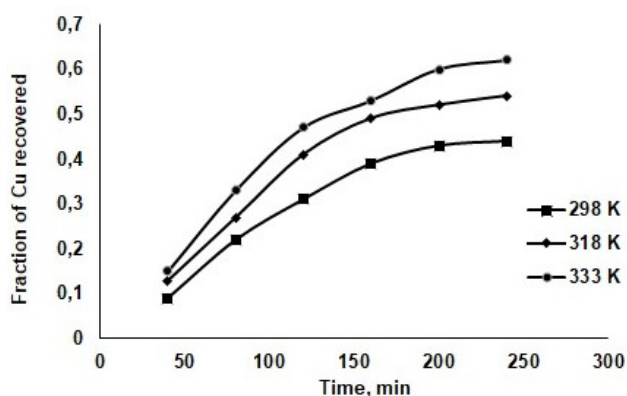


Figure 1 – Effect of temperature and leaching duration on copper recovery into solution (1M NH_4OH , particle size 90% < 200 mesh, S:L = 10 pct, stirring rate 800 rpm)

Effect of NH_4OH concentration. The influence of NH_4OH concentration on copper recovery into the solution has been investigated by varying the reagent concentration from 1 to 4 M at constant values of temperature (333 K), solid-to liquid ratio (10 pct), and stirring rate (800 rpm). The results obtained are present in Fig. 2.

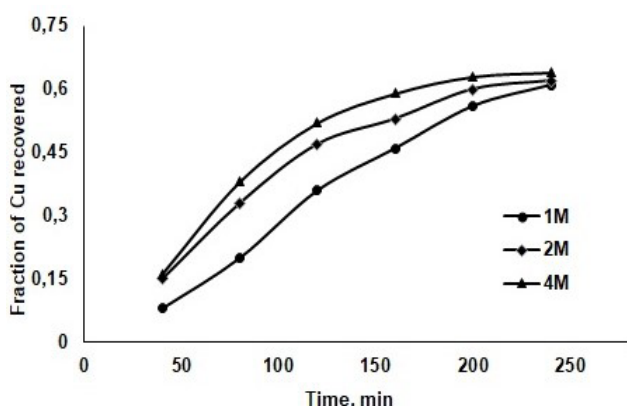


Figure 2 – Effect of NH_4OH concentration and leaching duration on copper recovery into solution (333 K, particle size 90% < 200 mesh, S:L = 10 pct, stirring rate 800 rpm)

As can be seen from Fig. 2, an increase in the concentration of NH_4OH leads to an increase of copper extraction into solution; however, 4 hours after the start of leaching, the concentration of the reagent practically ceases to affect the degree of copper recovery, which reaches a plateau at 62%.

The following aspects should be taken into account when discussing the effect of NH_4OH concentration on the leaching of copper from slag. Firstly,

it is the stoichiometry of the reactions (Eqs. 1-4). According to the above-mentioned equations, 1M of copper requires from 1M (for chalcocite) to 8 M (for chalcopyrite) moles of ammonia to leach. If we take into account that the copper content in the slag is 1.26 wt.%, and the solid-to-liquid ratio at leaching (10 pct), then the theoretical ammonia consumption for copper leaching will be about 0.10 mol per 1 litre of solution (without taking into account the equilibrium constants of the reactions of copper minerals with ammonia). Another point is related to the fact that an increase in the concentration of ammonia in solution leads to a decrease in the concentration of oxygen. Oxygen, in turn, is an important component of the reaction mixture (see Eqs. 1-4).

Effect of stirring rate. Stirring is a very important process in the ammonia leaching of copper from slag. The experiments carried out in the absence of stirring showed a very low (up to 18%) recovery of copper into solution even with prolonged (up to 5 hours) leaching. This circumstance indicates that the limiting stage of copper leaching reactions is the mass transfer of oxygen and ammonia to the surface of copper minerals. The effect of stirring rate on copper recovery at constant values of NH_4OH concentration (1M), temperature (333 K), and solid-to liquid ratio (10 pct), is presented in Fig. 3.

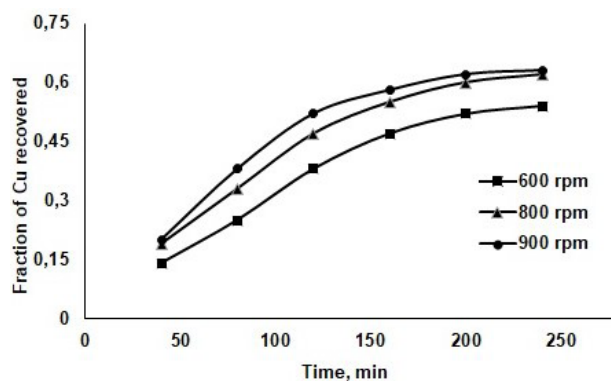


Figure 3 – Effect of stirring rate and leaching duration on copper recovery into solution (1M NH_4OH , 333 K, particle size 90% < 200 mesh, S:L = 10 pct)

The value of copper recovery increases with stirring rate up to 800 rpm; above this rate, copper recovery does not affect by the stirring rate. Apparently, up to a value of 800 rpm, the leaching process is controlled by mass transfer, and above this value, the leaching rate is controlled by inner diffusion of the rate of chemical reactions.

Effect of solid-to-liquid ratio. Solid-to-liquid ratio, or pulp density, is a very important parameter in hydrometallurgy. The decrease in pulp density, as a rule, intensifies the leaching process. On the other hand, at low pulp density, there is an overrun of the leaching agent and the content of the target metal in the solution after leaching is reduced. Therefore, it was important to find the minimum value of the pulp density, providing an acceptable extraction of copper into solution. The results of the experiments on determining the influence of solid-to-liquid ratio on the copper recovery at the constant values of NH_4OH concentration (1M), temperature (333 K), and stirring rate (800 rpm), is presented in Fig.4.

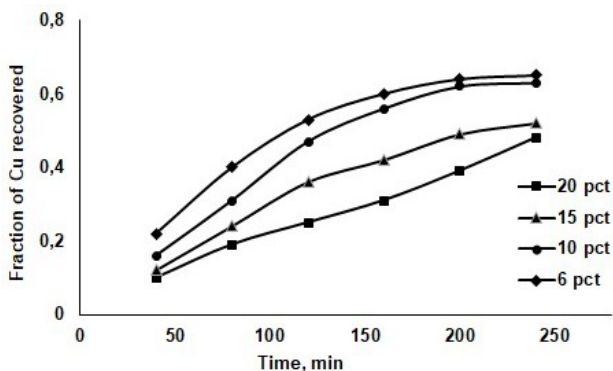


Figure 4 – Effect of solid-to-liquid ratio and leaching duration on copper recovery into solution (1M NH_4OH , 333 K, particle size 90% < 200 mesh, 800 rpm)

Increasing pulp density from 6 to 20 pct negatively affects the copper recovery. But, the values of copper recovery at 6 and 10 pct are almost the same. In both cases, the copper recovery values reach a plateau (64-65%) with a leaching time of 180 minutes.

Process kinetics. The shrinking core model was widely applied for the rate expression of leaching reactions in hydrometallurgy [25]. In this work, mixture kinetics model proposed by Ekmekyapar et al. [26] was used. The model is expressed by the following equation:

$$1 - 2(1-X)^{1/3} + (1-X)^{2/3} = k\tau \quad (6)$$

where X is the fraction of the recovered component, k is the apparent rate constant, and τ is the leaching duration.

The straight lines in the Fig.5 demonstrate that the leaching process is controlled by mixture kinetics.

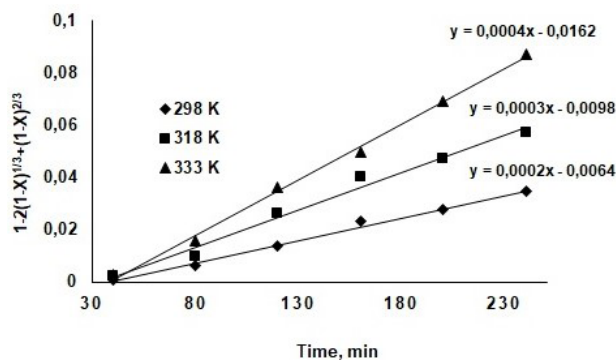


Figure 5 – Plot of $(1-2(1-X)^{1/3}+(1-X)^{2/3}) = k\tau$ vs time (1M NH_4OH , particle size 90% < 200 mesh, 800 rpm, S:L = 10 pct)

The apparent rate constants for the reactions of copper dissolution have been found as 0.0002, 0.0003 and 0.0004 min^{-1} for 298, 318 and 333 K, respectively.

In order to determine the activation energy of the reactions of copper dissolution (Eqs. 1-4), $\ln k$ versus $1/T$ was plotted (see Fig.6).

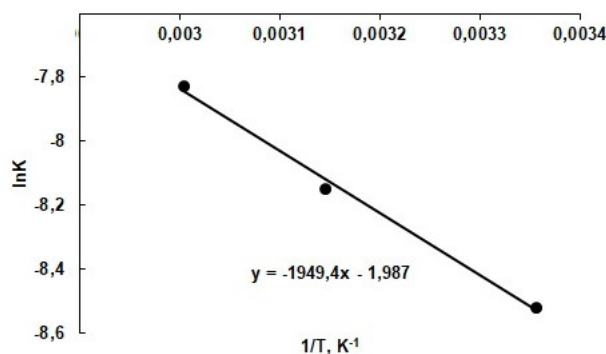


Figure 6 – Arrhenius plot (1M NH_4OH , particle size 90% < 200 mesh, 800 rpm, S:L = 10 pct)

The slope of the Arrhenius plot gives the E/R value, from which activation energy was calculated as 16.2 ± 0.7 kJ/mol. The relatively low value of the activation energy indicates that the leaching process is controlled mainly by diffusion processes rather than by the rate of chemical reactions.

For the calculating pre-exponential factor, the Arrhenius equation was used:

$$k = A e^{\frac{-E_a}{RT}} \quad (7)$$

where k is the apparent rate constant, A is the pre-exponential factor, E_a is the activation energy, R is the universal gas constant, and T is the absolute temperature.

According to the Eq.7, pre-exponential factor for the reaction of copper ammonia leaching was calculated to be $0.138 \pm 0.001 \text{ min}^{-1}$.

Conclusions

From the results of this study, the following conclusions were made regarding the characterization of copper smelter slag obtained from the Balkhash copper plant and the ammonia leaching of this slag.

In the copper smelter slag, copper mainly presents as copper sulfides (Cu_2S , CuFeS_2 , CuS) and oxide (Cu_2O).

Temperature, stirring rate, as well as pulp density have an impact on the copper recovery into solution when ammonia leaching of the slag, while the concentration of NH_4OH almost does not affect on the level of copper extraction. The stirring rate influences the process below 800 rpm, and pulp density has an impact on the process above 10 pct.

At the conditions of 1M NH_4OH , $T = 333 \text{ K}$, particle size $90\% < 200$ mesh, solid-to-liquid ratio 10 pct, stirring rate 800 rpm, and leaching duration 180 min, 65% of copper is extracted into the solution.

Shrinking core model with mixture kinetics adequately describes the process of ammonia leaching of copper from smelter slag.

The activation energy of the chemical reactions is calculated to be $16.2 \pm 0.7 \text{ kJ/mol}$ indicating that the leaching process is controlled mainly by mass transfer processes rather than by the rate of chemical reactions.

References

1. Kaksonen A. H., Särkijärvi S., Puhakka J. A., Peuraniemi E., Junnikkala S., Tuovinen O. H. (2017). Solid phase changes in chemically and biologically leached copper smelter slag. *Miner Eng.*, vol. 106, pp. 97-101.
2. Das B., Mishra B. K., Angadi S., Pradhan S. K., Prakash S., Mohanty J. (2010). Characterization and recovery of copper values from discarded slag. *Waste Manage Res.*, no. 28(6), pp. 561-567.
3. Sueoka Y., Sakakibara M. (2013). Primary phases and natural weathering of smelting slag at an abandoned mine site in southwest Japan. *Minerals*, no. 3(4), pp. 412-426.

4. Miganei L., Gock E., Achimovičová M., Koch L., Zobel H., Kähler J. (2017). New residue-free processing of copper slag from smelter. *J Clean Prod.*, vol. 164, pp. 534-542.

5. Potysz A., van Hullebusch E. D., Kierczak J., Grybos M., Lens P. N., Guibaud G. (2015). Copper metallurgical slags—current knowledge and fate: a review. *Crit Rev Env Sci Tec.*, vol. 45(22), pp. 2424-2488.

6. Onuaguluchi O., Eren Ö. (2012). Recycling of copper tailings as an additive in cement mortars. *Constr Build Mater.*, vol. 37, 723-727.

7. Pappu A., Saxena M., Asolekar S. R. (2007). Solid wastes generation in India and their recycling potential in building materials. *Build Environ*, vol. 42(6), pp. 2311-2320.

8. Murari K., Siddique R., Jain K. K. (2015). Use of waste copper slag, a sustainable material. *J Mater Cycles Waste*, vol. 17(1), pp. 13-26.

9. Nadirov R. K. (2019). Recovery of valuable metals from copper smelter slag by sulfation roasting. *T Indian I Metals*, vol. 72(3), pp. 603-607.

10. Banza A. N., Gock E., Kongolo, K. (2002). Base metals recovery from copper smelter slag by oxidising leaching and solvent extraction. *Hydrometallurgy*, vol. 67(1-3), pp. 63-69.

11. Yang Z., Rui-lin M., Wang-dong N., Hui, W. (2010). Selective leaching of base metals from copper smelter slag. *Hydrometallurgy*, vol. 103(1-4), 25-29.

12. Turan M. D., Sari Z. A., Miller, J. D. (2017). Leaching of blended copper slag in microwave oven. *T Nonferr Metal Soc.*, vol. 27(6), pp. 1404-1410.

13. Kaksonen A. H., Särkijärvi S., Puhakka J. A., Peuraniemi E., Junnikkala S., Tuovinen O. H. (2016). Chemical and bacterial leaching of metals from a smelter slag in acid solutions. *Hydrometallurgy*, vol. 159, pp. 46-53.

14. Meshram P., Bhagat L., Prakash U., Pandey B. D., Abhilash. (2017). Organic acid leaching of base metals from copper granulated slag and evaluation of mechanism. *Can Metall Quart.*, vol. 56(2), pp. 168-178.

15. Çalban T., Çolak S., Yeşilyurt M. (2005). Optimization of leaching of copper from oxidized copper ore in $\text{NH}_3\text{-(NH}_4)_2\text{SO}_4$ medium. *Chem Eng Commun.*, vol. 192(11), pp. 1515-1524.

16. Bingöl D., Canbazoglu M., Aydoğan S. (2005). Dissolution kinetics of malachite in ammonia/ammonium carbonate leaching. *Hydrometallurgy*, vol. 76(1-2), pp. 55-62.

17. Meng X., Han, K. N. (1996). The principles and applications of ammonia leaching of metals—a review. *Min Proc Ext Met Rev.*, vol. 16(1), pp. 23-61.
18. Radmehr V., Koleini S. M. J., Khalesi M. R., Mohammadi M. R. T. (2013). Ammonia Leaching: A new approach of copper industry in hydrometallurgical processes. *Journal of The Institution of Engineers (India): Series D*, vol. 94(2), pp. 95-104.
19. Radmehr V., Koleini S. M., Khalesi M. R., Tavakoli M. R. (2012). Ammonia leaching in the copper industry: a review. In *XXVI international mineral processing congress (IMPC) proceedings/New Delhi, India/24–28 September* (pp. 02512-02523).
20. Nadirov R., Syzdykova L., Zhussupova A. (2017). Copper smelter slag treatment by ammonia solution: Leaching process optimization. *J Cent South Univ.*, vol. 24(12), pp. 2799-2804.
21. Roy S., Sarkar S., Datta A., Rehani S. (2016). Importance of mineralogy and reaction kinetics for selecting leaching methods of copper from copper smelter slag. *Sep Sci Technol.*, vol. 51(1), pp. 135-146.
22. Bidari E., Aghazadeh V. (2015). Investigation of Copper Ammonia Leaching from Smelter Slags: Characterization, Leaching and Kinetics. *Metall Mater Trans B*, vol. 46(5), pp. 2305-2314.
23. Peretrutov A. A., Chubenko M. N., Kim P. P., Yakunin Y. I. (2009). Combined solubility of copper and zinc oxides in ammonia-ammonium solutions. *Russ J Phys Chem A*, vol. 83(8), pp. 1422-1425.
24. Liu Z. X., Yin Z. L., Hu H. P., Chen, Q. Y. (2012). Leaching kinetics of low-grade copper ore with high-alkalinity gangues in ammonia-ammonium sulphate solution. *J Cent South Univ.*, vol. 19(1), pp. 77-84.
25. Safari V., Arzpeyma G., Rashchi F., Mostoufi, N. (2009). A shrinking particle–shrinking core model for leaching of a zinc ore containing silica. *Int J Miner Process.*, vol. 93(1), pp. 79-83.
26. Ekmekyapar A., Oya R., Künkül, A. (2003). Dissolution kinetics of an oxidized copper ore in ammonium chloride solution. *Chem Biochem Eng Q*, vol. 17(4), pp. 261-266.

¹Nasim Pourebrahim , ¹Amirhussein Elhamirad ,
^{2*}Soodabeh Einafshar , ¹Mohammad Armin 

¹Sabzevar Branch (IAUS) Islamic Azad University, Sabzevar Branch (IAUS)
 Sabzevar Khorasan Razavi, Iran.

²Department of Agricultural Engineering Institute, Khorasan Razavi Agricultural and
 Natural Resources Research and Education Center, AREEO, Mashhad, Iran,
 e-mail: soodabeheyn@yahoo.com

Thin layer drying models, antioxidative activity and phenolic compounds of rose petals (*Rosa damascena* Mill.) in tray dryer

Abstract: The drying behavior of the Damask rose (*Rosa damascena* Mill.) petals in a thin layer hot air drying at 35, 45 and 55°C and 0.4, 1.2 and 2 (m·s⁻¹) air velocity levels, was investigated. The Midilli was the most suitable model among 14 different thin-layer models for showing the thin-layer drying characteristics. At the experimental temperature (35-55°C) and air velocity levels (0.4, 1.2 and 2 m·s⁻¹) the effective moisture diffusivity was 2.02×10⁻¹²- 11.3×10⁻¹² (m²·s⁻¹) and the activation energy varied from 56.3 to 64.5 (kJ·mol⁻¹). Total anthocyanin content (TAC) ranged 77-240 (mg·L⁻¹). The rose petal extracts showed higher DPPH (59.51%) and lower FRAP (1213.24 μmol(Fe⁺²)·L⁻¹), at an increasing temperature from 35 to 55°C. Results showed that the higher temperature caused less TAC. At 45-55°C and air velocities 0.4-1.2 (m·s⁻¹) the number of anthocyanins increased significantly, but at air velocities, 1.2- 2 (m·s⁻¹) a decrease was observed.

Key words: *Rosa Damascena* Mill., Thin layer dryer, Anthocyanin, Phenolic compounds, Antioxidative power.

Introduction

Damask rose (*Rosa damascena* Mill.) is an ornamental plant from the family Rosaceae with more than 200 species and approximately 18000 cultivars. Damask rose is widely cultivated in Iran, Turkey, Bulgaria, India, Morocco, France, China, Italy, Libya, South Russia and the Ukraine. It is used for producing rose oil, water, concrete (rose oil solid), and absolute, which are significant base materials for the medicine, food products, and cosmetic industry [1]. Some factors like genotype of Damask rose, environment conditions, the time of harvesting, and the technology of processing and distillation, substantially affect the amount, percentage and compounds of rose essential oil and extract [2]. Numerous compounds can be extracted from pistil, ovary and sepal of Rose flower such as flavonoids, glycosides, terpenes and anthocyanins. Studies shows that Damask rose and rosehip seed oils are significantly rich in unsaturated fatty acids (omega fatty acid), bitter principle, organic acids and tanning matter [3]. Dried flowers are also used as flavor and laxative agents [1].

The short harvest duration (40 days) of Rose flower and its high moisture make the transportation and storage a difficult task [4]. The destruction of high fresh petals occurs at high speed rates due to the growth of the living organisms such as bacteria, molds and yeasts. Therefore, drying at the appropriate moisture content is an important step in the process [5]. Drying rose petals would introduce new utilization opportunities such as decorative, herbal, aromatic, hydrotherapeutic and cosmetic uses. In addition, with an increased demand for using the roses in health and aroma therapy, the importance of preserving color, flavor, and essential oils during the drying process has been identified [6].

Drying method is one of the oldest processes for product preservation and protection. This technique decreases humidity from ~ 85% wb to ~% 8-12 wb. The drying process should be completed in a short period of time to prevent the decomposition and minimize the used energy for the business concerns [7]. The most common commercial technique of drying food and chemical products is air drying. Hot air drying in food processing decreases the drying

time and hence maintains the dried product quality [8]. Therefore, the temperature and humidity levels of drying air, drying speed, and drying duration should be optimized to achieve the highest product quality [9].

Thermal and physical characteristics such as heat and mass transfer, moisture diffusion, activation energy, and energy consumption are essential in the design of agricultural crops dryers [10]. The drying process and apparatus modeling are substantially important in order to optimize the operation parameters and improve the performance of the drying system. Thin layer drying removes the moisture from a porous material by evaporation, in which drying air is passed through a thin layer of the material until it reaches a moisture balance. The external factors of the process, the type and size of the product, and the internal diffusion mechanisms control the drying rate [11].

Economic justification, quality, and quantity of the dried petals are dependent on the proper drying methods. Therefore, designing an effective operating system to minimize the drying process time and optimize energy consumption is required. The objectives of this paper are to 1) investigate the drying behavior of Damask rose petals through thin-layer drying 2) determine the best mathematical model for describing the drying process kinetics and 3) evaluate the effects of hot air velocity and temperature on qualitative properties of petals.

Materials and methods

Sample Preparation

Fresh rose flowers were picked up early in the morning, April to May 2018, from Gonabad, Khorasan Razavi province, Iran. Samples were transported to the laboratory and petals were separated before drying.

Chemicals

The applied chemicals and solvents were analytical reagent grade and were supplied by Merck (Darmstadt, Germany) and Sigma-Aldrich (St. Louis, MO) Chemical Companies.

Experimental Design

A laboratory-model tray dryer, equipped with installed instrumentations was used for the drying test. Different parts of dryer were air inlet and outlet parts, control unit and drying chamber (in which perforated trays are placed horizontally). The specifications of the fabricated dryer along with instrumentations are all explained in detail in [12]. Before the start of the drying process, the desirable

constant temperature was obtained by the electrical heaters. To execute a drying run at each temperature, the dryer turned on 30 minutes so that it would stabilize at the specified temperature and air velocity [12]. About 10 g of fresh petals were spread on the shelves as a thin layer and kept in the drying chamber. Drying experiments were conducted at the temperature of 35, 45 and 55°C and hot air velocities of 0.4, 1.2 and 2 m·s⁻¹. The reduced moisture content of petals was recorded every 2 minutes to achieve a constant weight and obtain the drying curves.

Mathematical modeling

Moisture ratio (MR) of the petal samples was obtained using equation (1):

$$MR = (M_t - M_e)/(M_0 - M_e) \quad (1)$$

where, M_t is the last moisture content, M_0 is the initial moisture content, and M_e is the equilibrium moisture content. In practice, M_e value is rather less than M_t or M_0 . Thus, the equation can be simplified as follows [13]:

$$MR = M_t/M_0 \quad (2)$$

Moisture ratio data were consistent with 14 thin-layer models that were mainly used to assess their suitability for thin layer drying kinetics of foods. MATLAB R2013 tool was used to fit the experimental data to the 14 thin-layer models. Three statistical parameters including coefficient of determination (R^2), root mean squares error (RMSE), and sum square error (SSE) were used to determine the performance of the models. For quality fit, R^2 value should be closed to one while SSE and RMSE values should be closed to zero.

Moisture Loss Kinetics

Fick's second law of unsteady state diffusion can describe the transport of moisture during the drying process that occurs in the falling rate period for most food materials [14]. It is calculated using the equation (3):

$$\frac{\partial M}{\partial t} = D_{eff} \nabla^2 M \quad (3)$$

where, D_{eff} is effective moisture diffusion ($m^2 s^{-1}$) and M is moisture content

Research shows that D_{eff} is related to temperature and the kind of material being dried, including its texture and structure [15]. For

sufficiently long period of drying, using the first term in the series in the equation is significant and therefore [16]:

$$MR = \frac{8}{\pi^2} \exp\left[\frac{-D_{eff}\pi^2 t}{4L^2}\right] \quad (4)$$

Taking the natural logarithm of the equation gives:

$$\ln(MR) = \ln\left(\frac{8}{\pi^2}\right) - \frac{\pi^2 D_{eff} t}{4L^2} \quad (5)$$

where, L is the half thickness of *Rosa damascena* petal (RDP). Hence, the effective moisture diffusivity (D_{eff}) is obtained by plotting the experimental drying data in terms of $\ln(MR)$ against drying time (s).

Energy of activation (E_a) in a sample is the minimum amount of energy required for the initiation of a drying process to cause moisture diffusion through the sample. Therefore, the activation energy was calculated using Arrhenius equation [10] as shown in Eq. (6):

$$D_{eff} = D_0 \cdot \exp\left(-\frac{E_a}{R_g T_{abs}}\right) \quad (6)$$

E_a : the energy of activation, D_0 : the pre-exponential factor of Arrhenius equation ($m^2 s^{-1}$), R_g : the universal gas constant ($8.3143 \text{ kJ} \cdot \text{mol}^{-1} \cdot \text{K}^{-1}$), and T_{abs} : the absolute air temperature ($^{\circ}\text{K}$). D_0 and the corresponding E_a were determined by plotting $\ln(D_{eff})$ versus $1/T$ [14].

Total Anthocyanin Content

Anthocyanin pigments undergo reversible structural transformations with a change in pH manifested by strikingly different absorbance spectra. The colored oxonium form predominates at pH 1.0 and the colorless hemiketal form at pH 4.5. The pH-differential method is based on this reaction, and permits accurate and rapid measurement of the total anthocyanins, even in the presence of polymerized degraded pigments and other interfering compounds. Briefly, transfer 1 mL extracted solution into 10 mL volumetric flask for preparing two dilutions of the sample, one adjust volume with potassium chloride buffer, pH 1.0, and the other with sodium acetate buffer, pH 4.5, diluting each. Let these dilutions equilibrate for 15 min. Measure the absorbance of each dilution at the 510 and 700 nm (to correct for haze), against a blank cell filled with distilled water [17]. TAC was expressed as cyanidin-3-glucoside (%w/w)

equivalents and measured by the following equation (7):

Total anthocyanin content

$$(\%W/W) = \frac{A}{\epsilon \cdot l} \times MW \times DF \times \frac{V}{W} \times 100\% \quad (7)$$

where,

$$A = (A_{520\text{nm}} - A_{700\text{nm}})_{\text{pH}1.0} - (A_{520\text{nm}} - A_{700\text{nm}})_{\text{pH}4.5}$$

MW (molecular weight): 449.2 for cyanidin-3-glucoside; DF : dilution factor; W : sample weight (mg); l : diameter of spectrophotometer cell (cm); ϵ : 26,900 M extinction coefficient in $\text{L} \cdot \text{mol}^{-1} \cdot \text{cm}^{-1}$ for cyd-3-glu; and 10^3 : factor for conversion from g to mg.

Determination of Antioxidant Activity

DPPH and FRAP assays were used to evaluate the total antioxidant activity.

The DPPH method: The radical scavenging activity of RPE (Rose petals extract) was tested according to the method described in [18]. RPE was mixed with 1 ml of 0.5 mM free radical 2, 2-diphenyl-1-picrylhydrazyl (DPPH) methanolic solution, stored in the dark for 30 min, and then the absorbance was measured at 517 nm. The radical scavenging activity (%RSA) of RPE was calculated by the following equation:

$$\%RSA = \frac{A_{\text{control}} - A_{\text{sample}}}{A_{\text{control}}} \times 100 \quad (8)$$

where A_{sample} is the absorbance of RPE at a particular level and A_{control} is the absorbance of the DPPH solution.

The FRAP method: The FRAP (Ferric reducing-antioxidant power) assay was performed by the 2, 4, and 6-Tripyridyl-S-triazine (TPTZ) following the method of Benzie and Strain [19]. FRAP reagent was prepared by mixing acetate buffer (0.3 M, pH=3.6), TPTZ solution (10 mM) and FeCl_3 (20 mM) in the ratio of 10:1:1. Briefly, 90 μL RPE (10 gr L^{-1}), 2700 μL of freshly prepared FRAP reagent and 270 μL distilled water were mixed and warmed to 37°C in a water bath and absorptions were determined at 595 nm. A standard curve was prepared using different concentrations of (200–2000 $\text{Fe}(\text{II}) \mu\text{mol} \cdot \text{L}^{-1}$).

Total phenolic content (TPC) determination

The total phenolic content was determined spectrophotometrically using the Folin Ciocalteu reagent described by Singleton and Rossi [20]. The calibration curve was plotted by absorbance measurements of various concentrations of Gallic acid (0.04–0.4 $\text{mg} \cdot \text{ml}^{-1}$) at 760 nm.

Results and discussion

Drying Model Investigation

The Model constants, R^2 , RMSE, and SSE for

14 thin layer drying models (at three different drying temperatures with three levels of hot air velocities) consistent with the moisture ratio are presented in Table 1.

Table 1 – Coefficient of determination range for some thin-layer drying models applied to *Rosa damascena* petals (RDP)

T (°C)	V (m.s ⁻¹)	Model name	Model equation	Coefficients						R ²	X ²	RMSE
				a	b	c	d	h	g			
35	0.4	Midilli	MR=a exp (-kτ ⁿ)+b ₁	0.9836	-0.00104			0.0062	1.24	0.999	0.00003	0.00522
45	0.4	Midilli	MR=a exp (-kτ ⁿ)+b ₁	0.9727	-0.00085			0.0185	1.256	0.999	0.00007	0.00780
55	0.4	Two term	MR=a exp (-bt)+c exp (-dt)	-14.02	0.1611	15.01	0.1544			0.999	0.00004	0.00585
35	1.2	Midilli	MR=a exp (-kτ ⁿ)+b ₁	0.9277	-0.00005			0.0012	1.733	0.995	0.00053	0.02218
45	1.2	Midilli	MR=a exp (-kτ ⁿ)+b ₁	0.9777	-0.00056			0.0320	1.146	0.999	0.00010	0.00946
55	1.2	Midilli	MR=a exp (-kτ ⁿ)+b ₁	0.9815	-0.00034			0.0428	1.33	0.998	0.00018	0.01208
35	2	Midilli	MR=a exp (-kτ ⁿ)+b ₁	0.9598	-0.00085			0.0043	1.315	0.999	0.00012	0.01056
45	2	Two term	MR=a exp (-bt)+c exp (-dt)	-17.74	0.1111	18.73	0.1073	0.0645		0.999	0.00005	0.00654
55	2	Jena&Das	MR=a exp (-kt ⁿ)+b ₁ +c	0.1729	0.6838	1.176				0.999	0.00005	0.00606

R^2 , RMSE and SSE values varied from 0.995 to 0.999, 0.00522 to 0.02218, and 0.0006 to 0.0246, respectively. Compared to other models, Midilli drying model had the highest R^2 and the minimum RMSE and SSE values, at 35 °C air temperature and 0.4 (m·s⁻¹) while the two term model had the best performance for air velocity of 0.4 m·s⁻¹ at 55°C and 2 m·s⁻¹ at 45°C. Jena & Das was the best model for air velocity of 2 m·s⁻¹ at 55 °C. For all the nine drying conditions, the Midilli was the most suitable model to show the thin-layer drying characteristics of the petals. Similar results were reported for *Rosa damascena* petals drying by Karimi and Bankar [21]. The Midilli model has been also successfully used to study the drying characteristics of agricultural products such as savory leaves and eggplant [22].

Effective Moisture Diffusivity and Activation Energy

Effective moisture diffusivity is influenced by temperature, air velocity and the kind of substance. The higher temperature and air velocity cause the shorter drying time due to increased thermal

gradients and mass transfer and as a result, drying rate increases [23]. The values of temperature, air velocity and effective moisture diffusivity are showed in Table 2.

Table 2 – Variations effective moisture diffusivity at different temperatures and hot air velocities

Temperature (°C)	Hot air velocity (m·s ⁻¹)	R ²	D _{eff} (m ² s ⁻¹)
35	0.4	0.95	2.2 × 10 ⁻¹²
45		0.96	4.85 × 10 ⁻¹²
55		0.99	7.68 × 10 ⁻¹²
35	1.2	0.97	2.42 × 10 ⁻¹²
45		0.98	4.9 × 10 ⁻¹²
55		0.98	11.3 × 10 ⁻¹²
35	2	0.94	2.02 × 10 ⁻¹²
45		0.99	5.25 × 10 ⁻¹²
55		0.98	9.29 × 10 ⁻¹²

An increase in the temperature at constant air velocity increased the effective moisture diffusivity. Moisture diffusivity for the petals showed a minimum value of $2.02 \times 10^{-12} \text{ m}^2 \cdot \text{s}^{-1}$ at 35°C for air velocity of $2 \text{ m} \cdot \text{s}^{-1}$ and a maximum value of $11.3 \times 10^{-12} \text{ m}^2 \cdot \text{s}^{-1}$ at air velocity of $1.2 \text{ m} \cdot \text{s}^{-1}$ and 55°C . The results demonstrate that at a constant air velocity, the higher temperature caused the more effective moisture diffusivity. The most effective moisture diffusivity was observed at 55°C . Similarly, Sharayi *et al.* [24] found that the maximum value of effective moisture diffusivity is at the highest temperature.

Drying temperature affects the internal mass transfer during drying, and ultimately the moisture diffusivity [14]. This is due to a higher heating energy that increases the water molecules' activities

and leads to a higher moisture diffusivity when samples are dried. Also, lower energy is required to remove the moisture at higher temperature because the water molecules are lightly bound to the food complex [25].

The Arrhenius equation was calculated for the activation energy (E_a) of air velocity values (9):

$$D_e = D_0 \cdot \exp\left(-\frac{E_a}{RT}\right) \quad (9)$$

E_a : The energy of activation ($\text{kJ} \cdot \text{mol}^{-1}$), R : universal gas constant ($8.3143 \text{ kJ} \cdot \text{mol}^{-1}$), T : absolute air temperature ($^\circ\text{K}$), D_0 : The pre-exponential factor of the Arrhenius equation ($\text{m}^2 \cdot \text{s}^{-1}$).

Figure 1 shows the plot of $\text{Ln}(D_{\text{eff}})$ versus $1/T$ at various treatments.

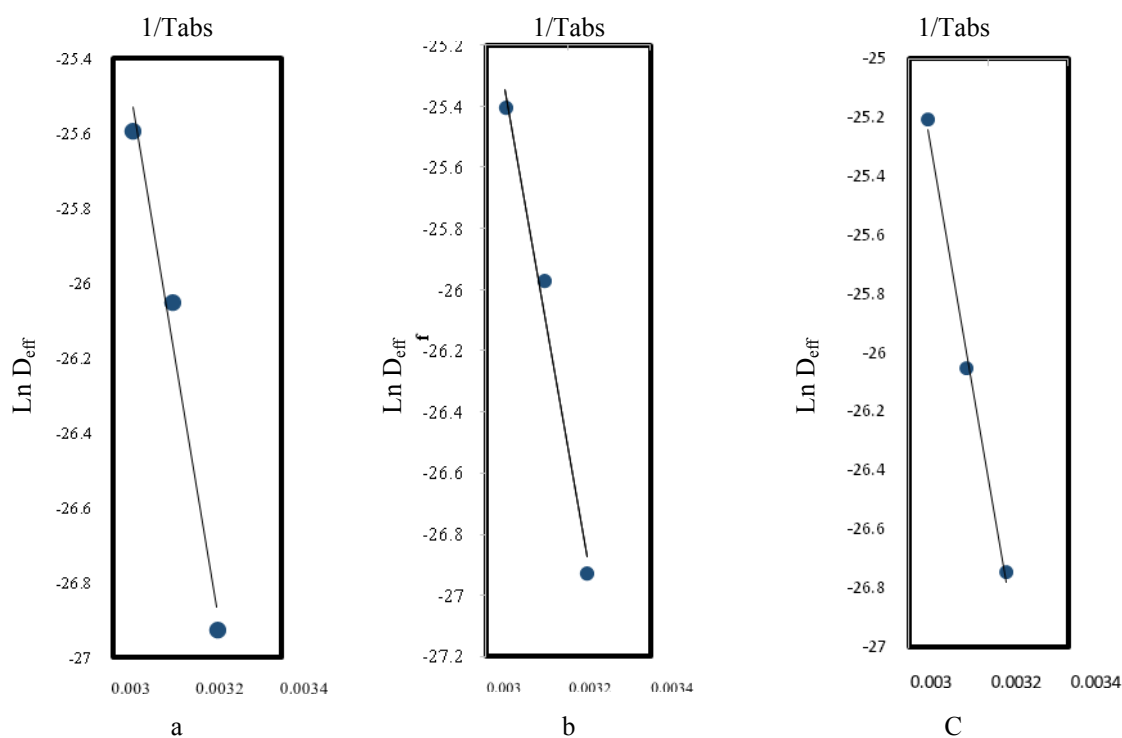


Figure 1 – Plotting experimental data for measuring of E_a : a: $0.4 \text{ m} \cdot \text{s}^{-1}$, b: $2 \text{ m} \cdot \text{s}^{-1}$ c: $1.2 \text{ m} \cdot \text{s}^{-1}$

$$\ln D_e = \ln D_0 - \frac{E_a}{RT} \quad (10)$$

The slope of the line (equation 10) was used for the calculation of the Activation energy (E_a) as follows

$$E_a = -(\text{slope} \times R) \quad (11)$$

In this study, the values of E_a were in the ranges of 56.3 to 64.5 $\text{kJ}\cdot\text{mol}^{-1}$, a result also reported by Sharayei *et al.* [24] for saffron petals. Aghbashlo *et al.* [10] and Doymaz [16] reported E_a of barberry and tomato varied from 110.837 to 130.61 and 17.40 to 32.94 $\text{kJ}\cdot\text{mol}^{-1}$, respectively.

Values of E_a and D_0 at air velocity are represented in Table 3. The maximum and minimum values of E_a (64.5 $\text{kJ}\cdot\text{mol}^{-1}$ and 56.3 $\text{kJ}\cdot\text{mol}^{-1}$) were at air velocity of 1.2 and 0.4 ($\text{m}\cdot\text{s}^{-1}$), respectively.

Table 3 – E_a and D_0 at different hot air velocities

Hot air velocity ($\text{m}\cdot\text{s}^{-1}$)	E_a (KJ mol^{-1})	D_0
0.4	56.3	7.5×10^{-3}
1.2	64.5	2.2×10^{-1}
2	64.3	1.7×10^{-1}

Temperature and Air Velocity Effects on Drying Time Duration

The fresh petals were dried in the air temperatures of 35, 45 and 55°C and different air velocity levels (0.4, 1.2 and 2 $\text{m}\cdot\text{s}^{-1}$). Figure 2 shows the decreasing trend of moisture content percentage over time due to temperature and air velocity.

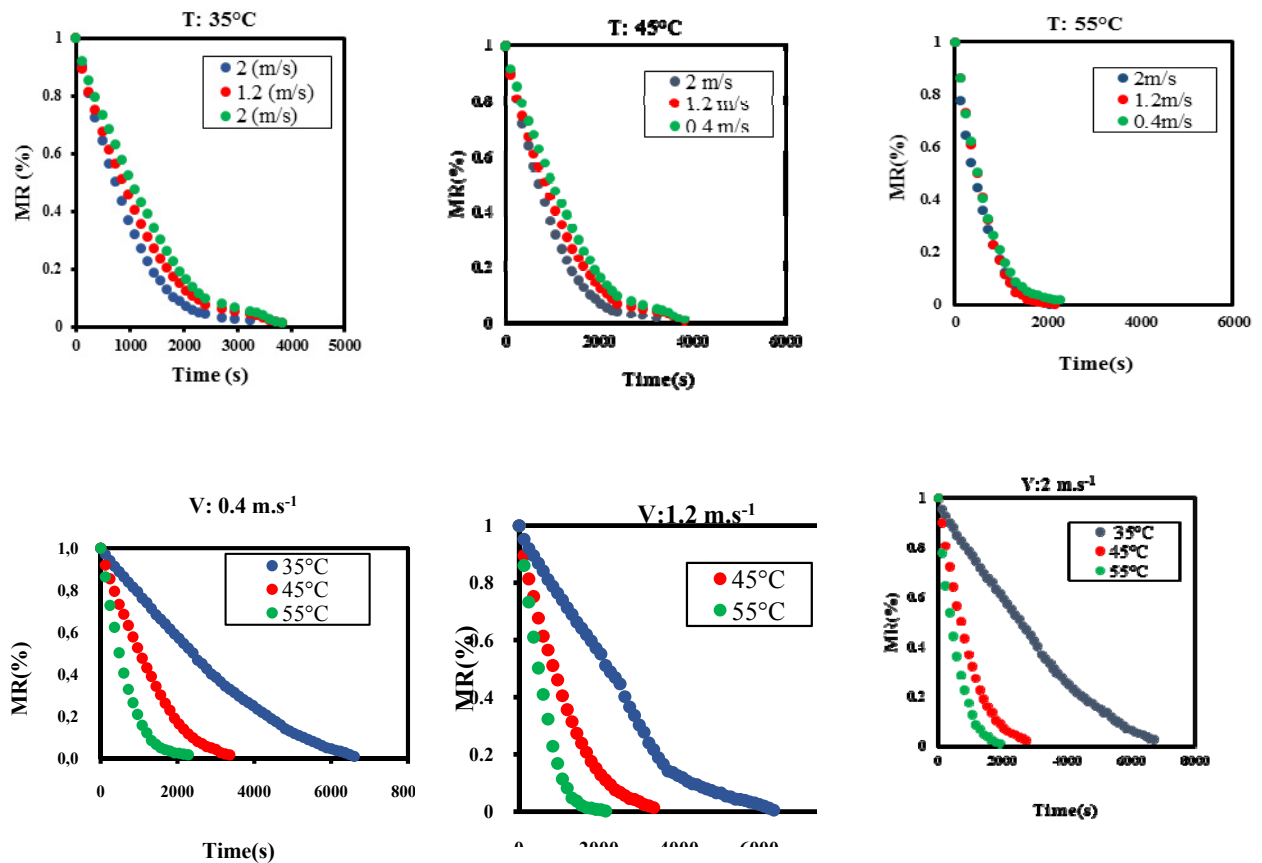


Figure 2 – Trend of variations of moisture content percentage with time for drying conditions

As shown in Table 4, the maximum (6720 s) and minimum (2040 s) drying times were at temperature of 35°C with air velocity of 0.4 $\text{m}\cdot\text{s}^{-1}$ and temperature of 55°C with air velocity of 2 $\text{m}\cdot\text{s}^{-1}$,

respectively. Drying time durations were 2000 – 7000 s at the 35, 45 and 55°C air temperatures and 0.4, 1.2 and 2 $\text{m}\cdot\text{s}^{-1}$ air velocity levels. The longest drying time was 3.5 times higher than those of the

shortest one. Figure 2 also demonstrates that the overall time of drying at 55°C was shorter than all the air velocities, suggesting that the temperature of drying was more effective than the air velocity. The increase in the temperature of drying increases the energy rate, the thermal gradient inside the product and also the accessible energy in the substrate for water transfer from the RDP. Therefore, higher temperatures lead to the faster drying rate and shorter drying time [26]. These results are similar to the findings of Kumar *et al.* [27] who dried different vegetables by the thin-layer dryer.

Table 4 – Time needed for removing moisture to 10% D.B. level for a combination of drying conditions

Temperature (°C)	Hot air velocity (ms ⁻¹)	Time (s)
35	0.4	6720
	1.2	6600
	2	6480
45	0.4	3360
	1.2	3240
	2	3240
55	0.4	2280
	1.2	2160
	2	2040

Increasing the hot air velocity reduced the moisture content of the RDP, and hence enhanced the drying rate. At first, RDP bulk water can be easily transferred to the surface and evaporated. With increasing the time of drying a significant decrease in the moisture was observed (Fig. 1). The internal moisture transfer rate is constant and does not evaporate easily. Therefore, the drying time is decreased with the increase of air velocity [28].

Influence of the Temperature and Air Velocity on RPE Properties

Anthocyanins that are natural dyes and food coloring agents are generally present in fruits and vegetables. They have beneficial health effects and possess strong antioxidative and antimicrobial activities. The presences of anthocyanins in RPE as quercetin-3-O-glucoside, kaempferol-3-O-

rhamnoside, and kaempferol-3-O-arabinoside have been reported by several researchers [29]. The antioxidative activities are affected by drying process such as air temperature and velocity [30].

In this study, the TAC was determined by the pH-differential method. The anthocyanin content in RPE was 77-240 mg·L⁻¹ (as cyanidin-3-glucoside) (Table 5). Similar results were reported for *Rosa damascena* petals by Ginova *et al.* [31]. TAC was in the same range (179-314 mg·L⁻¹) that has been previously reported by Bayram *et al.* [18] for samples from seven industrial-scale plantations. TAC of extracts obtained from edible flowers (Poppy, Red tulip, Rose and Roselle) in the same study were found within the range of 10 to 405 mg·kg⁻¹ dry extract. The TAC in the dried rose petals is more than fruits such as red grape (26.7 mg·L⁻¹) and apple (1.3-2.3 mg·L⁻¹) and less than of red fruit juices such as Sweet cherry (256.6 mg·L⁻¹) Blackberry (739.93 mg·L⁻¹), Sour cherry (369.39 mg·L⁻¹), Black currant (1543.8 mg·L⁻¹) and Chokeberry (3042.2 mg·L⁻¹) [32-33]. Our results show that the temperature had a significant impact on the TAC, the lower temperature caused the more TAC (Table 5). Increasing the air velocity from 0.4 to 1.2 (m·s⁻¹), at the temperature of 45-55°C, caused an increasing the amount of anthocyanins increased. However, at the air velocity of 1.2-2 (m·s⁻¹), a decrease was observed showing that the air velocity at the 35°C did not have a significant impact on the total anthocyanin.

Antioxidant activity of RPE were examined by applying the 2,2-diphenyl-1-picrylhydrazyl (DPPH) radical scavenging method and FRAP assay. The methanol extracts showed higher DPPH (30.01 vs 59.51%) scavenging power and lower FRAP (992.27 vs 1213.24 μmol (Fe⁺²)·L⁻¹) with increasing temperature from 35 to 55°C (Table 5). The DPPH depends on structural conformation, whereas FRAP assay is less sensitive toward hydrophilic antioxidants and the interaction of antioxidant compounds. Thus, DPPH may not show the accurate antioxidant capacity of compounds compared to the latter [34].

Table 5 – Effect of drying air temperature and velocity on total anthocyanin content (TAC) and antioxidant activity

Temperature (°C)	Velocity of air (ms ⁻¹)	TAC (mg.c3g/L of extract)	RSA (%)	Folin (mg of GA/g of extract)	FRAP (μmol (Fe ²⁺)L ⁻¹)
55	2	160.10±9.09b	59.51±1.96a	661.33±2.11a	992.27±12.47d
	1.2	180.59±4.76b	58.37±2.70a	643.33±5.03a	1001.78±4.11c
	0.4	77.40±14.62c	54.71±2.60a	658.33±4.98a	1119.39±8.19b
45	2	135.06±8.78c	31.97±11d	612.33±8.05b	837.24±7.53d
	1.2	239.02±9.07a	34.77±0.66cd	618.33±6.66b	1006.53±7.58c
	0.4	158.59±5.15b	52.08±1.75ab	624±9.88b	1261.15±6.36a
35	2	223.08±9.83a	43.69±1.16bc	537.33±8.7d	1206.71±5.99a
	1.2	220.05±9.47a	44.26±2.68bc	581.66±5.44c	1092.06±3.41b
	0.4	229.91±8.20a	30.01±1.21d	577.2±7.67c	1213.24±10.22a

There is a positive relationship between total phenolic content and Radical scavenging capacity (DPPH); and some research have observed a high correlation. But some other researchers reported negative correlation between total phenolic content and antioxidant activity because total phenolic compounds do not contain all the antioxidants present in the extract [35].

Acknowledgments

The authors would like to thank the technical support by Department of Agricultural Engineering Institute, Khorasan Razavi Agricultural and Natural Resources Research and Education Center, AREEO, Mashhad/IRAN.

References

- Mahboubi, M. Rosa damascene as holy ancient herb with novel applications// J. trad. Compl. Med. -2016. – 6. -P. 10-16.
- Yang, L, Ren, J, Wang, Y. Chemical investigation of volatiles emitted from flowers of three varieties of Damask Rose cultivated in Beijing// Hort. Environ. Biotechnol. -2014. -55(6). - P. 524-530.
- Kazaz, S, Baydar, H, Erbas, S, Variations in Chemical Compositions of *Rosa damascena* Mill. and *Rosa canina* L. Fruits, Czech// J. Food Sci. - 2009. – 27(3). –P. 178–184.
- Baydar, H, Schulz, H, Kruger, H, Erbas, S, Kineci, S. Influences of fermentation time, hydro-distillation time and fractions on essential oil composition of damask rose (*Rosa Damascena* Mill.)// J. Essent oil Bear Pl. -2008. – 11. – P. 224-232.
- Balladin, D.A, Headley, O. Solar drying of rose (*Rosa* sp.) petals// Renewable Energy. -1999. – P. – 249-255.
- Haghighi, M, Tehranifar, A, Nikbakht, A, Kafi, M, Research and current profile of Iranian production of Damask Rose (*Rosa Damascena* Mill.), In: VIIIth Int. People- Plant Symp. Acta Hort. ISHS. -2008. -P. 251-254.
- Brennan, J.G. Drying. Theory of air- drying. In: Encyclopedia of food sciences and nutrition, Caballero B, Trugo LC, Finglas PM (eds.), Academic Press, Elsevier Sci. Ltd., Oxford, UK// - 2003. – P. -1913-1917.
- Maskan, M. Drying, Shrinkage and rehydration characteristics of kiwi fruits during hot air and microwave drying// J. Food Eng. -2001. – 48(2). – P.:177-182.
- Bayhan, A.K, Boyar, S, Caglar, M.F, Akdeniz, R.C, Kayaalp, O. Design of the experimental dryer for medical & aromatic plants// Hungarian Agri. Eng. -2011.- 23.- P. 5-8.
- Aghbashlo, M, Kianmehr, MH, Akhijahani, HS. Modeling of thin-layer drying of potato slices in length of continuous band dryer// J. Energy Conv. Manage.-2009. -50.5. – P. 1348-1355.
- Omid, M, Yadollahinia, A.R, Rafiee, S. A thin-layer drying model for paddy dryer. In the International conference on Innovations in Food and Bioprocess Technologies, 12th–14th December 2006, AIT, Pathumthani, Thailand.
- Chaji, H, Hedayatzadeh, M. Quality assessment and kinetics of dehydrated watermelon seeds: Part 1.// Eng. in Agri. Environ. Food, -2017. - 10. – P.178–185.
- Doymaz, I., Sahin, M. Effect of temperature and pre-treatment on drying and rehydration characteristics of broccoli slices// J. of Food Meas. Charac. -2016. – 10(2). –P. 364-373.

14. Nwajinka, C.O, Nwuba E.I.U, Udoye B.O. Moisture diffusivity and activation energy of drying of melon seeds// *Int. J. App. Sci. Eng.* -2014. – 2(2). –P. 37-43.
15. Rizvi, S.S.H. Thermodynamics of foods in dehydration, In *Engineering Properties of Foods*, M. A. Rao & S. S. H. Rizvi (eds). -1986. Marcel Dekker. New York, P. 196.
16. Doymaz, I. Air-drying characteristics of tomatoes// *J. Food Eng.* -2007. – 78(4). –P.1291-1297.
17. Lee, J, Durst, R.W, Wrolstad, R.E. Determination of Total Monomeric Anthocyanin Pigment Content of Fruit Juices, Beverages, Natural Colorants, and Wines by the pH Differential Method: Collaborative Study// *J. AOAC Inter.* -2005. – 88(5). – P. 1269-1278.
18. Bayram, O, Sagdic, O, Ekici, L. Natural food colorants and bioactive extracts from some edible flowers// *J. App. Bot. Food Qual.* -2015. -88. P.170 – 176.
19. Benzie, I, Strain, J. The Ferric reducing ability of plasma (FRAP) as a measure of antioxidant activity. The FRAP assay// *Anal. Bioch.* -1996. -189. – P. 70-76.
20. Singleton, V.L, Rossi, Jr J.A. Colorimetry of total phenolics with phosphomolybdic phosphotungstic acid reagents// *Am. J. Enol. Viticul.*-1965. – 16. –P.144-158.
21. Karimi Akandi, S.R, Bankar, A., Rosa Damascena Mill. Moisture modeling in hot air dryer using mathematic models and artificial neural network, Iran// *J. Med. Arom. Pl.* -2014. -30(2). – P. 250-259.
22. Arslan, D., Ozcan, M.M. Evaluation of drying methods with respect to drying kinetics, mineral content, and color characteristics of savory leaves // *Food and bioprocess technology.* – 2012. – 5(3), P. 983-991.
23. Minaei, S, Motevali, A, Najafi, GH. H, Mousavi Seyedi, S.R. Influence of drying methods on activation energy, effective moisture diffusion and drying rate of pomegranate arils (*Punica Granatum*)// *AJCS.* -2011. – 6(4). –P.584-591.
24. Sharayei, P, Hedayatizadeh, M, Chaji H, Einafshar, S. Studying the thin-layer drying kinetics and qualitative characteristics of dehydrated saffron petals// *J. of Food Proc. Preserv.* -2018. – 42(2). – P:1-9.
25. Amira, T, Saber, C, Fethizayrouba, K. Moisture diffusivity and shrinkage of fruit and cladode of ountice ficus-indica during infrared drying// *J. food proc.* -2014. – 1. P. 1-9.
26. Mohammad, Z, Seyed, H. S. Barat, G. Kinetic drying and mathematical modeling of Apple slices in dehydration process// *J. food proc. tech.*-2013. – 4(7). – P. 1-4.
27. Kumar, N, Sarkar, B.C, Sharma H.K. Development and characterization of extruded product of carrot pomace, rice flour and pulse powder// *Afr. J. Food Sci.* -2010. -4. –P.703–17.
28. Nadi, F. Development of a New Model for Mass Transfer Kinetics of Petals of *Echium amoenum* Fisch. & C.A. Mey. under Fluidized Bed Conditions// *Food Technol. Biotechnol.* -2016. -54(2). –P. 217–227.
29. Schieber, A, Mihalev, K, Berardini, N, Mollov, P, Carle, D. Flavonol Glycosides from Distilled Petals of *Rosa damascene* Mill., *Zeitschrift für Naturforschung*, 60(5-6):379-84 (2005).
30. López-Vidaña, E.C, Figueroa, I.P, Cortés, F.B, Rojano, B.A, Ocañ, A.N. Effect Of Temperature On Antioxidant Capacity During Drying Process Of *Mortiño (Vaccinium meridionale Swartz)*// *Int. J. Food Prop.* – 2016. – 20(2). – P. 294-305.
31. Ginova, A, Mihalev, K, Kondakova, V, Antioxidant Capacity of Petals and Leaves from Different Rose (*Rosa damascene* Mill.) Plantations in Bulgaria// *Int. J. Pure & App. Bios.* -2013. – 1(2). P. 38-43.
32. Jakobek, L, Seruga, M, Medvidovic-Kosanovic, M, Novak, I. Anthocyanin content and antioxidant activity of various red fruit juices// *Deut. Leb.-Rund.* -2007. -103(2). -P:58-64.
33. Wu, X, Beecher, G.R, Holden, J.M, Hytowitz, D.B, Gebhardt, S.E, Prior, R.L. Concentrations of Anthocyanins in Common Foods in the United States and Estimation of Normal Consumption// *J. Agric. Food Chem.* -2006. -54. –P. 4069-4075.
34. Kaur, T.C, and Kapoor, H.C. Antioxidant in fruits and vegetable-The millennium's health// *Intl. J. Food Sci. Technol.* -2001. – 36. P.703–725.
35. Tawaha, K, Alali, F.Q, Gharaibeh, M, Mohammad, M, and El-Elimat, T. Antioxidant activity and total phenolic content of selected Jordanian plant species// *Food Chem.* -2007. -104. – P.1372-1378.